Dissertation

Lipidomic analysis of human serum samples from different gut microbial background and different health conditions

submitted by

Dipl. Ing. (FH) / Msc

Thomas Züllig

for the Academic Degree of

Doctor of Medical Science

(Dr. scient. Med)

at the

Medical University of Graz

Center for Medical Research

Under the Supervision of

Priv.-Doz. Mag. Dr.rer.nat. Harald KÖFELER

2021

DECLARATION

I hereby declare that this thesis is my own original work and that I have fully acknowledged by name all of those individuals and organisations that have contributed to the research for this thesis. Due acknowledgement has been made in the text to all other material used. Throughout this thesis and in all related publications I followed the “Guidelines of the Medical University of Graz on Good Scientific Practice“.

12.07.2021

Disclosure's

A Metabolomics Workflow for Analyzing Complex Biological Samples Using a Combined Method of Untargeted and Target-List Based Approaches

by Thomas Züllig [1,†],Martina Zandl-Lang [2,†],Martin Trötzmüller [1],Jürgen Hartler [3], Barbara Plecko [2] andHarald C. Köfeler [1,]

[1] Core Facility Mass Spectrometry, Medical University of Graz, 8036 Graz, Austria

[2] Department of Paediatrics and Adolescent Medicine, Division of General Paediatrics, University Childrens' Hospital Graz, Medical University of Graz, 8036 Graz, Austria

[3] Institute of Pharmaceutical Sciences, University of Graz, 8036 Graz, Austria

[†] These authors have contributed equally to this work.

Metabolites 2020, 10(9), 342; https://doi.org/10.3390/metabo10090342

REVIEW

Lipidomics from sample preparation to data analysis: a primer

Thomas Züllig[1], Martin Trötzmüller[1] & Harald C. Köfeler[1]

[1] Core Facility Mass Spectrometry, Medical University of Graz, 8036 Graz, Austria

Analytical and Bioanalytical Chemistry volume 412, pages 2191–2209 (2020)

https://doi.org/10.1007/s00216-019-02241-y

ACKNOWLEDGEMENTS

I would like to thank everyone who supported me in all facets with contributions on the content of the work, but also for the nice conversations over coffee.

I specifically want to thank Priv.-Doz. Dr. med. Univ. Tatjana Stojakovic for the uncomplicated supervision of this work.

Great thanks go to Dipl.-Ing. Dr. tech Martin Trötzmüller for providing invaluable help and assistance whenever I had any questions.

My deepest thanks go to Dr. rer. Nat. Harald Köfeler for his supervision and the opportunity to realize this work.

Also, my thanks go to the whole Core Facility team, Ing. Stefanie Maria Rappold, Christine Pein, Dipl. Ing. Verena Buchgraber and of course Ing. Birgit Reiter, they were in any cases very supportive and working with them was fun.

My thanks also go to our shared postdoc from Pediatrics Martina Zandl-Lang. The collaboration with her has always been great.

Last but not least, I want to thank Mag. Barbara Weißensteiner for her moral support and her useful correctional work.

The thesis was conducted at the Docteral School for Translational Molecular and Cellular Biosciences

This work was supported by the BMWFW-10.420/0005-WF/V/3c/2017 (Austrian Federal Ministry of Education, Science and Research)

Table of Contents

ABBREVIATIONS AND ACRONYMS

ACN	acetonitrile
ANOVA	analysis of variance
aPE	alkenyl phosphatidylethanolamine
BMI	body mass index
BMP	Bis(monoacylglycero)phosphate
CCS	collision cross section
CE	cholesterol ester
Cer	ceramide
CHOL	cholesterol
CL	cardiolipin
DESI	desorption electrospray ionization
DG	diacylglycerol
DTIM	drift tube ion mobility
ESI	electrospray ionisation
FA	fatty acid
GL	glycerolipid
GP	glycerophospholipids
HCD	higher energy collision dissociation
HexCer	hexosylceramide
HILIC	hydrophilic interaction liquid chromatography
HPLC	high performance liquid chromatography
IMS	ion mobility spectrometry
IPA	isopropanol
IT	ion trap
LC	liquid chromatography
LDA	Lipid Data Analyzer
LIPID MAPS	LIPID Metabolites and Pathways Strategy
LLOD	lower limit of detection
LLOQ	lower limit of quantification
LPA	lysophosphatidic acid
LPC	lysophosphatidylcholine
LPE	lysophosphatidylethanolamine
m/z	mass to charge ratio
MALDI	matrix-assisted laser desorption ionization
MeOH	methanol
MG	monoaxylglycerol
MS	mass spectrometry
MS/MS MS2	tandem mass spectrometry
MTBE	methyl *tert* butyl ether
NCE	normalized collision energy
NP	normal phase

OHS	over head shaker
PA	phosphatidic acid
PC	phosphatidylcholine
PE	phosphatidylethanolamine
PI	phosphatidylinositol
PK	plyketides
ppm	parts per million
PR	prenol
QTOF	quadrupole time of flight
RPLC	reverse phase liquid chromatography
RSD	relative standard deviation
RT	retention time
SL	saccherolipids
SM	sphingmyelin
SP	sphingolipid
SPE	solid phase extraction
ST	sterol lipids
SWATH-MS	sequential windowed acquisition of all theoretical fragment ion mass spectra
TG	triacylglycerol
TIC	total ion chromatogram
UHPLC	ultrahigh performance liquid chromatography
USB	ultra sonic bath

LIST OF FIGURES AND TABLE

ZUSAMMENFASSUNG

Lipide sind Moleküle mit großer struktureller Vielfalt und sind für eine Vielzahl biologischer Funktionen verantwortlich. Eine Deregulation des Lipidstoffwechsels kann erhebliche Auswirkungen auf verschiedene Krankheiten und pathogene Zustände wie zum Beispiel Lungenkrebs, Diabetes und Alzheimer haben. Die klinische Lipidomik ist ein relativ junges Forschungsgebiet und noch nicht gleich etabliert wie z.B. klinische Proteomik oder Metabolomik. Es werden Anstrengungen unternommen, um Probenmessungen und Datenanalysen zu standardisieren, um die Anforderungen für den klinischen Bereich zu optimieren. Die klinische Lipidomik hat das Potenzial eines leistungsstarken Werkzeugs für die krankheitsspezifische Diagnose, insbesondere wenn die Funktion des Lipidstoffwechsels und deren Enzyme besser verstanden werden. In dieser Arbeit stellen wir einen globalen Lipidomik Workflow von der Probenvorbereitung über die Datenverarbeitung bis zur statistischen Datenanalyse vor. Dabei wurden 3 große humane Serumprobenkohorten mit unterschiedlichen Phänotypen und eine Interventionsstudie mit einer kalorienarmen Diät mit Adipositas Patienten analysiert. Insgesamt wurden mehr als 1850 Serumproben mit einer Analysezeit von über 185 Tagen mit einem Q Exactive Focus Massenspektrometer gemessen. Die Interventionsstudie zeigte einen reversiblen Effekt im Lipidprofil zwischen der sechswöchigen kalorienarmen Diät und der normalen Nahrungsaufnahme für weitere sechs Wochen. Wir konnten auch Unterschiede im Phänotyp-spezifischen Lipidprofil in der Tomorrow Kohorte der gesunden Gruppe im Vergleich zur Diabetesgruppe feststellen. Dabei waren 235 Lipidspezies aus allen detektierten Lipidklassen signifikant unterschiedlich (adj. P-Wert $\leq$ 0,05). Mehrere Triglyceridspezies zeigten eine mehr als zweifache Veränderung im Vergleich zur Kontrollgruppe.

Zusätzlich konnten auch Unterschiede zwischen anderen Gruppen beobachtet werden, z.B. bei Herz-Kreislauf-Erkrankungen und rheumatoider Arthritis. Die Daten wurden an unseren Projektpartner übermittelt, um sie mit Metabolomics- und Mikrobiomdaten zu vergleichen.

ABSTRACT

Lipids are molecules with great structural diversity and are responsible for a large number of biological functions. Dysregulation of lipid metabolism can have significant effects on various diseases and pathogenic conditions such as lung cancer, diabetes, and Alzheimer's disease.

Clinical lipidomics is a relatively new area of research and may show a lack of sensitivity to changes in response to certain diseases caused by problems of insufficient standardization in sample preparation, sample measurement, and data analysis. However, if lipid profiles and their role in the interaction of the metabolic pathway are better understood, it has the potential of a powerful tool for disease-specific diagnosis and therapy. In this thesis we present a global lipidomic workflow from sample preparation and data processing to statistical data analysis including batch drift normalization. With this workflow, we were able to process 3 large human serum sample cohorts with different phenotype backgrounds and an intervention study on obesity patients on a low-calorie diet with a total of over 1850 serum samples and an analysis time of over 185 days measured with the Q Exactive Focus mass spectrometer. The intervention study showed a reversible effect in the lipid profile between the six-week low-calorie diet and the normal food intake for a further six weeks.

We were also able to determine differences in the phenotype-specific lipid profile in Tomorrow's cohort of the healthy group compared to the diabetes group. We identified 235 significantly different lipids (adj. P-value ≤ 0.05) across all lipid subclasses with multiple triacylglycerol species with more than twofold changes compared to the healthy group. We could also find differences between other phenotype-specific groups, e.g. cardiovascular disease and rheumatoid arthritis. The data were also transmitted to our project partner in order to compare them with metabolomics and microbiome data.

INTRODUCTION

In the past few decades, biomedicine and nutritional science have made significant advances to develop from cellular to molecular research technologies. This has led to the knowledge that health is a state of homeostasis not only for our various eukaryotic cells, but also for the millions of living microorganisms that are in symbiosis in (e.g. intestines) or on (e.g. skin) our human body. As this project is part of a bigger consortium, the overall aim is to find a homeostasis indicator as biomarker for health and nutrition.

Gut microbiota and nutrition are important to human health and gastrointestinal homeostasis as they play a role in the activity and development of the immune system (1), explain energy harvest from nutrition (2), and maintenance of mucosal integrity and regulation of intestinal epithelial renewal (3). Nowadays it is widely recognized that disorders in the gut microbiome are linked to many different diseases, including: i) metabolic disorders e. g. obesity and/ or type 2 diabetes (4-6), ii) cardiovascular diseases e. g. heart failure and atherosclerosis (7, 8), iii) chronic-inflammatory diseases e. g. rheumatoid arthritis and colitis (9, 10) and iv) defined malignancies e. g. colonic and gastric cancer (11, 12). As noted above, the gut microbiome disorders and their diversity of many different diseases imply that a microbiome corresponds to a health-related state of symbiotic homeostasis. The microbiome is not only a mirror of our health, it can also be influenced by nutrition. Since disturbances of the gut microbiome are associated with so many different disease entities, a favorable microbiome is likely to be a reliable indicator of the condition of symbiotic homeostasis associated with health. Arumugam et.al., (2011) showed that 3 major clusters of gut microbiota (enterotypes) are present (Prevotella, Ruminococcus, and Bacteriodetes) regardless of nationality, age, BMI, and gender-specific phenotype (13).

Long-term diet is a strong predictor of individual enterotype, carbohydrate-rich diet is associated with Prevotella type and the intake of protein and animal-based fat are associated with Bacteriodetes type (14). Cultural differences in diet give us further insight and are in line with long-term diet. A high-fiber diet in rural villages in Africa showed accumulation of Prevotella, and in the United States, the corresponding diet high in animal protein and

saturated fat showed more Bacteroides (15). Intervention studies demonstrated rapid microbiome shifts based on nutrition (16). The question arises as to how the enterotype influences the metabotype, since both are highly complex systems. Recent studies have shown that the microbiota and its host interact, leading to the model of the microbiome-host metabolic axis (17). This axis assumes a combined metabolism in which the substrates of the host and the microbiome influence each other, e.g. choline metabolism, short-chain fatty acids and the production of bile.

This work will provide the BioNuGut consortium with the lipidomics data of the jointly analyzed human serum cohorts in order to achieve the overall goal of identifying bio-patterns of gut microbiome metabolites in human serum that indicate the symbiotic homeostasis of humans and microbes, which is indicating a healthy nutrition and human health in general.

The aims of this study therefore are: i) to develop all necessary methods and to implement quality characteristics for sample processing and thus to analyze large amounts of data. ii) To analyze the cohorts (FoCus n = 905; PopGen, n = 399; TOMORROW, n = 400; and an intervention study n = 120) with a robust mass spectrometry method. iii) To develop a workflow for data processing with available tools and statistical analysis. The final lipidomics data will be transmitted to our German partner and merged with their omics data for further comparative analysis. The focus here is on comparing the metabotype (metabolomics and lipidomics) with the phylogenetic composition of the bacterial community.

1 Theoretical background

In the living organism, lipids are important organic compounds that have various biological functions, from energy storage (e.g. triglyceride), to building structures for cellular membranes (e.g. glycerophospholipids), or intra- and extracellular cell signaling (e.g. diglycerols). One of the main databases collecting information on lipids is LIPID MAPS, which contains 45664 entries (curated, 23711; computationally generated, 21953). The classification system was introduced in 2005 and is based on 8 different lipid classes (Figure 1). Each class has its hierarchical subclass based on different features (e.g. headgroups, bonding type, backbone structure). Lipids are macromolecules with a non-hydrophilic and a hydrophilic part (e.g. hydrophobic: acyl/alkyl, isoprene or sphingosine; hydrophilic: headgroup) (18, 19).

Fatty acids (FA) are the least complex lipid structure, based on a carboxylic acid and an aliphatic chain, which can be un/saturated, branched, and can have 4 to 28 carbon atoms with major species of 16 and 18 carbons. In higher eukaryotes, most FA have even number of carbons and, when unsaturated, are *cis*-configured. FA can be seen as building blocks for several other more complex lipids e.g. triglycerides, glycerophospholipids or cholesterol esters, where they appear as fatty acyl chains.

Glycerolipids (GL) main subclasses are tri-, di-, and mono- glycerols (TG, DG, MG). They contain esterified acyl-chains to the hydroxyl groups of glycerol, either one, two or three and play an essential role in energy storage.

Glycerophospholipids (GP) are very similar to the GL class with an additional phosphate group which is linked at the *sn*-3 position of the glycerol backbone. There are several GP subclasses, which are defined by their head groups linked to the phosphate group e.g. choline, ethanolamine, glycerol, serine, or inositol. The simplest of them is the phosphatidic acid (PA) without a head group.

There are also sub-classes with different chain binding types, not only are acylated chains on the glycerol backbone, but also alkylated chains are variants or lysophospholipid with only one acyl/alkyl chain. Phospholipids are the most important part of bilayers of cellular membranes. Sphingolipids (SP) are containing a sphingoid base e.g. sphingosine, as structural backbone. Common sphingolipids are ceramides (Cer) with a fatty acid or sphingomyelin (SM) with a fatty acid and a choline headgroup. Other subclasses found are variants with one up to several hexoses e.g. hexosylceramides (HexCer) and gangliosides. One of the functions is to build up the cell surface around the peripheral and central nervous system (20).

Sterol lipids (ST) are based on cholesterol with different derivates e.g. cholesterol esters (CE) with an attached acyl-chain or bile acids as well as hormones e.g. estrogens, corticoids, and androgens (18). Prenol lipids (PR) are originating from two precursors and contain lipids such as vitamins E, K or the coenzyme Qx.

Saccharolipids (SL) are lipids, where acyl/alky groups are linked to a sugar backbone commonly found in plants, fungi, and bacteria. And the last of these eight lipid classes are polyketides (PK), which are a highly diverse group. They are secondary metabolites from different plants, fungi, bacteria, or invertebrates built by polymerization of propionyl and acetyl groups, among them are tetracycline.

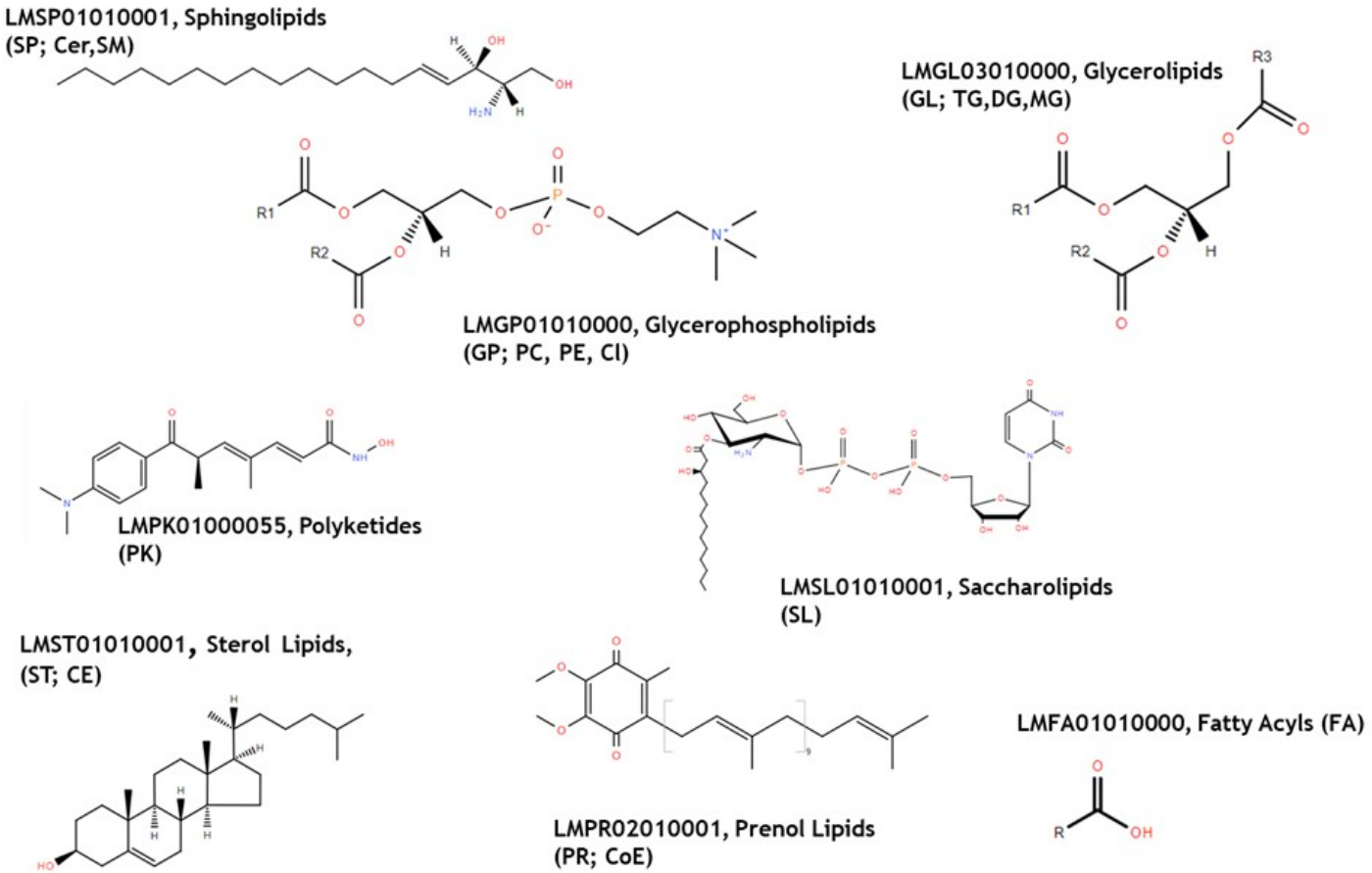

Figure 1 Overview of the 8 main lipid classes by International Lipids Classification and Nomenclature Committee. Shown is a representative structure of each lipid class.

1.1 Preanalytical steps in lipidomics

Before samples can be analyzed and processed, a few steps are required. As a first step, when samples are taken, they should be prevented from further biological activity or degradation, e.g. it is known that freezing processes can hydrolyze cardiolipin (CL) to monolysocardiolipin (21), and that lysophosphatidic acid (LPA) or lysophosphatidyl-choline (LPC) increase in concentration when left at room temperature (22, 23). Samples stored in methanol at pH higher than 6 and temperature higher than 20°C, lysophospholipid regioisomers change into a new stable equilibrium (24). Therefore, samples should be directly processed e.g. extraction, precipitation, or shock freezing and stored at least at minus 80°C as short as possible, especially if targets are susceptible of oxidation or degradation e.g. lysolipids, oxylipins, or phospholipids.

Preparation of heterogenic solid samples

Different tissue types e.g. skin, liver, cells, or lung are heterogenic and to some extent solid. To ensure that extraction solvents can access organelle compartments equally, methods for homogenizing samples are commonly used. The most suitable method depends on the type of tissue. Frequently used methods are i) liquid nitrogen frozen samples crushing with pestle and mortar (e.g. Bessman Tissue Pulverizers), ii) grinder which works with shearing forces (e.g. ULTRA-TURRAX), iii) bead based methods using beads with a diameter of 0.1 to 2 mm and are often combined with enzymatic solutions e.g. collagenase. There are shaking vessel types (e.g. MIXER MILL) and agitator shaft types (e.g. DYNO®-MILL). (iv) Another commonly used method is the cavity bomb, which relies on decompressing liquid nitrogen, or ultrasonic sound (25-28). To a certain extent, all methods have physical and/or chemical effects on the sample. Ice can be used to reduce heat effects or buffers to stabilize and reduce oxidation and/or lysis.

Lipid extraction with organic solvents

Lipids have hydrophobic properties that can be utilized to reduce unwanted chemical compounds such as proteins or metabolites to simplify complex matrices of biological samples with the aim of increasing the signal-to-noise ratios, reproducibility, and reduction of device contamination. The Folch extraction protocol was published in 1957 and is one of the 4 most common extraction protocols in lipidomics. It is a mixture of methanol with chloroform in a 1:2 ratio combined with a wash step with water to remove non-lipid compounds (29). Bligh and Dyer (30) developed another very popular method based on chloroform/methanol/water mixture. Matyash *et al.* (2008) exchanged the toxic chloroform with methyl tert-butyl ether (MTBE) and proposed a solvent ratio of 5/1.5/1.25 (MTBE/MeOH/H_20, v/v/v) (31). This ratio increased the total volume of organic compound compared to the other methods. One advantage of MTBE is that the organic phase is on top, not on the bottom, as is the case with chloroform extraction. This simplifies sample handling and reduces the risk of contamination. Löfgren *et al.* (2016) published a 2-step extraction method, where in a first step samples are diluted in butanol/methanol (3/1) mixture followed by heptane/ethyl acetate (3/1, 1% acetic acid) into a 2-phase system. They demonstrated with snap frozen tissue their procedure and compared it with MTBE and Folch extraction methods. The results were similar, but the automation allowed the sample throughput to be increased to 96 samples per 4 hours (32). Sarafian *et al.*, (2014) used serum to compare 4 precipitation methods with MeOH, ACN, IPA, and IPA/ACN to 4 extraction methods with dichloromethane, chloroform, MTBE and hexane. They concluded that IPA precipitation had the best overall performance due to the simple and time-saving process. The lipid coverage and recovery were comparable to the extraction methods based on chloroform and MTBE (33). However, it is unclear whether the precipitation processes contain more non-lipid content than the extraction processes. This could have a negative effect on the robustness and can lead to increased contamination of the UPLC-MS device. There is also a 3-phase extraction protocol with hexane, methyl acetate, acetonitrile, and water, resulting in an upper phase where e.g. triacylglycerols (TG) and other neutral lipids are present; in a middle phase with more polar lipids e.g. glycerophospholipids as well as sphingolipids. These two phases

can be analyzed in separate runs or together, depending on the number of samples and the scientific question (34). Not only are the chemical properties of the solvents important for good extraction performance, but the pH range can also have a positive effect. Anionic lipids e.g. sphingosine-1-phophate (LPA), phosphatidic acids (PA), or lysophosphatidic acid (LPA) showed a better extraction efficiency with the addition of acid, since this neutralizes the anionic properties and the elution in organic solvent is higher. The disadvantage of acidic extraction processes is higher hydrolysis, e.g. lysophospholipids, consequently the extraction must be carefully controlled to avoid false positive results (35).

Lipid isolation with solid phase extraction

Solid phase extraction (SPE) is often used, especially in targeted analytical approaches. It benefits from the specific binding of physico-chemical properties and enables the detection of low-concentration compounds. It is the opposite of a broad lipidomic approach with as many classes as possible and is mainly used for special applications, e.g. the enrichment of gangliosides from the aqueous fraction of a lipid fluid extraction (36), or to increase selectivity by purifying and enriching certain classes of lipids and to simplify data processing in shotgun lipidomics (37). It can also be used to fractionate lipid classes prior to LC-MS analysis for separation of isobaric species and classes (38).

Sample derivatization

The reasons for derivatizing lipid samples are: i) to increase the ionization efficiency, e.g. derivatization of hydroxyl groups (sterols oxysterols) by oxidation to a keto group in a first step, followed by the introduction of a quaternary nitrogen, which greatly increases the ionization efficacy by electrospray (39). ii) to add selective compounds to be used in neutral loss scans and precursor ion scans, e.g. to methylate phosphate groups with diazomethane for

selective detection of bis(monoacylglycerol)phosphates (BMP) and phosphatidylglycerols (PG) with shotgun mass spectrometry (40). iii) to mask groups to protect and conserve the structure before analysis, and to label structure for quantification, e.g. The methylation of phosphate groups of phosphatidylinositol phosphates (PIP) is not meant to increase the selectivity as described above, but to improve the ion transfer by lowering interactions of the free phosphates with the surrounding surfaces and, in addition, the increase of the ESI efficiency in positive mode, as described above (41). iv) To introduce an isotopic label for differential quantitation e.g. Methylation of glycerophospholipids with diazomethyl (trimethyl) silane for methanolic acidification, whereby the hydrogen of the hydrochloric acid is exchanged for a deuterium, which leads to a 2 Da mass shift. This was demonstrated with several glycerophospholipids subclasses (PA, PI, PIP, PS, and PG) (42). v) Another widely used derivatization technique is multiplexing, which is used for quantification with a triple quadrupole mass spectrometer. It enables quantification by derivatization with multiple isotopic tags e.g. free fatty acid labeling (43).

Mass Spectrometry in Lipidomics

There are two main categories of MS-based lipidomics measurement methods. On the one hand there is shotgun lipidomics, and on the other hand there is liquid chromatography, where compounds are separated before analysis. In addition, there are several different types of mass spectrometer that allow different approaches e.g. low-resolution MS such as triple quadrupole or a combination with ion trap (QTrap), which is primarily used in the field of targeted approaches. However, there are also trends towards additional features in terms of selectivity such as ion mobility to add an extra separation step to the workflow, or different ionization types for in-depth structural elucidation as well as imaging methods to focus on histological questions. In the next subsections these methods are briefly described.

Mass spectrometry in combination with liquid chromatography

The most popular method in lipidomics is reverse-phase LC coupled with a mass spectrometer. Reverse phase columns can separate lipids based on non-polar parts, based primarily on the length and degree of unsaturation of the acyl/alkyl chain. The interaction increases with the length of the chains and decreases with the degree of unsaturation. These effects are shown in Figure 2 for a few cholesterol esters occurring in human blood plasma with the indication of the black arrow (acyl chain length) and the blue arrow (unsaturation degree)

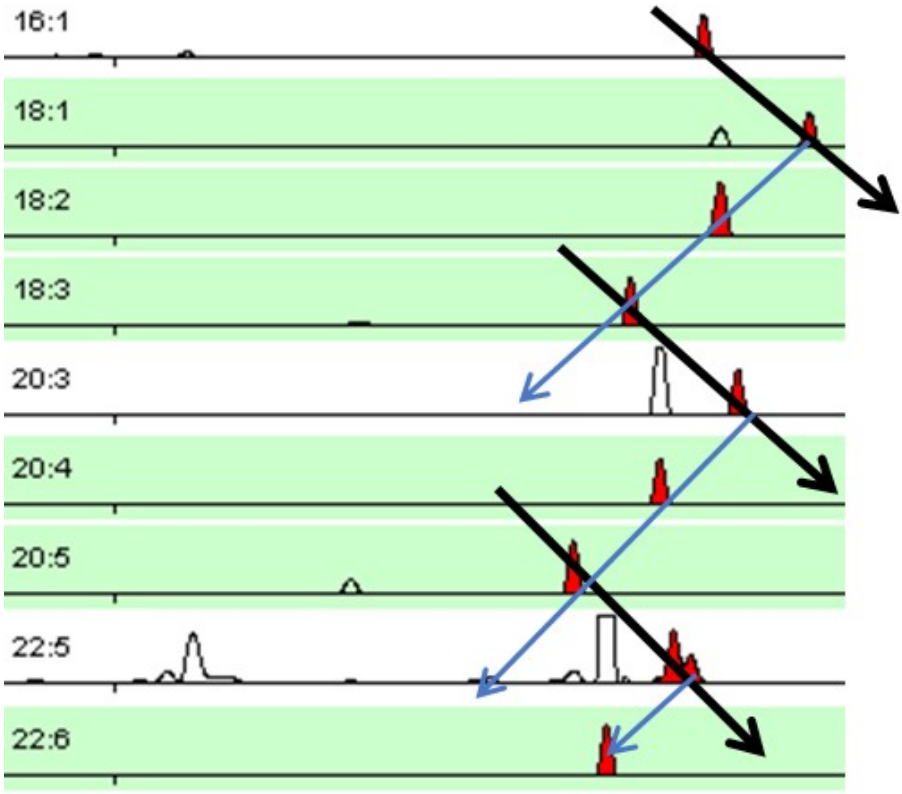

Figure 2 Separation of lipids based on their lipophilic moieties, e.g. chain length and degree of saturation as an example cholesterol esters (CE) with an C8 reverse phase column. Black arrows: Number of carbon atoms in the acyl chain; Blue arrows: Degree of saturation acyl chain; green: MS^2 data available

The reverse phase nano-LC variant is not that widely used in lipidomics. One of the reasons is that the robustness of the nano-LC can still be a challenge. However, reports showed a 3.4 fold increase in lipids detected compared to normal columns due to higher sensitivity (44), making nano-LC an interesting alternative to classic reversed-phase methods. In addition to reverse phase chromatography, the most frequently used method is liquid chromatography with hydrophilic interaction (HILIC) (36, 45, 46). It separates lipids by their polar head group instead of the backbone and the acyl/alky chains. That means all lipids from the same subclasses (e.g. PC, or PE) elute within a small retention time window, which can lead to an unresolved chromatographic peak with mixed lipid species. Therefore, the selectivity of HILIC methods depends more on MS than on chromatographic separation. Combined with high-resolution MS, which provides sufficient selectivity, the simultaneous elution of subclasses simplifies quantification as internal standards (IS) are ionized simultaneously with their targets, especially approaches that use one to a few IS for each subclass. This is a similar quantification approach to shotgun lipidomics (36, 47).

As noted above the acyl/alky chain dependent separation with reverse phase chromatography leads to wider RT windows respectively to complete separation of lipid species although not of molecular species. This can benefit the in-depth structural elucidations compared to HILIC (48, 49). However, in terms of quantification with one or a few internal standards, RT often varies widely in relation to the quantified target, which can lead to ion suppression and inaccurate quantification. Nowadays, several internal standards of non-naturally occurring, mostly odd chain lipids, or deuterium-labeled standards are used for quantification or normalization (50, 51). To complete the overview of the various LC methods in lipidomics, there are also normal-phase LC methods that are not as compatible with ESI ionization due to the non-polar eluent used. Nevertheless, they are required for special applications, for example in chiral chromatography in combination with chemical ionization at atmospheric pressure (APCI) for the detailed analysis of non-polar compounds such as TGs (36).

However, there are not only different methods of chromatographic separation available, but there is also a wide variety of MS instruments with a range of properties that are used in lipidomics. There are two categories of approaches: Targeted methods that focus on known

compounds are easier to apply because fragmentation patterns and retention time information are known, and the IS can be selected accordingly. Because of this information, low-resolution MS are widely spread e.g. triple quadrupole in multi reaction monitoring (MRM) mode (52, 53). The strength of tandem mass spectrometry lies in its high sensitivity, but it is usually used for one or a few lipid classes, since the mass transitions have to be applied manually with RT.

However, there are also targeted approaches with low-resolution MS with similar results, in which over 300 lipid species from 11 different lipid subclasses could be identified (54). These numbers are similar to the results of semi-targeted approaches with high-resolution MS. Targeted methods are not only used on low-resolution MS, alternatively, high-resolution methods can also be used with a parallel reaction monitoring (PRM) mode at a Q Exactive MS. Peng *et al.*, (2017) demonstrated a method with high-resolution MS with a targeted workflow for profiling sphingolipids (45, 55). Another targeted method are high-resolution approaches based on Q-TOF devices. Hajek *et al.*, (2017) used an HILIC column in combination with a Q-TOF to detect gangliosides in biological samples and found 145 gangliosides from 19 different subclasses, one of the highest numbers of gangliosides so far reported in biological samples (36).

Nowadays untargeted or approaches with generically generated long target-lists are mostly carried out in combination with high-resolution mass spectrometry. High resolution MS notably increases the selectivity due to mass resolution and mass accuracy. These features enable better structural elucidation of unknown compounds. There are two main differences in terms of acquisition mode: On the one hand data dependent acquisition (DDA) mode, on the other hand the data independent Acquisition (DIA). Several lipidomic approaches depending on DDA are published (38, 56-59), these approaches are based on a full-scan and a data dependent fragmentation scan. In order to decide which precursors to isolate and fragment, certain options can be chosen, e.g. scan of the top n precursors, a target-list of precursors, or both can be used as shown in Figure 3.

This also enables semi-targeted or targeted approaches in terms of precursor isolation and fragmentation but not for the full-scan which remains untargeted. Clearly, the advantage of non-targeted approaches is that unexpected and novel lipids can be discovered or re-analyzed at a later point in time. On the other hand, there must be some sort of reference material for the detection of a new compound, which can be a library or an in silico generated database. Otherwise, it is very unlikely that a new compound will be identified. MS^2 spectra are aiding identification as well as in-depth structural elucidation.

Since the time is a limiting factor in MS approaches with LC, MS^2 spectra cannot be generated from all precursors. In order to overcome this limitation within targeted or semi-targeted approaches, reversed phase separation can be used as described in Figure 2, by simply approximating between MS^2-identified lipids. Alternatively, there is also a DIA approach in which 100 percent MS^2 coverage can be achieved, since the fragmentation in DIA is independent to the precursor-ion. DIA is not as common in lipidomics compared to other omics fields. One of the reasons is that DIA approaches use wider m/z selection windows for fragmentation compared to the DDA approach, where selection windows are approximately 1.5 Da wide. This can be a problem with data deconvolution caused by lipid isomers and other similar structures (60). However, there are several studies that support a DIA approach to lipidomics. Yan *et al.* (2018) showed the differences in the lipid profile in an LC-SWATH-MS approach with a cohort of schizophrenia patients. They used a scan range from 100 to 1160 m/z with an m/z window of 40 Da combined with a reverse-phase LC. They could identify 17 lipid sub-classes with a total of 445 identified lipid species (61). Schlotterbeck *et al.,* (2019) used an RPLC-SWATH-MS method with an QTof-MS to study the lipidome in coronary artery disease in platelets (62).

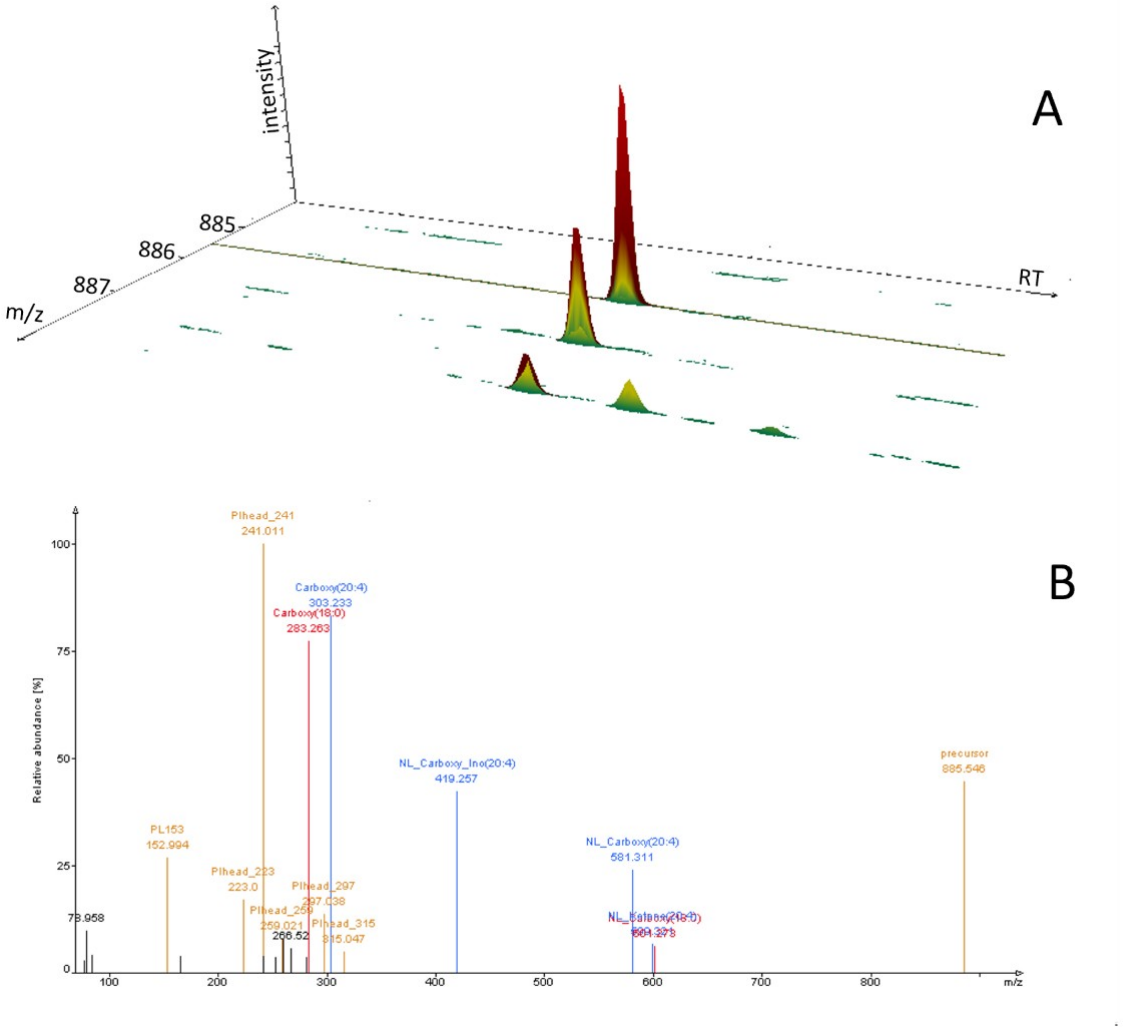

Figure 3: Extracted ion chromatogram (21 – 26 min) of PI 38:4 with natural isotopes (panel A) and linked centroid fragmented MS^2 data from serum QC-sample (panel B). Data are obtained with a Q Exactive MS (R: 70,000, m/z 200) with HCD fragmentation (R: 15,000, m/z 200). NL – Neutral loss; Ino – inositol.

Shotgun mass spectrometry in the field of lipidomics

Shotgun mass spectrometry or direct infusion electrospray ionization (ESI) was firstly introduced in 1994 (63), at that time triple quadrupole-based MS methods were state of the

art. The approach is based on selective ionization of certain lipid classes followed by intra-source separation, neutral loss scan, and precursor ion scan of fatty acid and head group fragments (64). Liebisch *et al.* (1999) adapted the direct injection to flow injection where a liquid chromatography is used without a separation column. This setup, in which the sample is injected into an isocratic flow of eluent, benefited from the injection automation of the HPLC. This approach has been applied in several methods to analyze different lipid classes (22, 65). The lack of gradient elution, which is a good way to reduce carry-over and to elute compounds with different physicochemical properties, is absent from this system to eliminate cross-contamination between samples. The nano ESI chip is an alternative to classic MS sources because every needle is used only once. This chip-based direct infusion from Advion Inc. (Ithaca, NY, USA) contains an array of up to 400 nano electrospray nozzles and is designed for single use, this means that each nozzle is used for one injection. Not only does it prevent carry over effects, but it also increases signal intensity and reduces the amount of sample volume (66, 67). One of the major benefits of shotgun lipidomics is the robust ionization environment which is particularly useful for quantitation methods. In HPLC lipidomics, several internal standards are used for each lipid subclass, especially for reversed-phase methods, since gradient elution changes the ionization environment massively. In shotgun lipidomics only one internal standard per lipid subclass is needed (64-66, 68). Shotgun lipidomics also faces challenges, a well-known one being ion suppression, especially when the samples are highly concentrated, and the target of interest is a low abundant compound in a complex matrix. Another problem can be the clogging of nano ESI which is widely used in the field of shotgun lipidomics. It is even a bigger problem with nano LC-MS methods that are less common. Low-resolution MS has some certain limitations without an LC dimension, the separation of PCs with odd-carbon numbered acyl chains cannot be discriminated from isobaric plasmalogens (69).

High-resolution mass spectrometry e.g. QTof (resolution up to 40.000), or Orbitrap technology are preferable to direct infusion lipidomics (70-72). Since high-resolution MS devices were available, methods were shifting to data dependent and data independent acquisition (DDA/DIA) combined with fast scanning instruments.

Gao *et al.* (2018) demonstrated a TripleTOF MS/MS^{ALL} method, which can provide MS/MS spectra for all masses with an isolation window of one Dalton in a range of 1000 Da (73). The benefit of this method is that MS/MS spectral coverage is 100 % over a broad mass range. In terms of quantitation MS/MS^{ALL} showed good results within the applied method for the mitochondrial cardiolipin quantitation. Of course, it can be difficult to link the precursor to the MS/MS fragment, which can lead to a loss of information regarding the identification of the lipid species. Another example of a similar approach is using a method based on the Orbitrap Fusion platform. Their method included 5 multiplexed MS analyses with two high-resolution (R = 45000 at m/z 200) scans at low m/z range of 350 – 600 and a higher m/z range of 550 – 1201, a MS^2 HCD fragmentation scan at a resolution of 30000 (m/z 200) and an MS^n scan with CID fragmentation analyzed within the Ion Trap (IT). They were able to identify 311 lipid species in the hippocampus and in the cerebellum of the mouse with 211 structural in-depth analyses (74). The desorption electrospray ionization (DESI) is another ionization method used in combination with direct infusion lipidomic mass spectrometry. It was shown that different types of adducts were produced when compared to ESI ionization, but the results were similar for lipids (75). DESI is also used in mass spectrometry imaging (MSI), which allows tissues to be ionized directly to create a lipidomic image of them (76). Complementary to DESI the coupling of matrix associated laser desorption (MALDI) with an LTQ-Orbitrap (R= 240000, m/z 400) was used for demonstrating a two-dimensional lipidomics image of a rat cerebellum at a lateral resolution of 40 µm (77).

Mass spectrometry combined with ion mobility

In recent years ion mobility spectrometry increased in popularity. Ion mobility is based on a physicochemical concept, where ions are immobilized or moved in an electrical field against a flow of an inert drift gas. This kind of separation is based on the size and shape of the molecule rather than on its chemical properties. Keating *et al.,* (2018) could demonstrate in a differential ion mobility spectrometry (DIMS) approach that isomeric lipids e.g. PC-O 36:4

and PE 38:4 can be separated (78). There is not only a direct separation advantage of an additional dimension, but also an introduced unit called the collision cross-section (CCS), which is unique for each molecule and comparable between different IMS techniques. There are efforts to build CCS databases, which are highly valuable in terms of compound identification (79-82). Ion mobility is not only used with Shotgun MS but can also be combined with LC. Hinz *et al.,* (2019) demonstrated the suitability of this technique for quantification and profiling of fatty acids and oxylipins with an LC-DTIM-MS approach. They reported that they were able to separate lipid conformers and dimers using IM (83). In general, two ways are used to obtain databases with CCS values. On the one hand, experimental CCS data were measured, on the other hand there are in silico predicted data based on the SMILES structure (80, 84).

Lipid annotation

To simplify the lipid annotation in terms of structural annotation level and simplify their names Liebisch *et al.* (2013) introduced commonly used shorthand annotation for lipids (69, 85), which is also used in this work. The different elucidation levels are shown in Figure 4 with the example of a PC 34:1. In literature often fully elucidated lipids are mentioned, which would mean for the example in Figure 4 that the *sn*-1, *sn*-2 position, isomerism type, double bond position, and headgroup is known. With lipidomic based mass spectrometry methods structures are usually determined to lipid species level (PC 34:1), where the head group, the sum of carbon atoms in the acyl chain respectively the number of double bonds, is known. In many cases it is also possible to annotate to the lipid composition level (PC 16:0_18:1), where the position (*sn*-1, *sn*-2) of the acyl chains is not known, but the acyl chains themselves with unknown position. For this purpose, a specific acyl chain fragment is searched in the MS^2 fragmentation spectrum. In the case of the lipid subclass PC, this can be performed in negative mode, where fragments of the acyl chain can be seen in the MS^2 spectrum (m/z 255.232, FA16:0; m/z 281.247, FA18:1). Up to composition level the annotation can be done

with standard high-resolution MS with fragmentation spectra, respectively also with triple quadrupole low-resolution mass spectrometer in a targeted mode, if retention time is known for ether-linked and other resolution dependent isobaric lipids.

For the double bond position or the detection of the *sn*-positions, fragmentation and high-resolution mass spectrometry alone are not sufficient. Therefore, different methods are needed such as ultra-violet induced photodissociation (UVPD) or ozone-induced dissociation (OzID). In cases of phospholipids and sphingolipids the detection of double bond position can be achieved with an Orbitrap instrument with a 192 nm UV laser, which produces cleaved fragments depending on the methylene bond (86, 87). OzID is based on the reaction of ozone with double bonds and these fragments can be detected (88). Zhang *et al.*, (2019) showed an LC-MS/MS workflow to identify and quantify PCs including *sn*-positioning with the potential of double bond position detection. Therefore, they used the photochemical paterno-büchi reaction to produce specific fragmentation in combination with a bicarbonate adduct on the choline headgroup (89).

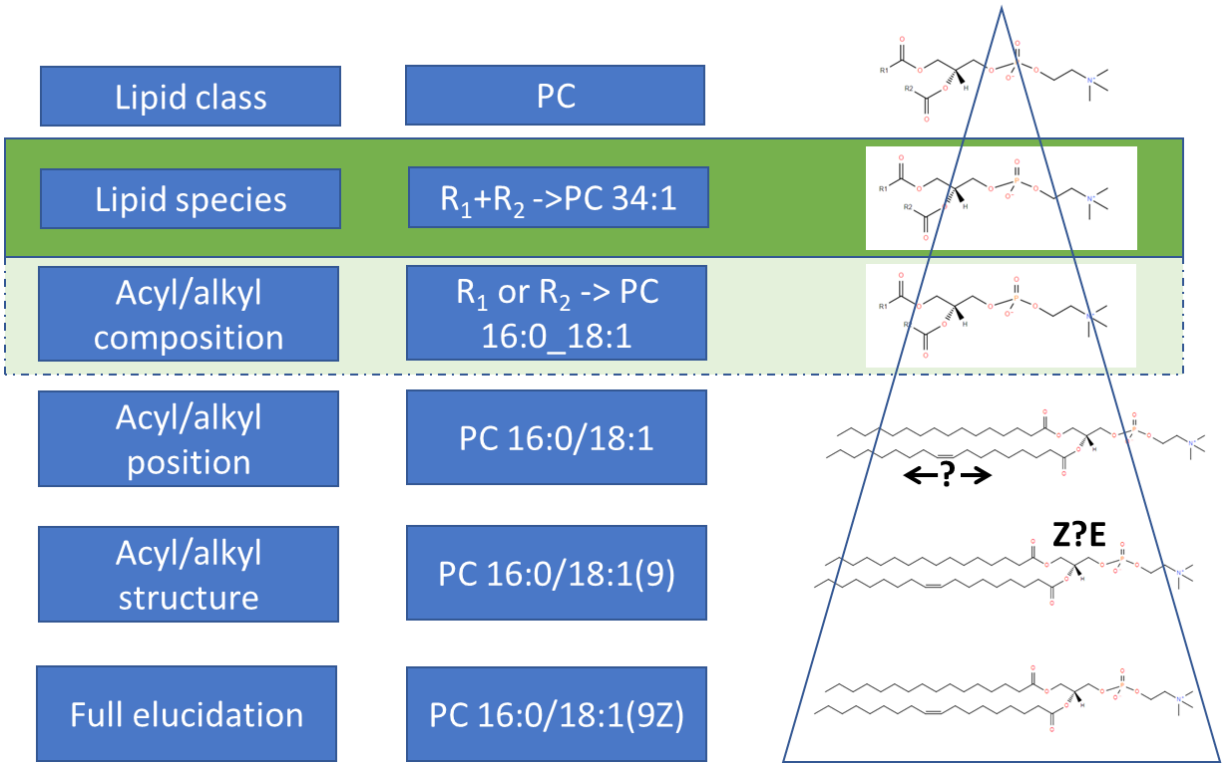

Figure 4 Lipid annotation levels shown as pyramid with an example (69, 85).

Data processing in lipidomics

Data processing in lipidomics respectively in mass spectrometry is an important point especially since the trend towards high-resolution mass spectrometry with more in-depth structural elucidation and machine learning approaches is increasing. The complexity of processing and analyzing the amount of data has also increased; this requires control and validation steps in order to obtain reliable results. One of the reasons is also the higher diversity of MS devices (e.g. QqQ, QToF, Orbitrap) and its vendor specific formats. As we used in this work an LC-MS based approach, we will just briefly discuss lipidome-based shotgun data processing tools.

Shotgun based data processing tools for lipidomics

The main difference between the shotgun lipidomics data processing compared to the LC-MS method is that all compounds are ionized at the same time and the selectivity depends only on the MS device. The shotgun MS' short acquisition times allow multiple experiments to be performed on a sample using different strategies e.g. ionization with different physiochemical conditions to improve coverage, or different extraction procedures (64, 90, 91).

Various specialized software tools are used to aggregate and process the data collected from various experiments. Yang *et al.*, (2009) showed an automated multidimensional mass spectrometry-based shotgun lipidomics approach, which is based on a building blocks concept. It is similar to a database with different blocks filled with information e.g. total number of carbon atoms, double bonds, masses, and structure parts like backbone head group and so on. In combination these blocks represent the whole lipid, and in best case also the fragment data obtained by MS^2 (92). This combinatorial approach is similar to the lipid structure and therefore the information is saved in the different "blocks", which can also be generated in silico to a large extent. Another highly adaptable software, the LipidXplorer, is based on query language and can be used for high-resolution, low-resolution approaches, as well as precursor scan, neutral loss scan, or top-down and bottom-up approaches (93-96).

Other frequently used tools are the vendor specific software LipidView/LipidProfiler (Sciex Applied Biosystems, Framingham, MA, USA), or the analysis of lipid experiments (ALEX), a tool with a graphical user interface for processing high-resolution data from multiplex shotgun experiments and with a powerful integrated database with reference information on 85 lipid subclasses representing 20,000 lipid species (97).

Data processing tools for LC-MS based lipidomics approaches

Compared to shotgun mass spectrometry, LC-MS-based approaches with their additional dimension of temporal separation show less simultaneous ionization, which is easier in terms of identification because of the increased selectivity, but not in terms of quantification. There are mainly two approaches (as described above), DDA and DIA methods, used in untargeted lipidomics. DDA workflows are more straightforward since the linking of precursor mass to fragmentation mass is depending on RT and is within 1 to 1.5 Da windows. However, the lack of coverage of the precursor ions with fragmentation spectra, limits the in-depth structural analysis. As mentioned earlier, there are ways to bypass the MS^2 identification with RT shifts between known lipid species. Although the detailed structural information is then limited to the annotation level of the lipid species. Molecular species can only be obtained with information about the corresponding neutral loss of acyl / alkenyl chains, unless there is a lipid subclass with only one chain e.g. LPC, or CE. Benton *et al.*, (2015) showed in an experiment with 40 metabolites an 85 % MS^2 coverage (98). In samples with a complex matrix, coverage of 50 to 60% is more realistic due to the co-eluting compounds and matrix effects. DIA approaches have a 100% MS^2 coverage, which is more difficult with the precursor linkage. There are different strategies, the classic approach is the all-ion fragmentation, which is vendor-dependent called AIF, MS^{All}, or MS^{E}. Since MS^{All} scans are the most difficult to associate with precursors, SWATH methods are more commonly used when additional isolation windows, such as 20-100 Da prior ion fragmentation are used. Ions are separated in a serial manner, which simplifies the data linking (99). When analyzing serum samples, both approaches produce several thousand features with additional MS^2 information. Various software tools are available to process such data (shown in Figure 6): there are all in one software tools (I), or toolboxes which can be used for specific parts (II, III, IV) of the whole workflow. In Figure 5, a data processing workflow with a few common analysis tools as well as data bases for annotation is summarized.

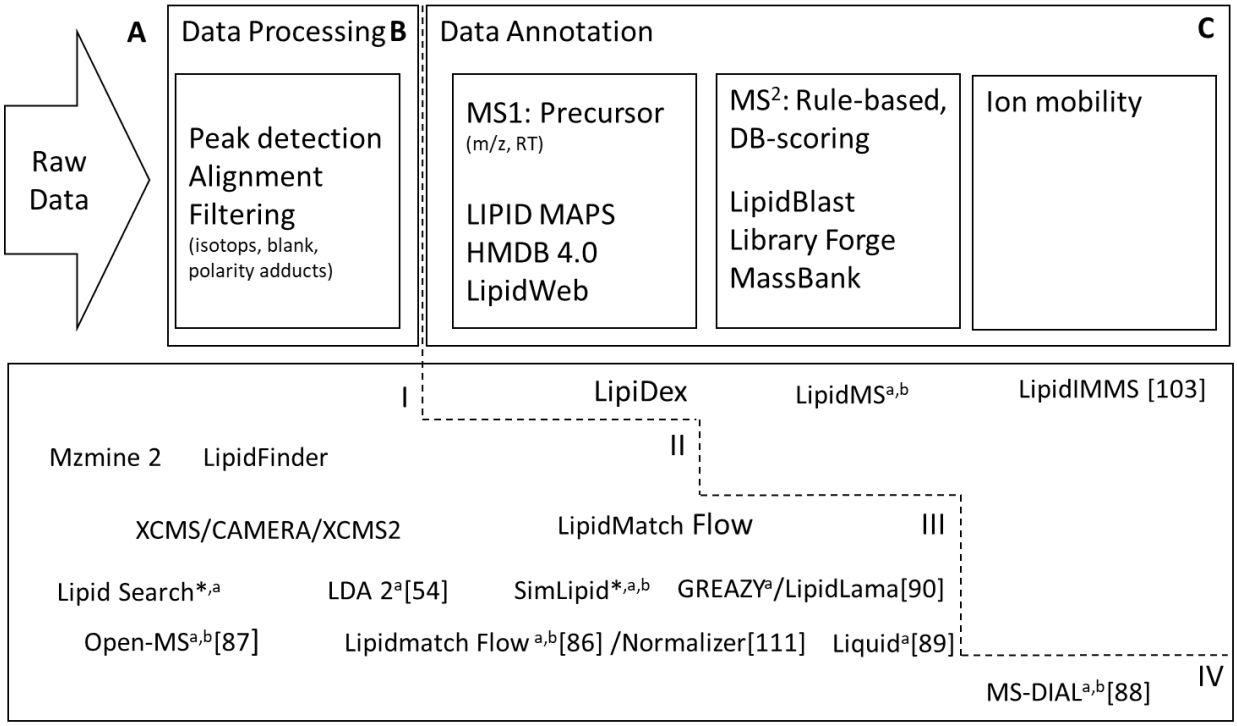

Figure 5 An Overview of different steps of data processing with available software tools used in the field of lipidomics. Starting with raw data processing (A) and peak detection (B) with software tools (I-IV), and data annotation based on MS^1, MS^2, or ion mobility (C), with software tools (II, III, or IV) (modified version of Fig.4 published under CC BY 4 (100))

Even if there are several tools available, workflows are similar. In a first step, vendor specific files are converted to an open format, unless using vendor specific data processing software. Most tools therefore are using msconvert from proteowizard (101, 102), or Reifyces abf converter (https://www.reifycs.com/AbfConverter). Sometimes they are integrated in other software tools but can also be used as standalone software package. In the next step features are generated with a peak picking algorithm from full-scan data. Features are signals which are recognized depending on algorithm but are not automatically a unique lipid structure. Regarding the number of expected lipid species, Tsugawa *et al.*, (2020) reported over 961 individual lipids at the molecular species level in SRM 1950 human plasma with 8 different sample extraction-MS approaches. The maximum for a single MS approach was reported with 495 lipid species, the minimum with 118 and an average of 318, the data were processed with

MS-Dial 4.0 (103). There are even higher numbers reported elsewhere, although this demonstrates that we can expect a few hundred lipid species out of several thousand features. The unknown and mainly undesired features can be noise, adducts respectively lipid isotopes, or artefacts. There are software tools using different strategies to reduce those unwanted features, for example blank samples can be utilized as a blueprint for noise reduction and environment-based signals, isotope correction can identify the naturally occurring isotopes, or to merge different adducts of the same molecule.

Typical software tools which are used for peak picking, and data filtering as well as data annotation based on precursor mass are XCMS, which is a widely spread tool in the field of metabolomics but also in lipidomics. XCMS is using the centWave algorithm for peak picking (104) and OBI-warp algorithm for RT alignment (105). The 3-D algorithm of LDA is depending on m/z signal, retention time, and signal intensity, as it is based on a semi-targeted approach, it also needs a target-list for lipid annotation (106). Semi-targeted means in this case, that analyzed data is untargeted, but the software uses a list to search for lipid annotation. Theoretically, there are no limits to the list, it could contain the 45,664 curated and computationally generated entries of LIPID MAPS database. There are also several filtering options e.g. isotope filtering to identify and remove corresponding M + 2 isotopes from the same species with one double bond less (106). The GUI based MZmine 2 (107) software package offers options of different algorithms based on MS-data quality and is used for peak picking to generate feature tables for further processing with more specialized software tools e.g. LipidMatch published workflow (108).

In the next step, after peak picking, filtering and RT alignment, the generated feature tables are compared with target lists or the database e.g. LipidHome (109) (LipidWeb), LIPID MAPS (110) or Human Metabolome Database (HMDB) (111), which are sources of experimentally or in-silico generated lipid species. It should be noted that up to MS 1 annotation step the difference between metabolomics and lipidomics annotation is very similar, even LDA can be used for metabolomics annotation in combination with untargeted software (112). In data dependent acquisition mode fragmentation spectra are detected and aligned to the feature table on the one hand to validate and identify lipid species and on the

other hand for in-depth lipid annotation, or for novel lipid identification with predictive databases. Software tools are handling fragmentation data differently. There are “scoring” based tools, which are often based on dot product or reverse-dot product. Therefore, a fragmentation database is used for comparison of the measured respectively the theoretical MS^2 spectra to the obtained spectra e.g. XCMS with the use of the reference database from METLIN (113, 114), Open-MS (115), MS-Dial (103), LipidDex (116, 117), or LipidBlast(118). The second big set of methods are rule-based decision methods, in which MS^2 fragments are assigned using rules based on acyl chains, head groups, neutral losses and their intensities or any other fragments. LipidMatch (108), LipidMS (119), LDA 2 (120), and LipidIMMS (82) are using this rule-based decision approach. One advantage is the flexibility of rule-based approaches, as these can be easily and robustly adapted with in-house experiments or literature values, with the disadvantage of MS device-specific fragmentation differences and dependencies on collision energy levels. Database scoring needs more computational power to compare large databases of reference spectra to the obtained spectra. Another problem is that DDA MS^2 spectra are mixed fragmentation spectra, because of the 1 to 1.5 DA ion selection window used to select precursor. This can lead to incorrect annotation if the scoring cut-off is too weak compared to custom tailored rule-based methods. At the end, both methods should be checked for plausibility to ensure that the annotation can be easily explained if results are not curated manually. Lipid annotation is a crucial part; therefore, the different annotation levels are discussed in detail in chapter Lipid annotation.

There are also several special tools for de novo identification of unknown features with MS^2 information. In silico fragmenters are software tools that follow a computational approach to find possible molecular structures on MS^1 and MS^2 information. The MetFrag 2.2 (121) tool uses a combinatorial approach based on database search and fragment prediction. Reference data are from the Kyoto Encyclopedia of Genes and Genomes (122), PubChem (123), or ChemSpider, and additionally offline databases are supported. There are also some options for additional filter criteria to increase the validity, such as retention time information, limitation of chemical elements or entire substructures to narrow search fields. CSI:FingerID, is a vector machine based method to predict precursor spectra with a focus on functional fragments and

groups (124). Competitive Fragmentation Modeling-ID 3.0 (CFM-ID) has implemented a rule-based fragmentation approach for lipids, based on 344 rules for 21 lipid subclasses, an experimental scoring database, and a chemical classification algorithm to help to find unknown compounds (125).

Approaches of batch drift correction and normalization strategies

Lipidomic studies with large cohorts, as analyzed in this work, require a longer measurement period, e.g. 500 samples require a detection time of 25 days with a one-hour method. During this long period of time, several problems can occur. The acquisition might be interrupted and even if there are no interruptions, systematic time-dependent errors are existing. Batch-dependent effects such as sensitivity drifts, changes in pH systems, changes in eluents concentration due to different eluent batch production, temperature, and vacuum changes during analysis are reasons for signal drifts. These errors are in addition to preanalytical errors e.g. changes in sample preparation, and if ignored are leading to less or false statistical significance between phenotype-associated differences (126). To control or correct batch drifts several normalization strategies are available (127). One of the simplest ways is to analyze a pooled QC in between the acquisition list on a regular basis for example between every 10^{th} sample. Another method is the use of internal standards to normalize or even quantify the lipids in each sample. The strength of using internal standards is that the signal in each sample can be corrected more precisely and even used for quantification, which helps to better compare data with literature values. The disadvantage is, that standards can be very expensive when analyzing many samples and lipid subclasses. The availability of reference material can also be a limiting factor.

The QC-based normalization has the advantage that all lipid species in the samples are also in the pooled QC and therefore each lipid species between the measured QC can be corrected individually. There are several software tools available with different algorithms and functions e.g. the LOESS regression based Batch Normalizer (128), the Systematic Error

Removal using Random Forest (SERRF) (129) which was tested with a lipid data set and compared with other algorithms, or the StatTarget, a vector machine-based normalization strategy (130). For normalization of data based on internal standards there are a few special tools such as Normalization method for metabolomics data using Optimal selection of Multiple Internal Standards NOMIS (131), Best-Matched internal standard B-Mis (132) or Cross-Contribution compensating Multiple Standard normalization (CCMS) (133). For the internal standard correction, however, not only special software tools can be used, but also Lipid Data Analyzer (134) and LipidMatch Normalizer (LMN) (135), which have integrated internal standard normalizer functions.

Overview of different Statistical tools

Various statistical tests and methods are available to analyze the immense amount of data from mass spectrometry experiments. Here we summarize a selection of these. The method of choice depends on the study design e.g. targeted, or untargeted approach, number of samples, research question, data quality, or data distribution. The most common methods are univariate tests. If the data is evenly distributed, a parametric test such as multi-group ANOVA can be used in combination with a Tukey HSD post hoc test. For nonparametric tests without normal distribution solutions are Kruskal-Wallis for more than 2 groups or Mann-Whitney U test for two groups.

Nowadays, multivariate tests are also commonly used, because they can enable discrimination between groups with small differences or if large numbers of lipids or metabolites are compared (136). When multiple covariates are involved in animal models or clinical studies, multivariate analysis is frequently used to find compounds associated with a particular disease status, with or without treatment, or between healthy and sick groups. Due to the dimensional reduction, multivariate methods can simplify the interpretation of variances in groups and the correlation of variables between groups (137). There are unsupervised and supervised methods. Unsupervised methods do not require additional information about phenotypes or

treatments. They are based only on the annotated compounds and their intensity. The best-known representatives of unsupervised methods are principal component analysis (PCA). The PCA algorithm correlates the data matrix in a principal compound into a new variable. The objective is that the first few principal compounds explain the major part of the proportion of variance. To ascertain the explained variance, the number of important principal compounds must be determined or, alternatively, a scree plot can be used to visualize them (138). Other unsupervised methods are clustering methods, such as k-means clustering, hierarchical clustering, or self-organizing map (138), which are less prominent in lipidomics or metabolomics. The supervised methods aim to understand and determine defined differences such as response to treatment or differences in phenotype, which can help to identify relevant compounds. Typical methods are (O)PLS ((Orthogonal) partial least squares) regression, which is based on response and prediction variables of a covariance, or as extension with orthogonal projection to reduce uncorrelated variables (139). A frequently used method in the field of metabolomics is a combination of discrimination analyses (OPLS-DA, or PLS-DA) to classify samples (140). There are many more classification methods e.g. support vector machine based methods (SVM), soft-independent modeling of class analogies (SIMCA), or K nearest neighbor (KNN) classification (141).

There are different software tools that can be used to analyze data using these algorithms. The most comprehensive free software tool (GNU-license) is MetaboAnalyst 5.0 (142-144), which contains workflows with data normalization for the analysis of the metabolic pathway, enrichment analysis, as well as a biomarker selection, integrative pathway analysis, or time series, and power analysis among other features. Another advantage of MetaboAnalyst is that the user has full control over every step of the analysis due to the R based code, which can be displayed through analysis. If simpler, more specific software is preferred, several packages are available in R to analyze data using multivariate methods e.g. LipidR, which takes into account the Lipid shorthand nomenclature, OPLS-DA, PLS-DA method, and other multivariate options, as well as enrichment analysis (145). The Metabolomics Univariate and Multivariate Analysis (Muma) package is another option that works directly with only one input file, where compounds are listed in the columns and samples in rows with a phenotype

or treatment information column. There are several more R based tools e.g. Bioconductor, and several vendor-specific options e.g. SIMCA (Sartorius, NI, Germany), that are easy to use and can deal with multivariate and univariate statistics.

2 Material and Methods

Chemicals and reference substances

The following chemical and reference substances were used from Sigma-Aldrich (St. Louis, MO, USA): tert-Butyl methyl ether, (MTBE, 650560-1L), Methanol Chromasolv, (MeOH, 34885), Ammonium formate (NH4COOH, 55674), from Honeywell (Charlotte, NC, USA): Acetonitrile chromasolv, (ACN, 34851-2,5L), Chloroform, (CHCl3, 1024441000), from Avanti (Alabaster,AL ,USA): N-heptadecanoyl-D-erythro-sphingosine (Cer 35:1, 860517P), 1,2-dipalmitoyl-sn-glycerol (DG 32:0, 111008), 1,2-didodecanoyl-sn-glycero-3-phosphocholine (PC 24:0, 850335P), 1,2-didodecanoyl-sn-glycero-3-phosphoethanolamine (PE 24:0, 850702P), 1-oleoyl-2-hydroxy-sn-glycero-3-phosphoethanolamine (LPE 18:1, 846725), 1-stearoyl-2-oleoyl-sn-glycero-3-phosphocholine (PC 36:1, 850467C), 1-stearoyl-2-linoleoyl-sn-glycero-3-phospho-L-serine (PS 26:2, 840063P), 1,2,3-trihexadecanoyl-sn-glycerol (TG 48:0, 33-1600), 1,3-stearin-2-elaidin (TG 54:1, 34-1804), 1-oleoyl-2-hydroxy-sn-glycero-3-phosphocholine (LPC 18:1, 845875), 1,2-dilauroyl-sn-glycero-3-phosphate (PA 24:0, 840635), 1-stearoyl-2-arachidonoyl-sn-glycero-3-phosphoethanolamine (PE 38:4, 850804), 1,2-dilauroyl-sn-glycero-3-phospho-(1'-rac-glycerol) (PG 24:0, 840435), 1-stearoyl-2-oleoyl-sn-glycero-3-phospho-(1'-rac-glycerol) (PG 34:1, 840503), 1-stearoyl-2-linoleoyl-sn-glycero-3-phospho-L-serine (PS 36:2, 840063), and from Larodan (Solna, AB, SWE): 1,2,3-trihexadecanoyl-sn-glycerol (TG 48:0, 33-1600), 1,3-stearin-2-elaidin (TG 54:1, 34-1804).

Sample storage and extraction

The sample extraction is based on the MTBE extraction method (31) and adapted to our workflow. The blood serum was stored at -80°C and thawed on ice shortly before extraction. 50 µl of the serum were transferred to a 12 ml Pyrex culture tube (DWK Life Sciences, Wertheim, BW, DE) for extraction, and 5 µl to a separate 12 ml Pyrex for the QC pool, where 5 µl of serum were collected from each sample. 10 µl (0.5 mM) of PE 24:0 were added to the 50 µl serum as internal standard for extraction control. 1.5 ml MeOH and 5 ml MTBE were added to the extraction mixture, shortly mixed, and placed in the ultrasonic bath (USB) for 10 min followed by 10 min overhead shaker (OHS). 1.25 ml deionized water (Milli-Q Elix, Merck KGaA, HE, Germany) were added and mixed on the OHS for an additional 10 min. When the organic upper phase was transferred, the samples in the Pyrex were centrifuged for 10 minutes with 5,840 g (Heraeus Multifuge 3S-R, Thermo Fisher Scientific, Waltham, MA, USA) at room temperature. The aquatic phase was extracted a second time with 2 ml of the organic phase of the aqueous saturated solution with MTBE/MeOH/H_2O (v/v/v; 10/3/2.5). The mixture was mixed for 10 min in the OHS for extraction and centrifuged again for 10 min with the same setting as in the first step. The upper phase was transferred to the organic phase from the first extraction step and evaporated in a speed vacuum concentrator (Savant SC250, RVT4104, Thermo Fisher Scientific, Waltham, MA, USA) at room temperature overnight. The aquatic phase was discarded. The dry extracts were re-eluted in 500 µl $CHCl_3$/MeOH (v/v; 1/1), transferred to a 1 ml HPLC vial and stored at -80°C. After all samples of a cohort had been extracted, the solvent was changed before analysis. Therefore, samples were shortly put into the USB and 50 µl of the sample were transferred into a 300 ml glass vial, 10 µl (50 µM) of PC 24:0 standard was added. Samples were evaporated in the speed vacuum concentrator, placed in 50 µl IPA/$CHCl_3$/MeOH (v/v/v; 90/5/5) and eluted again. The resuspended samples were placed in the USB for a few seconds, vortexed properly and briefly stored in the freezer at -20 °C or directly put in the UHPLC autosampler before analysis.

Liquid chromatographic separation

To separate the serum lipids, a gradient elution on a Waters (Waters, Milford, MA, USA) BEH C8 (100 x 1 mm, 1.7 µm) column was used, thermostated at 50 °C in a Vanquish UHPLC system (Thermo Fisher Scientific, Waltham, MA, USA). Deionized water with 1 vol % of 1 M aqueous ammonium formate and 0.1 vol% formic acid as additives were used as eluent A, and acetonitrile/isopropanol (v/v, 5/2) as eluent B. Gradient elution was used as published from Triebl *et al.,* (2017), started with 50 % eluent B increasing to 100 % continuously over 40 minutes, and it was held for 10 minutes before re-equilibrating at starting condition of 50 % eluent B. A constant solvent flow of 150 µl min^{-1} was used. Autosampler temperature was set at 8 °C and 2 µl sample volume was injected. Autosampler wash solution was IPA and rear piston solvent was 10 vol% MeOH in water.

Mass spectrometry method

This method is an adaptation to the Q Exactive Focus mass spectrometer (Thermo Fisher Scientific, Waltham, MA, USA) and based on the previous published method of Triebl *et al.* (2017). The MS was used in full scan mode (resolution 70,000, m/z 200, profile data) with data dependent acquisition for MS^2 data (resolution 17,500, m/z 200, centroid data). A HESI II Ion source was used and the source parameters were chosen as follows: Source Voltage 4500 (+) respectively 3800 (-), Capillary Temperature 275 (+) resp. 300 (-), Sheath gas 25 (+) resp. 30 (-), Aux Gas 8 (+) resp. 10 (-), Probe Heater Temp. 300 (+) resp. 325 (-), and S-Lens radio frequency level of 55. Scan range in positive mode was 160 to 1150 m/z and in negative mode 300 to 1900 m/z. To obtain the fragment ion spectra, discovery mode in combination with a target list was used. Since the Focus variant of the Q Exactive family is limited to fragment only the top 3 precursor masses, an inclusion list was used to obtain additional MS^2 spectra (Supplement Table 3) and to increase MS^2 spectra of simultaneously eluted compounds a 10 s dynamic exclusion time was set.

Data processing

The data processing was split into two parts (shown in Figure 6), as for our in-house lipidomics approach we used the Lipid Data Analyzer 2.6, a raw data processing and target list-based annotation software with a rule-based decision to consider fragmentation ions for accurate annotation (105, 119). The drawback of LDA is the time-consuming analysis of large data sets as processed in this study. The benefits of graphically assisted manual curation of lipids do not work properly with our available IT system in combination with the large number of samples as analyzed in this study. Another available software tool we use in-house is the Tracefinder 4.1 (Thermo Fisher Scientific, Waltham, MA, USA) a fast targeted list-based data processing tool for quantification. Therefore, we decided to use a combined approach of these two software tools. The LDA was used to process the measured QC samples with consideration of MS^2 data, or/and retention time shifts based on the total saturation level of acyl chains, the total number of C-atoms of acyl chains, and the isotopic distribution filtering to remove false positive isotopic ions. With this approach we can benefit of the superior lipid annotation and filtering properties of LDA within a manageable number of samples and time. These results were converted into a target list with m/z value, and retention time information to process the analyzed cohort samples with Tracefinder 4.1.

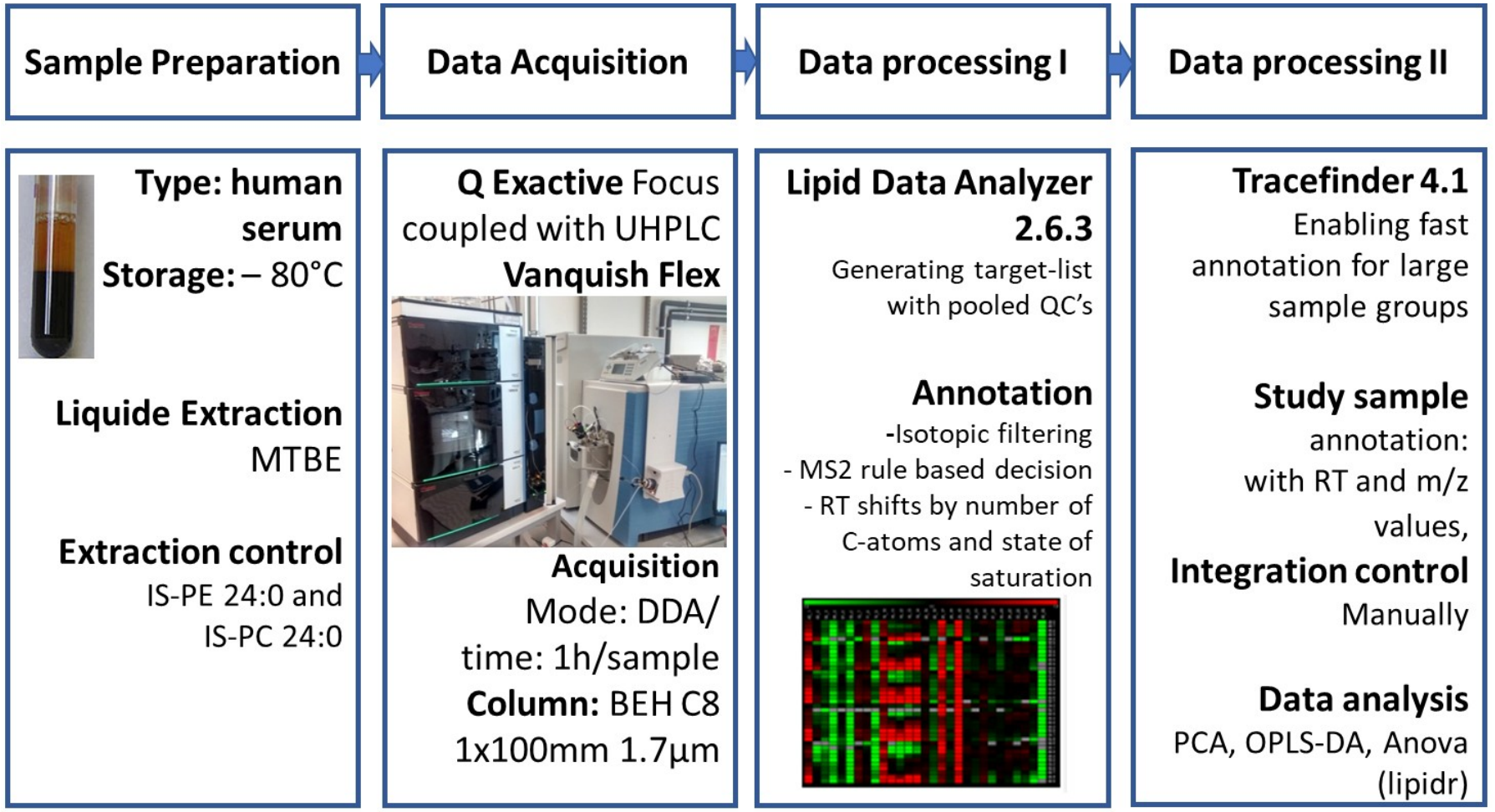

Figure 6 Lipidomics workflow; from sample to data analysis. An overview of the developed workflow in this thesis

LDA processing settings

To process the QC samples, we used the version 2.6.3_9 of LDA with the MS settings file OrbiTrap_exactive as shown in supplement (Supplement Table 2).

Data analysis and data visualization

Statistic data analysis as well as data visualization were achieved with R 4.0.4 respectively R studio 1.4.1103. Figures were mainly generated with ggplot2 package (145), multivariate analysis with the lipidR package (144), and univariate statistics with ggpubr package. To handle data dplyr was used (146) among others. Additionally, to produce ROC analysis we used carat package in combination with Mlevel package.

Method adaptation and evaluation

Collision energy adaption

To adapt our in-house lipidomics method (148) originally developed on the Orbitrap Velos Pro to the Q Exactive Focus mass spectrometer (Thermo Fisher Scientific, Waltham, MA, USA) we used a mix of lipid standards (Cer 15:1, DG 32:0, LPE 18:1, PC 24:0, PC 36:1, PS 36:2, TG 48:0, TG 54:1) with a concentration of 10 µM and injected 2 µl of the mix with different NCE settings (10, 12, 15, 17, 20 and 25) in positive mode. In negative mode the experiment was repeated with NCE of 12, 15, 20, and 25. A different purchased standards set was used with LPC 18:1, LPE 18:1, PA 24:0, PC 36:1, PE 38:4, PG 24:0, PG 34:1, PS 34:1, and PS 36:2 in a concentration of 10 µM.

Evaluation of linear behavior of the detected lipids

Because of the high numbers of detected lipids in this semi-targeted approach it is not possible to validate the method in a classical way by determination of the concentration, determination of linear ranges, and limits of detection as LLOD or LLOQ (lower limit of detection/quantification). Although we are mainly interested in the up and down regulation of lipids between groups with different health status, we have only proven that the set of lipids we are able to detect are detectable in a certain range of higher and lower concentration. Therefore, we extracted different amounts of pooled QC samples (5, 10, 20, 30 40, 50, 75, 100, and 150 µl) to simulate different lipid concentrations. The extraction procedure is mentioned above (section Sample storage and extraction). In our standard approach we extracted 50 µl serum, and thus we tested a concentration range between 10 and 300 % of our targeted extraction concentration.

Cohorts

We analyzed 3 different cohorts respectively subsets of them. The Alberta's Tomorrow project form Canada includes 443 participates with 207 in the control group, 120 with cardiovascular diseases (CVD), 36 with diabetes, 39 healthy, 28 with inflammatory bowel diseases (IBD) and 13 with rheumatoid arthritis (RA), the FoCus cohort from Kiel includes 905 participants with 351 patients in the control group, 218 with CVD conditions, 72 with inflammatory diseases, 211 with metabolic diseases, and 52 with manifested or previous oncological diseases. For the PopGen cohort there is currently no metadata available and therefore PopGen will not be included in the health status comparison in the results chapter. The FoCus and the Tomorrow cohort were selected to have overlaps in health status to validate the results. There is only limited metadata information available, therefore we only included the known data in the statistical analysis.

The 38 participants (two dropouts) of the intervention study are between 25 and 70 years old and obese with a BMI between 40.4 and 56.2. 17 of them had hypertension, 7 with diabetes

and hypertension. 9 of them are male and the rest female. All participants had a low-calorie diet for the first 6 weeks period, followed by a stabilization phase with normal food for another 6 weeks. Samples were taken at the beginning, after the first 6 weeks and at the end.

3 Results

3.1 Method optimization

3.1.1 In-house lipidomic method adaption to the Q Exactive™ Focus mass spectrometer

Our in-house lipidomic method was optimized on an Orbitrap Velos Pro (Thermo Fisher Scientific, Waltham, MA, USA), a hybrid mass spectrometer with an Orbitrap, a linear ion trap analyzer, and a quadrupole filter. Data dependent acquisition with the Orbitrap Velos Pro is based on parallel MS^2 and MS^1 ion analyzing. For generation and detection of MS^2 spectra, the ions are fragmented with collision-induced dissociation (CID) at 50 eV and analyzed in the ion trap as a low-resolution spectrum. The MS^1 full scan spectra is analyzed in the second analyzer the high-resolution Orbitrap (100,000, m/z 400).

The Q Exactive (Thermo Fisher Scientific, Waltham, MA, USA), is missing the ion trap and both ions are analyzed serial in the Orbitrap mass analyzer, in full scan mode with a maximum resolution of 70,000 at m/z 200. The MS^2 spectra are fragmented with higher energy collision dissociation (HCD) and analyzed with the lowest resolution option of 17,500 at m/z 200. Due to the difference that the ions in the C-trap are fragmented with HCD and not in the ion trap with low energy collision-induced dissociation (CID), the different fragmentation energies of the method had to be reevaluated. Therefore, a set of purchased standards had been used with different collision energies to achieve similar fragmentation spectra, which is important for data annotation with LDA. Since the annotation decisions with the LDA are rule-based, the fragments should be coherent within a certain framework, these

can contain both intensities and ratios. If the fragmentation profile is too different between certain spectra, the fragmentation rules can also be adjusted as a second option. Figure 7 shows the fragmentation patterns of different lipid standards in dependency of normalized collision energy (10, 12, 15, 17, 20, and 25 NCE) in positive mode. As expected, as the energy increases the fragment ions are increased as well and the parent ions are decreased.

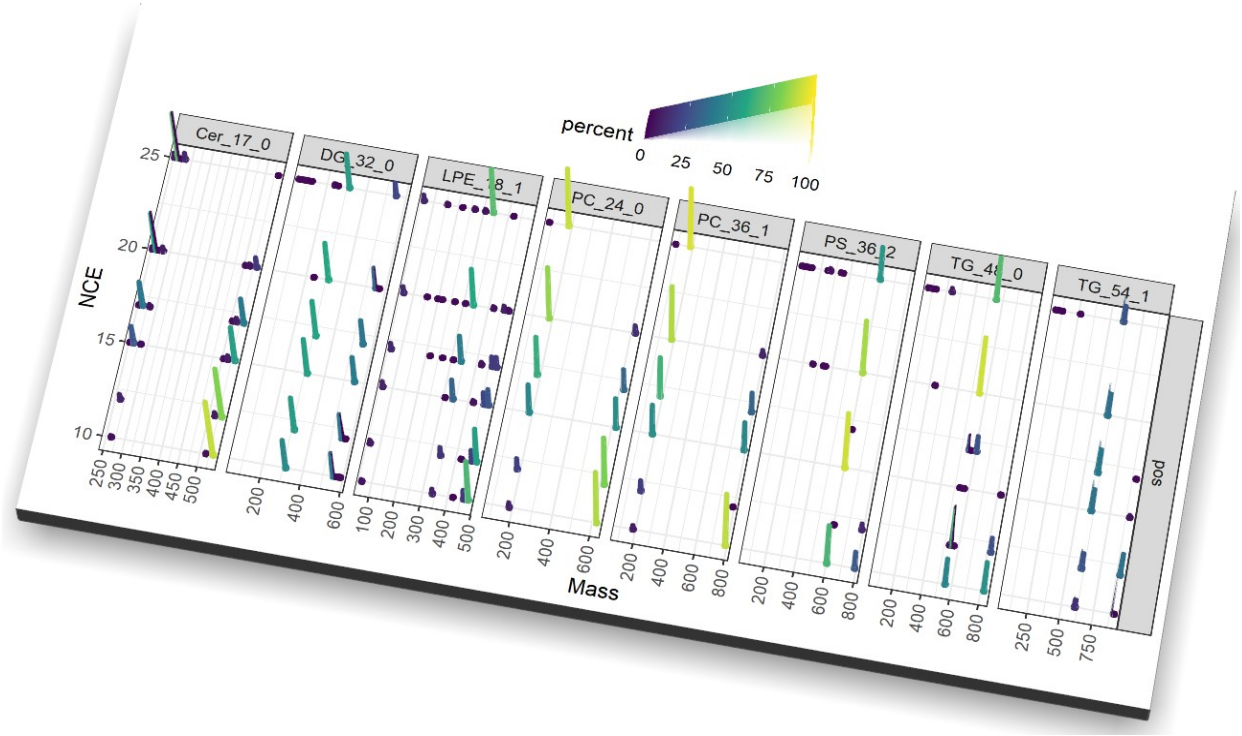

Figure 7 Influence of normalized collision energy (NCE) on fragmentation profiles of different lipid standards (Cer 17:0, DG 32:0, LPE 18:1, PC 24:0, PC 36:1, PS 36:2, TG 48:0, TG 54:1). Represented as a percentage of the total fragments per standard and NCE

These standards are detected without a serum matrix and are not representative of the entire lipid class due to the different chain lengths and degrees of saturation within the lipid classes. However, we could demonstrate that normalized collision energies between 15 and 25 showed good results in positive mode as well as in negative mode. In regard to our requirement profile, in which a remaining signal of the precursor ion is prefred in combination with high

specific fragment ion. The used fragmentation energy for each lipid class is shown in Supplement Table 1. The final HCD fragmentation energy is at least half the 50 eV used in the CID method. We even found better fragmentation profiles in the cholesterol ester subclass compared to the original method with the Orbitrap Velos Pro (data not shown).

Linear behavior of detect lipids in pooled QC samples.

In order to control and prove the concentration-dependent linear behavior of the detected lipids with our method, we extracted different amounts of pooled QCs (5 to 150ml, n=3), which corresponds to a range from 10 to 300% of the standard concentration. Figure 8 shows the concentration dependent behavior of the 424 (Supplement Table 4) detected lipid species of the pooled serum samples, with the two internal lipid standards (PC 24:0, PE 24:0). For visualization of the results we used a histogram of the coefficient of determination **(B)**, and a scatterplot with a linear regression of the pooled QC extraction volumes as integrated peak area (**A**). Since lipid standards are independent of the concentration, the coefficient of determination is close to zero (R^2, 0.06 PC 24:0 and 0.55 PE 24:0) and recognizable as horizontal line in Figure 8A. 78.8 % of detected lipids corresponds to a strong linear behavior with a coefficient of determination equal to or larger as 0.9. 16 % showed a weaker linear behavior between 0.9 and 0.5 R^2, and the last 5.2 % showed a week linear behavior smaller than 0.5 R^2. These had to be reintegrated manually or removed from the target list, which explains also that we found more lipid species in our analysis than reported in the cohorts.

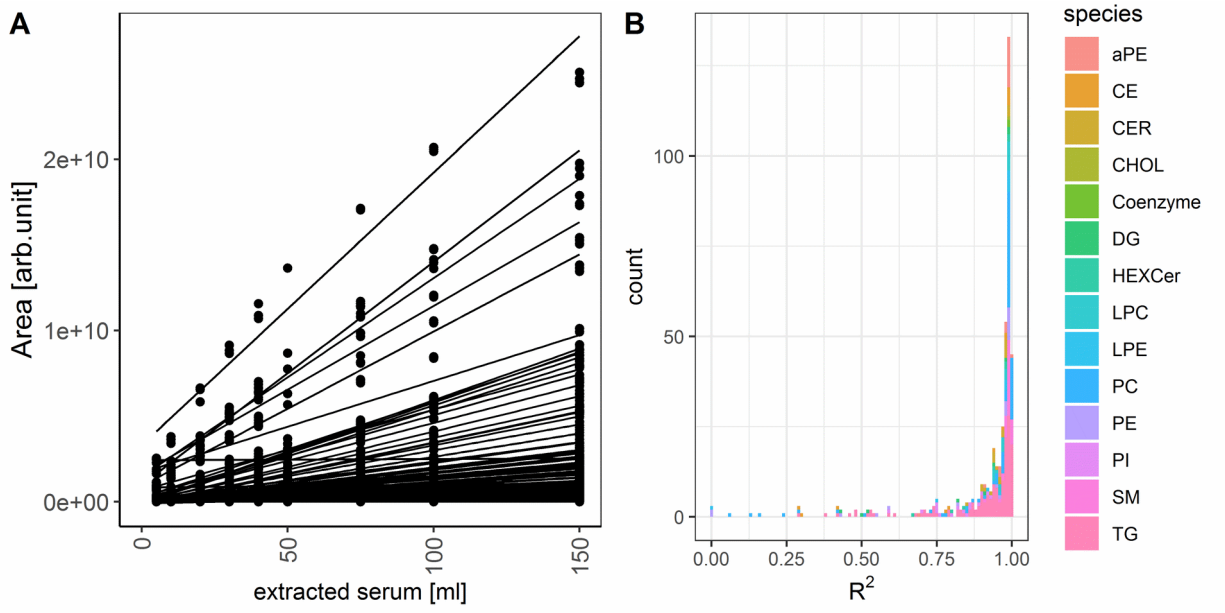

Figure 8 Effect of the concentration of the 426 detected lipid species in human serum including internal standard (PE 24:0, PC 24:0). **A** – shows the detected peak areas of the 426 lipid species sorted by extraction volume with a linear fit to visualized the linearity. **B** – Coefficient of determination of each lipid visualized as histogram and colored by lipid class.

Lipid separation with LC-MS

The temporal dimension of liquid chromatography separation of the lipids was adapted to the Vanquish UHPLC according to our in-house method (146). The one-hour separation of the lipids showed good separation and helps in reducing co-eluting lipids to increase scan time for full scan spectra and MS^2 spectra of the targeted analytes. All lipids were measured between 2 and 45 minutes and each lipid species is clustered to a certain start and end point depending on chain length, chain saturation and head group shown in Figure 9. Retention time stability was controlled in the FoCus cohort (n= 905) with a %RSD smaller than <0.25 for PC 24:0 and <0.24 for PE 24:0.

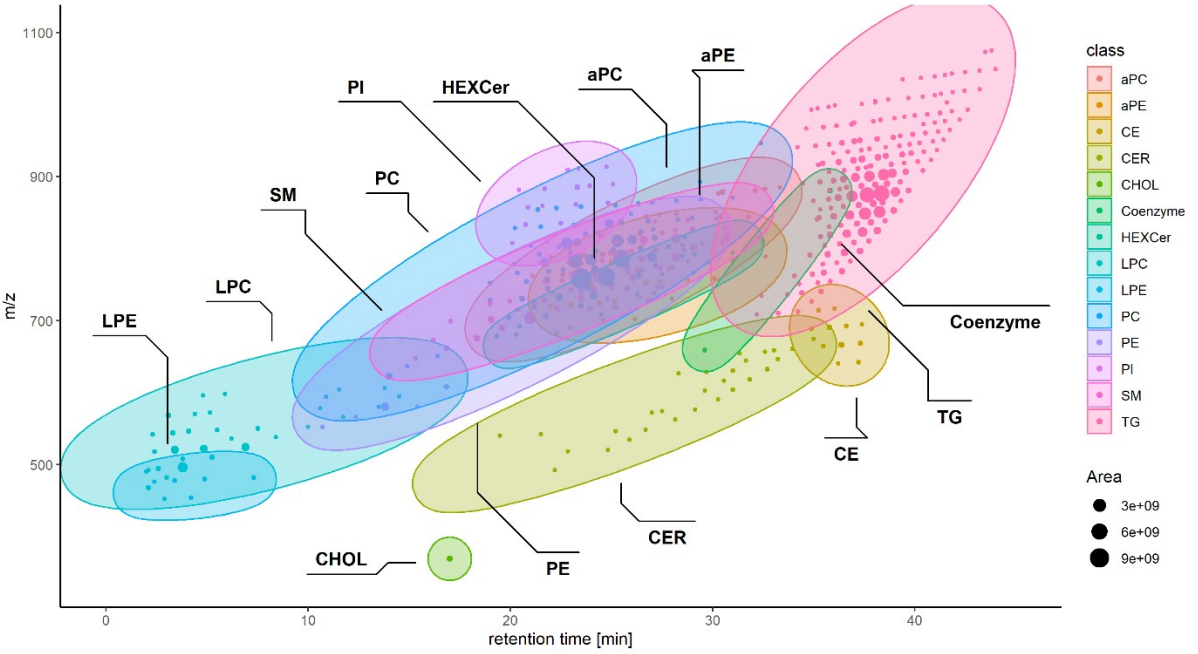

Figure 9 Overview of retention time dependent lipid class elution with the BEH C8 column (100 x 1 mm, 1.7 µm) from waters. (Data: QC sample_20 form PopGen cohort)

Data processing

Batch drift correction

The analysis time for one polarity was approximately 26 days, due to the large number of samples, e.g. FoCus cohort (n = 905 and additional 20% pooled QC extracted blanks samples). During such a long acquisition time, the MS device becomes contaminated. This can lead to a loss of sensitivity as well as discrepancies in retention time and mass accuracy. For these reasons we implemented a normalization strategy. Several methods are available as mentioned in section Approaches of batch drift correction and normalization strategies We used a random forest based method because it had already been tested with lipidomics data, which is called systematic defect removal with random forest (SERRF) (128). It can be executed as R code or as an online tool at https://slfan.shinyapps.io/ShinySERRF/.

The aim of the batch correction is to ensure that only systematic errors are eliminated and phenotypic differences are retained during the process. As a reference for systemic error correction, we use the pooled quality control that is representative of the entire cohort and was stored in the injection solvent at -80 °C (IPA/MeOH/CHCl3). In order to monitor the changes in the detected QC samples over time, we analyzed one of these pooled QC samples at every 10^{th} or 12^{th} sample position in the acquisition list. This information was used in the random forest-based algorithm to correct for systematic errors in the samples measured between the pooled QCs. Figure 10 shows the differences before and after batch correction as principal compound analysis (PCA) which shows a linear systematic distribution of the QC (red dots) in the “Before-plot”, which are transformed to a small cluster in the “After-plot” batch correction. The histogram of RSD illustrates the differences of all found compounds colored by lipid species and showed that in the FoCus cohort all major lipid species were decreased under 0.25 RSD. All cohorts and the intervention study were corrected with this tool (data not shown).

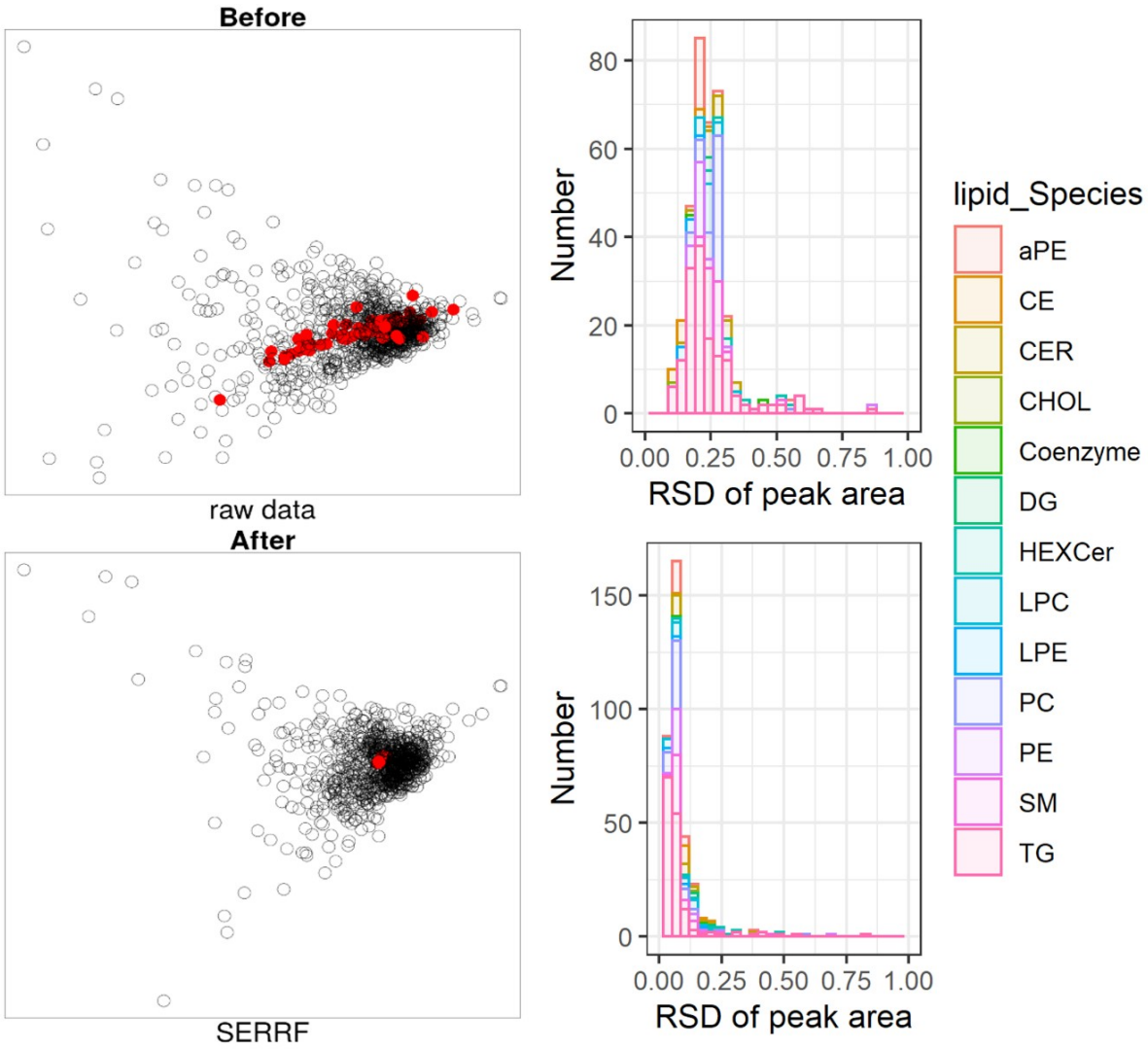

Figure 10 QC-based batch correction with SERRF (systematic error removal using random forest) of the FoCus cohort. Left side PCA before and after correction, right side RSD of found compounds before and after batch correction.

Results Cohorts

In general, processing data is a very important and time-consuming part of MS-based lipidomics, especially when large cohorts are involved. One of the reasons lipid annotation is time consuming is because excluding incorrectly annotated lipids still requires manual curation, due to the presence of isobaric or isomeric lipids or similar compounds. We are

using in our lab the Lipid Data Analyzer (LDA) for raw file processing, data integration, and lipid annotation in combination with an extended target-list as standard software tool. Since we were dealing in this project with larger cohorts then usually, we were not able to use LDA to process the data in combination with our technical equipment. Therefore, we only processed selected pooled QC samples with LDA to generate a target list with precursor mass, RT and analyzed the raw data of the cohorts with Tracefinder 4.1. This approach allows lipid identification with the benefits of the high-quality annotation of the LDA software and the faster processing and annotation with Tracfinder 4.1.

In the four sample sets we were able to detect and annotate around 380 lipid species (FoCus; 371, Tomorrow; 378, PopGen; 395, and intervention study; 382) from 13 different lipid subclasses, and cholesterol (Figure 11a). The Venn diagram illustrates the shared lipid species within the cohorts and the intervention study (Figure 11b). The number of found lipid species in all sample sets were 306, the individual highest number were found in the PopGen cohort with 395 lipid species, and the lowest number of lipid species were found in the FoCus cohort. The reasons for the discrepancy can be diverse: different longtime storage condition of the sample cohorts, different device performance and sample handling during extraction as well as storage time in autosamplers, etc.

Reports of the number of lipids found in serum or plasma vary widely. The numbers generally depend on the extraction method, MS device, annotation software, and several other factors. According to the literature, it is to be expected that, depending on the method and device, between 100 and 600 lipids can be annotated in human serum (103, 149, 150). But there are also reports with larger numbers of lipids found, especially when the structure elucidation is increased to the level of molecular species. We also checked whether a sample stands out in terms of abundances compared to others. Therefore, the total lipid abundances as a bar graph and as a box plot of lipid species were compared with all samples in each cohort (Supplement Figure 1). We found one sample of the PopGen cohort that was suspicious and therefore was excluded.

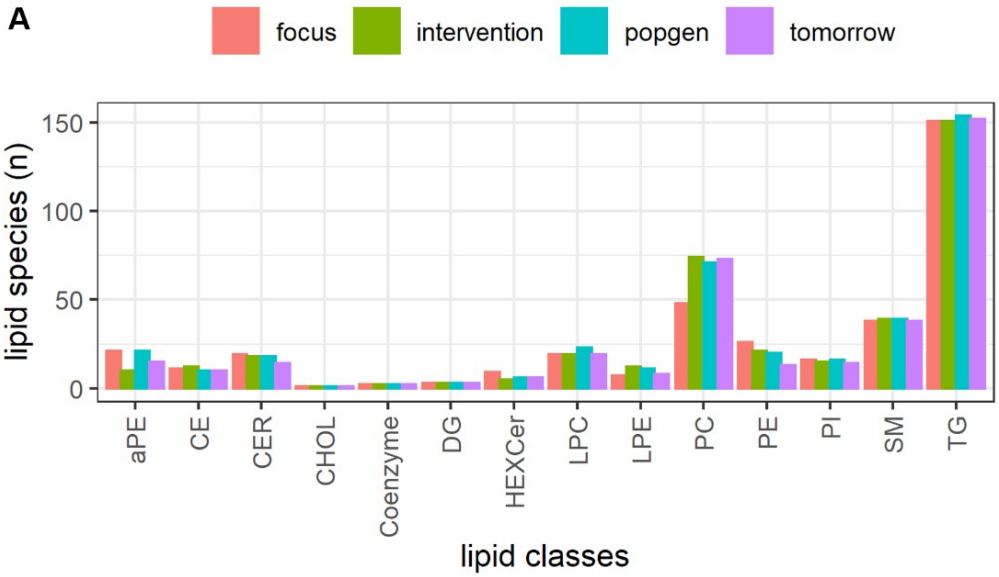
A
focus
intervention
popgen
tomorrow
lipid species (n)
150
100
50
0
aPE
CE
CER
CHOL
Coenzyme
DG
HEXCer
LPC
LPE
PC
PE
PI
SM
TG
lipid classes

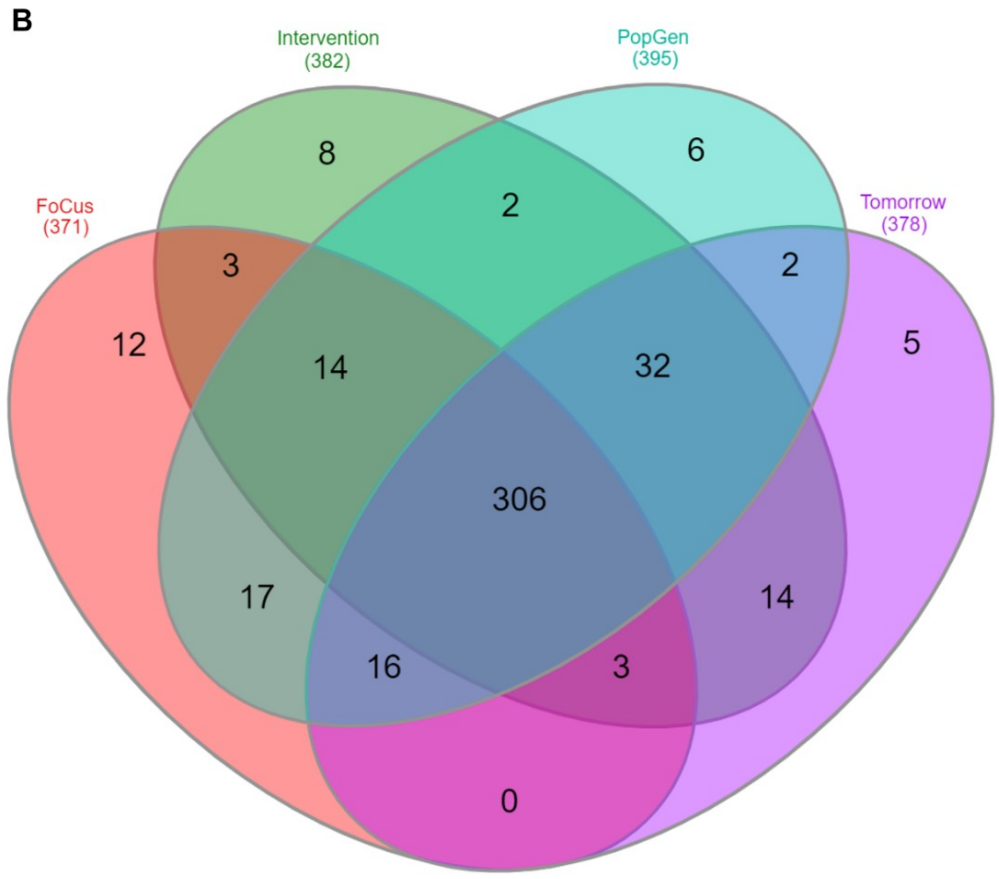
B
Intervention
(382)
PopGen
(395)
FoCus
(371)
Tomorrow
(378)
8
6
2
3
2
12
14
32
5
306
17
14
16
3
0

Figure 11 Overview of the found lipid classes and number of lipid species in all 3 cohorts (FoCus, PopGen, Tomorrow) and the intervention study in the top figure and on the Bottom a Venn diagram (151) which shows the common lipid species between the cohorts and the intervention study.

Intervention study

The data analyzed of the candidates participated in the intervention study (n=38) are obese with a BMI between 40.4 and 56.2 at time point t1. Seven candidates have diabetes in combination with hypertension. 17 of the non-diabetes patients have hypertension and the rest (n=14) are without hypertension and without diabetes. More details of the intervention study are not part of this thesis and will be publish elsewhere with consideration of all data (metabolomics, lipidomic and microbiome sequencing data). PCA showed that the differences between time points t1 and t2 are bigger than these between time points t1 and t3 (Figure 12).

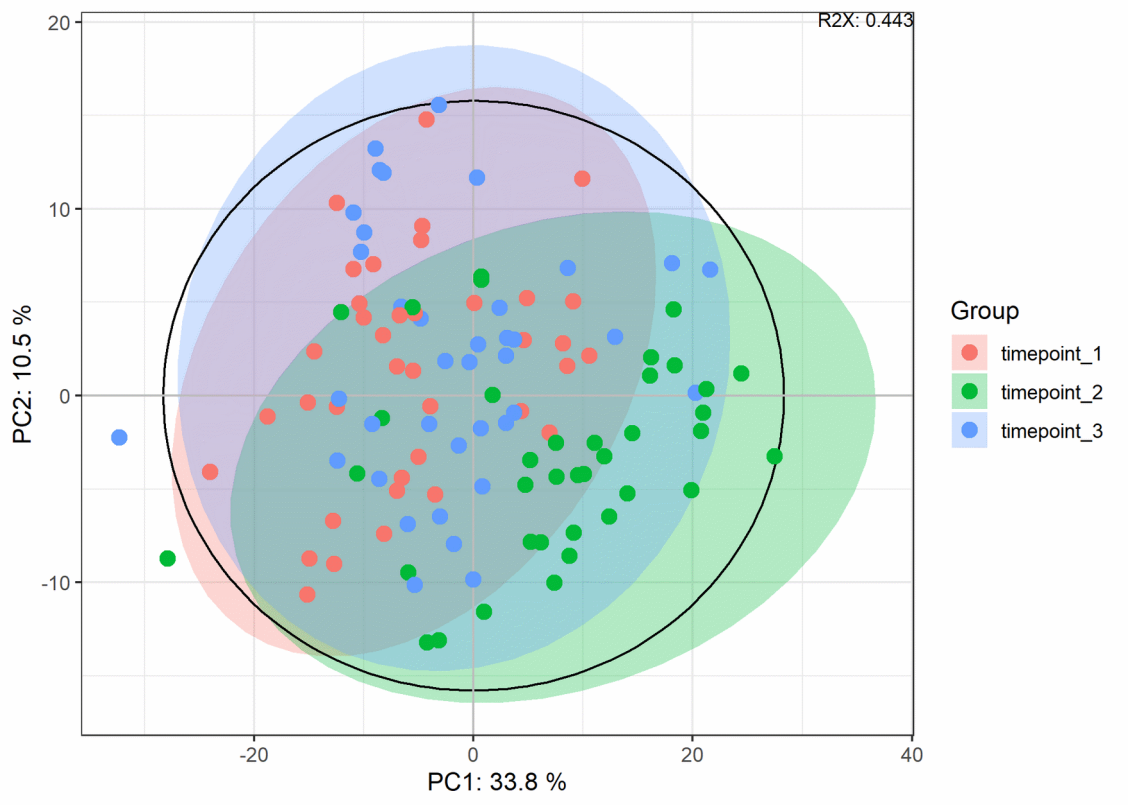

Figure 12 PCA of obese candidates in a low-calorie intervention study data obtained at 3 time points: t1 – before treatment, t2 – after 6 weeks liquid low-calorie diet, t3 – 6 weeks normalization phase with normal food.

To find out the main contributor to the differences between the time points we used supervised statistics orthogonal partial least square – discriminant analysis (OPLS-DA) shown in Figure 13

The OPLS-DA plots showed separation between both time points. However, the separation between t1 and t2 is with p1 – 22% much stronger than between t1 and t3 p1 – 5.66 %. the top 20 lipid species which contributed most to this model belonging to the SM, LPC, LPE, PC, aPE, and TG classes (Table 1). The minor effect of the separation between t1 and t3 are mainly contributed from ceramides and sphingomyelins (Table 1). In addition, we also used the OPLS-DA model to test whether there are differences in the lipidome of diabetic and non-diabetic patients and between hypertensive and non-hypertensive patients. We tested every

time point separately and found only minor differences between these parameters, similar to t1 versus t3 where the model showed problems with R2Y and Q2 consistency (shown in Supplement Figure 2).

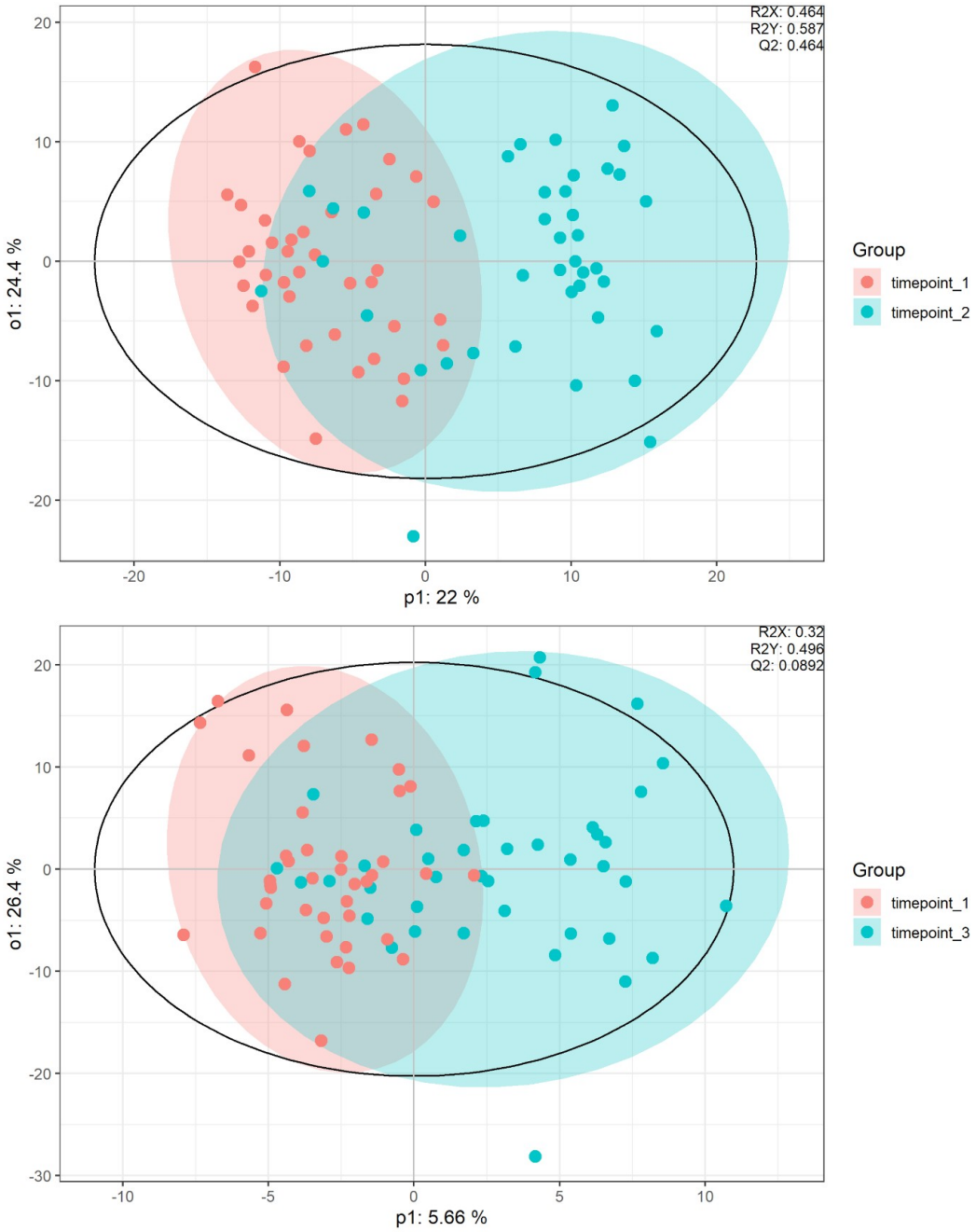

Figure 13 OPLS-DA plots of obese candidates in a low-calorie diet intervention study. Top side shows differences of time point t1 and t2, bottom side between time point t1 and t3

Table 1: The 20 most contributing lipid species to the OPLS-DA model separation between t1 and t2 or t1 and t3 . cl = chain length, cs = chain saturation

time point 1-2				time point 1-3		
lipid species	total_cl	total_cs	molrank	Molecule	total_cl	total_cs
SM 40:5	22	4	1	LPC 20:1	20	1
PC 32:2	32	2	2	PC 44:5	44	5
LPC 18:3	18	3	3	SM 40:1	22	0
LPC 14:0	14	0	4	CER 42:1	24	0
SM 40:4	22	3	5	CER 40:1	22	0
PC 36:4	36	4	6	CER 36:1	18	0
SM 38:3	20	2	7	LPC 19:0	19	0
TG 47:1	47	1	8	SM 36:2	18	1
TG 55:1	55	1	9	SM 38:1	20	0
LPE 20:3	20	3	10	SM 36:1	18	0
PC 38:3	38	3	11	CER 44:1	26	0
PC 36:6	36	6	12	SM 44:4	26	3
PC 30:1	30	1	13	SM 44:2	16	1
TG 46:1	46	1	14	TG 52:1	52	1
TG 48:1	48	1	15	CER 38:1	20	0
aPE 40:4	40	4	16	SM 43:1	25	0
TG 46:0	46	0	17	CER 43:1	25	0
CE 18:3	18	3	18	SM 41:1	23	0
PC 29:0	29	0	19	CER 41:1	23	0
TG 50:0	50	0	20	PC 42:7	42	7

We also tested statistically significant differences with a univariate statistical model between time points t1 and t2 and found that 247 out of 382 lipid species are statistically significant across all subclasses (adj. p.value <= 0.05). 55 even had a fold change over 2. The most frequently represented subclass with 72 percent of significant lipid species were triglycerides followed by gylcerophosphatidylcholine with 10 percent. Figure 14 shows the differences visualized as volcano plot between time point t1 and t2 aggregated by lipid subclasses. Between time point t1 and t3, only 4 lipid species were significant and none had a fold change over 2 (Supplement Figure 3). These results showed that the low-calorie diet has a strong negative effect on the serum lipidome over all lipid classes because in most cases they were found at lower concentrations. It also shows that after the stabilization phase (second 6-week cycle) there were no significant differences unless these 4 lipids.

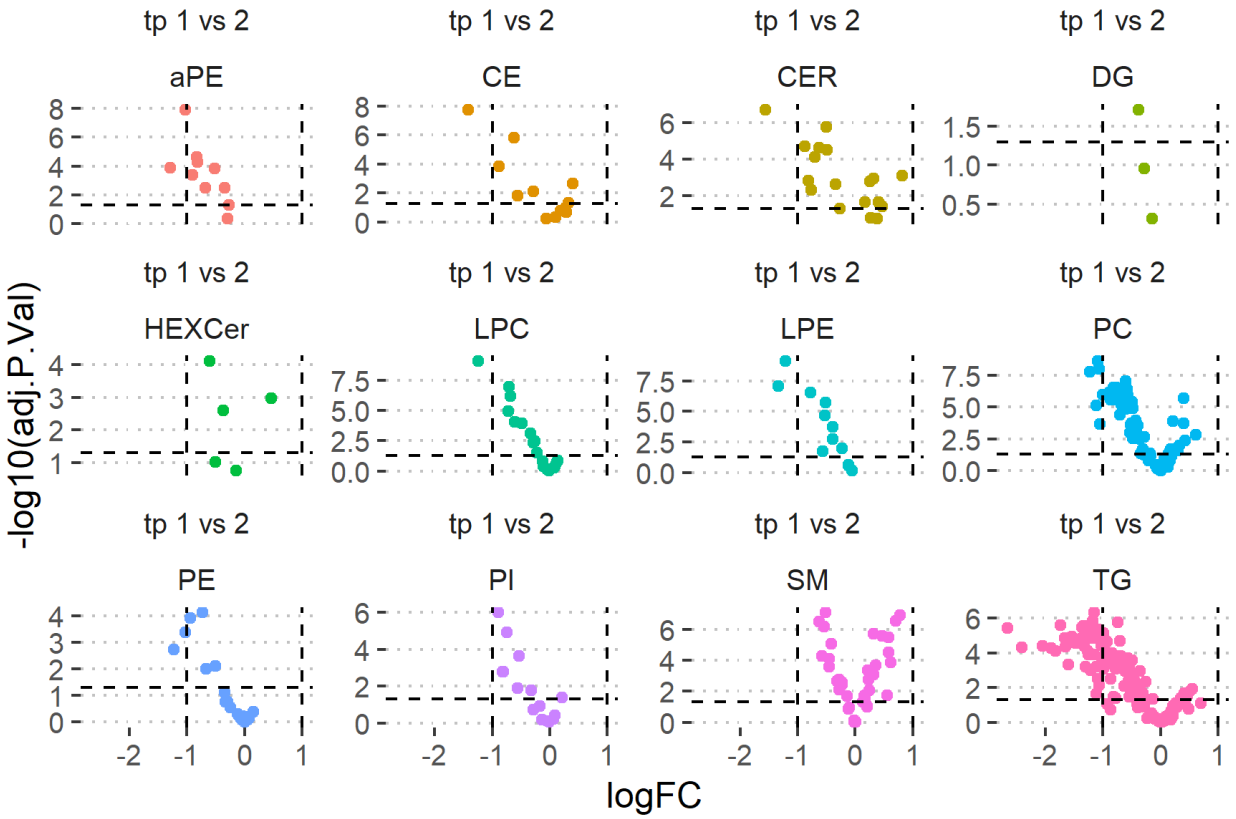

Figure 14 Volcano plots of obese candidates in a low-calorie intervention study data obtained at 3 time points shown only time point (tp) t1 vs t2. t2 – after 6 weeks liquid based low-calorie diet, logFC – log 2, fold change, vertical dashed line indicates ± 2 fold change, vertical dashed line shows significant level adj. P. Value ≤ 0.05. Coenzyme Q and cholesterol have been removed from the figure for the sake of clarity

Furthermore, we were interested in changes of acyl/alkyl chains in terms of saturation and/or chain length. To do this, we aggregated the different classes according to the number of chains and compared time point t1 with t2 or t1 with t3 results are shown in Figure 15. i) Lipids with only one chain (LPC, LPE, CE) showed at time point t2 an area count reduction at chain length of 14, 18 and 20 carbon atoms and a reduction by total chain saturated of 1-4 double bounds. At time point t3 there were no differences to time point t1, which we already expected because of the previous reported results which showed no major effects between these two time points. ii) Detected lipid subclasses with 2 acyl/alkyl chains (PE, PC, PI, DG, Cer, HexCer, and aPE) showed an increase at the lower and upper end of the total chain

length and a decrease in between at time point t2 compared to time point t1. With regard to the saturation levels between these two time points, a general decrease could be observed. Between time point t1 and t3 no major differences of both, chain length and saturation level, were detected. iii) The only group of lipids with 3 acyl chains were the TG subclass, they showed the largest reduction between 40 and 55 total chain length at time point t2 and at time point t3. In the case of unsaturated chain levels, an increase was observed at time point t2, depending on the saturation level, and at time point t3 there was a slight decrease across all saturation levels.

The observation of changes in the total chain length and the total unsaturation level is limited to general observations, for that it would be even more interesting to compare changes of individual acyl/alkyl chains. However, this is not possible due to the annotation level limitations and for this we would need in-depth annotation at the molecular species level. With the combination of the lipid subclasses with the same number of chains we were at least within similar conditions and thought that it is best practice regarding the annotation level of lipid species. The individual changes in total chain unsaturation for each lipid species can be found in Supplement Figure 5 and the total chain length in Supplement Figure 6 in the Appendix.

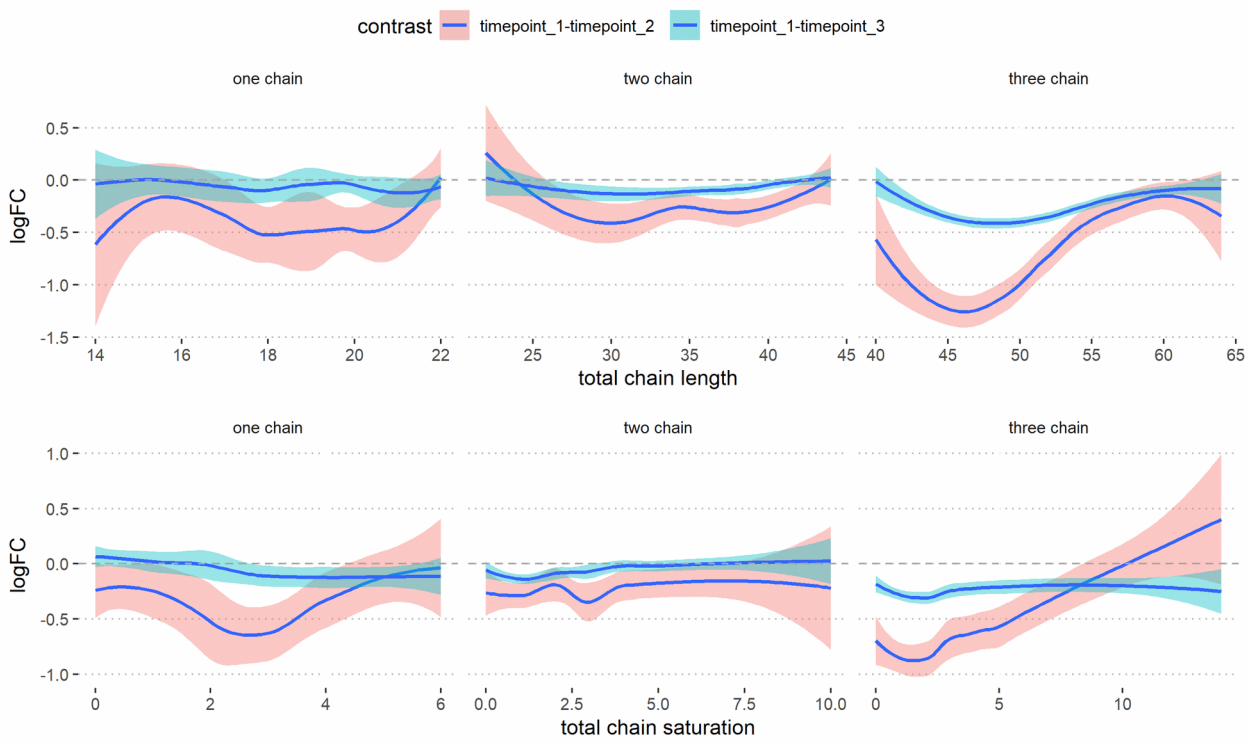

Figure 15 Overview of lipid subclasses aggregated by number of chains on top the changes in total chain length are shown and on the bottom the changes of total unsaturated bonds interpolated with leoss regression algorithm. logFC – log2 fold change

Cohorts

We analyzed Tomorrow, PopGen and FoCus cohorts with similar types of diseases (section Cohorts). Since the clinical metadata of the PopGen cohort is up to now not available, we will exclude it from further analysis at least for the moment. First, we did multivariate clustering with PCA to get an overview about potential differences (Figure 16) followed by supervised multivariate clustering to explore differences between the control group and each health status on a lipid species level shown in Figure 17.

The PCA of the FoCus cohort showed no health-specific clustering, in contrast to the Tomorrow cohort, which showed minor clusters between rheumatoid arthritis (RA), inflammatory bowel disease (IBD), and diabetes versus healthy candidates (Figure 16).

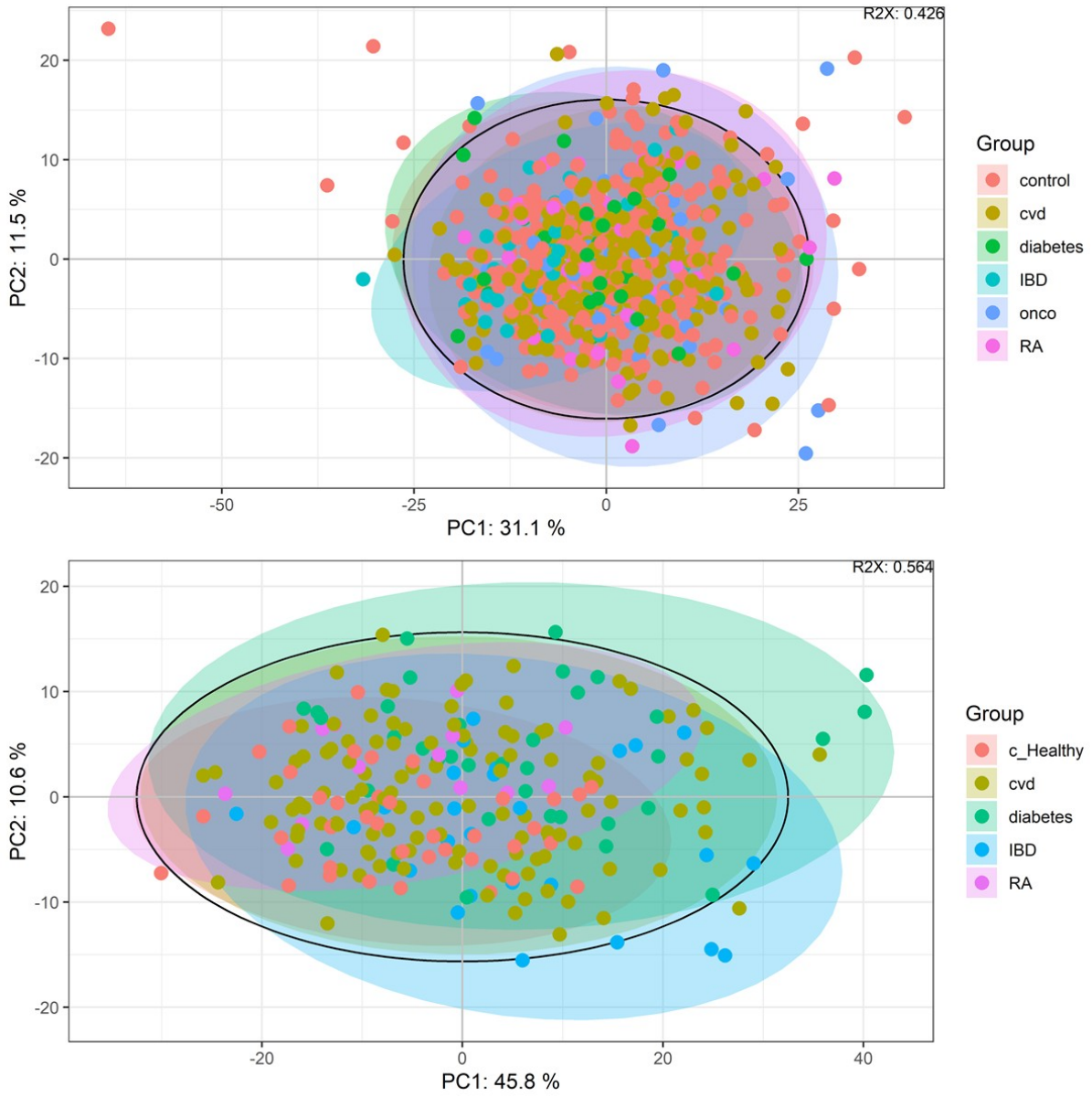

Figure 16 PCA of candidates with different health condition of FoCus (top-side) or Tomorrow (bottom-side) cohort. cvd – cardiovascular disease, IBD – Inflammatory Bowel Disease, RA – Rheumatoid Arthritis, onco – malignancies

The supervised model of OPLS-DA showed similar results as PCA in the FoCus cohort. The model could not discriminate correlated differences between control and the different health statuses (

In the Tomorrow cohort the diabetes versus the health group showed best separation with a total R2X: 0.578, R2Y: 0.551, and Q2: 0.439, all other pairs are better than within the FoCus cohort but the predictive value Q2 as well as the R2Y value with under 0.25 is too low to accept the model. The 50 main drivers of the differences between diabetes and healthy condition are shown in Supplement Table 5. 48 of the 50 main drivers were TG species, and the other two were DG species (DG 26:2, DG 36:3), all from the glycerolipid class. This could also be an obesity trend, but since we do not have metadata on Tomorrow's cohort weight, we cannot test this assumption. None the less, we already showed that we could not identify differences in the lipidome between obese with and without diabetes (Supplement Figure 2) from the data of the intervention study.

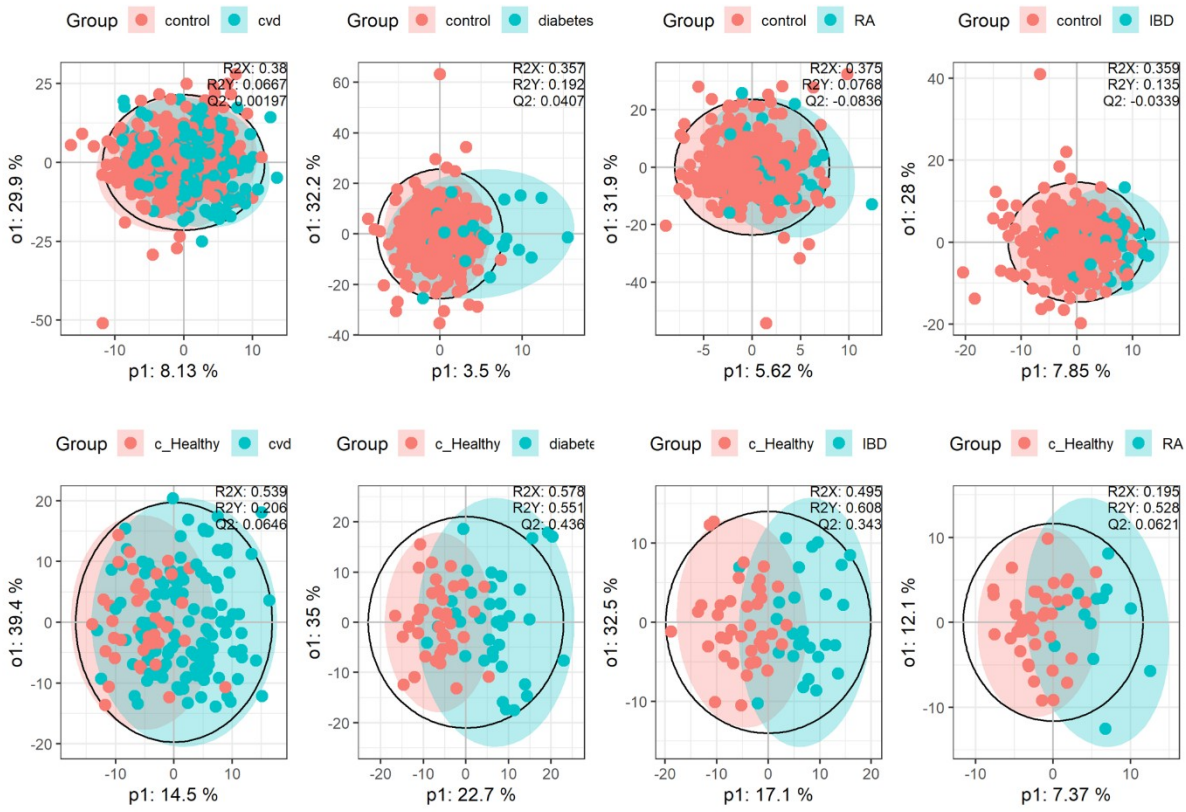

Figure 17 OPLS-DA plots of candidates with different health condition. top row shows differences of the FoCus cohort, and bottom row the differences of the Tomorrow cohort, R2X – shows the explained variation of the whole model, R2Y - shows how good the model could separate condition 1 from condition 2 (1 – perfect, 0 - no separation), and Q2 – predicts

how good the system can explain the separation of condition 1 and 2. Q2 and R2Y should not differ > 0.3 otherwise the separation is unbalanced.

In the group of healthy patients compared to the group of patients with cardiovascular disease in the Tomorrow cohort, 62 lipid species were found to be statistically significant (adjust p-Value ≤ 0.05). Two of them, both belonging to the PI species, were lower and the other 60 were more abundant in the CVD group. The main contributors were TG subclass with 55 lipid species, 4 PC species and one was from the HEXCer subclass. With regard to the fold changes, only 6 TG species were changed more than 2-fold.

Between the Healthy and the IBD group 236 out of total 378 lipid species were statistically significant, which is over 62 percent of total species. 79 of a total of 154 were TG species, 63 of 74 were PC species, 31 of 38 were SM species, 17 of 19 were LPC species, all of the 14 identified ceramide species and the remaining 32 lipid species were from 8 other lipid subclasses. The abundance shift is similar to that of the CVD group compared to the healthy group. In the healthy group only 3 species were upregulated and overall, only 13 with a change in folds of more than 2. The RA group showed no statistically significant lipid species compared to the healthy group. Due to the good separation of the diabetes group in the OPLS-DA analysis from the 4 groups with an altered state of health, we expected the best results also with univariate statistics. A total of 235 lipid species were statistically significant between diabetes and the healthy control group, which corresponds to more than 62% of total lipid species. The largest lipid subclass was TG with 143 lipid species, similar to the results of the other health conditions compared to the healthy group. Only 5 lipid species were less abundant compared to the healthy control group in the diabetes group, and 88 lipid species (2 PE, 86 TG) in total had a higher fold change than 2, with 38 of them also being among the 50 main drivers of the OPLS-DA model. The results are summarized as volcano plots in Figure 18B, and information of all statistically tested lipids are in Supplement Table 6 for the FoCus cohort and in Supplement Table 7 for the Tomorrow cohort.

We also compared total chain length and saturation levels. The results of them in IBD, diabetes and CVD showed that the chain lengths are higher abundant in all three groups of the

different acyl/alkyl chains compared to the healthy group (Figure 18C). In the group of three acyl chains (TG), the diabetes group even showed a more than two-fold increase in the total chain length for lengths between 55 and 62 carbon atoms. With regard to the total number of unsaturated bonds, a similar picture emerges in the TG group. All different health conditions are higher than in the healthy group, in particular the diabetes group again showed a more than two-fold increase. Additional information for total chain length (Supplement Figure 9, Supplement Figure 10) and total unsaturation level (Supplement Figure 12, Supplement Figure 13) for all lipid species are separately listed available in the appendix.

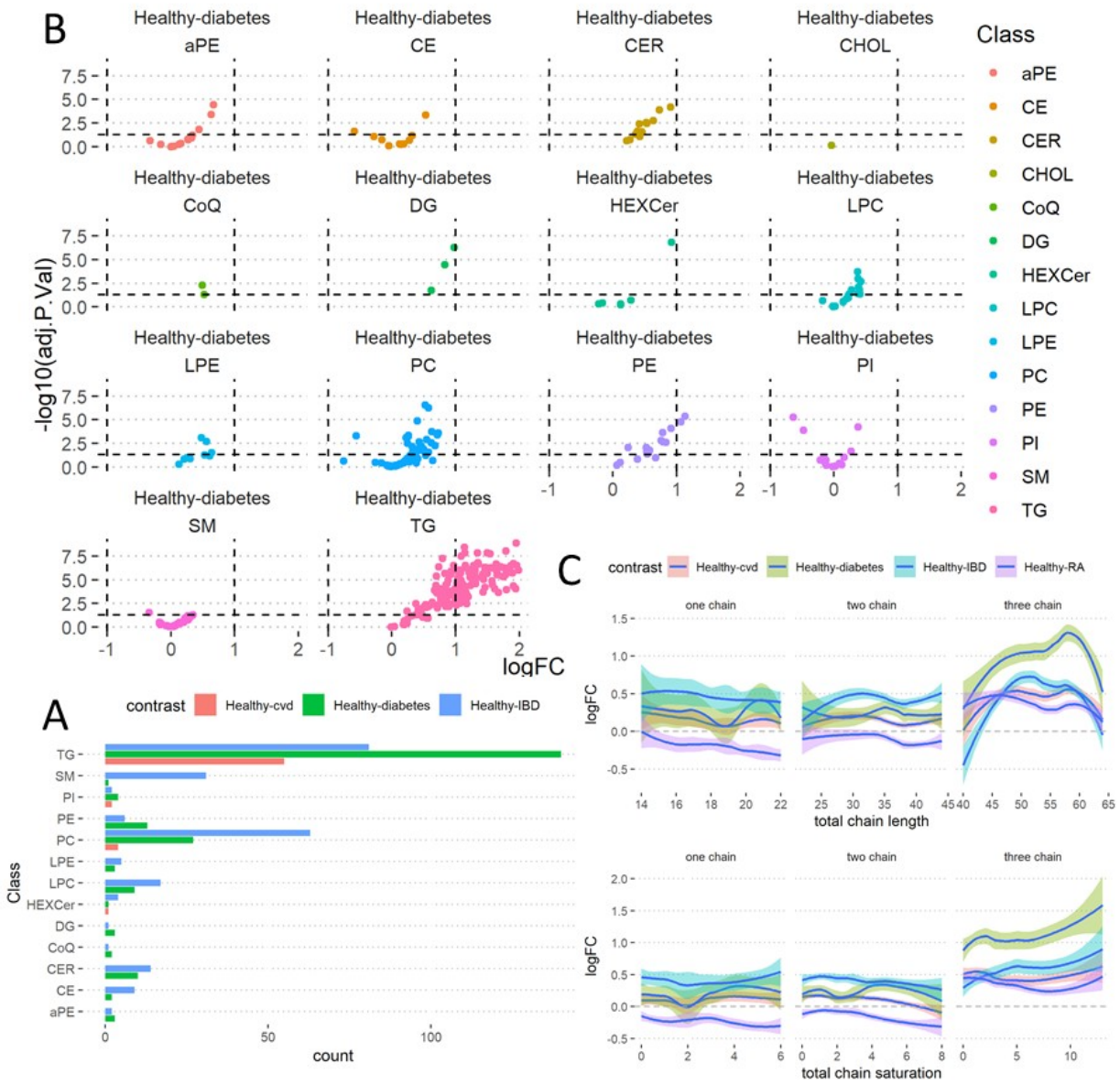

Figure 18 Overview of univariate statistic of the Tomorrow cohort. A The number of significant lipids found in the various health status groups compared to healthy candidates. Volcano plot **B** shows the differences between group Healthy and diabetes, which showed best separation of these groups in OPLS-DA analysis. **C** - Overview of lipid subclasses of the differences between health status and cvd, diabetes, IBD, and RA. Aggregated by number of chains on top the changes in total chain length are shown and on the bottom the changes of total unsaturated bonds interpolated with leoss regression, logFC – log2 fold change

4 Discussion

Omics studies are often hypothesis generating projects. With the aim of finding as many compounds as possible and using statistical methods to determine which compounds show the biggest effect in order to identify differences between different groups with different health conditions. As simple as the approach is, the challenge is to validate the results and find "bias-free" health status-specific effects. Often there is no information or known mechanism that could explain the diagnosed differences. Therefore, it can be difficult to come up with a plausible explanation for changes when the biochemistry behind is unknown. One strategy is to create a new hypothesis with potential mechanisms, which can be tested. Another solution, if no plausible mechanism is known, is to validate the results with literature data to reduce the risk that differences were only accidental or due to other unknown effects.

In this study two separate cohorts with similar health status groups were analyzed and used to evaluate results. As noted in the results section the Tomorrow cohort showed between diabetes and control group most promising changes. To validate these results, we used receiver operating characteristic curve (ROC) models, on the one hand to show the diagnostic ability of the top 20 lipid species with the best discriminatory capacity of the OPLS-DA model and validated these findings with the FoCus cohort (Figure 19). The Area under the curve (AUC) value of the multivariate ROC curves analysis showed a good discrimination level of 0.88. This is in contrast to the data of the FoCus cohort, which showed a poor discrimination of 0.61. As the groups between healthy candidates (FoCus = 351, Tomorrow = 39) and diabetes (FoCus = 27, Tomorrow = 36) are unbalanced we also used the more robust Precision Recall Gain curve method for unbalanced groups (152). Results showed that there was no discrimination in the FoCus cohort AUC-PRG, and the differences in the Tomorrow cohort could not be confirmed. To explain the differences probably full metadata could help to verify the similarity of the two cohorts in general and since diabetes is often associated with other risks such as cardiovascular disease and/or obesity, it could have a major impact on the results of observed differences in lipid metabolism. The other health conditions of the cohorts were also compared with the ROC-AUC method of the 20 main drivers form OPLS-

DA model and are shown in the Supplement Figure 14. Since the discrimination of the other groups compared to the healthy group are less distinct, the AUC-ROC reflected that too (CVD vs Healthy, AUC-ROC, Tomorrow – 0.61 and FoCus – 0.67; IBD vs Healthy, AUC-ROC, Tomorrow – 0.79, FoCus – 0.67; RA vs Healthy, AUC-ROC, Tomorrow – 0.75, FoCus – 0.55).

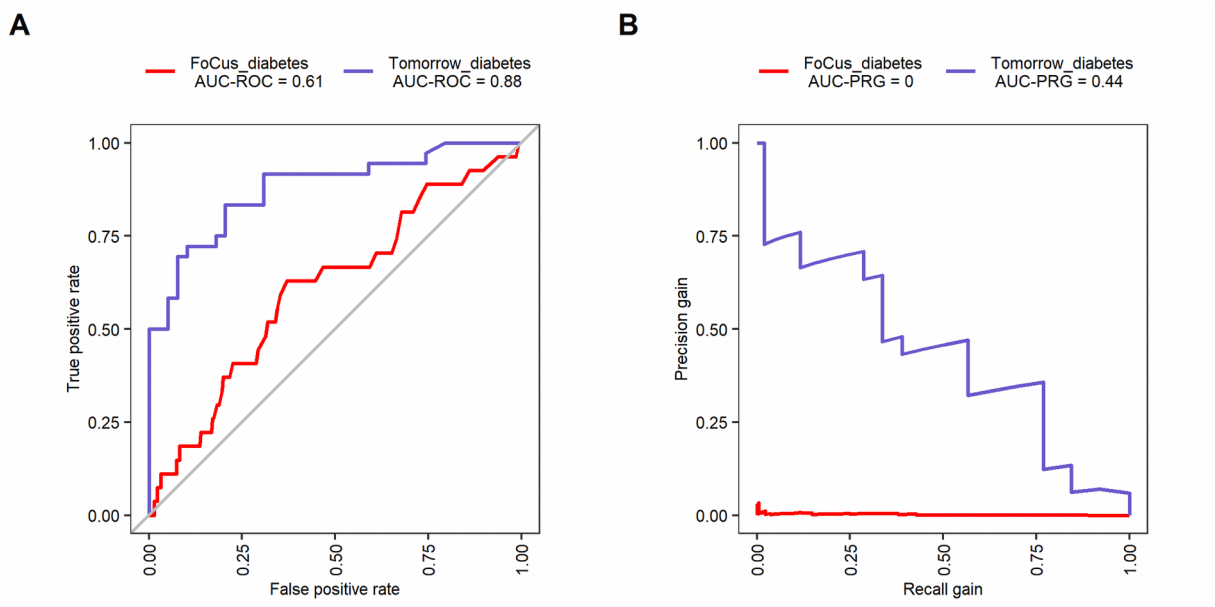

Figure 19 ROC (A) and Precision-Recall-Gain (B) curves of the top 20 contributing lipid species between diabetes and health status of the Tomorrow cohort (blue line) and validation FoCus cohort as to validate results (red line).

Diabetes related changes in the lipidome

The analysis of this study showed a large number of significantly changed lipids between the diabetes and healthy groups, especially in the TG subclass. Due to the large number of significant lipid species, and the different outcome of the two cohorts (Tomorrow vs FoCus) the interpretation has increased in complexity. Therefore, we wanted to compare and discuss our results with results from the literature. Meikle *et al.*, (2013) exanimated patients with prediabetes, Typ 2 Diabetes (T2D) and to a control group with normal glucose tolerance values. From the 259 detected lipids species 135 were significant of the T2D group compared

to control group (153). They showed correlation between T2D and control group in the following subclasses: **Cer↑**, **DG↑,** dhCer↑, **HexCer→,** LPC(O)↓, **PC→**, PC(O)↓, PC(P)↓, **PE↑,** PG↑, PI↑, SM↑, and **TG↑**, which confirmed our results to some extent. The Tomorrow cohort showed the following trend ($p < 0.05$, bold – same as in Meikle et al.) aPE→**,** **PE↑**, CE→, **Cer↑,** cholesterol→**,** CoQ→, **DG↑,** **HexCer→,** LPC→, LPE↑, **PC↑**, **PE↑,** PI→, **SM→,** and **TG↑** upregulated, only PI was differently associated of the measured lipid subclasses, which are shared between both studies.

We could find similar results as previously reported not only at the lipid class level, but also on the species level, they showed that T2D diabetic patients had higher concentration levels of total ceramides and of the following species C18:0, C20:0 and C24:1 (154). In the Tomorrow cohort we found these 3 ceramides increased within the diabetes patient group, but also several other ceramide species were increased (Figure 20).

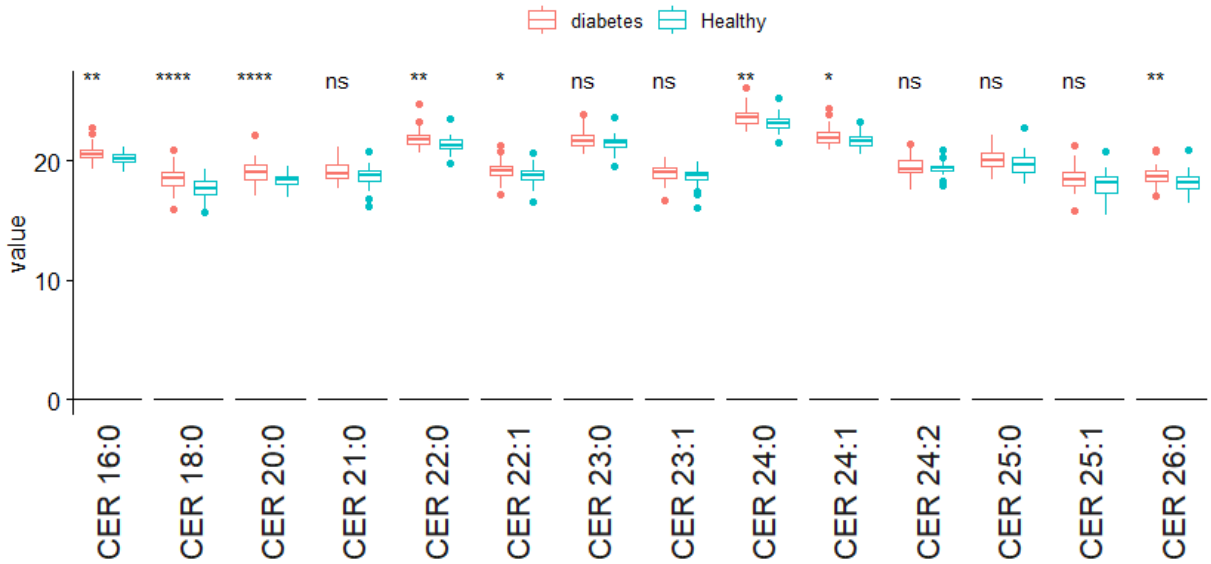

Figure 20 ceramides of the Tomorrow cohort tested with t-test. *- $p \leq 0.05$, ** - $p \leq 0.01$, *** - $p \leq 0.001$, **** - $p \leq 0.0001$, ns – $p > 0.05$, assumption of the additional (d18:1)

Chew *et al.*, (2019) showed in a large-scale lipidomics study the associations between plasma sphingolipids and T2D, that 2 distinct SMs were associated with a higher risk (SM(d16:1/18:0), SM(d18:1/18:0)) (155). Due to the prediction improvement of the SM

d16:0/18:0 we cannot compare our data directly because we only annotate at species level and not molecular species. Although we could not observe an increase of SM on subclass level in general but on species level: SM 31:1 was in the diabetes group decreased and SM(35:1, 36:1, 36:2,18:1, 40:1, 40:5, 42:1, 43:0, 43:1) were significantly increased.

Cardiovascular disease related lipidome changes

Cardiovascular disease (CVD) is the number one cause of death in the western world and a ubiquitous research topic. In term of changes in lipidomics of plasma Stegemann *et al.*, (2014) showed in a cohort study with 685 plasma samples with 145 lipid species from 8 different subclasses that individual subclasses CE, LPC, PC, PE, SM and TG were associated with cardiovascular diseases (156). They found that the lipid subclasses of TG and CE with a low total number of carbon and a low total number of double bonds are predictive of CVD. Overall, the strongest predictors they described were TG 54:2, CE 16:1 and PE 36:5. In the Tomorrow cohort these three lipid species were not significantly different only PE 36:5 was significant in the FoCus cohort.

We also did ROC and precision gain curve analysis of these three analytes for showing the predictive value which was in our case poor. They were close to random results (shown Figure 21). In terms of changes in total number of carbons and total number of double bonds our results showed in some parts a similar trend, TG with 0 and 1 total numbers of double bonds are significantly different and higher in the CVD group of TG but not in the CE subclass. Lower total chain length is not increased between the groups (shown in Figure 21E). In general, the data are not complementary although there are differences in the analysis method. They used an L1-regularized Cox regression with least absolute shrinkage and selection operator algorithm (LASSO), which considered additional to the lipid species, age, sex and the use of statin as explanatory variables. In our analysis only the lipid information was used, we could not include the same additional explanatory variable due to metadata limitations.

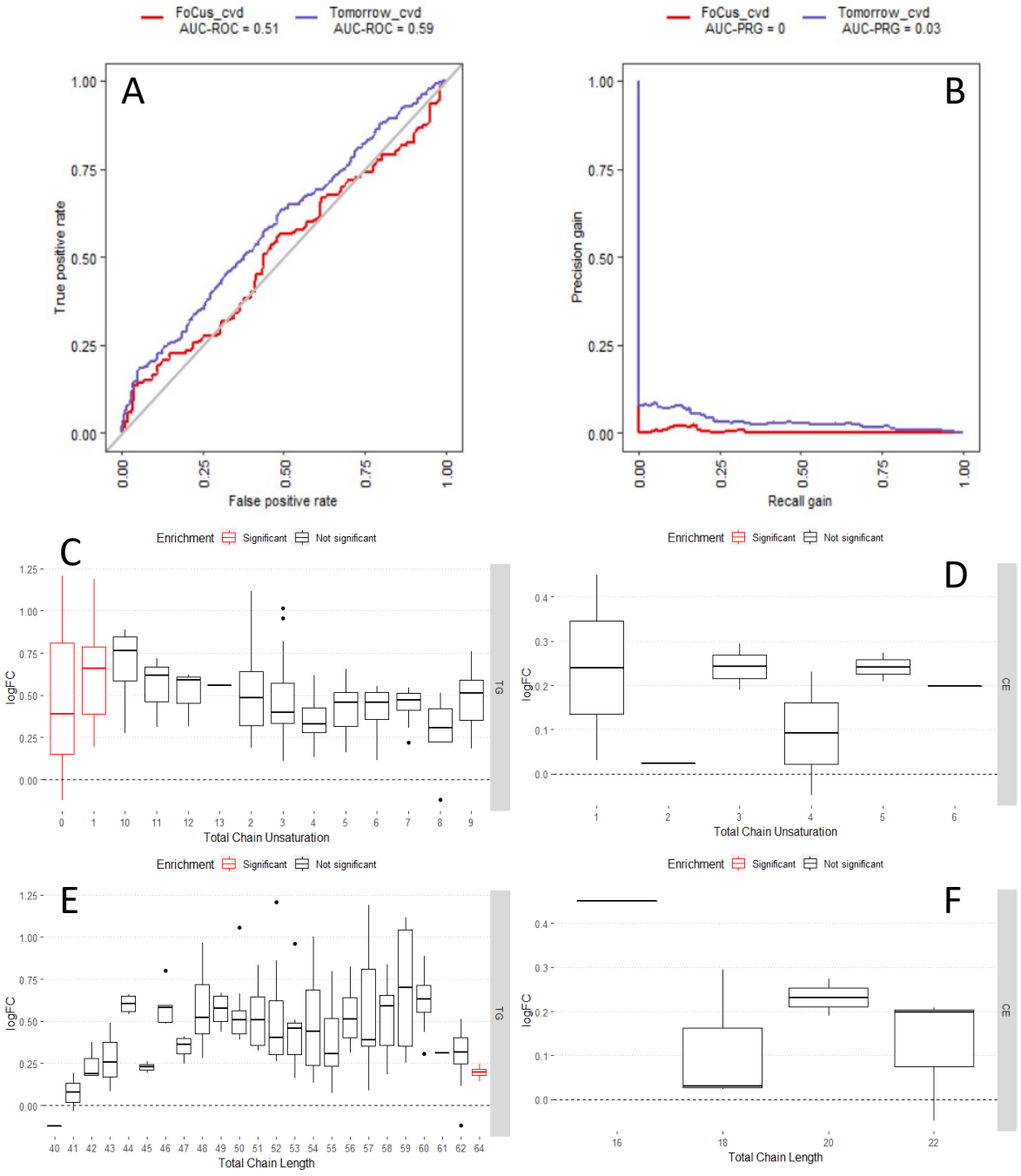

Figure 21 ROC (**A**) and Precision-Recall-Gain (**B**) curves of the CE 16:1, PE 36:5 and TG 54:2 the three best predictors of the Stegemann *et al.* (2014) for CVD risk. Tomorrow cohort - blue line and FoCus cohort - red line. Total Chain Unsaturation enrichment of TG (**C**) and CE (**D**) and Total Chain Length enrichment of TG (**E**) and CE (**F**) of the Tomorrow cohort. Results are shown as log2 fold change and red boxplots are statistically significant. Enrichment analysis were processed with lipidr (144).

Inflammatory bowel disease related lipidome changes

IBD are several inflammatory conditions of the small intestine and the colon (e.g. Crohn's disease). Guan *et al.*, (2020) analyzed on a UPLC-QTOF-MS-based platform lipids to identify biomarkers between IBD patients and control. They identified (PLS-DA based ROC analysis) 44 lipid species with multivariate methods as biomarker candidates with ≥ 80 % sensitivity and specificity between IBD and control group (16 FA, 4 GLP, 9 PR, 2 SP, and 13 ST) (157). We only found three lipid species in common of the GLP class due to their more lipophilic method than ours with a focus on fatty acids among others. These 3 common lipid species were significantly different from the control group and the subclass showed a general trend towards an increase in the IBD group of the Tomorrow cohort compared to the control group. In case of the 3 LPC species the trend was exactly the opposite of the results in the publication of Guan *et al.*, they are significant but downregulated instead of upregulated.

Another lipidomic based study of plasma from Fan *et al.*, (2015) compared 40 patients with subgroup of ulcerative colitis (UC) or Crohn's disease (CD) with 83 healthy volunteers (158). They found 333 lipid species and 86 were statistically significant between CD vs Control. They used a logistic regression adjusted model by including sex, age, waist circumference, smoking, and diastolic blood pressure. The most dominant group they found were ether lipids from PC and PE as plasmalogens or alkenyl variants and the trend was a decreased abundance level in CD patients. They argued that oxidative stress could be the reason for the decrease. In our data we only could identify alkenyl phosphatidylethanolamine species and the tendency was a not a significant increase, only three out of 12 were statistically significant and not the same species as mentioned in the study of Fan *et al.*, (2015).

Another study showed that PS are increased in CD patients more than 2-fold compared to healthy patients. As we were not able to detect PS or LPS with our method we could not compare these results. They also showed significant differences between PC of healthy and CD patients, where PC was decreased in the CD group (159). In our case PC species of the

Tomorrow cohort are increased and not decreased. A main difference of the studies is, that not the same metadata are considered in the analysis models, which makes it difficult to compare the outcomes directly.

Rheumatoid arthritis disease related lipidome changes

Rheumatoid arthritis is an autoimmune inflammatory disease and the cause of the disease is not fully understood. Significant decreases of FA 16:0, 18:2, 18:3 and alteration to a higher degree of unsaturation are published (161). One untargeted lipidomic study of Łuczaj *et al.*, (2018) identified 114 phosphlipids in plasma were they found with score analysis (variable importance in projection - VIP) between RA and control group 16 significant lipids (LPC 16:1, PC 34:3, PC 36:3, PC 38:3, PC 40:2, PC 40:3, PC 42:3, PE 30:1, PI 36:1, PI 36:2, PI 36:3, PI 36:4, PI 38:3, PI 38:4, SM 40:1, SM d40:2) (160). Compared to the results of the Tomorrow cohort, only PI 36:3 of these was significantly different to the control group.

Miltenberger-Miltenyi *et al.*, (2020) analyzed 82 blood serum samples of 19 patients with established RA, 18 patients with early untreated RA, 13 patients early untreated without fulfilling the classification criteria, 12 with established SPA, and 20 patients as healthy controls. The lipid subclass focused in that study was ceramides and monohexosylceramide (HexCer) (162). They analyzed sphingosine (d18:1) and several lipid species of Cer and HexCer which they combined to one subclass and did regression analysis. Results showed increased levels of sphingosine and HexCer in patients with established RA. Early established RA showed only significantly increased sphingosine. Data in the Tomorrow cohort showed no significant changes in the Cer and HexCer lipid subclasses but the species of Cer 40:1↑, 40:2↓ and 41:2↓ were significantly different. In the HexCer subclass only the species 42:1 was significantly increased compared to the control group. Overall, the publication in the field of RA in combination with untargeted lipidomics are very limited, and comparison of data from different study cohorts is difficult due to different methods and patient cohorts.

5 Conclusion

In summary, in the current study we were able to process and analyze large cohorts of clinical blood serum samples from different health background, and an intervention study of a low-calorie liquid diet, with a state-of-the-art bench top mass spectrometer and with a comprehensive data processing method including statistical analysis with multivariate and univariate tools. We could show that not only the change in lipid profile is important also the change of total chain length and total saturation level are important. As this study was part of a multi-omics center study our present work might contribute to the other omics data and for further studies with similar biological groups.

The limitation of this study is - among others - the restricted access of metadata of the study cohorts, and the difficulty to use humans as a model because of the high diversity of the phenotypes (genetics, epigenetics and the environmental interactions), which could be a reason that the validation cohort did not show similar results. Therefore, outcome of such studies is difficult in interpretation and comparison. However, past and future work were used to validate results, and complementary methods with cell culture or animal studies could be powerful tools to elucidate the mechanisms behind non-specific results from omics studies like this one. Comparing literature data can also be challenging as long as many different approaches in terms of annotation and data analysis are used without strict standardization rules.

References

1. Planer JD, Peng Y, Kau AL, Blanton LV, Ndao IM, Tarr PI, et al. Development of the gut microbiota and mucosal IgA responses in twins and gnotobiotic mice. Nature. 2016;534(7606):263-6.
2. Turnbaugh PJ, Ley RE, Mahowald MA, Magrini V, Mardis ER, Gordon JI. An obesity-associated gut microbiome with increased capacity for energy harvest. Nature. 2006;444(7122):1027-31.
3. Hörmann N, Brandão I, Jäckel S, Ens N, Lillich M, Walter U, et al. Gut microbial colonization orchestrates TLR2 expression, signaling and epithelial proliferation in the small intestinal mucosa. PLoS One. 2014;9(11):e113080.
4. Pedersen HK, Gudmundsdottir V, Nielsen HB, Hyotylainen T, Nielsen T, Jensen BA, et al. Human gut microbes impact host serum metabolome and insulin sensitivity. Nature. 2016;535(7612):376-81.
5. Ley RE, Turnbaugh PJ, Klein S, Gordon JI. Microbial ecology: human gut microbes associated with obesity. Nature. 2006;444(7122):1022-3.
6. Vrieze A, Van Nood E, Holleman F, Salojärvi J, Kootte RS, Bartelsman JF, et al. Transfer of intestinal microbiota from lean donors increases insulin sensitivity in individuals with metabolic syndrome. Gastroenterology. 2012;143(4):913-6.e7.
7. Tang WH, Hazen SL. The contributory role of gut microbiota in cardiovascular disease. J Clin Invest. 2014;124(10):4204-11.
8. Trøseid M, Ueland T, Hov JR, Svardal A, Gregersen I, Dahl CP, et al. Microbiota-dependent metabolite trimethylamine-N-oxide is associated with disease severity and survival of patients with chronic heart failure. J Intern Med. 2015;277(6):717-26.
9. Rehman A, Rausch P, Wang J, Skieceviciene J, Kiudelis G, Bhagalia K, et al. Geographical patterns of the standing and active human gut microbiome in health and IBD. Gut. 2016;65(2):238-48.
10. Van de Wiele T, Van Praet JT, Marzorati M, Drennan MB, Elewaut D. How the microbiota shapes rheumatic diseases. Nat Rev Rheumatol. 2016;12(7):398-411.
11. Lertpiriyapong K, Whary MT, Muthupalani S, Lofgren JL, Gamazon ER, Feng Y, et al. Gastric colonisation with a restricted commensal microbiota replicates the promotion of neoplastic lesions by diverse intestinal microbiota in the Helicobacter pylori INS-GAS mouse model of gastric carcinogenesis. Gut. 2014;63(1):54-63.
12. Zambirinis CP, Pushalkar S, Saxena D, Miller G. Pancreatic cancer, inflammation, and microbiome. Cancer J. 2014;20(3):195-202.
13. Arumugam M, Raes J, Pelletier E, Le Paslier D, Yamada T, Mende DR, et al. Enterotypes of the human gut microbiome. Nature. 2011;473(7346):174-80.
14. Wang J, Linnenbrink M, Künzel S, Fernandes R, Nadeau MJ, Rosenstiel P, et al. Dietary history contributes to enterotype-like clustering and functional metagenomic content in the intestinal microbiome of wild mice. Proc Natl Acad Sci U S A. 2014;111(26):E2703-10.
15. De Filippo C, Cavalieri D, Di Paola M, Ramazzotti M, Poullet JB, Massart S, et al. Impact of diet in shaping gut microbiota revealed by a comparative study in children from Europe and rural Africa. Proc Natl Acad Sci U S A. 2010;107(33):14691-6.
16. Wu GD, Chen J, Hoffmann C, Bittinger K, Chen YY, Keilbaugh SA, et al. Linking long-term dietary patterns with gut microbial enterotypes. Science. 2011;334(6052):105-8.

17. Nicholson JK, Holmes E, Kinross J, Burcelin R, Gibson G, Jia W, et al. Host-gut microbiota metabolic interactions. Science. 2012;336(6086):1262-7.
18. Fahy E, Subramaniam S, Brown HA, Glass CK, Merrill AH, Murphy RC, et al. A comprehensive classification system for lipids. Journal of Lipid Research. 2005;46(5):839-61.
19. Fahy E, Alvarez-Jarreta J, Brasher CJ, Nguyen A, Hawksworth JI, Rodrigues P, et al. LipidFinder on LIPID MAPS: Peak filtering, MS searching and statistical analysis for lipidomics. Bioinformatics. 2019;35(4):685--7.
20. Schnaar RL. Gangliosides of the Vertebrate Nervous System. J Mol Biol. 2016;428(16):3325-36.
21. Kim J, Hoppel CL. Comprehensive approach to the quantitative analysis of mitochondrial phospholipids by HPLC-MS. J Chromatogr B Analyt Technol Biomed Life Sci. 2013;912:105-14.
22. Liebisch G, Drobnik W, Lieser B, Schmitz G. High-throughput quantification of lysophosphatidylcholine by electrospray ionization tandem mass spectrometry. Clin Chem. 2002;48(12):2217-24.
23. Scherer M, Schmitz G, Liebisch G. High-throughput analysis of sphingosine 1-phosphate, sphinganine 1-phosphate, and lysophosphatidic acid in plasma samples by liquid chromatography-tandem mass spectrometry. Clin Chem. 2009;55(6):1218-22.
24. Okudaira M, Inoue A, Shuto A, Nakanaga K, Kano K, Makide K, et al. Separation and quantification of 2-acyl-1-lysophospholipids and 1-acyl-2-lysophospholipids in biological samples by LC-MS/MS. J Lipid Res. 2014;55(10):2178-92.
25. Jurowski K, Kochan K, Walczak J, Baranska M, Piekoszewski W, Buszewski B. Analytical Techniques in Lipidomics: State of the Art. Crit Rev Anal Chem. 2017;47(5):418-37.
26. Wolf C, Quinn PJ. Lipidomics: practical aspects and applications. Prog Lipid Res. 2008;47(1):15-36.
27. Vasconcelos B, Teixeira JC, Dragone G, Teixeira JA. Optimization of lipid extraction from the oleaginous yeasts Rhodotorula glutinis and Lipomyces kononenkoae. AMB Express. 2018;8(1):126.
28. Goldberg S. Mechanical/physical methods of cell disruption and tissue homogenization. Methods Mol Biol. 2008;424:3-22.
29. Folch J, Lees M, Sloane Stanley GH. A simple method for the isolation and purification of total lipides from animal tissues. J Biol Chem. 1957;226(1):497-509.
30. Bligh EG, Dyer WJ. A rapid method of total lipid extraction and purification. Can J Biochem Physiol. 1959;37(8):911-7.
31. Matyash V, Liebisch G, Kurzchalia TV, Shevchenko A, Schwudke D. Lipid extraction by methyl-tert-butyl ether for high-throughput lipidomics. Journal of Lipid Research. 2008;49(5):1137-46.
32. Lofgren L, Stahlman M, Forsberg GB, Saarinen S, Nilsson R, Hansson GI. The BUME method: a novel automated chloroform-free 96-well total lipid extraction method for blood plasma. J Lipid Res. 2012;53(8):1690-700.
33. Sarafian MH, Gaudin M, Lewis MR, Martin FP, Holmes E, Nicholson JK, et al. Objective set of criteria for optimization of sample preparation procedures for ultra-high throughput untargeted blood plasma lipid profiling by ultra performance liquid chromatography-mass spectrometry. Anal Chem. 2014;86(12):5766-74.
34. Vale G, Martin SA, Mitsche MA, Thompson BM, Eckert KM, McDonald JG. Three-phase liquid extraction: a simple and fast method for lipidomic workflows. J Lipid Res. 2019;60(3):694-706.

35. Triebl A, Trotzmuller M, Eberl A, Hanel P, Hartler J, Kofeler HC. Quantitation of phosphatidic acid and lysophosphatidic acid molecular species using hydrophilic interaction liquid chromatography coupled to electrospray ionization high resolution mass spectrometry. Journal of Chromatography A. 2014;1347:104-10.
36. Hajek R, Jirasko R, Lisa M, Cifkova E, Holcapek M. Hydrophilic Interaction Liquid Chromatography-Mass Spectrometry Characterization of Gangliosides in Biological Samples. Anal Chem. 2017;89(22):12425-32.
37. Jin R, Li L, Feng J, Dai Z, Huang YW, Shen Q. Zwitterionic hydrophilic interaction solid-phase extraction and multi-dimensional mass spectrometry for shotgun lipidomic study of Hypophthalmichthys nobilis. Food Chem. 2017;216:347-54.
38. Sala P, Potz S, Brunner M, Trotzmuller M, Fauland A, Triebl A, et al. Determination of Oxidized Phosphatidylcholines by Hydrophilic Interaction Liquid Chromatography Coupled to Fourier Transform Mass Spectrometry. International Journal of Molecular Sciences. 2015;16(4):8351-63.
39. Griffiths WJ, Gilmore I, Yutuc E, Abdel-Khalik J, Crick PJ, Hearn T, et al. Identification of unusual oxysterols and bile acids with 7-oxo or 3beta,5alpha,6beta-trihydroxy functions in human plasma by charge-tagging mass spectrometry with multistage fragmentation. J Lipid Res. 2018;59(6):1058-70.
40. Wang M, Palavicini JP, Cseresznye A, Han X. Strategy for Quantitative Analysis of Isomeric Bis(monoacylglycero)phosphate and Phosphatidylglycerol Species by Shotgun Lipidomics after One-Step Methylation. Anal Chem. 2017;89(16):8490-5.
41. Clark J, Anderson KE, Juvin V, Smith TS, Karpe F, Wakelam MJ, et al. Quantification of PtdInsP3 molecular species in cells and tissues by mass spectrometry. Nat Methods. 2011;8(3):267-72.
42. Lee JC, Byeon SK, Moon MH. Relative Quantification of Phospholipids Based on Isotope-Labeled Methylation by Nanoflow Ultrahigh Performance Liquid Chromatography-Tandem Mass Spectrometry: Enhancement in Cardiolipin Profiling. Anal Chem. 2017;89(9):4969-77.
43. Narayana VK, Tomatis VM, Wang T, Kvaskoff D, Meunier FA. Profiling of Free Fatty Acids Using Stable Isotope Tagging Uncovers a Role for Saturated Fatty Acids in Neuroexocytosis. Chem Biol. 2015;22(11):1552-61.
44. Danne-Rasche N, Coman C, Ahrends R. Nano-LC/NSI MS Refines Lipidomics by Enhancing Lipid Coverage, Measurement Sensitivity, and Linear Dynamic Range. Anal Chem. 2018;90(13):8093-101.
45. Peng B, Weintraub ST, Coman C, Ponnaiyan S, Sharma R, Tews B, et al. A Comprehensive High-Resolution Targeted Workflow for the Deep Profiling of Sphingolipids. Anal Chem. 2017;89(22):12480-7.
46. Scherer M, Schmitz G, Liebisch G. Simultaneous quantification of cardiolipin, bis(monoacylglycero)phosphate and their precursors by hydrophilic interaction LC-MS/MS including correction of isotopic overlap. Anal Chem. 2010;82(21):8794-9.
47. Cifkova E, Holcapek M, Lisa M, Ovcacikova M, Lycka A, Lynen F, et al. Nontargeted quantitation of lipid classes using hydrophilic interaction liquid chromatography-electrospray ionization mass spectrometry with single internal standard and response factor approach. Anal Chem. 2012;84(22):10064-70.
48. Holcapek M, Liebisch G, Ekroos K. Lipidomic Analysis. Anal Chem. 2018;90(7):4249-57.
49. Knittelfelder OL, Weberhofer BP, Eichmann TO, Kohlwein SD, Rechberger GN. A versatile ultra-high performance LC-MS method for lipid profiling. J Chromatogr B Analyt Technol Biomed Life Sci. 2014;951-952:119-28.

50. Fauland A, Kofeler H, Trotzmuller M, Knopf A, Hartler J, Eberl A, et al. A comprehensive method for lipid profiling by liquid chromatography-ion cyclotron resonance mass spectrometry. J Lipid Res. 2011;52(12):2314-22.
51. Triebl A, Burla B, Selvalatchmanan J, Oh J, Tan SH, Chan MY, et al. Shared reference materials harmonize lipidomics across MS-based detection platforms and laboratories. J Lipid Res. 2020;61(1):105-15.
52. Triebl A, Weißengruber S, Trötzmüller M, Lankmayr E, Köfeler HC. Quantitative analysis of N acylphosphatidylethanolamine molecular species in rat brain using solid phase extraction combined with reversed phase chromatography and tandem mass spectrometry detection. Journal of Separation Science. 2016;in press.
53. Quehenberger O, Armando AM, Brown AH, Milne SB, Myers DS, Merrill AH, et al. Lipidomics reveals a remarkable diversity of lipids in human plasma. Journal of Lipid Research. 2010;51(11):3299-305.
54. Khan MJ, Codreanu SG, Goyal S, Wages PA, Gorti SKK, Pearson MJ, et al. Evaluating a targeted multiple reaction monitoring approach to global untargeted lipidomic analyses of human plasma. Rapid Commun Mass Spectrom. 2020;34(22):e8911.
55. Schott HF, Krautbauer S, Horing M, Liebisch G, Matysik S. A Validated, Fast Method for Quantification of Sterols and Gut Microbiome Derived 5alpha/beta-Stanols in Human Feces by Isotope Dilution LC-High-Resolution MS. Anal Chem. 2018;90(14):8487-94.
56. Triebl A, Trotzmuller M, Hartler J, Stojakovic T, Kofeler HC. Lipidomics by ultrahigh performance liquid chromatography-high resolution mass spectrometry and its application to complex biological samples. Journal of Chromatography B. 2017;1053:72-80.
57. Xuan Q, Hu C, Yu D, Wang L, Zhou Y, Zhao X, et al. Development of a High Coverage Pseudotargeted Lipidomics Method Based on Ultra-High Performance Liquid Chromatography-Mass Spectrometry. Anal Chem. 2018;90(12):7608-16.
58. Contrepois K, Mahmoudi S, Ubhi BK, Papsdorf K, Hornburg D, Brunet A, et al. Cross-Platform Comparison of Untargeted and Targeted Lipidomics Approaches on Aging Mouse Plasma. Sci Rep. 2018;8(1):17747.
59. Cajka T, Smilowitz JT, Fiehn O. Validating Quantitative Untargeted Lipidomics Across Nine Liquid Chromatography-High-Resolution Mass Spectrometry Platforms. Anal Chem. 2017;89(22):12360-8.
60. Raetz M, Bonner R, Hopfgartner G. SWATH-MS for metabolomics and lipidomics: critical aspects of qualitative and quantitative analysis. Metabolomics. 2020;16(6):71.
61. Yan L, Zhou J, Wang D, Si D, Liu Y, Zhong L, et al. Unbiased lipidomic profiling reveals metabolomic changes during the onset and antipsychotics treatment of schizophrenia disease. Metabolomics. 2018;14(6):80.
62. Schlotterbeck J, Chatterjee M, Gawaz M, Lämmerhofer M. Comprehensive MS/MS profiling by UHPLC-ESI-QTOF-MS/MS using SWATH data-independent acquisition for the study of platelet lipidomes in coronary artery disease. Anal Chim Acta. 2019;1046:1-15.
63. Han XL, Gross RW. Electrospray-Ionization Mass Spectroscopic Analysis of Human Erythrocyte Plasma-Membrane Phospholipids. Proceedings of the National Academy of Sciences of the United States of America. 1994;91(22):10635-9.
64. Han XL, Gross RW. Shotgun lipidomics: Electrospray ionization mass spectrometric analysis and quantitation of cellular lipidomes directly from crude extracts of biological samples. Mass Spectrometry Reviews. 2005;24(3):367-412.
65. Liebisch G, Drobnik W, Reil M, Trumbach B, Arnecke R, Olgemoller B, et al. Quantitative measurement of different ceramide species from crude cellular extracts by electrospray ionization tandem mass spectrometry (ESI-MS/MS). Journal of Lipid Research. 1999;40(8):1539-46.

66. Schwudke D, Oegema J, Burton L, Entchev E, Hannich JT, Ejsing CS, et al. Lipid profiling by multiple precursor and neutral loss scanning driven by the data-dependent acquisition. Analytical Chemistry. 2006;78(2):585-95.
67. Hsu FF. Mass spectrometry-based shotgun lipidomics - a critical review from the technical point of view. Anal Bioanal Chem. 2018;410(25):6387-409.
68. Nielsen I, Vidas Olsen A, Dicroce-Giacobini J, Papaleo E, Andersen KK, Jäättelä M, et al. Comprehensive Evaluation of a Quantitative Shotgun Lipidomics Platform for Mammalian Sample Analysis on a High-Resolution Mass Spectrometer. J Am Soc Mass Spectrom. 2020;31(4):894-907.
69. Liebisch G, Vizcaino JA, Kofeler H, Trotzmuller M, Griffiths WJ, Schmitz G, et al. Shorthand notation for lipid structures derived from mass spectrometry. Journal of Lipid Research. 2013;54(6):1523-30.
70. Horing M, Ejsing CS, Hermansson M, Liebisch G. Quantification of Cholesterol and Cholesteryl Ester by Direct Flow Injection High-Resolution Fourier Transform Mass Spectrometry Utilizing Species-Specific Response Factors. Anal Chem. 2019;91(5):3459-66.
71. Bielow C, Mastrobuoni G, Orioli M, Kempa S. On Mass Ambiguities in High-Resolution Shotgun Lipidomics. Anal Chem. 2017;89(5):2986-94.
72. Schuhmann K, Srzentic K, Nagornov KO, Thomas H, Gutmann T, Coskun U, et al. Monitoring Membrane Lipidome Turnover by Metabolic (15)N Labeling and Shotgun Ultra-High-Resolution Orbitrap Fourier Transform Mass Spectrometry. Anal Chem. 2017;89(23):12857-65.
73. Gao F, McDaniel J, Chen EY, Rockwell HE, Nguyen C, Lynes MD, et al. Adapted MS/MS(ALL) Shotgun Lipidomics Approach for Analysis of Cardiolipin Molecular Species. Lipids. 2018;53(1):133-42.
74. Almeida R, Pauling JK, Sokol E, Hannibal-Bach HK, Ejsing CS. Comprehensive lipidome analysis by shotgun lipidomics on a hybrid quadrupole-orbitrap-linear ion trap mass spectrometer. J Am Soc Mass Spectrom. 2015;26(1):133-48.
75. Abbassi-Ghadi N, Jones EA, Gomez-Romero M, Golf O, Kumar S, Huang J, et al. A Comparison of DESI-MS and LC-MS for the Lipidomic Profiling of Human Cancer Tissue. J Am Soc Mass Spectrom. 2016;27(2):255-64.
76. Klein DR, Feider CL, Garza KY, Lin JQ, Eberlin LS, Brodbelt JS. Desorption Electrospray Ionization Coupled with Ultraviolet Photodissociation for Characterization of Phospholipid Isomers in Tissue Sections. Anal Chem. 2018;90(17):10100-4.
77. Ellis SR, Paine MRL, Eijkel GB, Pauling JK, Husen P, Jervelund MW, et al. Automated, parallel mass spectrometry imaging and structural identification of lipids. Nat Methods. 2018;15(7):515-8.
78. Keating JE, Glish GL. Dual Emitter Nano-Electrospray Ionization Coupled to Differential Ion Mobility Spectrometry-Mass Spectrometry for Shotgun Lipidomics. Anal Chem. 2018;90(15):9117-24.
79. Blazenovic I, Shen T, Mehta SS, Kind T, Ji J, Piparo M, et al. Increasing Compound Identification Rates in Untargeted Lipidomics Research with Liquid Chromatography Drift Time-Ion Mobility Mass Spectrometry. Anal Chem. 2018;90(18):10758-64.
80. Zhou Z, Tu J, Zhu ZJ. Advancing the large-scale CCS database for metabolomics and lipidomics at the machine-learning era. Curr Opin Chem Biol. 2018;42:34-41.
81. Leaptrot KL, May JC, Dodds JN, McLean JA. Ion mobility conformational lipid atlas for high confidence lipidomics. Nat Commun. 2019;10(1):985.
82. Zhou Z, Shen X, Chen X, Tu J, Xiong X, Zhu ZJ. LipidIMMS Analyzer: Integrating multi-dimensional information to support lipid identification in ion mobility - Mass spectrometry based lipidomics. Bioinformatics. 2019;35(4):698--700.

83. Hinz C, Liggi S, Mocciaro G, Jung S, Induruwa I, Pereira M, et al. A Comprehensive UHPLC Ion Mobility Quadrupole Time-of-Flight Method for Profiling and Quantification of Eicosanoids, Other Oxylipins, and Fatty Acids. Anal Chem. 2019;91(13):8025-35.
84. Zhou Z, Tu J, Xiong X, Shen X, Zhu ZJ. LipidCCS: Prediction of Collision Cross-Section Values for Lipids with High Precision To Support Ion Mobility-Mass Spectrometry-Based Lipidomics. Anal Chem. 2017;89(17):9559-66.
85. Liebisch G, Fahy E, Aoki J, Dennis EA, Durand T, Ejsing CS, et al. Update on LIPID MAPS classification, nomenclature, and shorthand notation for MS-derived lipid structures. Journal of Lipid Research. 2020;61(12):1539-55.
86. Ryan E, Nguyen CQN, Shiea C, Reid GE. Detailed Structural Characterization of Sphingolipids via 193 nm Ultraviolet Photodissociation and Ultra High Resolution Tandem Mass Spectrometry. J Am Soc Mass Spectrom. 2017;28(7):1406-19.
87. Williams PE, Klein DR, Greer SM, Brodbelt JS. Pinpointing Double Bond and sn-Positions in Glycerophospholipids via Hybrid 193 nm Ultraviolet Photodissociation (UVPD) Mass Spectrometry. J Am Chem Soc. 2017;139(44):15681-90.
88. Brown SHJ, Mitchell TW, Blanksby SJ. Analysis of unsaturated lipids by ozone-induced dissociation. Biochimica Et Biophysica Acta-Molecular and Cell Biology of Lipids. 2011;1811(11):807-17.
89. Zhang W, Zhang D, Chen Q, Wu J, Ouyang Z, Xia Y. Online photochemical derivatization enables comprehensive mass spectrometric analysis of unsaturated phospholipid isomers. Nat Commun. 2019;10(1):79.
90. Han X, Yang K, Gross RW. Microfluidics-based electrospray ionization enhances the intrasource separation of lipid classes and extends identification of individual molecular species through multi-dimensional mass spectrometry: development of an automated high-throughput platform for shotgun lipidomics. Rapid Commun Mass Spectrom. 2008;22(13):2115-24.
91. Jiang X, Cheng H, Yang K, Gross RW, Han X. Alkaline methanolysis of lipid extracts extends shotgun lipidomics analyses to the low-abundance regime of cellular sphingolipids. Anal Biochem. 2007;371(2):135-45.
92. Yang K, Cheng H, Gross RW, Han X. Automated lipid identification and quantification by multidimensional mass spectrometry-based shotgun lipidomics. Anal Chem. 2009;81(11):4356-68.
93. Herzog R, Schwudke D, Shevchenko A. LipidXplorer: Software for Quantitative Shotgun Lipidomics Compatible with Multiple Mass Spectrometry Platforms. Curr Protoc Bioinformatics. 2013;43:14 2 1-30.
94. Herzog R, Schuhmann K, Schwudke D, Sampaio JL, Bornstein SR, Schroeder M, et al. LipidXplorer: a software for consensual cross-platform lipidomics. PLoS One. 2012;7(1):e29851.
95. Herzog R, Schwudke D, Schuhmann K, Sampaio JL, Bornstein SR, Schroeder M, et al. A novel informatics concept for high-throughput shotgun lipidomics based on the molecular fragmentation query language. Genome Biol. 2011;12(1):R8.
96. Schwudke D, Hannich JT, Surendranath V, Grimard V, Moehring T, Burton L, et al. Top-down lipidomic screens by multivariate analysis of high-resolution survey mass spectra. Anal Chem. 2007;79(11):4083-93.
97. Husen P, Tarasov K, Katafiasz M, Sokol E, Vogt J, Baumgart J, et al. Analysis of lipid experiments (ALEX): a software framework for analysis of high-resolution shotgun lipidomics data. PLoS One. 2013;8(11):e79736.

98. Benton HP, Ivanisevic J, Mahieu NG, Kurczy ME, Johnson CH, Franco L, et al. Autonomous metabolomics for rapid metabolite identification in global profiling. Anal Chem. 2015;87(2):884-91.
99. Fenaille F, Barbier Saint-Hilaire P, Rousseau K, Junot C. Data acquisition workflows in liquid chromatography coupled to high resolution mass spectrometry-based metabolomics: Where do we stand? J Chromatogr A. 2017;1526:1-12.
100. Zullig T, Trotzmuller M, Kofeler HC. Lipidomics from sample preparation to data analysis: a primer. Anal Bioanal Chem. 2020;412(10):2191-209.
101. Adusumilli R, Mallick P. Data conversion with proteoWizard msConvert. 2017.
102. Holman JD, Tabb DL, Mallick P. Employing ProteoWizard to convert raw mass spectrometry data. Current Protocols in Bioinformatics. 2014.
103. Tsugawa H, Ikeda K, Takahashi M, Satoh A, Mori Y, Uchino H, et al. A lipidome atlas in MS-DIAL 4. Nat Biotechnol. 2020;38(10):1159-63.
104. Tautenhahn R, Bottcher C, Neumann S. Highly sensitive feature detection for high resolution LC/MS. BMC Bioinformatics. 2008;9:1--16.
105. Mahieu NG, Genenbacher JL, Patti GJ. A roadmap for the XCMS family of software solutions in metabolomics. Curr Opin Chem Biol. 2016;30:87-93.
106. Hartler J, Trotzmuller M, Chitraju C, Spener F, Kofeler HC, Thallinger GG. Lipid Data Analyzer: unattended identification and quantitation of lipids in LC-MS data. Bioinformatics. 2011;27(4):572-7.
107. Pluskal T, Castillo S, Villar-Briones A, Orei. MZmine 2: Modular framework for processing, visualizing, and analyzing mass spectrometry-based molecular profile data. BMC Bioinformatics. 2010;11.
108. Koelmel JP, Kroeger NM, Ulmer CZ, Bowden JA, Patterson RE, Cochran JA, et al. LipidMatch: an automated workflow for rule-based lipid identification using untargeted high-resolution tandem mass spectrometry data. BMC Bioinformatics. 2017;18(1):331.
109. Foster JM, Moreno P, Fabregat A, Hermjakob H, Steinbeck C, Apweiler R, et al. LipidHome: a database of theoretical lipids optimized for high throughput mass spectrometry lipidomics. PLoS One. 2013;8(5):e61951.
110. Fahy E, Sud M, Cotter D, Subramaniam S. LIPID MAPS online tools for lipid research. Nucleic Acids Res. 2007;35(Web Server issue):W606-12.
111. Wishart DS, Feunang YD, Marcu A, Guo AC, Liang K, Vazquez-Fresno R, et al. HMDB 4.0: the human metabolome database for 2018. Nucleic Acids Res. 2018;46(D1):D608-D17.
112. Zullig T, Zandl-Lang M, Trotzmuller M, Hartler J, Plecko B, Kofeler HC. A Metabolomics Workflow for Analyzing Complex Biological Samples Using a Combined Method of Untargeted and Target-List Based Approaches. Metabolites. 2020;10(9).
113. Smith CA, O'Maille G, Want EJ, Qin C, Trauger SA, Brandon TR, et al. METLIN: a metabolite mass spectral database. Ther Drug Monit. 2005;27(6):747-51.
114. Benton HP, Wong DM, Trauger SA, Siuzdak G. XCMS2: Processing tandem mass spectrometry data for metabolite identification and structural characterization. Analytical Chemistry. 2008.
115. Pfeuffer J, Sachsenberg T, Alka O, Walzer M, Fillbrunn A, Nilse L, et al. OpenMS – A platform for reproducible analysis of mass spectrometry data. Journal of Biotechnology. 2017;261(May):142--8.
116. Hutchins PD, Russell JD, Coon JJ. Mapping Lipid Fragmentation for Tailored Mass Spectral Libraries. Journal of the American Society for Mass Spectrometry. 2019.
117. Hutchins PD, Russell JD, Coon JJ. LipiDex: An Integrated Software Package for High-Confidence Lipid Identification. Cell Syst. 2018;6(5):621-5 e5.

118. Cajka T, Fiehn O. LC-MS-Based Lipidomics and Automated Identification of Lipids Using the LipidBlast In-Silico MS/MS Library. Methods Mol Biol. 2017;1609:149-70.
119. Alcoriza-Balaguer MI, Garca-Caaveras JC, Lpez A, Conde I, Juan O, Carretero J, et al. LipidMS: An R Package for Lipid Annotation in Untargeted Liquid Chromatography-Data Independent Acquisition-Mass Spectrometry Lipidomics. Analytical Chemistry. 2019;91(1):836--45.
120. Hartler J, Triebl A, Ziegl A, Trtzmller M, Rechberger GN, Zeleznik OA, et al. Deciphering lipid structures based on platform-independent decision rules. Nature Methods. 2017;14(12):1171--4.
121. Ruttkies C, Schymanski EL, Wolf S, Hollender J, Neumann S. MetFrag relaunched: incorporating strategies beyond in silico fragmentation. J Cheminform. 2016;8:3.
122. Kanehisa M, Araki M, Goto S, Hattori M, Hirakawa M, Itoh M, et al. KEGG for linking genomes to life and the environment. Nucleic Acids Res. 2008;36(Database issue):D480-4.
123. Wang Y, Xiao J, Suzek TO, Zhang J, Wang J, Bryant SH. PubChem: a public information system for analyzing bioactivities of small molecules. Nucleic Acids Res. 2009;37(Web Server issue):W623-33.
124. Dührkop K, Shen H, Meusel M, Rousu J, Böcker S. Searching molecular structure databases with tandem mass spectra using CSI:FingerID. Proceedings of the National Academy of Sciences. 2015;112:12580-5.
125. Djoumbou-Feunang Y, Pon A, Karu N, Zheng J, Li C, Arndt D, et al. CFM-ID 3.0: Significantly Improved ESI-MS/MS Prediction and Compound Identification. Metabolites. 2019;9(4):72.
126. Sampson JN, Boca SM, Shu XO, Stolzenberg-Solomon RZ, Matthews CE, Hsing AW, et al. Metabolomics in epidemiology: sources of variability in metabolite measurements and implications. Cancer Epidemiol Biomarkers Prev. 2013;22(4):631-40.
127. Li B, Tang J, Yang Q, Li S, Cui X, Li Y, et al. NOREVA: normalization and evaluation of MS-based metabolomics data. Nucleic Acids Res. 2017;45(W1):W162-W70.
128. Wang SY, Kuo CH, Tseng YJ. Batch Normalizer: a fast total abundance regression calibration method to simultaneously adjust batch and injection order effects in liquid chromatography/time-of-flight mass spectrometry-based metabolomics data and comparison with current calibration methods. Anal Chem. 2013;85(2):1037-46.
129. Fan S, Kind T, Cajka T, Hazen SL, Tang WHW, Kaddurah-Daouk R, et al. Systematic Error Removal Using Random Forest for Normalizing Large-Scale Untargeted Lipidomics Data. Anal Chem. 2019;91(5):3590-6.
130. Luan H, Ji F, Chen Y, Cai Z. statTarget: A streamlined tool for signal drift correction and interpretations of quantitative mass spectrometry-based omics data. Anal Chim Acta. 2018;1036:66-72.
131. Sysi-Aho M, Katajamaa M, Yetukuri L, Oresic M. Normalization method for metabolomics data using optimal selection of multiple internal standards. BMC Bioinformatics. 2007;8:93.
132. Boysen AK, Heal KR, Carlson LT, Ingalls AE. Best-Matched Internal Standard Normalization in Liquid Chromatography-Mass Spectrometry Metabolomics Applied to Environmental Samples. Anal Chem. 2018;90(2):1363-9.
133. Redestig H, Fukushima A, Stenlund H, Moritz T, Arita M, Saito K, et al. Compensation for systematic cross-contribution improves normalization of mass spectrometry based metabolomics data. Anal Chem. 2009;81(19):7974-80.
134. Hartler J, Trötzmuller M, Chitraju C, Spener F, Köfeler HC, Thallinger GG. Lipid Data Analyzer: unattended identification and quantitation of lipids in LC-MS data. Bioinformatics. 2011;27(4):572-7.

135. Koelmel JP, Cochran JA, Ulmer CZ, Levy AJ, Patterson RE, Olsen BC, et al. Software tool for internal standard based normalization of lipids, and effect of data-processing strategies on resulting values. BMC Bioinformatics. 2019;20(1):217.
136. Hocher B, Adamski J. Metabolomics for clinical use and research in chronic kidney disease. Nat Rev Nephrol. 2017;13(5):269-84.
137. Jové M, Portero-Otín M, Naudí A, Ferrer I, Pamplona R. Metabolomics of human brain aging and age-related neurodegenerative diseases. J Neuropathol Exp Neurol. 2014;73(7):640-57.
138. Jolliffe IT, Cadima J. Principal component analysis: a review and recent developments. Philos Trans A Math Phys Eng Sci. 2016;374(2065):20150202.
139. Trygg J, Wold S. Orthogonal projections to latent structures (O-PLS). Journal of Chemometrics. 2002;16(3):119-28.
140. Bylesjö M, Rantalainen M, Cloarec O, Nicholson JK, Holmes E, Trygg J. OPLS discriminant analysis: combining the strengths of PLS-DA and SIMCA classification. Journal of Chemometrics. 2006;20(8-10):341-51.
141. Wang T, Shao K, Chu Q, Ren Y, Mu Y, Qu L, et al. Automics: an integrated platform for NMR-based metabonomics spectral processing and data analysis. BMC Bioinformatics. 2009;10:83.
142. Chong J, Soufan O, Li C, Caraus I, Li S, Bourque G, et al. MetaboAnalyst 4.0: towards more transparent and integrative metabolomics analysis. Nucleic Acids Res. 2018;46(W1):W486-W94.
143. Chong J, Wishart DS, Xia J. Using MetaboAnalyst 4.0 for Comprehensive and Integrative Metabolomics Data Analysis. Curr Protoc Bioinformatics. 2019;68(1):e86.
144. Chong J, Xia J. Using MetaboAnalyst 4.0 for Metabolomics Data Analysis, Interpretation, and Integration with Other Omics Data. Methods Mol Biol. 2020;2104:337-60.
145. Mohamed A, Molendijk J, Hill MM. lipidr: A Software Tool for Data Mining and Analysis of Lipidomics Datasets. J Proteome Res. 2020;19(7):2890-7.
146. Wickham H. ggplot:2 Elegant Graphics for Data Analysis. Springer-Verlag New York; 2016.
147. Wickham H, François R. dplyr: A Grammar of Data Manipulation. 2014.
148. Triebl A, Trotzmuller M, Hartler J, Stojakovic T, Kofeler HC. Lipidomics by ultrahigh performance liquid chromatography-high resolution mass spectrometry and its application to complex biological samples. J Chromatogr B Analyt Technol Biomed Life Sci. 2017;1053:72-80.
149. Lísa M, Cífková E, Khalikova M, Ovčačíková M, Holčapek M. Lipidomic analysis of biological samples: Comparison of liquid chromatography, supercritical fluid chromatography and direct infusion mass spectrometry methods. J Chromatogr A. 2017;1525:96-108.
150. Koelmel JP, Li X, Stow SM, Sartain MJ, Murali A, Kemperman R, et al. Lipid Annotator: Towards Accurate Annotation in Non-Targeted Liquid Chromatography High-Resolution Tandem Mass Spectrometry (LC-HRMS/MS) Lipidomics Using A Rapid and User-Friendly Software. Metabolites. 2020;10(3).
151. Heberle H, Meirelles GV, da Silva FR, Telles GP, Minghim R. InteractiVenn: a web-based tool for the analysis of sets through Venn diagrams. BMC Bioinformatics. 2015;16:169.
152. Flach PA, Kull M. Precision-Recall-Gain curves: PR analysis done right. Proceedings of the 28th International Conference on Neural Information Processing Systems - Volume 1; Montreal, Canada: MIT Press; 2015. p. 838–46.

153. Meikle PJ, Wong G, Barlow CK, Weir JM, Greeve MA, MacIntosh GL, et al. Plasma lipid profiling shows similar associations with prediabetes and type 2 diabetes. PLoS One. 2013;8(9):e74341.
154. Haus JM, Kashyap SR, Kasumov T, Zhang R, Kelly KR, Defronzo RA, et al. Plasma ceramides are elevated in obese subjects with type 2 diabetes and correlate with the severity of insulin resistance. Diabetes. 2009;58(2):337-43.
155. Chew WS, Torta F, Ji S, Choi H, Begum H, Sim X, et al. Large-scale lipidomics identifies associations between plasma sphingolipids and T2DM incidence. JCI Insight. 2019;5.
156. Stegemann C, Pechlaner R, Willeit P, Langley SR, Mangino M, Mayr U, et al. Lipidomics profiling and risk of cardiovascular disease in the prospective population-based Bruneck study. Circulation. 2014;129(18):1821-31.
157. Guan S, Jia B, Chao K, Zhu X, Tang J, Li M, et al. UPLC-QTOF-MS-Based Plasma Lipidomic Profiling Reveals Biomarkers for Inflammatory Bowel Disease Diagnosis. J Proteome Res. 2020;19(2):600-9.
158. Fan F, Mundra PA, Fang L, Galvin A, Moore XL, Weir JM, et al. Lipidomic Profiling in Inflammatory Bowel Disease: Comparison Between Ulcerative Colitis and Crohn's Disease. Inflamm Bowel Dis. 2015;21(7):1511-8.
159. Iwatani S, Iijima H, Otake Y, Amano T, Tani M, Yoshihara T, et al. Novel mass spectrometry-based comprehensive lipidomic analysis of plasma from patients with inflammatory bowel disease. J Gastroenterol Hepatol. 2020;35(8):1355-64.
160. Bruderlein H, Daniel R, Boismenu D, Julien N, Couture F. Fatty acid profiles of serum phospholipids in patients suffering rheumatoid arthritis. Prog Lipid Res. 1981;20:625-31.
161. Łuczaj W, Moniuszko-Malinowska A, Domingues P, Domingues MR, Gindzienska-Sieskiewicz E, Skrzydlewska E. Plasma lipidomic profile signature of rheumatoid arthritis versus Lyme arthritis patients. Arch Biochem Biophys. 2018;654:105-14.
162. Miltenberger-Miltenyi G, Cruz-Machado AR, Saville J, Conceição VA, Calado Â, Lopes I, et al. Increased monohexosylceramide levels in the serum of established rheumatoid arthritis patients. Rheumatology (Oxford). 2020;59(8):2085-9.

APPENDIX

PUBLICATION RECORD (as of 07/2021)

Züllig T, Zandl-Lang M, Trotzmuller M, Hartler J, Plecko B, Kofeler HC. 2020. A Metabolomics Workflow for Analyzing Complex Biological Samples Using a Combined Method of Untargeted and Target-List Based Approaches. Metabolites 10.

Züllig T, Kofeler HC. 2020. High Resolution Mass Spectrometry in Lipidomics. Mass Spectrom Rev.

Züllig T, Trotzmuller M, Kofeler HC. 2020. Lipidomics from sample preparation to data analysis: a primer. Anal Bioanal Chem 412:2191-2209.

Parey K, Haapanen O, Sharma V, Kofeler H, Züllig T, Prinz S, Siegmund K, Wittig I, Mills DJ, Vonck J, Kuhlbrandt W, Zickermann V. 2019. High-resolution cryo-EM structures of respiratory complex I: Mechanism, assembly, and disease. Sci Adv 5:eaax9484.

Leithner K, Triebl A, Trotzmuller M, Hinteregger B, Leko P, Wieser BI, Grasmann G, Bertsch AL, Züllig T, Stacher E, Valli A, Prassl R, Olschewski A, Harris AL, Kofeler HC, Olschewski H, Hrzenjak A. 2018. The glycerol backbone of phospholipids derives from noncarbohydrate precursors in starved lung cancer cells. Proc Natl Acad Sci USA 115:6225-6230.

Ruth C, Zuellig T, Mellitzer A, Weis R, Looser V, Kovar K, Glieder A. 2010. Variable production windows for porcine trypsinogen employing synthetic inducible promoter variants in Pichia pastoris. Syst Synth Biol 4:181-191.

Hyka P, Züllig T, Ruth C, Looser V, Meier C, Klein J, Melzoch K, Meyer HP, Glieder A, Kovar K. 2010. Combined use of fluorescent dyes and flow cytometry to quantify the physiological state of Pichia pastoris during the production of heterologous proteins in high-cell-density fed-batch cultures. Appl Environ Microbiol 76:4486-4496.

LIST OF SUPPLEMENT FIGURES AND TABLES

Supplement Table 1. Used fragmentation energy adapted to different lipid classes in positive and negative mode.

Lipid Class	Adduct	NCE	Time Range [min]		mode
aPC	$[M+H]^+$	20	20	40	pos
aPE	$[M+H]^+$	20	20	40	pos
dhCer	$[M-OH]^+$	15	0	58	pos
HexCer	$[M-OH]^+$	15	0	58	pos
LPC	$[M+H]^+$	20	2	10	pos
LPE	$[M+H]^+$	25	2	15	pos
LPS	$[M+H]^+$	25	2	15	pos
MG	$[M+NH_4]^+$	20	0	10	pos
PC	$[M+H]^+$	23	18	30	pos
PE	$[M+H]^+$	23	10	35	pos
PS	$[M+H]^+$	23	10	35	pos
SM	$[M+H]^+$	17	15	40	pos
TG	$[M+NH_4]^+$	15	29	45	pos
DG	$[M+Na]^+$	15	19	40	pos
CE	$[M+NH_4]^+$	15	0	58	pos
Cer	$[M-OH]^+$	15	0	58	pos
aPC	$[M+HCO_2]^-$	15	0	58	neg
aPE	$[M+HCO_2]^-$	15	0	58	neg
CL	$[M-H]^-$	15	0	58	neg
LPA	$[M-H]^-$	15	0	58	neg
LPC	$[M+HCO_2]^-$	13	0	58	neg
LPE	$[M-H]^-$	21	0	58	neg
LPI	$[M-H]^-$	15	0	58	neg
PA	$[M-H]^-$	19	0	58	neg
PC	$[M+HCO_2]^-$	15	10	32	neg
PE	$[M-H]^-$	20	9	30	neg
PG	$[M-H]^-$	21	10	30	neg
PI	$[M-H]^-$	24	15	35	neg
PS	$[M-H]^-$	20	10	30	neg

Supplement Table 2. Used data processing settings with Lipid Data Analyzer

Key	Value	Key	Value
LDA-version	2.6.3_9	profileSteepnessChange1	1.5
rawFile	5_1.raw	profileSteepnessChange2	1.8
machineName	OrbiTrap_exactive	profileIntensityCutoff1	0.15
neutronMass	1.005	profileIntensityCutoff2	0.2
coarseChromMzTolerance	0.015	profileGeneralIntCutoff	0.03
MS2	true	profilePeakAcceptanceRange	0.012
basePeakCutoff	0.1	profileSmoothingCorrection	0
massShift	0	profileMaxRange	0.03
threeDViewerDefaultTimeResolution	2	smallChromMzRange	0.004
threeDViewerDefaultMZResolution	0.005	smallChromSmoothRepeats	3
ms2PrecursorTolerance	0.03	smallChromMeanSmoothRepeats	0
ms2MzTolerance	0.02	smallChromSmoothRange	2
ms2MinIntsForNoiseRemoval	100	smallChromIntensityCutoff	0.03
ms2IsobarSCExclusionRatio	0.01	broadChromSmoothRepeats	5
ms2IsobarSCFarExclusionRatio	0.1	broadChromMeanSmoothRepeats	0
ms2IsobaricOtherRtDifference	2	broadChromSmoothRange	2
chainCutoffValue	0.01	broadChromIntensityCutoff	0
ms2ChromMultiplicationFactorForInt	10	broadChromSteepnessChangeNoSmall	1.33
threeDViewerMs2DefaultTimeResolution	1	broadChromIntensityCutoffNoSmall	0.05
threeDViewerMs2DefaultMZResolution	1	finalProbeTimeCompTolerance	0.1
maxFileSizeForChromTranslationAtOnce	600	finalProbeMzCompTolerance	5.00E-04
chromMultiplicationFactorForInt	1000	overlapDistanceDeviationFactor	1.5
chromLowestResolution	1	overlapPossibleIntensityThreshold	0.15
chromSmoothRange	8	overlapSureIntensityThreshold	0.7
chromSmoothRepeats	4	overlapPeakDistanceDivisor	3
use3D	true	overlapFullDistanceDivisor	6
isotopeCorrection	false	peakDiscardingAreaFactor	1000
removeFromOtherIsotopes	true	isotopeInBetweenTime	30
respectIsotopicDistribution	true	isoInBetweenAreaFactor	3
useNoiseCutoff	true	isoNearNormalProbeTime	30
noiseCutoffDeviationValue	2	relativeAreaCutoff	0.05
scanStep	2	relativeFarAreaCutoff	0.05
profileMzRangeExtraction	0.05	relativeFarAreaTimeSpace	30
profileTimeTolerance	5	relativeIsoInBetweenCutoff	0.5
profileIntThreshold	5	isoInBetweenMaxTimeDistance	300
broaderProfileTimeTolerance	3	twinPeakMzTolerance	0.01
profileSmoothRange	0.0025	closePeakTimeTolerance	10
profileSmoothRepeats	1	twinInBetweenCutoff	0.95

profileMeanSmoothRepeats	2	unionInBetweenCutoff	0.8
profileMzMinRange	0.002	sparseData	false

Supplement Table 3 Inclusion list of the lipidomics acquisition method for positive and negative mode**.** (xx-xx): - number of carbon atoms, :(x-x) – number of double bonds.

		Positive
		(12-17):(0-2)
		(18-19):(0-4)
	SM	(20-30):(0-6)
		(4-6):0
		(10-10):(0-1)
		(12-12):(0-2)
		(14-14):(0-3)
		(16-18):(0-4)
		(20-20):(0-6)
		(22-22):(0-7)
	MG	(24-26):(0-8)
		(20-29):(0-3)
		(30-31):(0-4)
		(32-33):(0-6)
		(34-37):(0-8)
		(38-39):(0-10)
	DG	(40-46):(0-12)
		(28-29):(0-2)
		(30-39):(0-4)
		(40-47):(0-6)
		(48-49):(0-8)
		(50-53):(0-10)
		(54-57):(0-12)
		(58-59):(0-14)
		(60-63):(0-16)
	TG	(64-70):(0-18)
		(6-9):0
		(10-13):(0-1)
		(14-15):(0-3)
		(16-17):(0-4)
		(18-19):(0-6)
	CE	(20-26):(0-8)
		(2-5):0
		(6-9):(0-1)
		(10-13):(0-2)
		(14-15):(0-3)
		(16-17):(0-4)
Cer	HexCer	(18-30):(0-6)
		(2,8):0
		(12,13,15,17,19,21,27-40):(0-2)
		(14,23,25):(0-3)
		(16,18,26):(0-4)
		(22,24):(0-6)
	dhCer	(20):(0-7)
	LPS	(6-9):0
		(10-11):(0-1)
		(12-15):(0-4)

			(16-19):(0-6)
			(20-26):(0-8)
			negativ and positive
			(20-29):(0-4)
			(30-35):(0-6)
			(36-37):(0-8)
			(38-39):(0-10)
PC	PE	PS	(40-48):(0-12)
			(20-29):(0-3)
			(30-35):(0-5)
			(36-37):(0-7)
			(38-39):(0-9)
	aPC	aPE	(40-48):(0-11)
			(6-9):0
			(10-11):(0-1)
			(12-15):(0-4)
			(16-19):(0-6)
	LPE	LPC	(20-26):(0-8)
			negativ
			(48-49):0
			(50-53):(0-2)
			(54-57):(0-4)
			(58-59):(0-6)
			(60-67):(0-8)
			(68-71):(0-10)
			(72-73):(0-12)
			(74-79,81,83,85,87,89,91,93,95,97,99,101,103):(0-14)
			(80):(0-16)
			(82):(0-18)
			(84):(0-20)
		CL	(86,88,90,92,94,96,98,100,102,104):(0-22)
			(20-29):(0-4)
			(30-35):(0-6)
			(36-37):(0-8)
			(38-39):(0-10)
	PG	PI	(40-48):(0-12)
			(6-9):(0-0)
			(10-11):(0-1)
			(12-15):(0-4)
			(16-19):(0-6)
	LPI	LPA	(20-26):(0-8)

Supplement Table 4 coefficient of determination of pooled QC with different extraction volumes (5, 10, 20, 30 40, 50, 75, 100, and 150 µl) detected with TraceFinder 4.1

Lipid species	R^2	Lipid species	R^2	Lipid species	R^2	Lipid species	R^2	Lipid species	R^2	Lipid species	R^2
aPE 38:2	1.0000	TG 60:9	0.9932	PE 36:3	0.9885	TG 51:1	0.9785	TG 57:3	0.9454	PC 22:0	0.8480
SM 16:0	0.9982	TG 58:8	0.9930	SM 21:0	0.9885	CER 22:1	0.9783	CER 24:0	0.9449	CER 26:0	0.8471
SM 22:0	0.9980	PC 36:0	0.9929	aPE 40:4	0.9884	CER 26:3	0.9782	TG 42:2	0.9441	HEXCER 18:1	0.8440
PC 38:6	0.9979	PC 31:1	0.9929	SM 26:1	0.9883	PC 42:8	0.9776	TG 62:4	0.9438	PI 32:0	0.8412
TG 60:7	0.9979	CoQ 50:10	0.9928	SM 23:2	0.9882	CER 26:2	0.9775	LPC 22:4	0.9434	TG 62:2	0.8374
PC 31:0	0.9977	PC 34:0	0.9928	PE 36:2	0.9881	TG 55:8	0.9774	TG 58:4	0.9433	TG 46:1	0.8341
TG 58:9	0.9975	TG 58:7	0.9926	PE 38:3	0.9881	TG 50:5	0.9769	TG 44:2	0.9426	TG 53:5	0.8328
PC 40:3	0.9975	DG 38:5	0.9925	aPE 38:6	0.9880	TG 57:5	0.9767	TG 42:1	0.9425	PE 26:0	0.8240
TG 54:6	0.9974	TG 56:6	0.9925	LPC 15:0	0.9878	TG 46:3	0.9767	LPC 22:6	0.9421	TG 51:4	0.8234
TG 54:5	0.9974	PC 28:0	0.9924	SM 25:2	0.9878	SM 19:1	0.9766	CER 26:1	0.9408	DG 36:4	0.8201
TG 44:0	0.9969	PE 36:4	0.9924	TG 57:8	0.9877	PC 40:2	0.9766	CE 20:2	0.9393	PI 38:4	0.8178
PC 32:0	0.9968	PC 38:1	0.9923	LPC 17:0	0.9876	TG 58:5	0.9765	DG 38:6	0.9388	TG 53:4	0.8162
TG 55:6	0.9968	SM 20:1	0.9923	TG 54:7	0.9876	HEXCER 22:0	0.9764	CER 24:1	0.9382	PI 36:1	0.8033
TG 52:1	0.9967	PC 38:2	0.9921	SM 24:0	0.9873	CER 24:2	0.9764	LPC 22:5	0.9375	HEXCER 24:0	0.7999
TG 56:5	0.9967	PC 35:0	0.9921	TG 52:6	0.9873	TG 53:2	0.9762	TG 41:1	0.9374	TG 57:1	0.7936
PC 36:6	0.9966	aPE 36:4	0.9920	TG 48:1	0.9873	PE 34:0	0.9759	TG 64:4	0.9374	CE 24:6	0.7919
PC 35:3	0.9965	aPE 36:1	0.9919	TG 60:8	0.9872	TG 60:12	0.9759	PC 40:7	0.9372	TG 46:5	0.7895
TG 60:10	0.9965	PC 37:5	0.9919	TG 49:4	0.9872	TG 48:4	0.9753	TG 60:5	0.9370	PC 39:3	0.7803
TG 53:6	0.9965	TG 50:1	0.9919	LPE 22:4	0.9872	aPE 34:4	0.9752	HEXCER 23:0	0.9366	CE 18:4	0.7761
TG 56:7	0.9963	SM 22:2	0.9918	HEXCER 22:1	0.9872	LPC 18:3	0.9745	TG 42:3	0.9356	PC 38:7	0.7743
PC 40:6	0.9962	TG 49:1	0.9918	PE 34:3	0.9871	LPC 16:1	0.9743	TG 55:7	0.9340	PI 38:3	0.7564
TG 56:8	0.9962	PC 31:2	0.9918	LPE 18:0	0.9871	SM 18:2	0.9743	TG 48:5	0.9334	PI 34:2	0.7547
PC 29:0	0.9962	CoQ 35:7	0.9918	LPC 14:0	0.9870	TG 45:1	0.9741	TG 40:0	0.9325	PI 40:5	0.7510
TG 54:4	0.9961	TG 48:0	0.9917	LPE 18:2	0.9870	TG 52:7	0.9739	CER 23:0	0.9293	TG 56:0	0.7505
PC 32:2	0.9961	PE 38:5	0.9917	TG 49:2	0.9870	TG 52:2	0.9738	TG 50:7	0.9291	PI 40:4	0.7466
PC 33:1	0.9960	aPE 40:6	0.9916	CE 20:5	0.9869	PC 36:2	0.9736	PI 32:1	0.9288	LPE 22:0	0.7459
PC 36:5	0.9960	LPC 18:0	0.9916	CER 20:0	0.9868	LPC 18:2	0.9735	TG 58:3	0.9275	TG 59:2	0.7397
SM 18:0	0.9959	SM 15:0	0.9916	aPE 42:6	0.9865	TG 62:11	0.9735	TG 50:8	0.9242	TG 58:2	0.7393
SM 14:1	0.9959	SM 16:1	0.9913	PC 34:1	0.9864	PC 42:5	0.9721	TG 51:0	0.9241	TG 51:3	0.7360
TG 48:3	0.9958	aPE 38:4	0.9912	PC 39:6	0.9864	TG 60:6	0.9716	TG 62:12	0.9234	TG 64:2	0.7285
PC 36:1	0.9958	PC 32:3	0.9912	LPE 18:1	0.9860	TG 42:0	0.9713	TG 53:1	0.9226	PC 36:4	0.7252
TG 52:4	0.9958	LPC 20:0	0.9912	TG 53:3	0.9859	PC 40:1	0.9709	TG 54:9	0.9214	TG 62:8	0.7236
PC 38:3	0.9957	PE 36:1	0.9910	SM 19:2	0.9857	PC 38:0	0.9697	TG 46:4	0.9189	TG 60:0	0.7149
SM 24:1	0.9957	PC 37:2	0.9910	SM 26:2	0.9857	TG 58:11	0.9686	PI 38:6	0.9183	TG 64:3	0.7075
PC 37:4	0.9956	PC 34:5	0.9908	TG 45:0	0.9855	LPC 20:2	0.9684	LPE 22:1	0.9159	TG 58:0	0.7024
TG 52:5	0.9955	aPE 34:1	0.9907	PE 36:5	0.9854	TG 57:9	0.9682	aPE 36:6	0.9149	PI 38:2	0.6963
SM 24:2	0.9955	TG 54:3	0.9907	TG 56:9	0.9849	CER 21:0	0.9674	DG 38:3	0.9147	aPE 36:5	0.6860
TG 50:3	0.9954	aPE 38:5	0.9905	aPE 40:7	0.9848	CER 23:1	0.9667	TG 60:3	0.9131	TG 62:1	0.6817
TG 54:2	0.9953	DG 36:2	0.9903	LPE 20:1	0.9847	CE 16:0	0.9667	TG 62:5	0.9109	HEXCER 20:2	0.6683
SM 13:0	0.9952	SM 20:0	0.9903	TG 55:4	0.9846	TG 54:1	0.9663	TG 55:2	0.9099	TG 49:5	0.6052
PC 35:2	0.9952	CE 18:3	0.9903	CE 20:3	0.9846	PC 28:1	0.9656	TG 40:1	0.9086	TG 62:6	0.5948
PC 36:3	0.9952	SM 17:1	0.9903	TG 56:4	0.9845	PC 38:4	0.9652	CER 25:1	0.9077	PI 40:6	0.5859
PC 33:0	0.9951	PE 40:5	0.9903	SM 23:0	0.9844	SM 20:2	0.9652	PC 26:0	0.9075	PE 40:9	0.5853
TG 46:0	0.9951	CHOL	0.9901	TG 52:3	0.9843	TG 50:6	0.9650	SM 26:0	0.9063	PE 24:0	0.5535
TG 48:2	0.9950	aPE 36:2	0.9900	PE 34:1	0.9842	TG 41:0	0.9643	TG 49:3	0.9049	TG 55:0	0.5381
TG 57:7	0.9949	PC 35:4	0.9899	LPC 18:1	0.9840	TG 56:10	0.9640	TG 60:2	0.9047	TG 57:4	0.5321
SM 22:1	0.9948	PC 42:4	0.9899	LPE 20:3	0.9838	aPE 42:7	0.9626	PI 36:4	0.9046	TG 59:0	0.5296
PC 32:1	0.9948	TG 47:0	0.9899	TG 56:3	0.9838	TG 56:2	0.9624	TG 62:3	0.9041	DG 38:4	0.5194
HEXCER 16:0	0.9948	SM 14:0	0.9897	TG 50:0	0.9837	TG 43:1	0.9613	TG 60:4	0.9037	TG 59:1	0.5151
TG 57:6	0.9947	TG 47:1	0.9897	SM 24:3	0.9834	SM 25:0	0.9605	CER 25:0	0.9031	PC 30:1	0.5145
CER 16:0	0.9946	PC 37:1	0.9897	TG 49:0	0.9833	LPC 20:3	0.9590	TG 58:12	0.8999	DG 36:5	0.4996
SM 21:1	0.9946	PC 42:6	0.9896	TG 45:2	0.9833	aPE 34:3	0.9582	TG 58:1	0.8974	TG 58:6	0.4821
CER 18:0	0.9943	PC 40:5	0.9896	TG 44:1	0.9831	CER 22:0	0.9581	CER 18:1	0.8971	TG 44:3	0.4759
aPE 34:2	0.9943	CE 18:2	0.9895	LPC 16:2	0.9831	aPE 38:1	0.9576	PI 38:5	0.8915	TG 57:0	0.4594
PC 37:6	0.9942	TG 51:2	0.9895	TG 46:2	0.9830	PE 38:6	0.9561	TG 43:2	0.8913	DG 36:3	0.4273
PC 33:2	0.9941	TG 62:10	0.9894	SM 25:1	0.9829	LPE 16:0	0.9558	TG 56:1	0.8907	PE 42:8	0.4268
LPC 19:0	0.9939	PC 44:5	0.9894	TG 50:4	0.9826	LPC 20:5	0.9555	TG 59:3	0.8907	TG 61:2	0.4246
PC 30:0	0.9939	PC 42:7	0.9894	PC 42:3	0.9825	CER 20:1	0.9550	PC 39:5	0.8866	PC 35:5	0.4211
SM 12:0	0.9938	CE 22:6	0.9893	HEXCER 24:1	0.9821	TG 62:7	0.9544	TG 40:2	0.8836	CE 24:7	0.4194
PC 34:3	0.9938	TG 58:10	0.9893	DG 38:2	0.9821	LPC 20:4	0.9533	TG 54:0	0.8774	TG 55:5	0.3764
TG 50:2	0.9937	PC 40:8	0.9893	LPE 22:5	0.9818	PC 42:2	0.9533	TG 47:2	0.8750	CE 22:4	0.3000
SM 19:0	0.9936	TG 51:5	0.9893	CER 16:1	0.9799	TG 54:8	0.9527	TG 56:11	0.8742	PC 34:4	0.2941
TG 60:11	0.9936	TG 43:0	0.9892	TG 53:7	0.9798	TG 52:0	0.9526	TG 60:1	0.8731	TG 62:0	0.2875

PC 38:5	0.9936	LPE 22:6	0.9892	CE 18:1	0.9797	PC 34:2	0.9522	PC 42:10	0.8662	CE 24:8	0.2861
PC 39:4	0.9935	LPC 20:1	0.9890	PE 38:7	0.9797	CE 22:5	0.9519	TG 57:2	0.8661	PC 38:8	0.2430
SM 18:1	0.9935	CE 20:4	0.9890	aPE 42:5	0.9794	TG 55:3	0.9515	TG 64:1	0.8643	PC 25:0	0.1604
PC 37:3	0.9935	aPE 40:5	0.9889	TG 51:6	0.9794	TG 62:9	0.9511	PI 36:3	0.8638	PC 23:0	0.1342
SM 17:0	0.9934	SM 23:1	0.9887	SM 22:3	0.9793	TG 60:13	0.9482	PI 36:2	0.8612	PC 24:0	0.0602
LPC 16:0	0.9934	LPE 20:4	0.9886	LPC 14:1	0.9792	TG 47:3	0.9469	TG 55:1	0.8594	LPE 22:2	0.0000
PC 35:1	0.9933	aPE 38:3	0.9886	SM 22:4	0.9786	PE 38:4	0.9460	PI 34:1	0.8505	PE 40:8	0.0000
PC 40:4	0.9932	aPE 36:3	0.9886	PE 40:7	0.9786	PC 44:4	0.9458	LPE 20:2	0.8481	PE 42:9	0.0000

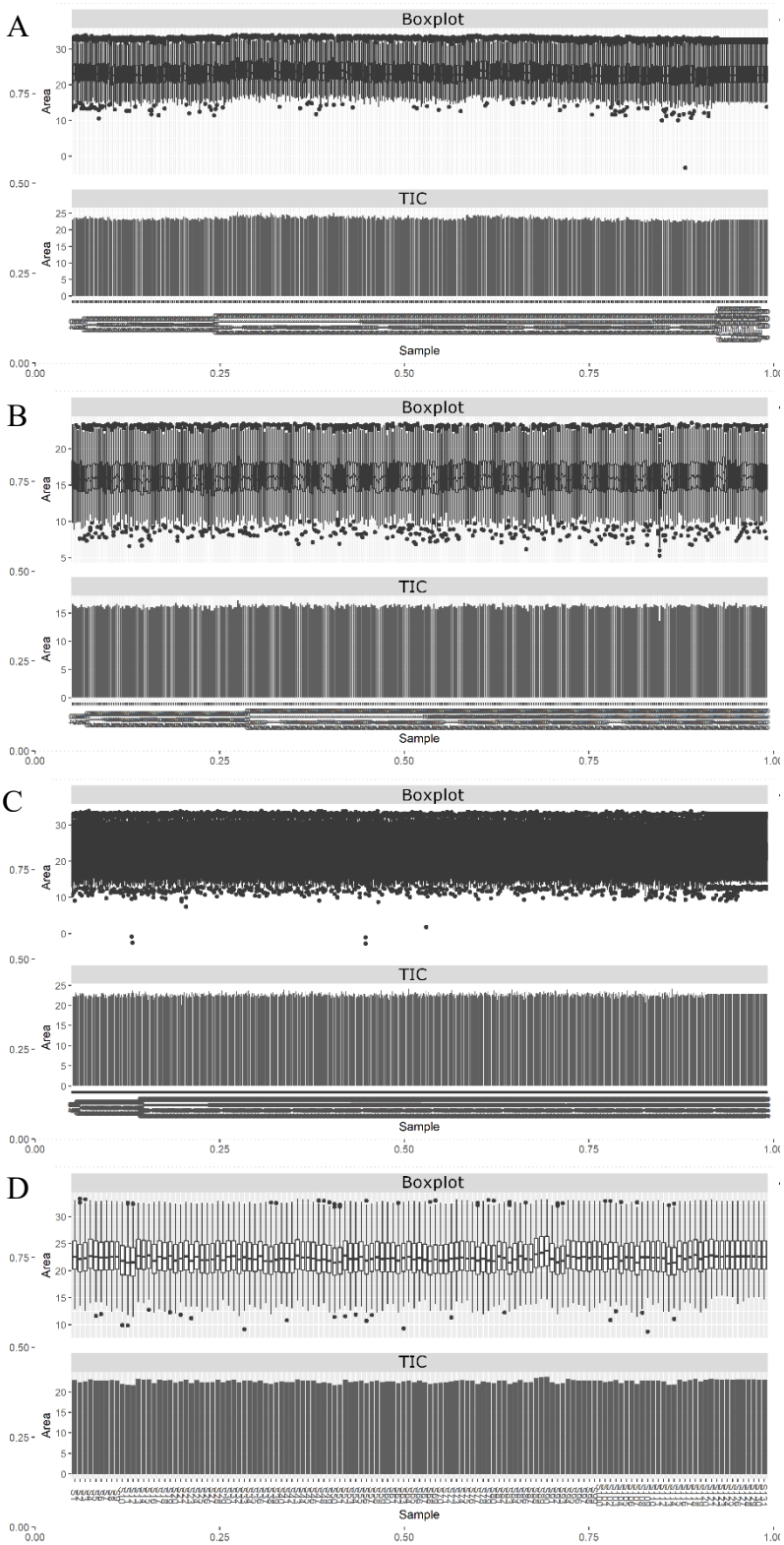
A
Boxplot
TIC
Area
Sample
B
Boxplot
TIC
Area
Sample
C
Boxplot
TIC
Area
Sample
D
Boxplot
TIC
Area
Sample

Supplement Figure 1 Overview of all sample shown as boxplot of all lipids and as sum (TIC) to show inconsistencies in the sample extraction or detection. Data shown as log2(area), A – Tomorrow, B – PopGen, C – FoCus, D – Intervention study. Sample B 339 is asymptotic and will be excluded.

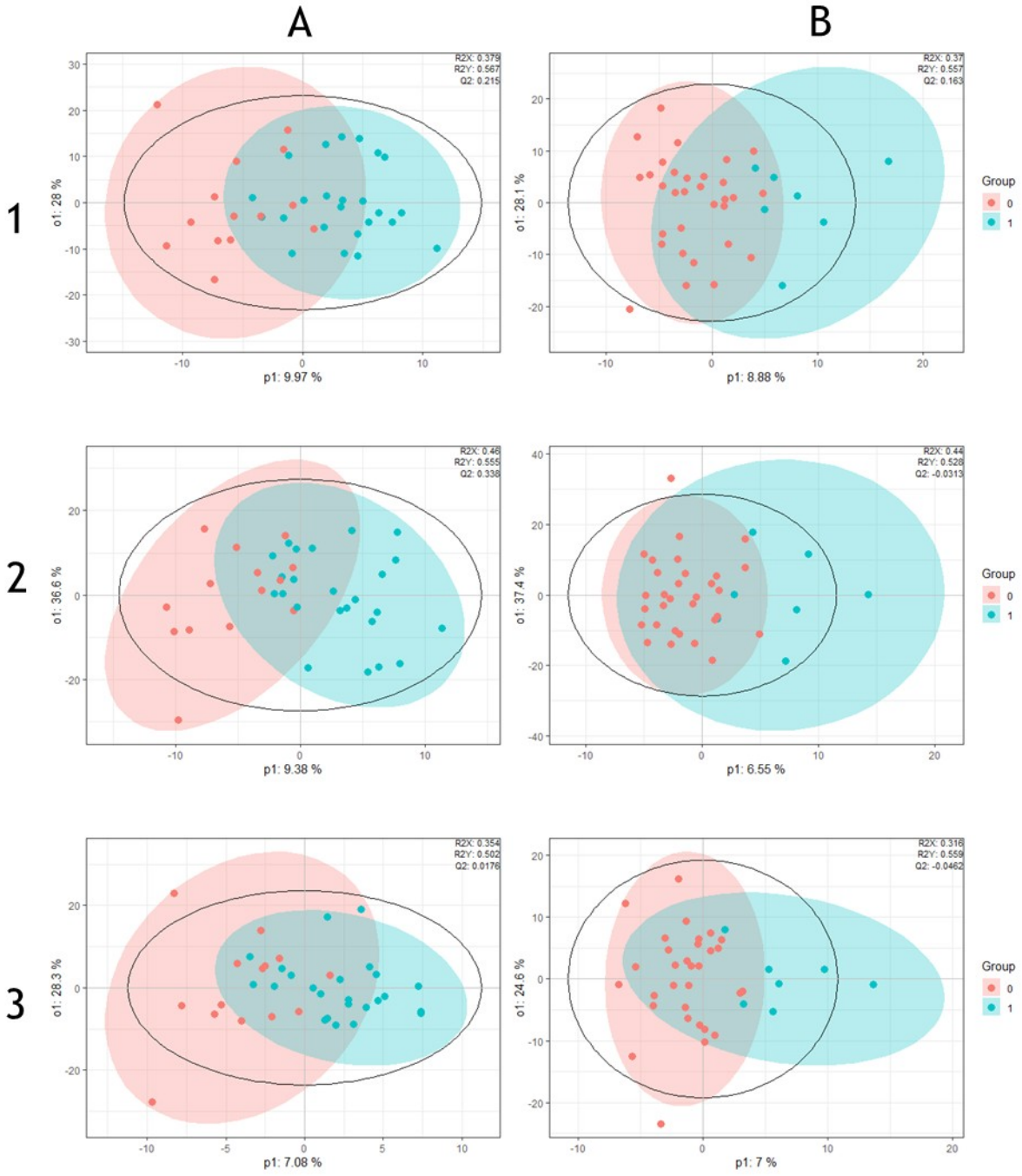

Supplement Figure 2 OPLS-DA plots of intervention study time point dependent (1,2, and 3) between obese control group (**0**) and health statues **A** (1-hypertension) or **B** (1-diabetes).

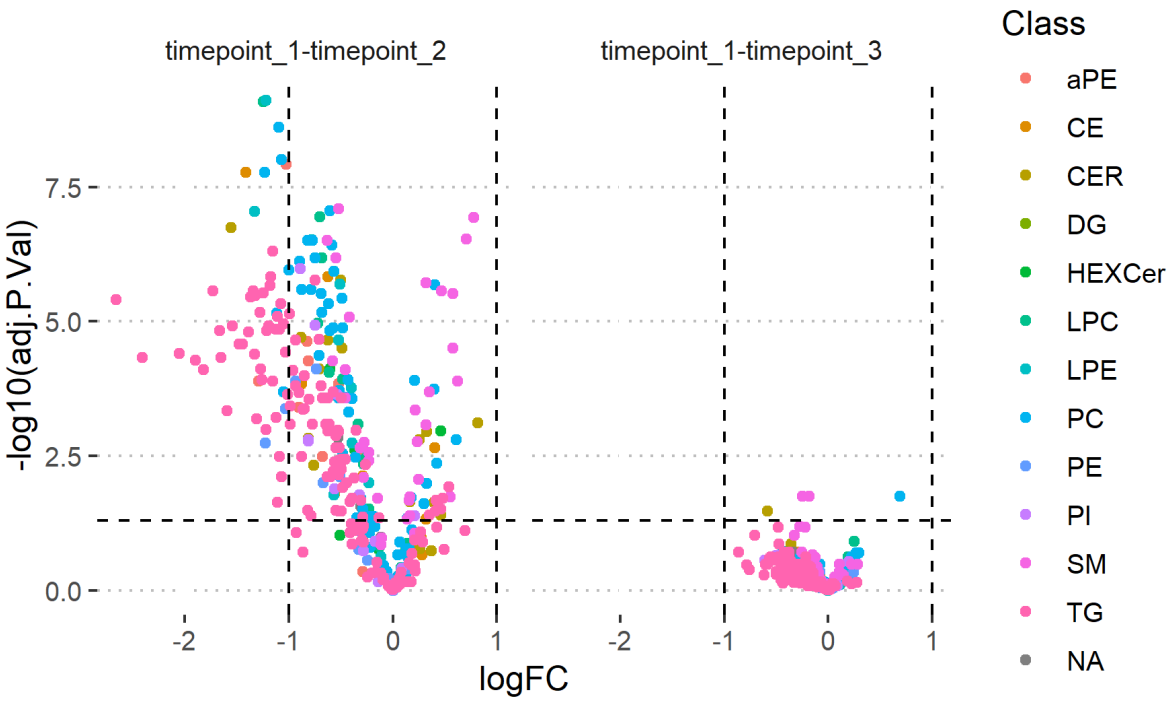

Supplement Figure 3 Volcano plots of obese candidates in a low-calorie intervention study data obtained at 3 time points and compared to starting point (time point_1). time point_2 – after 6 weeks liquid based low-calorie diet, time point_3 – 6 weeks normalization phase with normal food. logFC – log 2, fold change

Supplement Table 5 The 50 main drivers of differences in the OPLS-DA model between diabetes and Healthy subjects shown in ().

Molecule	rank	Molecule	rank	Molecule	rank	Molecule	rank	Molecule	rank
TG 58:6	1	TG 60:6	11	TG 53:2	21	TG 48:2	31	TG 55:6	41
TG 52:2	2	TG 56:4	12	TG 51:1	22	TG 54:7	32	TG 58:3	42
TG 52:1	3	TG 60:9	13	TG 53:3	23	TG 56:1	33	TG 56:8	43
TG 52:3	4	TG 51:2	14	TG 52:4	24	TG 60:5	34	TG 60:1	44
TG 50:2	5	TG 50:3	15	TG 50:0	25	TG 56:6	35	DG 36:3	45
TG 58:5	6	TG 55:4	16	TG 52:0	26	TG 48:0	36	TG 58:2	46
TG 54:6	7	TG 53:1	17	TG 55:5	27	TG 54:0	37	TG 51:0	47
TG 54:2	8	TG 54:1	18	TG 48:1	28	TG 57:5	38	TG 49:4	48
DG 36:2	9	TG 58:7	19	TG 56:7	29	TG 60:3	39	TG 57:4	49
TG 50:1	10	TG 56:2	20	TG 51:3	30	TG 60:10	40	TG 49:1	50

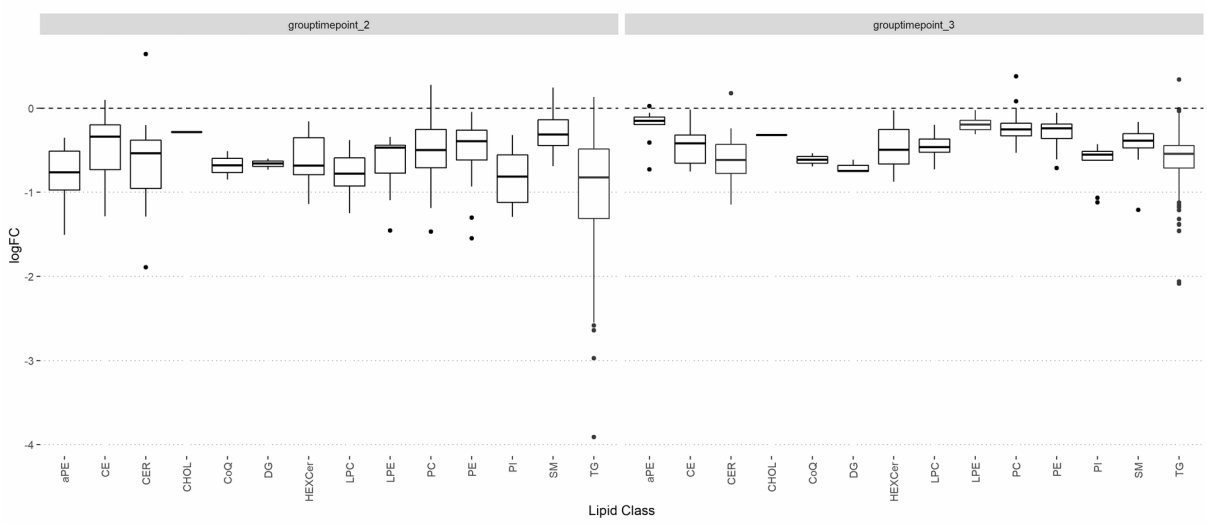

Supplement Figure 4 Overview of the log2 fold changes of lipid classes of the different health statues groups to control group (Intervention study)

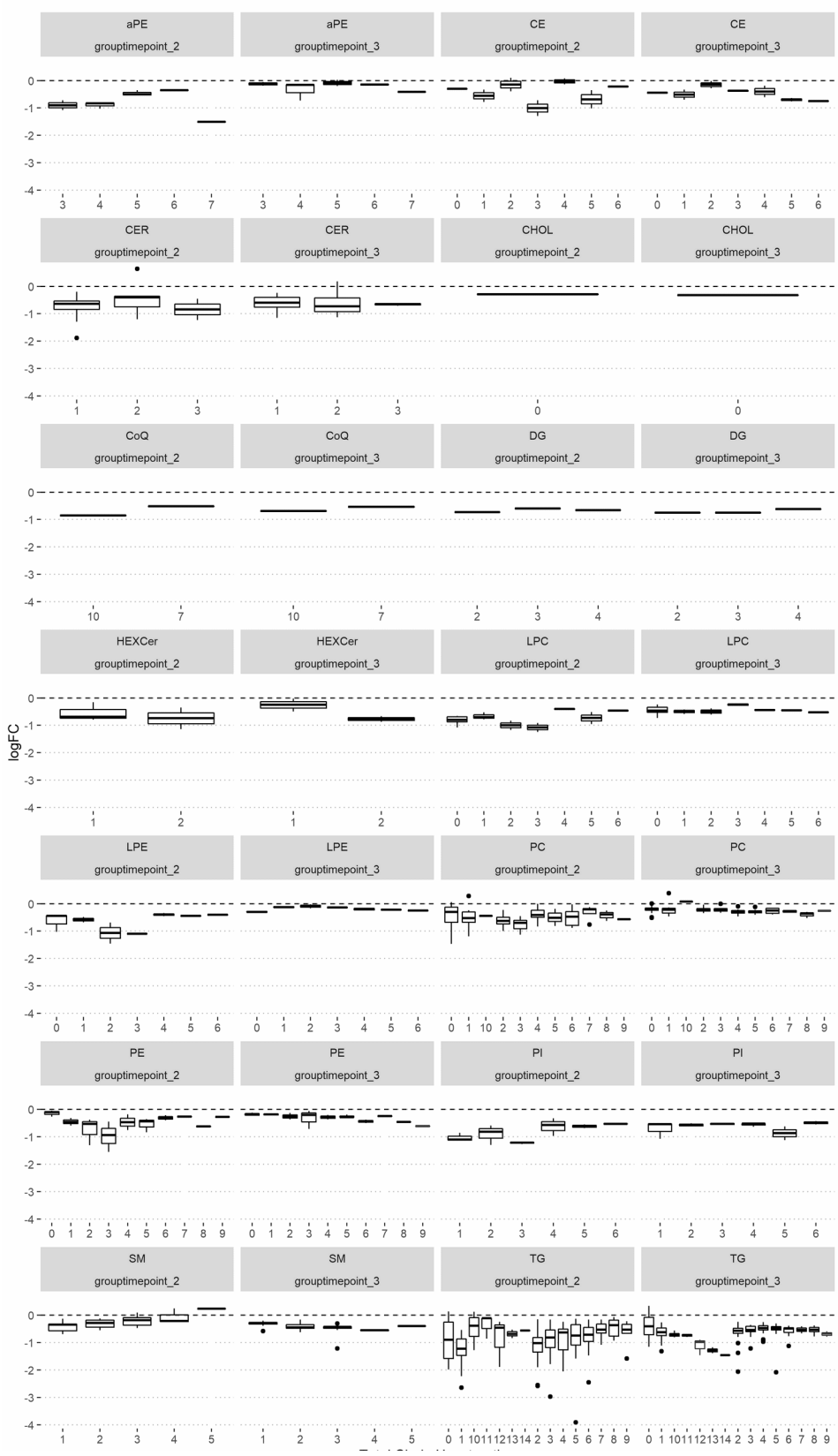
aPE
grouptimepoint_2
aPE
grouptimepoint_3
CE
grouptimepoint_2
CE
grouptimepoint_3
CER
grouptimepoint_2
CER
grouptimepoint_3
CHOL
grouptimepoint_2
CHOL
grouptimepoint_3
CoQ
grouptimepoint_2
CoQ
grouptimepoint_3
DG
grouptimepoint_2
DG
grouptimepoint_3
HEXCer
grouptimepoint_2
HEXCer
grouptimepoint_3
LPC
grouptimepoint_2
LPC
grouptimepoint_3
LPE
grouptimepoint_2
LPE
grouptimepoint_3
PC
grouptimepoint_2
PC
grouptimepoint_3
PE
grouptimepoint_2
PE
grouptimepoint_3
PI
grouptimepoint_2
PI
grouptimepoint_3
SM
grouptimepoint_2
SM
grouptimepoint_3
TG
grouptimepoint_2
TG
grouptimepoint_3
logFC

Supplement Figure 5 Overview of the total chain unsaturation arranged by lipid class and health statues group shown as log2 fold change to the control group (Intervention study)

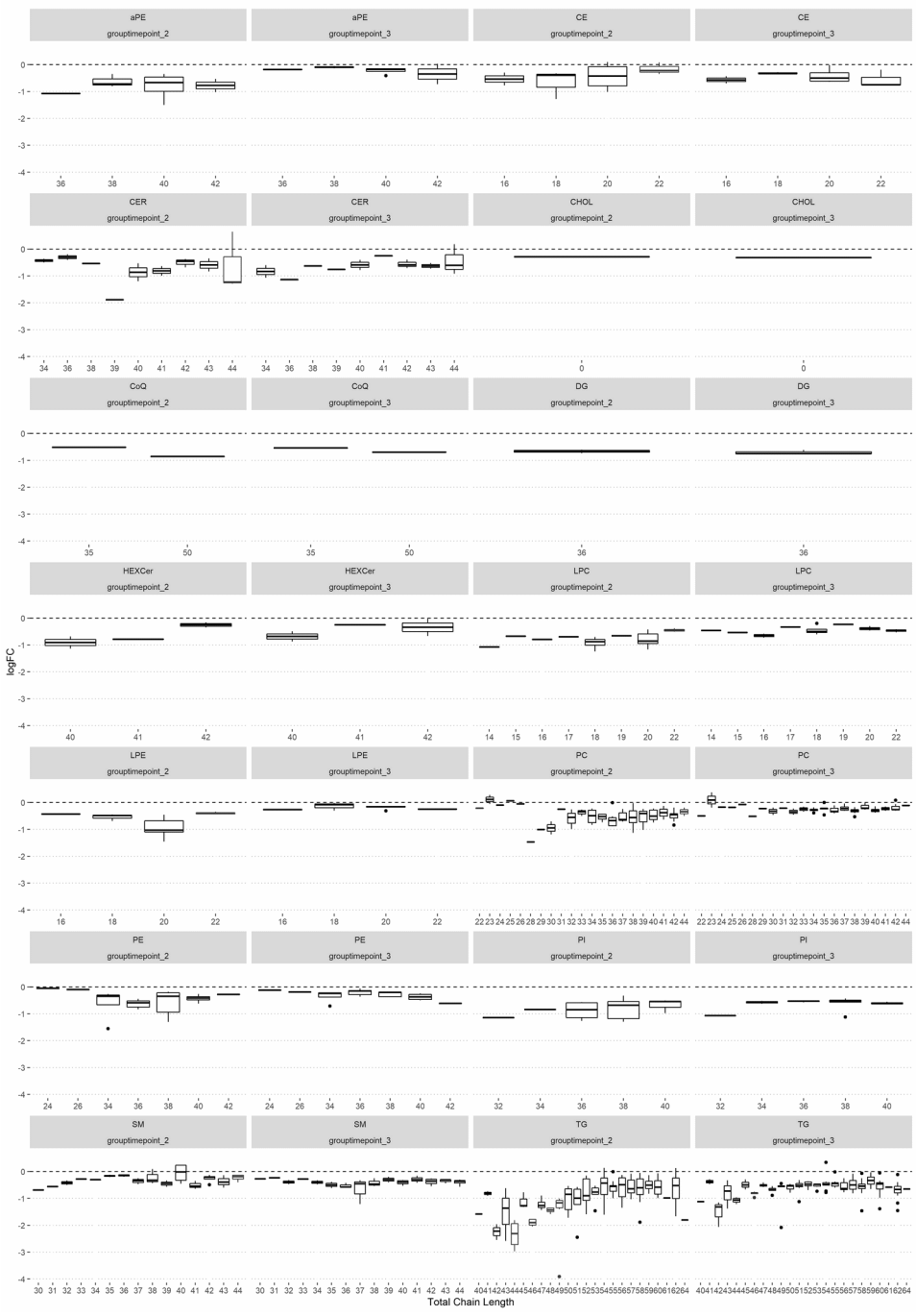

Supplement Figure 6 Overview of the total chain length arranged by lipid class and health statues group shown as log2 fold change to the control group (Intervention study)

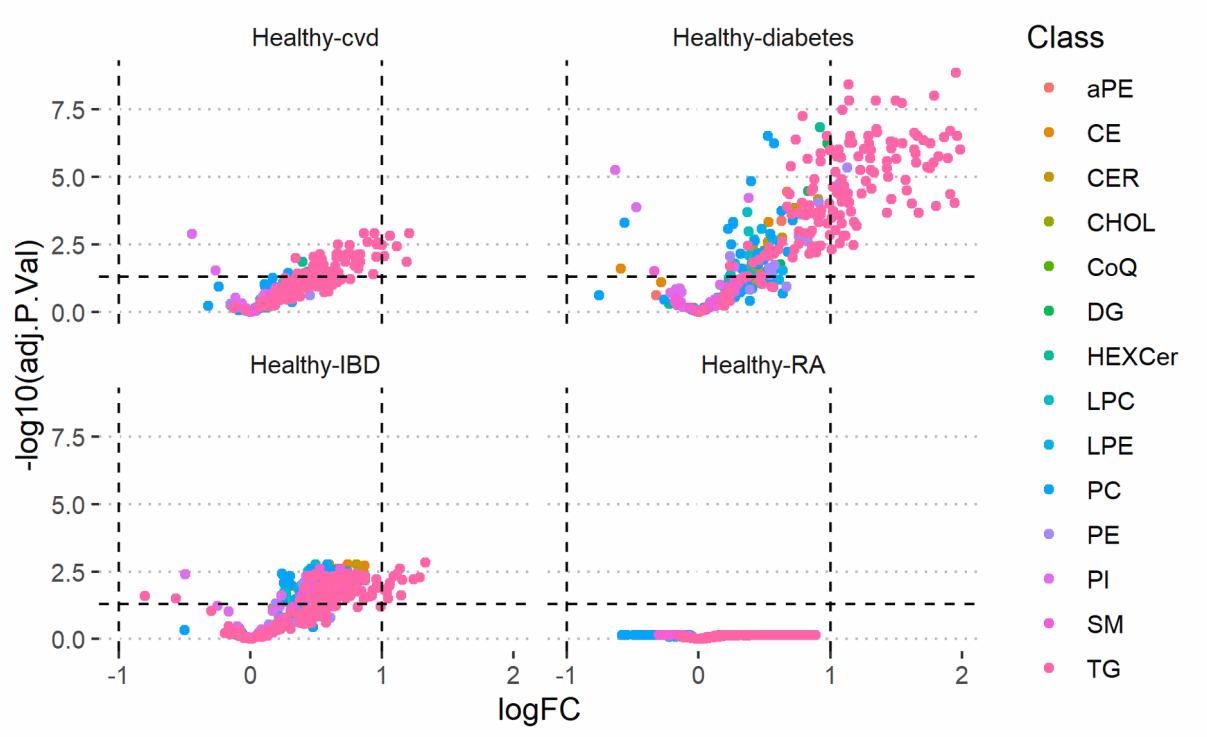

Supplement Figure 7 Volcano plot of the Tomorrow cohorts shows the healthy group versus the health condition (cvd, diabetes, IBD, or RA). logFC – log 2, fold change

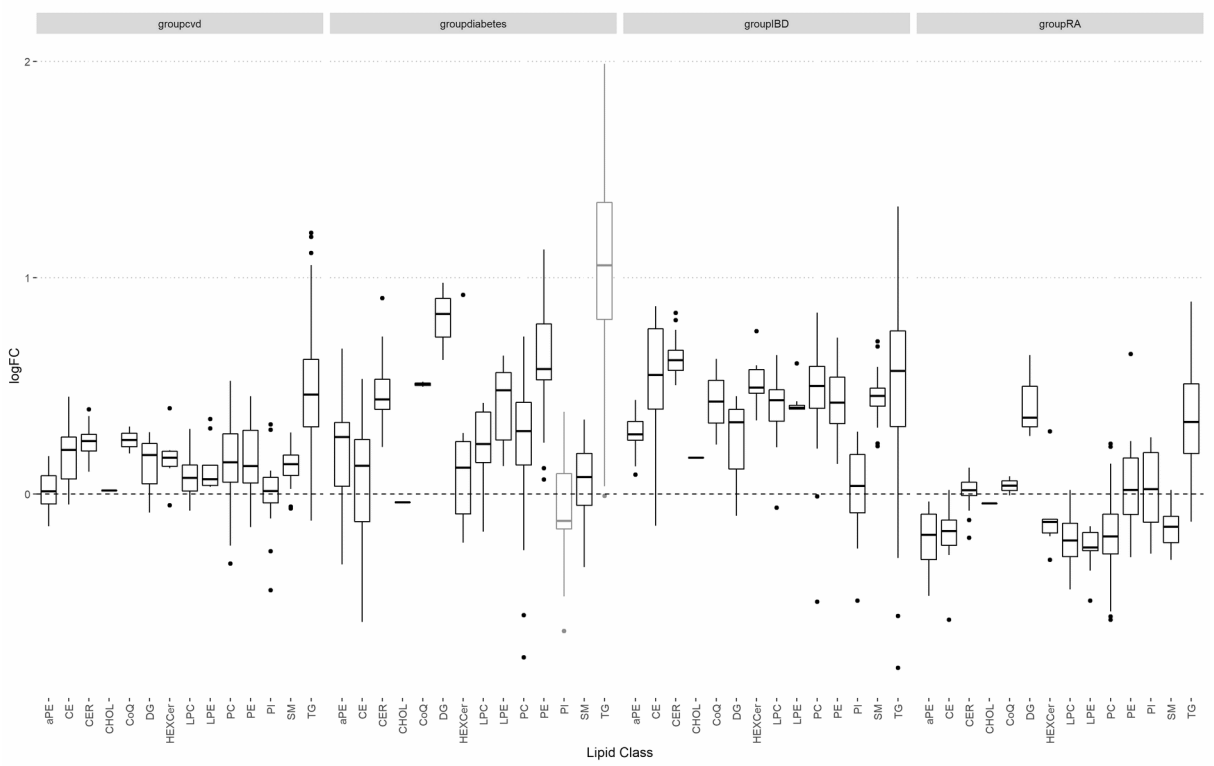

Supplement Figure 8 Overview of the log2 fold changes of lipid classes of the different health statues groups to control group (Tomorrow)

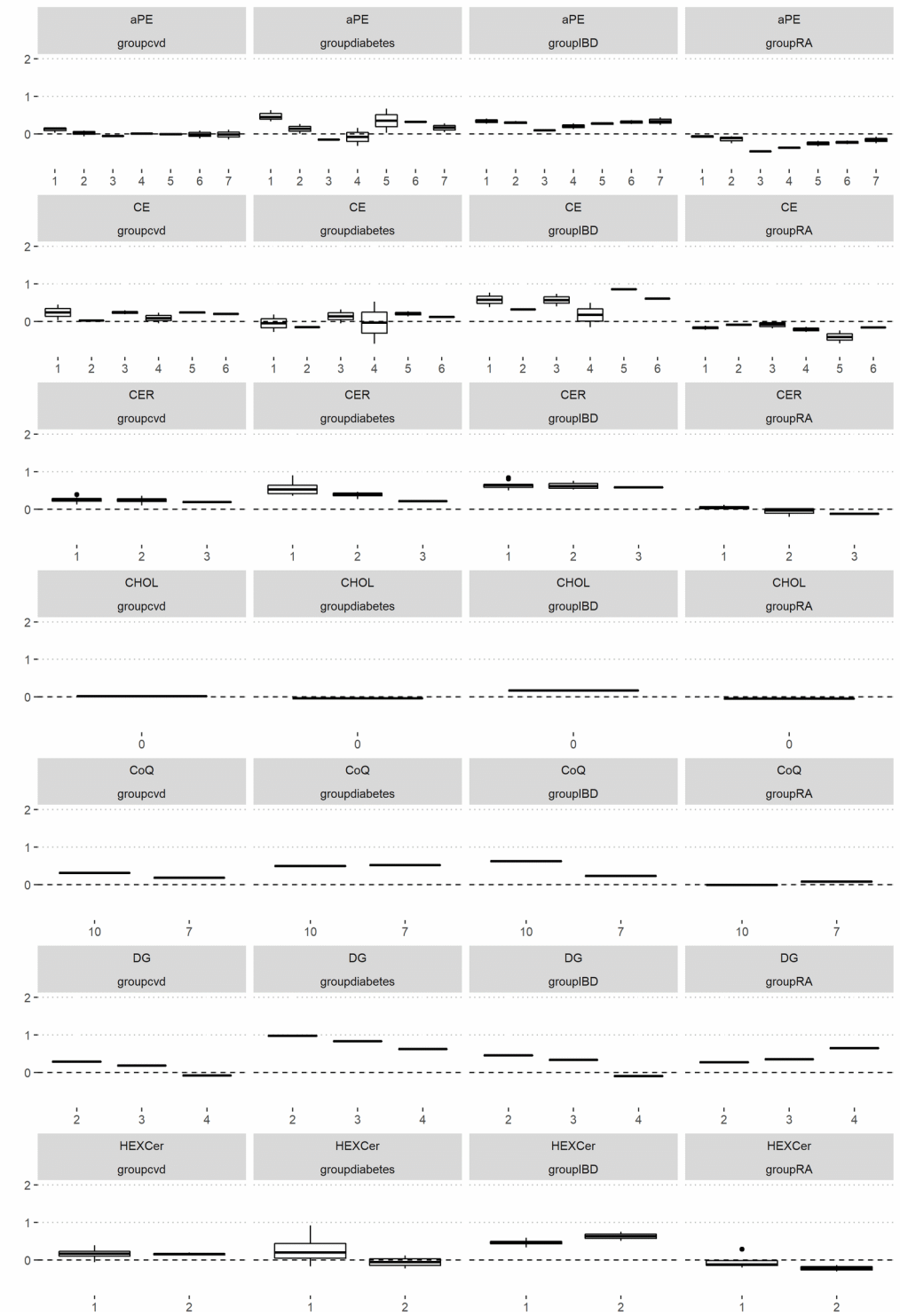
aPE
groupcvd
aPE
groupdiabetes
aPE
groupIBD
aPE
groupRA
CE
groupcvd
CE
groupdiabetes
CE
groupIBD
CE
groupRA
CER
groupcvd
CER
groupdiabetes
CER
groupIBD
CER
groupRA
CHOL
groupcvd
CHOL
groupdiabetes
CHOL
groupIBD
CHOL
groupRA
CoQ
groupcvd
CoQ
groupdiabetes
CoQ
groupIBD
CoQ
groupRA
DG
groupcvd
DG
groupdiabetes
DG
groupIBD
DG
groupRA
HEXCer
groupcvd
HEXCer
groupdiabetes
HEXCer
groupIBD
HEXCer
groupRA

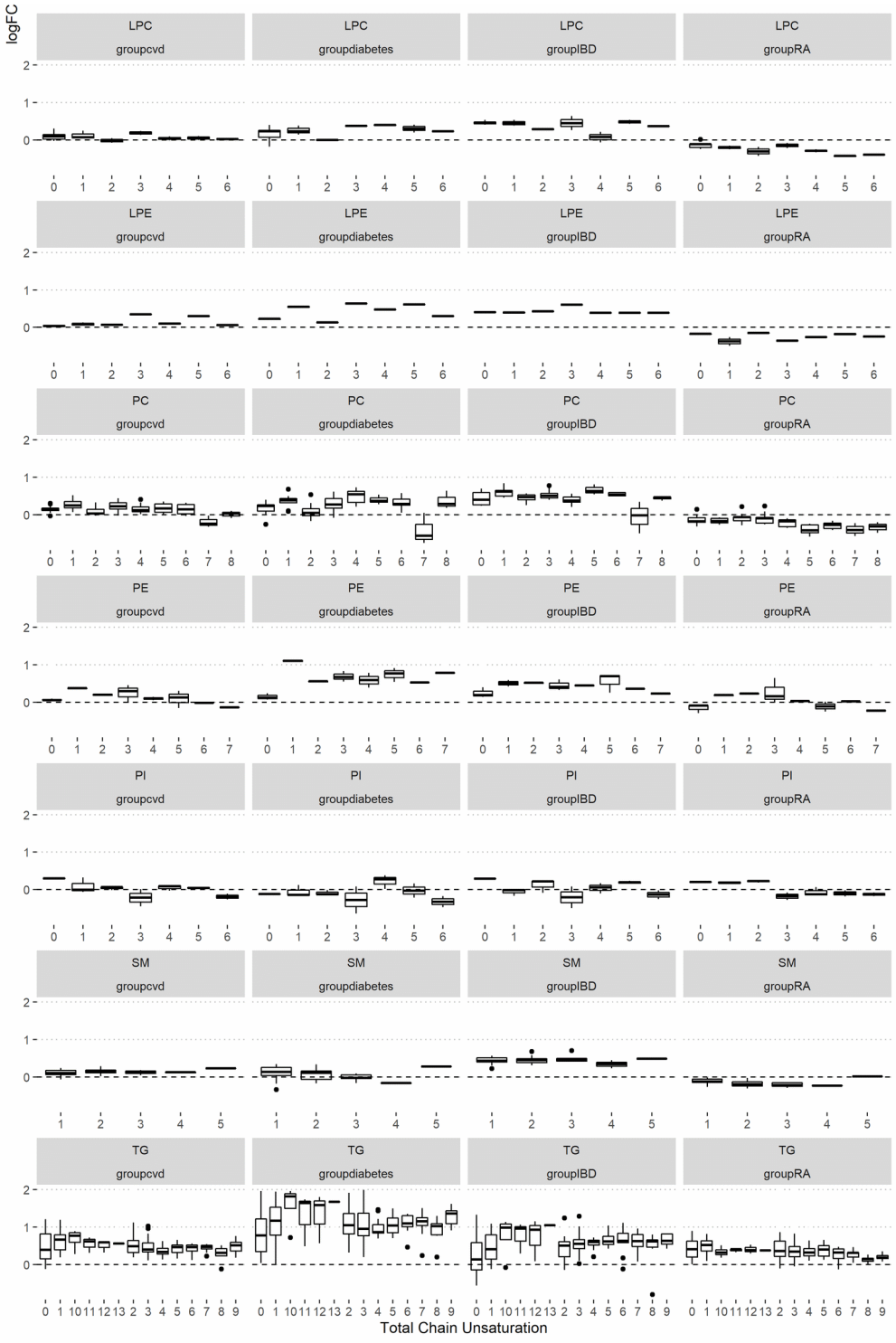

Supplement Figure 9 Overview of the total chain unsaturation arranged by lipid class and health statues group shown as log2 fold change to the control group (Tomorrow)

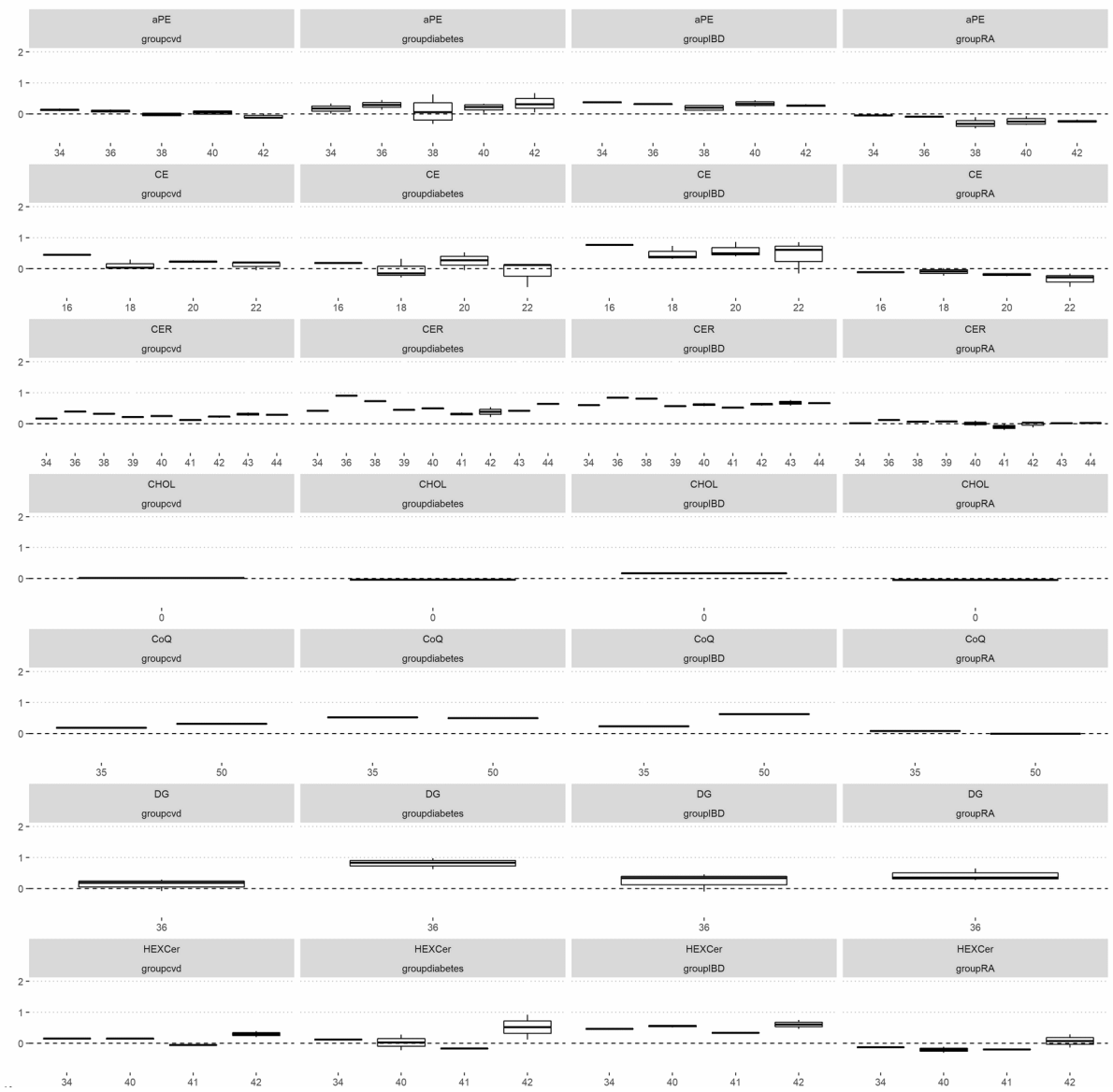
aPE
groupcvd
aPE
groupdiabetes
aPE
groupIBD
aPE
groupRA
CE
groupcvd
CE
groupdiabetes
CE
groupIBD
CE
groupRA
CER
groupcvd
CER
groupdiabetes
CER
groupIBD
CER
groupRA
CHOL
groupcvd
CHOL
groupdiabetes
CHOL
groupIBD
CHOL
groupRA
CoQ
groupcvd
CoQ
groupdiabetes
CoQ
groupIBD
CoQ
groupRA
DG
groupcvd
DG
groupdiabetes
DG
groupIBD
DG
groupRA
HEXCer
groupcvd
HEXCer
groupdiabetes
HEXCer
groupIBD
HEXCer
groupRA

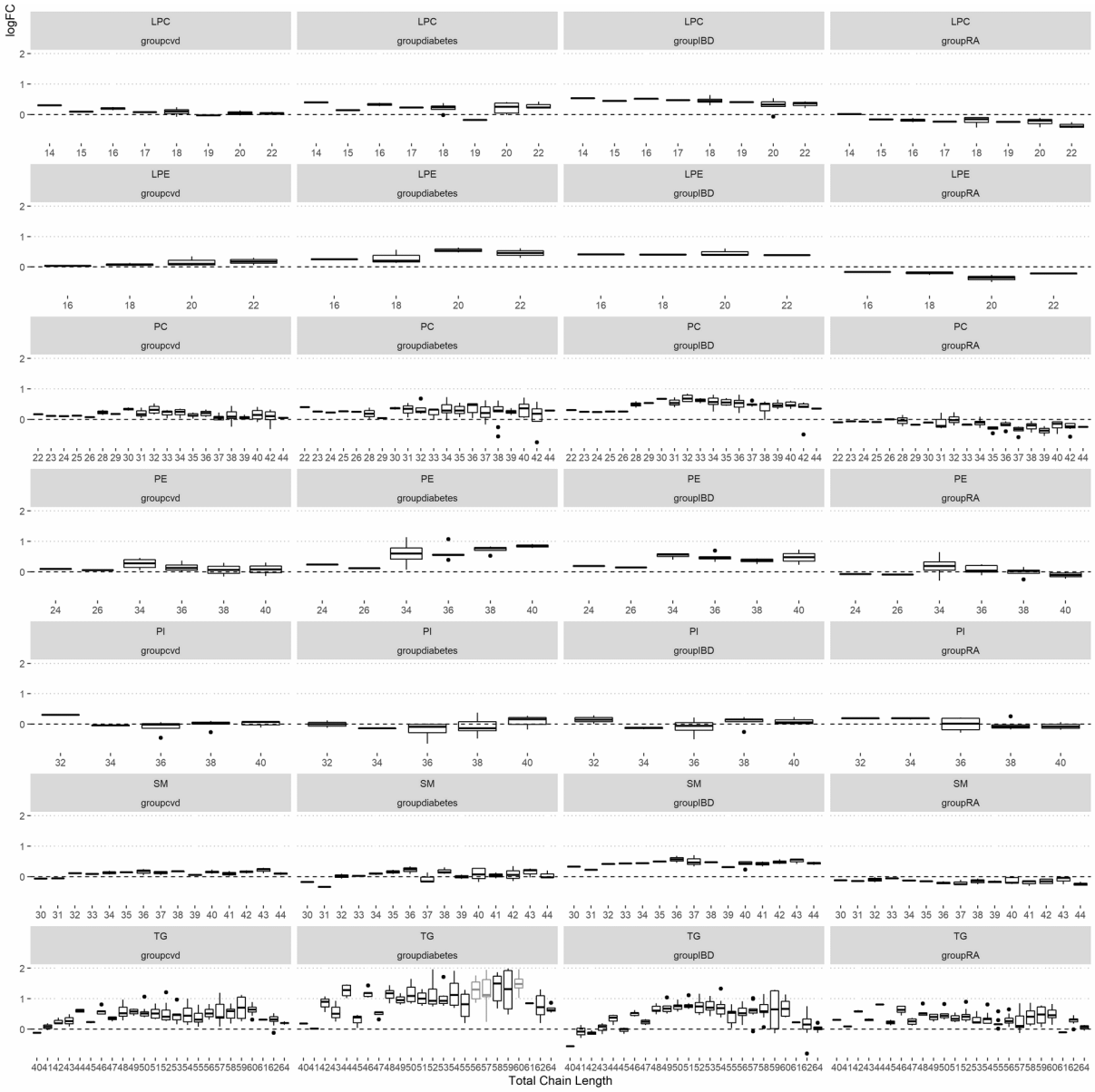

Supplement Figure 10 Overview of the total chain length arranged by lipid class and health statues group shown as log2 fold change to the control group (Tomorrow)

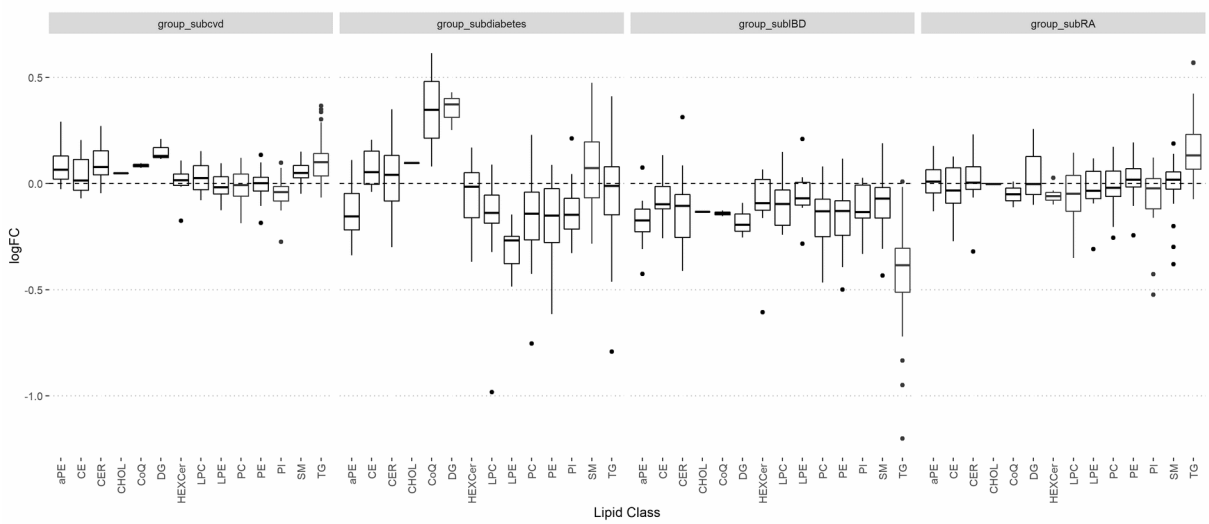

Supplement Figure 11 Overview of the log2 fold changes of lipid classes of the different health statues groups to control group (FoCus)

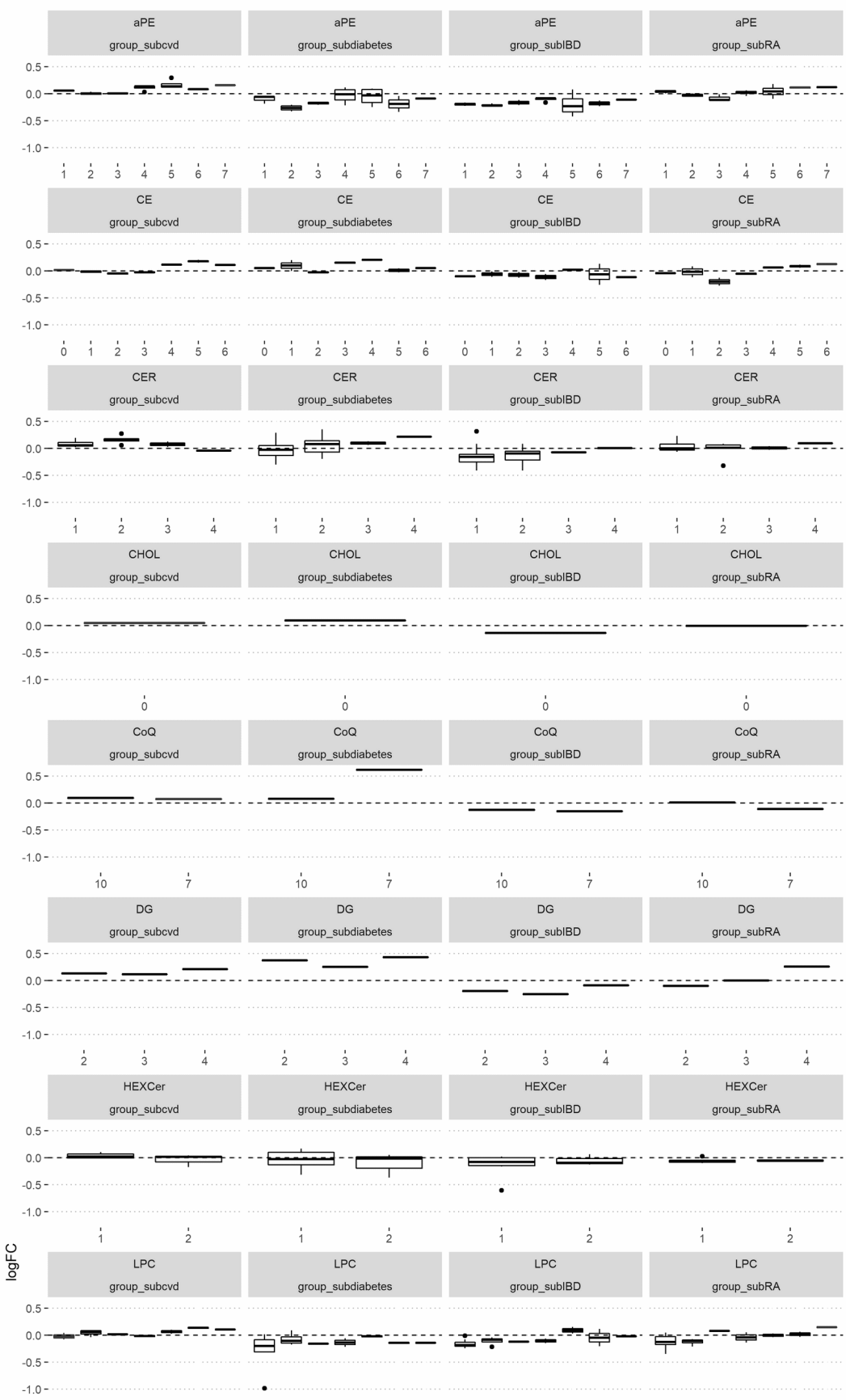
aPE
group_subcvd
aPE
group_subdiabetes
aPE
group_subIBD
aPE
group_subRA
CE
group_subcvd
CE
group_subdiabetes
CE
group_subIBD
CE
group_subRA
CER
group_subcvd
CER
group_subdiabetes
CER
group_subIBD
CER
group_subRA
CHOL
group_subcvd
CHOL
group_subdiabetes
CHOL
group_subIBD
CHOL
group_subRA
CoQ
group_subcvd
CoQ
group_subdiabetes
CoQ
group_subIBD
CoQ
group_subRA
DG
group_subcvd
DG
group_subdiabetes
DG
group_subIBD
DG
group_subRA
HEXCer
group_subcvd
HEXCer
group_subdiabetes
HEXCer
group_subIBD
HEXCer
group_subRA
LPC
group_subcvd
LPC
group_subdiabetes
LPC
group_subIBD
LPC
group_subRA
logFC

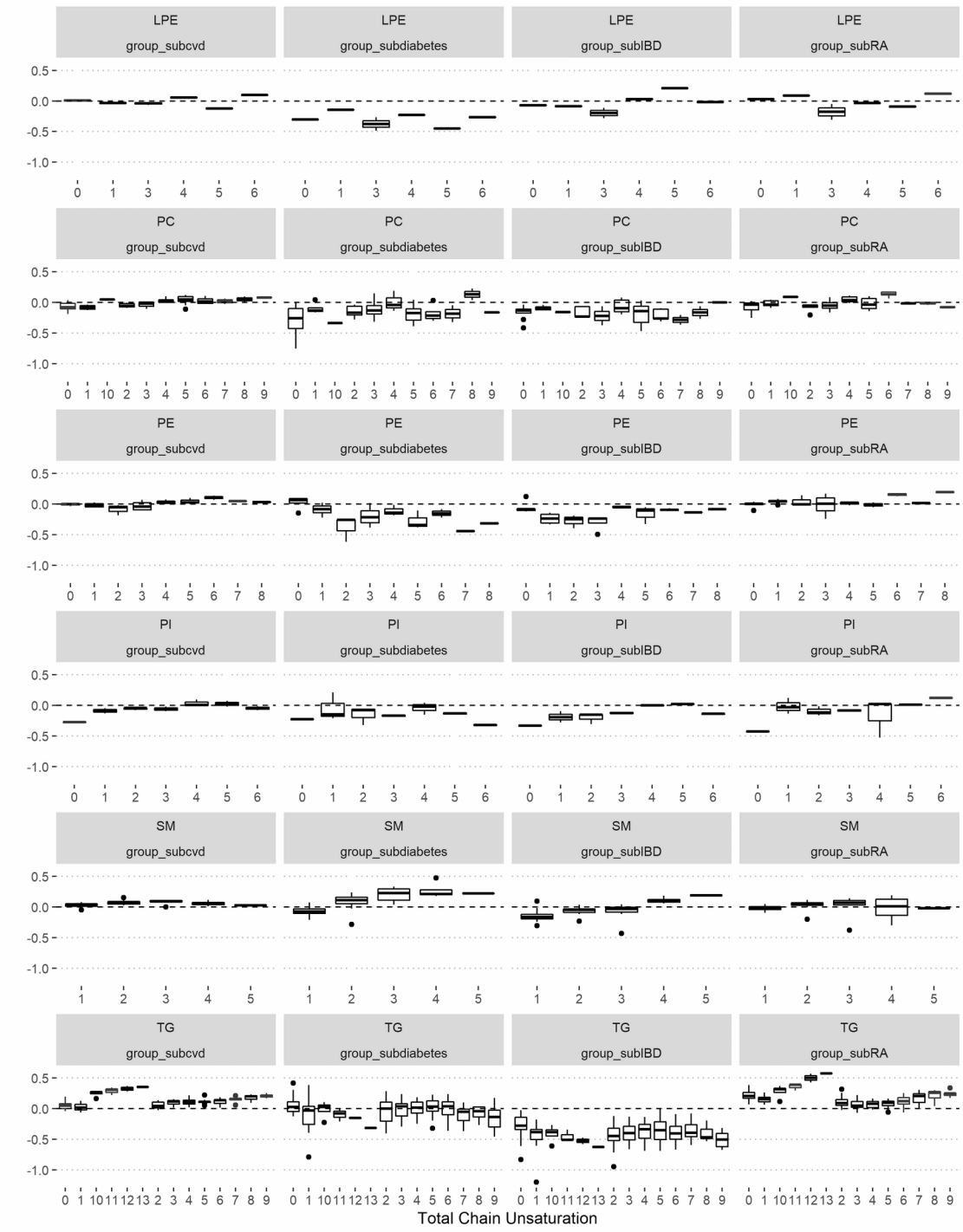

Supplement Figure 12 Overview of the total chain unsaturation arranged by lipid class and health statues group shown as log2 fold change to the control group (FoCus)

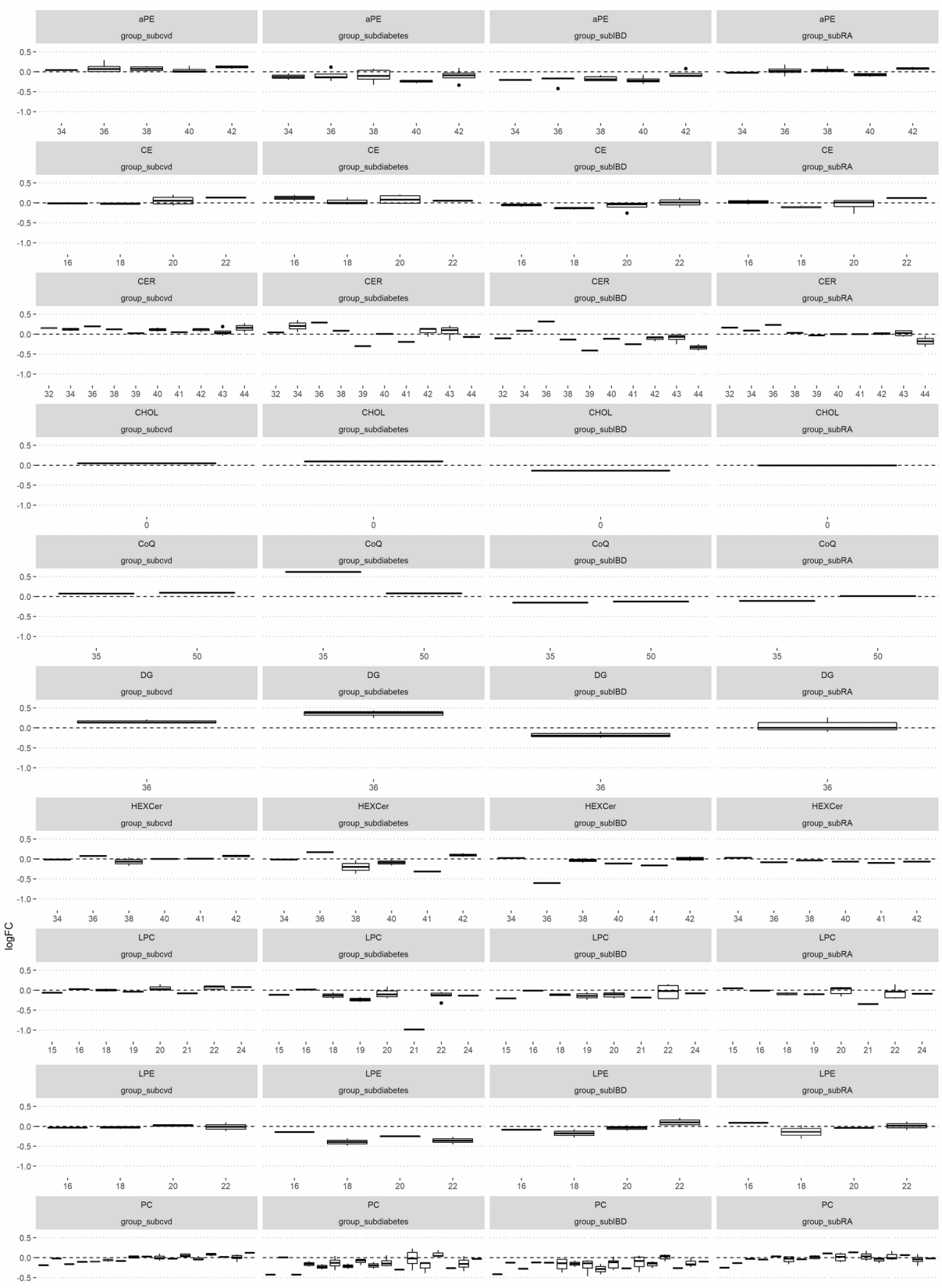
aPE
group_subcvd
group_subdiabetes
group_subIBD
group_subRA
CE
CER
CHOL
CoQ
DG
HEXCer
LPC
LPE
PC
logFC

Supplement Figure 13 Overview of the total chain length arranged by lipid class and health statues group shown as log2 fold change to the control group (FoCus)

Supplement Table 6 Overview of the T-test between lipid species and lipid subclasses of healthy condition (group 1) and cardiovascular diseases (cvd), diabetes, rheumatoid arthritis (RA) and inflammation bowel diseases (IBD) (group 2) of the Tomorrow cohort.

ID	class	group 1	group2	p-value	p.signif	group2	p-value	p.signif	group2	p-value	p.signif	group2	p-value	p.signif	group2	p-value	p.signif	method
1	aPE	control	cvd	0.0838	ns	diabetes	0.2161	ns	IBD	0.0541	ns	RA	0.8688	ns	onco	0.5374	ns	T-test
2	CE	control	cvd	0.5211	ns	diabetes	0.6072	ns	IBD	0.5559	ns	RA	0.8846	ns	onco	0.6512	ns	T-test
3	CER	control	cvd	0.0234	*	diabetes	0.8130	ns	IBD	0.1777	ns	RA	0.8492	ns	onco	0.1324	ns	T-test
4	CHOL	control	cvd	0.1797	ns	diabetes	0.2584	ns	IBD	0.0269	*	RA	0.9824	ns	onco	0.1066	ns	T-test
5	CoQ	control	cvd	0.5904	ns	diabetes	0.2737	ns	IBD	0.6591	ns	RA	0.8740	ns	onco	0.9685	ns	T-test
6	DG	control	cvd	0.1982	ns	diabetes	0.1880	ns	IBD	0.4462	ns	RA	0.8307	ns	onco	0.7034	ns	T-test
7	HEXCer	control	cvd	0.8670	ns	diabetes	0.6845	ns	IBD	0.3780	ns	RA	0.6558	ns	onco	0.8259	ns	T-test
8	LPC	control	cvd	0.7036	ns	diabetes	0.3259	ns	IBD	0.5112	ns	RA	0.6718	ns	onco	0.9472	ns	T-test
9	LPE	control	cvd	0.8946	ns	diabetes	0.1269	ns	IBD	0.7904	ns	RA	0.8376	ns	onco	0.7255	ns	T-test
10	PC	control	cvd	0.8584	ns	diabetes	0.2178	ns	IBD	0.1322	ns	RA	0.9174	ns	onco	0.2283	ns	T-test
11	PE	control	cvd	0.9965	ns	diabetes	0.1684	ns	IBD	0.1385	ns	RA	0.8240	ns	onco	0.4384	ns	T-test
12	PI	control	cvd	0.2824	ns	diabetes	0.1856	ns	IBD	0.1751	ns	RA	0.5095	ns	onco	0.5410	ns	T-test
13	SM	control	cvd	0.2074	ns	diabetes	0.5191	ns	IBD	0.3820	ns	RA	0.9819	ns	onco	0.1132	ns	T-test
14	TG	control	cvd	0.0001	***	diabetes	0.5482	ns	IBD	0.0000	****	RA	0.0047	**	onco	0.0001	***	T-test

ID	Lipids	group 1	group2	p-value	p.signif	group2	p-value	p.signif	group2	p-value	p.signif	group2	p-value	p.signif	group2	p-value	p.signif	method
1	aPE 34:1	control	cvd	0.2559	ns	diabetes	0.6779	ns	IBD	0.0218	*	RA	0.9514	ns	onco	0.9318	ns	T-test
2	aPE 34:2	control	cvd	0.4986	ns	diabetes	0.1476	ns	IBD	0.0392	*	RA	0.5431	ns	onco	0.2251	ns	T-test
3	aPE 36:1	control	cvd	0.1089	ns	diabetes	0.5822	ns	IBD	0.0848	ns	RA	0.3792	ns	onco	0.6393	ns	T-test
4	aPE 36:2	control	cvd	0.8964	ns	diabetes	0.0846	ns	IBD	0.0830	ns	RA	0.8287	ns	onco	0.5631	ns	T-test

XXX

5	aPE 36:3	control	cvd	0.9169	ns	diabetes	0.2896	ns	IBD	0.0947	ns	RA	0.2427	ns	onco	0.5831	ns	T-test
6	aPE 36:4	control	cvd	0.0064	**	diabetes	0.3241	ns	IBD	0.0409	*	RA	0.8359	ns	onco	0.4733	ns	T-test
7	aPE 36:5	control	cvd	0.0060	**	diabetes	0.5150	ns	IBD	0.0706	ns	RA	0.4383	ns	onco	0.8072	ns	T-test
8	aPE 38:1	control	cvd	0.2440	ns	diabetes	0.0688	ns	IBD	0.0455	*	RA	0.6001	ns	onco	0.5246	ns	T-test
9	aPE 38:2	control	cvd	0.8366	ns	diabetes	0.0044	**	IBD	0.0735	ns	RA	0.9760	ns	onco	0.9982	ns	T-test
10	aPE 38:3	control	cvd	0.7040	ns	diabetes	0.2859	ns	IBD	0.3113	ns	RA	0.9283	ns	onco	0.4777	ns	T-test
11	aPE 38:4	control	cvd	0.0012	**	diabetes	0.5720	ns	IBD	0.2794	ns	RA	0.5072	ns	onco	0.1472	ns	T-test
12	aPE 38:5	control	cvd	0.0065	**	diabetes	0.4885	ns	IBD	0.0409	*	RA	0.9320	ns	onco	0.1462	ns	T-test
13	aPE 38:6	control	cvd	0.0271	*	diabetes	0.6415	ns	IBD	0.0071	**	RA	0.1843	ns	onco	0.0480	*	T-test
14	aPE 40:2	control	cvd	0.6159	ns	diabetes	0.0097	**	IBD	0.0339	*	RA	0.5618	ns	onco	0.8858	ns	T-test
15	aPE 40:3	control	cvd	0.8803	ns	diabetes	0.0645	ns	IBD	0.0825	ns	RA	0.1546	ns	onco	0.8552	ns	T-test
16	aPE 40:4	control	cvd	0.5815	ns	diabetes	0.1516	ns	IBD	0.3627	ns	RA	0.6271	ns	onco	0.9734	ns	T-test
17	aPE 40:5	control	cvd	0.0580	ns	diabetes	0.2205	ns	IBD	0.0429	*	RA	0.5802	ns	onco	0.7812	ns	T-test
18	aPE 42:4	control	cvd	0.0027	**	diabetes	0.3756	ns	IBD	0.2822	ns	RA	0.7232	ns	onco	0.0667	ns	T-test
19	aPE 42:5	control	cvd	0.0143	*	diabetes	0.5072	ns	IBD	0.5404	ns	RA	0.3483	ns	onco	0.2372	ns	T-test
20	aPE 42:6	control	cvd	0.1493	ns	diabetes	0.0090	**	IBD	0.2026	ns	RA	0.3874	ns	onco	0.1936	ns	T-test
21	aPE 42:7	control	cvd	0.0200	*	diabetes	0.5548	ns	IBD	0.3462	ns	RA	0.3174	ns	onco	0.0496	*	T-test
22	CE 16:0	control	cvd	0.7900	ns	diabetes	0.5155	ns	IBD	0.0349	*	RA	0.6207	ns	onco	0.3187	ns	T-test
23	CE 16:1	control	cvd	0.6630	ns	diabetes	0.3273	ns	IBD	0.9644	ns	RA	0.5819	ns	onco	0.0748	ns	T-test
24	CE 18:1	control	cvd	0.6662	ns	diabetes	0.9926	ns	IBD	0.0532	ns	RA	0.0969	ns	onco	0.8864	ns	T-test
25	CE 18:2	control	cvd	0.4647	ns	diabetes	0.6724	ns	IBD	0.0412	*	RA	0.0531	ns	onco	0.5783	ns	T-test
26	CE 18:3	control	cvd	0.5449	ns	diabetes	0.4037	ns	IBD	0.0592	ns	RA	0.4792	ns	onco	0.5976	ns	T-test
27	CE 20:2	control	cvd	0.0975	ns	diabetes	0.9471	ns	IBD	0.7928	ns	RA	0.0066	**	onco	0.2914	ns	T-test
28	CE 20:3	control	cvd	0.8624	ns	diabetes	0.3072	ns	IBD	0.5972	ns	RA	0.7612	ns	onco	0.4140	ns	T-test
29	CE 20:4	contro	cvd	0.0087	**	diabetes	0.0841	ns	IBD	0.7715	ns	RA	0.4628	ns	onco	0.0794	ns	T-test

30	CE 20:5	control	cvd	0.0055	**	diabetes	0.8398	ns	IBD	0.0543	ns	RA	0.7516	ns	onco	0.1255	ns	T-test
31	CE 22:5	control	cvd	0.1408	ns	diabetes	0.7603	ns	IBD	0.2722	ns	RA	0.4645	ns	onco	0.2241	ns	T-test
32	CE 22:6	control	cvd	0.0513	ns	diabetes	0.6721	ns	IBD	0.2973	ns	RA	0.3035	ns	onco	0.1594	ns	T-test
33	CER 32:1	control	cvd	0.0099	**	diabetes	0.7908	ns	IBD	0.3436	ns	RA	0.0977	ns	onco	0.0139	*	T-test
34	CER 34:1	control	cvd	0.0124	*	diabetes	0.4818	ns	IBD	0.1197	ns	RA	0.1148	ns	onco	0.1140	ns	T-test
35	CER 34:2	control	cvd	0.0048	**	diabetes	0.0031	**	IBD	0.5255	ns	RA	0.3872	ns	onco	0.7905	ns	T-test
36	CER 36:1	control	cvd	0.0018	**	diabetes	0.0547	ns	IBD	0.0088	**	RA	0.0253	*	onco	0.0537	ns	T-test
37	CER 38:1	control	cvd	0.0157	*	diabetes	0.4912	ns	IBD	0.1623	ns	RA	0.7718	ns	onco	0.0998	ns	T-test
38	CER 39:1	control	cvd	0.7889	ns	diabetes	0.0609	ns	IBD	0.0007	***	RA	0.7947	ns	onco	0.4467	ns	T-test
39	CER 40:1	control	cvd	0.1028	ns	diabetes	0.8877	ns	IBD	0.0750	ns	RA	0.9759	ns	onco	0.6833	ns	T-test
40	CER 40:2	control	cvd	0.0063	**	diabetes	0.8939	ns	IBD	0.4590	ns	RA	0.9985	ns	onco	0.1855	ns	T-test
41	CER 41:1	control	cvd	0.4081	ns	diabetes	0.1410	ns	IBD	0.0051	**	RA	0.9312	ns	onco	0.6944	ns	T-test
42	CER 41:2	control	cvd	0.2991	ns	diabetes	0.2171	ns	IBD	0.0440	*	RA	0.9631	ns	onco	0.5501	ns	T-test
43	CER 42:1	control	cvd	0.2169	ns	diabetes	0.5859	ns	IBD	0.0456	*	RA	0.7297	ns	onco	0.5865	ns	T-test
44	CER 42:2	control	cvd	0.0010	***	diabetes	0.1729	ns	IBD	0.1642	ns	RA	0.8142	ns	onco	0.0598	ns	T-test
45	CER 42:3	control	cvd	0.0025	**	diabetes	0.1903	ns	IBD	0.4612	ns	RA	0.5437	ns	onco	0.0562	ns	T-test
46	CER 43:1	control	cvd	0.4366	ns	diabetes	0.1517	ns	IBD	0.0338	*	RA	0.5649	ns	onco	0.7405	ns	T-test
47	CER 43:2	control	cvd	0.0027	**	diabetes	0.3604	ns	IBD	0.7057	ns	RA	0.5263	ns	onco	0.9201	ns	T-test
48	CER 43:3	control	cvd	0.6522	ns	diabetes	0.4597	ns	IBD	0.0677	ns	RA	0.7202	ns	onco	0.2736	ns	T-test
49	CER 43:4	control	cvd	0.6415	ns	diabetes	0.3017	ns	IBD	0.9796	ns	RA	0.5452	ns	onco	0.0721	ns	T-test
50	CER 44:1	control	cvd	0.4170	ns	diabetes	0.6567	ns	IBD	0.0190	*	RA	0.7030	ns	onco	0.7696	ns	T-test
51	CER 44:2	control	cvd	0.0508	ns	diabetes	0.7691	ns	IBD	0.1331	ns	RA	0.3705	ns	onco	0.0982	ns	T-test
52	CHOL 0:0	control	cvd	0.1797	ns	diabetes	0.2584	ns	IBD	0.0269	*	RA	0.9824	ns	onco	0.1066	ns	T-test
53	CoQ 50:10	control	cvd	0.0330	*	diabetes	0.4757	ns	IBD	0.1823	ns	RA	0.9165	ns	onco	0.2488	ns	T-test

54	CoQ 35:7	control	cvd	0.5701	ns	diabetes	0.0041	**	IBD	0.4937	ns	RA	0.6270	ns	onco	0.8221	ns	T-test
55	DG 36:2	control	cvd	0.0977	ns	diabetes	0.0201	*	IBD	0.2020	ns	RA	0.4965	ns	onco	0.6925	ns	T-test
56	DG 36:3	control	cvd	0.0985	ns	diabetes	0.0810	ns	IBD	0.0782	ns	RA	0.9876	ns	onco	0.8719	ns	T-test
57	DG 36:4	control	cvd	0.0733	ns	diabetes	0.0930	ns	IBD	0.6633	ns	RA	0.4419	ns	onco	0.4033	ns	T-test
58	HEXCer 34:1	control	cvd	0.7036	ns	diabetes	0.8657	ns	IBD	0.7335	ns	RA	0.6880	ns	onco	0.7253	ns	T-test
59	HEXCer 36:1	control	cvd	0.5988	ns	diabetes	0.6736	ns	IBD	0.0655	ns	RA	0.7491	ns	onco	0.6250	ns	T-test
60	HEXCer 38:1	control	cvd	0.4649	ns	diabetes	0.8039	ns	IBD	0.8166	ns	RA	0.6525	ns	onco	0.2687	ns	T-test
61	HEXCer 38:2	control	cvd	0.0504	ns	diabetes	0.1365	ns	IBD	0.6315	ns	RA	0.8352	ns	onco	0.6261	ns	T-test
62	HEXCer 40:1	control	cvd	0.8288	ns	diabetes	0.0956	ns	IBD	0.1878	ns	RA	0.2862	ns	onco	0.7475	ns	T-test
63	HEXCer 40:2	control	cvd	0.7488	ns	diabetes	0.9135	ns	IBD	0.2138	ns	RA	0.5771	ns	onco	0.1178	ns	T-test
64	HEXCer 41:1	control	cvd	0.9149	ns	diabetes	0.0165	*	IBD	0.0900	ns	RA	0.2720	ns	onco	0.4302	ns	T-test
65	HEXCer 42:1	control	cvd	0.0348	*	diabetes	0.2424	ns	IBD	0.6192	ns	RA	0.5673	ns	onco	0.9932	ns	T-test
66	HEXCer 42:2	control	cvd	0.3181	ns	diabetes	0.6813	ns	IBD	0.3340	ns	RA	0.3644	ns	onco	0.1310	ns	T-test
67	LPC 15:0	control	cvd	0.1255	ns	diabetes	0.3169	ns	IBD	0.0205	*	RA	0.4511	ns	onco	0.4358	ns	T-test
68	LPC 16:0	control	cvd	0.4869	ns	diabetes	0.8805	ns	IBD	0.8814	ns	RA	0.8864	ns	onco	0.6988	ns	T-test
69	LPC 18:0	control	cvd	0.2586	ns	diabetes	0.5980	ns	IBD	0.3415	ns	RA	0.6207	ns	onco	0.1476	ns	T-test
70	LPC 18:3	control	cvd	0.4880	ns	diabetes	0.0622	ns	IBD	0.1617	ns	RA	0.1815	ns	onco	0.7491	ns	T-test
71	LPC 19:0	control	cvd	0.3294	ns	diabetes	0.0380	*	IBD	0.0269	*	RA	0.1864	ns	onco	0.0806	ns	T-test
72	LPC 19:1	control	cvd	0.4142	ns	diabetes	0.1465	ns	IBD	0.6059	ns	RA	0.4346	ns	onco	0.0934	ns	T-test
73	LPC 20:0	control	cvd	0.4995	ns	diabetes	0.0617	ns	IBD	0.0200	*	RA	0.0456	*	onco	0.4165	ns	T-test
74	LPC 20:1	control	cvd	0.2835	ns	diabetes	0.3390	ns	IBD	0.2162	ns	RA	0.1502	ns	onco	0.6655	ns	T-test
75	LPC 20:2	control	cvd	0.6823	ns	diabetes	0.1331	ns	IBD	0.1491	ns	RA	0.3730	ns	onco	0.6855	ns	T-test
76	LPC 20:3	control	cvd	0.9470	ns	diabetes	0.5315	ns	IBD	0.5132	ns	RA	0.5057	ns	onco	0.3063	ns	T-test
77	LPC 20:4	control	cvd	0.0076	**	diabetes	0.9756	ns	IBD	0.6490	ns	RA	0.6708	ns	onco	0.2127	ns	T-test
78	LPC 20:5	contro	cvd	0.0175	*	diabetes	0.1779	ns	IBD	0.0898	ns	RA	0.6888	ns	onco	0.2500	ns	T-test

79	LPC 21:0	control	cvd	0.2227	ns	diabetes	0.0060	**	IBD	0.1163	ns	RA	0.0557	ns	onco	0.1830	ns	T-test
80	LPC 22:0	control	cvd	0.7429	ns	diabetes	0.0404	*	IBD	0.0645	ns	RA	0.0862	ns	onco	0.2751	ns	T-test
81	LPC 22:1	control	cvd	0.2112	ns	diabetes	0.6221	ns	IBD	0.0708	ns	RA	0.1556	ns	onco	0.4353	ns	T-test
82	LPC 22:4	control	cvd	0.5941	ns	diabetes	0.7458	ns	IBD	0.0753	ns	RA	0.6744	ns	onco	0.8034	ns	T-test
83	LPC 22:5	control	cvd	0.0090	**	diabetes	0.2018	ns	IBD	0.2183	ns	RA	0.7450	ns	onco	0.8617	ns	T-test
84	LPC 22:6	control	cvd	0.0143	*	diabetes	0.1799	ns	IBD	0.8060	ns	RA	0.0835	ns	onco	0.0896	ns	T-test
85	LPC 24:1	control	cvd	0.1530	ns	diabetes	0.3695	ns	IBD	0.4276	ns	RA	0.5354	ns	onco	0.5383	ns	T-test
86	LPE 16:1	control	cvd	0.6277	ns	diabetes	0.4426	ns	IBD	0.6719	ns	RA	0.4482	ns	onco	0.5468	ns	T-test
87	LPE 18:0	control	cvd	0.8244	ns	diabetes	0.0037	**	IBD	0.4015	ns	RA	0.7208	ns	onco	0.8510	ns	T-test
88	LPE 18:3	control	cvd	0.4236	ns	diabetes	0.0237	*	IBD	0.3273	ns	RA	0.1165	ns	onco	0.6409	ns	T-test
89	LPE 20:3	control	cvd	0.7414	ns	diabetes	0.0744	ns	IBD	0.5918	ns	RA	0.6510	ns	onco	0.8297	ns	T-test
90	LPE 20:4	control	cvd	0.1231	ns	diabetes	0.0435	*	IBD	0.7273	ns	RA	0.6399	ns	onco	0.4307	ns	T-test
91	LPE 22:5	control	cvd	0.1415	ns	diabetes	0.1801	ns	IBD	0.2584	ns	RA	0.5984	ns	onco	0.3890	ns	T-test
92	LPE 22:6	control	cvd	0.0238	*	diabetes	0.0279	*	IBD	0.8429	ns	RA	0.0901	ns	onco	0.0357	*	T-test
93	PC 24:0.IS	control	cvd	0.1576	ns	diabetes	0.3848	ns	IBD	0.3197	ns	RA	0.4795	ns	onco	0.2884	ns	T-test
94	PC 26:0	control	cvd	0.6742	ns	diabetes	0.9470	ns	IBD	0.3142	ns	RA	0.2005	ns	onco	0.6925	ns	T-test
95	PC 29:0	control	cvd	0.0146	*	diabetes	0.0162	*	IBD	0.0346	*	RA	0.7888	ns	onco	0.6987	ns	T-test
96	PC 30:0	control	cvd	0.0919	ns	diabetes	0.1068	ns	IBD	0.3079	ns	RA	0.6492	ns	onco	0.0863	ns	T-test
97	PC 30:1	control	cvd	0.0960	ns	diabetes	0.6519	ns	IBD	0.5019	ns	RA	0.7052	ns	onco	0.0680	ns	T-test
98	PC 31:0	control	cvd	0.0654	ns	diabetes	0.0237	*	IBD	0.1526	ns	RA	0.8105	ns	onco	0.9491	ns	T-test
99	PC 31:1	control	cvd	0.0921	ns	diabetes	0.3027	ns	IBD	0.3924	ns	RA	0.6958	ns	onco	0.5403	ns	T-test
100	PC 32:0	control	cvd	0.8102	ns	diabetes	0.2316	ns	IBD	0.6002	ns	RA	0.7420	ns	onco	0.1276	ns	T-test
101	PC 32:1	control	cvd	0.4049	ns	diabetes	0.7975	ns	IBD	0.7976	ns	RA	0.8210	ns	onco	0.0722	ns	T-test
102	PC 32:2	control	cvd	0.1177	ns	diabetes	0.2377	ns	IBD	0.0063	**	RA	0.3377	ns	onco	0.2169	ns	T-test

103	PC 32:3	control	cvd	0.1228	ns	diabetes	0.1441	ns	IBD	0.0210	*	RA	0.1877	ns	onco	0.4259	ns	T-test
104	PC 33:1	control	cvd	0.0387	*	diabetes	0.1687	ns	IBD	0.4056	ns	RA	0.6245	ns	onco	0.8195	ns	T-test
105	PC 33:2	control	cvd	0.0321	*	diabetes	0.0158	*	IBD	0.0043	**	RA	0.3689	ns	onco	0.2776	ns	T-test
106	PC 34:0	control	cvd	0.2841	ns	diabetes	0.3198	ns	IBD	0.1251	ns	RA	0.8251	ns	onco	0.2818	ns	T-test
107	PC 34:2	control	cvd	0.5266	ns	diabetes	0.5158	ns	IBD	0.1439	ns	RA	0.3801	ns	onco	0.7506	ns	T-test
108	PC 34:4	control	cvd	0.9056	ns	diabetes	0.7938	ns	IBD	0.0909	ns	RA	0.7397	ns	onco	0.0096	**	T-test
109	PC 34:5	control	cvd	0.4905	ns	diabetes	0.3509	ns	IBD	0.0113	*	RA	0.7569	ns	onco	0.0508	ns	T-test
110	PC 35:4	control	cvd	0.8974	ns	diabetes	0.3578	ns	IBD	0.0648	ns	RA	0.2728	ns	onco	0.2205	ns	T-test
111	PC 35:5	control	cvd	0.5664	ns	diabetes	0.0973	ns	IBD	0.0032	**	RA	0.5500	ns	onco	0.4627	ns	T-test
112	PC 36:0	control	cvd	0.3063	ns	diabetes	0.0108	*	IBD	0.2751	ns	RA	0.2575	ns	onco	0.3179	ns	T-test
113	PC 36:1	control	cvd	0.3559	ns	diabetes	0.3173	ns	IBD	0.3522	ns	RA	0.2650	ns	onco	0.4953	ns	T-test
114	PC 36:2	control	cvd	0.9143	ns	diabetes	0.3586	ns	IBD	0.1368	ns	RA	0.3547	ns	onco	0.9520	ns	T-test
115	PC 36:4	control	cvd	0.1541	ns	diabetes	0.4822	ns	IBD	0.6079	ns	RA	0.2205	ns	onco	0.0024	**	T-test
116	PC 36:5	control	cvd	0.1364	ns	diabetes	0.2283	ns	IBD	0.0345	*	RA	0.6113	ns	onco	0.0753	ns	T-test
117	PC 36:6	control	cvd	0.7754	ns	diabetes	0.1778	ns	IBD	0.0056	**	RA	0.3039	ns	onco	0.0184	*	T-test
118	PC 37:6	control	cvd	0.6469	ns	diabetes	0.0281	*	IBD	0.0087	**	RA	0.1644	ns	onco	0.6677	ns	T-test
119	PC 38:3	control	cvd	0.7227	ns	diabetes	0.3450	ns	IBD	0.5907	ns	RA	0.4264	ns	onco	0.0845	ns	T-test
120	PC 38:4	control	cvd	0.0010	**	diabetes	0.2813	ns	IBD	0.4154	ns	RA	0.1397	ns	onco	0.0020	**	T-test
121	PC 38:5	control	cvd	0.3083	ns	diabetes	0.1750	ns	IBD	0.6340	ns	RA	0.2358	ns	onco	0.7727	ns	T-test
122	PC 38:6	control	cvd	0.2072	ns	diabetes	0.1572	ns	IBD	0.2228	ns	RA	0.0757	ns	onco	0.0337	*	T-test
123	PC 38:7	control	cvd	0.6535	ns	diabetes	0.0545	ns	IBD	0.0022	**	RA	0.8842	ns	onco	0.4615	ns	T-test
124	PC 38:8	control	cvd	0.4282	ns	diabetes	0.3267	ns	IBD	0.1863	ns	RA	0.8582	ns	onco	0.3193	ns	T-test
125	PC 39:3	control	cvd	0.3059	ns	diabetes	0.4444	ns	IBD	0.0120	*	RA	0.7569	ns	onco	0.2833	ns	T-test
126	PC 39:4	control	cvd	0.3628	ns	diabetes	0.1899	ns	IBD	0.0710	ns	RA	0.8653	ns	onco	0.1385	ns	T-test
127	PC 39:5	contro	cvd	0.4743	ns	diabetes	0.0086	**	IBD	0.4416	ns	RA	0.2126	ns	onco	0.7264	ns	T-test

128	PC 40:4	control	cvd	0.4655	ns	diabetes	0.2142	ns	IBD	0.3305	ns	RA	0.8961	ns	onco	0.1337	ns	T-test
129	PC 40:5	control	cvd	0.0150	*	diabetes	0.6903	ns	IBD	0.6473	ns	RA	0.5077	ns	onco	0.4924	ns	T-test
130	PC 40:6	control	cvd	0.0414	*	diabetes	0.7622	ns	IBD	0.3368	ns	RA	0.0947	ns	onco	0.0214	*	T-test
131	PC 41:6	control	cvd	0.7517	ns	diabetes	0.0703	ns	IBD	0.0270	*	RA	0.5772	ns	onco	0.2705	ns	T-test
132	PC 42:10	control	cvd	0.3130	ns	diabetes	0.0246	*	IBD	0.0647	ns	RA	0.4383	ns	onco	0.2016	ns	T-test
133	PC 42:2	control	cvd	0.2745	ns	diabetes	0.0986	ns	IBD	0.0062	**	RA	0.0183	*	onco	0.9948	ns	T-test
134	PC 42:3	control	cvd	0.9243	ns	diabetes	0.2211	ns	IBD	0.0240	*	RA	0.5229	ns	onco	0.4410	ns	T-test
135	PC 42:4	control	cvd	0.8671	ns	diabetes	0.4271	ns	IBD	0.1431	ns	RA	0.9577	ns	onco	0.0531	ns	T-test
136	PC 42:5	control	cvd	0.0337	*	diabetes	0.0102	*	IBD	0.1081	ns	RA	0.1609	ns	onco	0.9317	ns	T-test
137	PC 42:7	control	cvd	0.2734	ns	diabetes	0.7381	ns	IBD	0.0314	*	RA	0.9006	ns	onco	0.1137	ns	T-test
138	PC 42:8	control	cvd	0.9254	ns	diabetes	0.7752	ns	IBD	0.4144	ns	RA	0.8559	ns	onco	0.1572	ns	T-test
139	PC 42:9	control	cvd	0.1416	ns	diabetes	0.2419	ns	IBD	0.9848	ns	RA	0.5217	ns	onco	0.5872	ns	T-test
140	PC 44:5	control	cvd	0.0564	ns	diabetes	0.8221	ns	IBD	0.3509	ns	RA	0.8943	ns	onco	0.0569	ns	T-test
141	PE 22:0	control	cvd	0.9336	ns	diabetes	0.0942	ns	IBD	0.0413	*	RA	0.7853	ns	onco	0.8423	ns	T-test
142	PE 23:0	control	cvd	0.8717	ns	diabetes	0.3052	ns	IBD	0.0585	ns	RA	0.5087	ns	onco	0.8412	ns	T-test
143	PE 24:0.IS	control	cvd	0.5694	ns	diabetes	0.7749	ns	IBD	0.2485	ns	RA	0.8189	ns	onco	0.6557	ns	T-test
144	PE 25:0	control	cvd	0.6254	ns	diabetes	0.3394	ns	IBD	0.4813	ns	RA	0.3898	ns	onco	0.3231	ns	T-test
145	PE 26:0	control	cvd	0.6337	ns	diabetes	0.1098	ns	IBD	0.1949	ns	RA	0.9921	ns	onco	0.4716	ns	T-test
146	PE 32:1	control	cvd	0.6363	ns	diabetes	0.9375	ns	IBD	0.5962	ns	RA	0.8315	ns	onco	0.2059	ns	T-test
147	PE 34:1	control	cvd	0.9858	ns	diabetes	0.6825	ns	IBD	0.3417	ns	RA	0.9166	ns	onco	0.1853	ns	T-test
148	PE 34:2	control	cvd	0.3558	ns	diabetes	0.0381	*	IBD	0.2245	ns	RA	0.8585	ns	onco	0.8547	ns	T-test
149	PE 34:3	control	cvd	0.2941	ns	diabetes	0.1329	ns	IBD	0.0798	ns	RA	0.3635	ns	onco	0.7504	ns	T-test
150	PE 35:1	control	cvd	0.4774	ns	diabetes	0.1422	ns	IBD	0.1296	ns	RA	0.6113	ns	onco	0.9354	ns	T-test
151	PE 35:2	control	cvd	0.0728	ns	diabetes	0.0206	*	IBD	0.1097	ns	RA	0.5103	ns	onco	0.9225	ns	T-test

152	PE 36:1	control	cvd	0.7095	ns	diabetes	0.2904	ns	IBD	0.0341	*	RA	0.7262	ns	onco	0.4317	ns	T-test
153	PE 36:2	control	cvd	0.7156	ns	diabetes	0.0441	*	IBD	0.0947	ns	RA	0.9371	ns	onco	0.8089	ns	T-test
154	PE 36:3	control	cvd	0.2055	ns	diabetes	0.0099	**	IBD	0.1850	ns	RA	0.6623	ns	onco	0.7210	ns	T-test
155	PE 36:4	control	cvd	0.9932	ns	diabetes	0.1248	ns	IBD	0.8681	ns	RA	0.8944	ns	onco	0.1225	ns	T-test
156	PE 36:5	control	cvd	0.7424	ns	diabetes	0.0496	*	IBD	0.1519	ns	RA	0.9030	ns	onco	0.2369	ns	T-test
157	PE 38:3	control	cvd	0.9653	ns	diabetes	0.9310	ns	IBD	0.2242	ns	RA	0.6352	ns	onco	0.4146	ns	T-test
158	PE 38:4	control	cvd	0.1471	ns	diabetes	0.1587	ns	IBD	0.6802	ns	RA	0.7942	ns	onco	0.1037	ns	T-test
159	PE 38:5	control	cvd	0.9820	ns	diabetes	0.0111	*	IBD	0.5315	ns	RA	0.9436	ns	onco	0.1695	ns	T-test
160	PE 38:6	control	cvd	0.3177	ns	diabetes	0.1608	ns	IBD	0.6827	ns	RA	0.4681	ns	onco	0.1211	ns	T-test
161	PE 40:3	control	cvd	0.3293	ns	diabetes	0.4129	ns	IBD	0.0539	ns	RA	0.2732	ns	onco	0.2089	ns	T-test
162	PE 40:4	control	cvd	0.7849	ns	diabetes	0.9402	ns	IBD	0.7269	ns	RA	0.8815	ns	onco	0.4506	ns	T-test
163	PE 40:5	control	cvd	0.1117	ns	diabetes	0.4335	ns	IBD	0.7522	ns	RA	0.6678	ns	onco	0.5706	ns	T-test
164	PE 40:6	control	cvd	0.0472	*	diabetes	0.5435	ns	IBD	0.4667	ns	RA	0.2182	ns	onco	0.0395	*	T-test
165	PE 40:7	control	cvd	0.5722	ns	diabetes	0.0320	*	IBD	0.5357	ns	RA	0.9392	ns	onco	0.4183	ns	T-test
166	PE 40:8	control	cvd	0.6250	ns	diabetes	0.0506	ns	IBD	0.6182	ns	RA	0.1841	ns	onco	0.5189	ns	T-test
167	PI 32:0	control	cvd	0.0049	**	diabetes	0.2324	ns	IBD	0.1099	ns	RA	0.5173	ns	onco	0.9125	ns	T-test
168	PI 32:1	control	cvd	0.1258	ns	diabetes	0.3006	ns	IBD	0.6670	ns	RA	0.5571	ns	onco	0.2258	ns	T-test
169	PI 34:1	control	cvd	0.0694	ns	diabetes	0.2300	ns	IBD	0.1157	ns	RA	0.8506	ns	onco	0.6720	ns	T-test
170	PI 34:2	control	cvd	0.0902	ns	diabetes	0.6533	ns	IBD	0.1064	ns	RA	0.9353	ns	onco	0.2935	ns	T-test
171	PI 36:1	control	cvd	0.2638	ns	diabetes	0.0339	*	IBD	0.0020	**	RA	0.4113	ns	onco	0.8039	ns	T-test
172	PI 36:2	control	cvd	0.2136	ns	diabetes	0.3997	ns	IBD	0.0168	*	RA	0.4358	ns	onco	0.5478	ns	T-test
173	PI 36:3	control	cvd	0.0190	*	diabetes	0.1543	ns	IBD	0.3017	ns	RA	0.4509	ns	onco	0.5125	ns	T-test
174	PI 36:4	control	cvd	0.8121	ns	diabetes	0.9046	ns	IBD	0.9138	ns	RA	0.8065	ns	onco	0.3559	ns	T-test
175	PI 38:2	control	cvd	0.3979	ns	diabetes	0.0177	*	IBD	0.0006	***	RA	0.3470	ns	onco	0.2012	ns	T-test
176	PI 38:3	contro	cvd	0.5925	ns	diabetes	0.2186	ns	IBD	0.0694	ns	RA	0.6204	ns	onco	0.4954	ns	T-test

177	PI 38:4	control	cvd	0.0019	**	diabetes	0.5216	ns	IBD	0.8271	ns	RA	0.8250	ns	onco	0.1412	ns	T-test
178	PI 38:5	control	cvd	0.5018	ns	diabetes	0.2670	ns	IBD	0.7335	ns	RA	0.8689	ns	onco	0.4914	ns	T-test
179	PI 38:6	control	cvd	0.1438	ns	diabetes	0.0202	*	IBD	0.2165	ns	RA	0.4169	ns	onco	0.1297	ns	T-test
180	PI 40:4	control	cvd	0.8066	ns	diabetes	0.2562	ns	IBD	0.9850	ns	RA	0.3676	ns	onco	0.9715	ns	T-test
181	PI 40:5	control	cvd	0.0807	ns	diabetes	0.1718	ns	IBD	0.7901	ns	RA	0.8971	ns	onco	0.2630	ns	T-test
182	PI 40:6	control	cvd	0.7877	ns	diabetes	0.0080	**	IBD	0.2113	ns	RA	0.3935	ns	onco	0.0783	ns	T-test
183	SM 30:1	control	cvd	0.4859	ns	diabetes	0.5893	ns	IBD	0.1052	ns	RA	0.7917	ns	onco	0.1525	ns	T-test
184	SM 31:1	control	cvd	0.2908	ns	diabetes	0.0906	ns	IBD	0.0329	*	RA	0.5515	ns	onco	0.7806	ns	T-test
185	SM 32:1	control	cvd	0.2145	ns	diabetes	0.5048	ns	IBD	0.0017	**	RA	0.9394	ns	onco	0.1262	ns	T-test
186	SM 32:2	control	cvd	0.1075	ns	diabetes	0.0393	*	IBD	0.5313	ns	RA	0.2723	ns	onco	0.0340	*	T-test
187	SM 33:1	control	cvd	0.6464	ns	diabetes	0.4029	ns	IBD	0.0128	*	RA	0.6082	ns	onco	0.7948	ns	T-test
188	SM 34:1	control	cvd	0.6852	ns	diabetes	0.4517	ns	IBD	0.6951	ns	RA	0.6277	ns	onco	0.6336	ns	T-test
189	SM 34:2	control	cvd	0.0117	*	diabetes	0.0136	*	IBD	0.6007	ns	RA	0.2788	ns	onco	0.0466	*	T-test
190	SM 34:3	control	cvd	0.0667	ns	diabetes	0.0130	*	IBD	0.7235	ns	RA	0.1032	ns	onco	0.2099	ns	T-test
191	SM 35:1	control	cvd	0.2082	ns	diabetes	0.9526	ns	IBD	0.1870	ns	RA	0.6280	ns	onco	0.5033	ns	T-test
192	SM 35:2	control	cvd	0.0557	ns	diabetes	0.5217	ns	IBD	0.2024	ns	RA	0.1633	ns	onco	0.1367	ns	T-test
193	SM 36:1	control	cvd	0.0194	*	diabetes	0.4408	ns	IBD	0.1223	ns	RA	0.4303	ns	onco	0.1268	ns	T-test
194	SM 36:2	control	cvd	0.0102	*	diabetes	0.1131	ns	IBD	0.4903	ns	RA	0.1506	ns	onco	0.0191	*	T-test
195	SM 36:3	control	cvd	0.0104	*	diabetes	0.0650	ns	IBD	0.8600	ns	RA	0.3195	ns	onco	0.2237	ns	T-test
196	SM 36:4	control	cvd	0.9005	ns	diabetes	0.0158	*	IBD	0.0036	**	RA	0.0746	ns	onco	0.7649	ns	T-test
197	SM 37:1	control	cvd	0.1776	ns	diabetes	0.8578	ns	IBD	0.0442	*	RA	0.5885	ns	onco	0.2056	ns	T-test
198	SM 37:2	control	cvd	0.3588	ns	diabetes	0.3995	ns	IBD	0.5611	ns	RA	0.5787	ns	onco	0.4606	ns	T-test
199	SM 38:1	control	cvd	0.2237	ns	diabetes	0.2998	ns	IBD	0.0058	**	RA	0.9499	ns	onco	0.0246	*	T-test
200	SM 38:2	control	cvd	0.1843	ns	diabetes	0.6890	ns	IBD	0.6388	ns	RA	0.3645	ns	onco	0.0189	*	T-test

201	SM 38:3	control	cvd	0.0211	*	diabetes	0.0080	**	IBD	0.5733	ns	RA	0.1672	ns	onco	0.0120	*	T-test
202	SM 39:1	control	cvd	0.8809	ns	diabetes	0.0726	ns	IBD	0.0001	****	RA	0.6991	ns	onco	0.1597	ns	T-test
203	SM 39:2	control	cvd	0.3070	ns	diabetes	0.2204	ns	IBD	0.6645	ns	RA	0.5167	ns	onco	0.2224	ns	T-test
204	SM 40:1	control	cvd	0.1961	ns	diabetes	0.7359	ns	IBD	0.1142	ns	RA	0.8806	ns	onco	0.2652	ns	T-test
205	SM 40:2	control	cvd	0.4318	ns	diabetes	0.7391	ns	IBD	0.0716	ns	RA	0.9822	ns	onco	0.0953	ns	T-test
206	SM 40:3	control	cvd	0.0076	**	diabetes	0.0146	*	IBD	0.7398	ns	RA	0.2223	ns	onco	0.0034	**	T-test
207	SM 40:4	control	cvd	0.0487	*	diabetes	0.0053	**	IBD	0.4050	ns	RA	0.0705	ns	onco	0.0206	*	T-test
208	SM 40:5	control	cvd	0.6327	ns	diabetes	0.0675	ns	IBD	0.0380	*	RA	0.8376	ns	onco	0.7551	ns	T-test
209	SM 41:1	control	cvd	0.8035	ns	diabetes	0.1118	ns	IBD	0.0049	**	RA	0.4989	ns	onco	0.1479	ns	T-test
210	SM 42:1	control	cvd	0.3716	ns	diabetes	0.2528	ns	IBD	0.0322	*	RA	0.3893	ns	onco	0.1851	ns	T-test
211	SM 42:2	control	cvd	0.0066	**	diabetes	0.0983	ns	IBD	0.3910	ns	RA	0.9550	ns	onco	0.0204	*	T-test
212	SM 42:3	control	cvd	0.0077	**	diabetes	0.0743	ns	IBD	0.3133	ns	RA	0.5437	ns	onco	0.0070	**	T-test
213	SM 42:4	control	cvd	0.1989	ns	diabetes	0.0488	*	IBD	0.3413	ns	RA	0.1214	ns	onco	0.0172	*	T-test
214	SM 43:1	control	cvd	0.2283	ns	diabetes	0.3851	ns	IBD	0.0368	*	RA	0.9332	ns	onco	0.5847	ns	T-test
215	SM 43:2	control	cvd	0.0046	**	diabetes	0.4152	ns	IBD	0.4555	ns	RA	0.6255	ns	onco	0.4037	ns	T-test
216	SM 43:3	control	cvd	0.9901	ns	diabetes	0.8406	ns	IBD	0.0417	*	RA	0.0664	ns	onco	0.3163	ns	T-test
217	SM 44:1	control	cvd	0.2946	ns	diabetes	0.3517	ns	IBD	0.0161	*	RA	0.3150	ns	onco	0.6953	ns	T-test
218	SM 44:2	control	cvd	0.0876	ns	diabetes	0.1337	ns	IBD	0.1047	ns	RA	0.1937	ns	onco	0.1024	ns	T-test
219	SM 44:3	control	cvd	0.0771	ns	diabetes	0.4944	ns	IBD	0.1069	ns	RA	0.7765	ns	onco	0.0678	ns	T-test
220	SM 44:4	control	cvd	0.4496	ns	diabetes	0.2554	ns	IBD	0.4184	ns	RA	0.6249	ns	onco	0.1238	ns	T-test
221	TG 40:0	control	cvd	0.9859	ns	diabetes	0.5898	ns	IBD	0.1703	ns	RA	0.3570	ns	onco	0.4641	ns	T-test
222	TG 41:0	control	cvd	0.9505	ns	diabetes	0.7704	ns	IBD	0.2451	ns	RA	0.4384	ns	onco	0.6129	ns	T-test
223	TG 42:0	control	cvd	0.7418	ns	diabetes	0.9252	ns	IBD	0.3049	ns	RA	0.3767	ns	onco	0.3783	ns	T-test
224	TG 42:1	control	cvd	0.9933	ns	diabetes	0.9625	ns	IBD	0.1859	ns	RA	0.4711	ns	onco	0.5087	ns	T-test
225	TG 42:2	contro	cvd	0.9528	ns	diabetes	0.9236	ns	IBD	0.1812	ns	RA	0.4249	ns	onco	0.6257	ns	T-test

226	TG 43:0	control	cvd	0.8951	ns	diabetes	0.7286	ns	IBD	0.3525	ns	RA	0.3652	ns	onco	0.4726	ns	T-test
227	TG 43:1	control	cvd	0.9797	ns	diabetes	0.9771	ns	IBD	0.1139	ns	RA	0.2790	ns	onco	0.3535	ns	T-test
228	TG 43:2	control	cvd	0.8655	ns	diabetes	0.8520	ns	IBD	0.0279	*	RA	0.3202	ns	onco	0.1964	ns	T-test
229	TG 44:0	control	cvd	0.7852	ns	diabetes	0.6992	ns	IBD	0.1948	ns	RA	0.4052	ns	onco	0.2858	ns	T-test
230	TG 44:1	control	cvd	0.8502	ns	diabetes	0.9198	ns	IBD	0.1947	ns	RA	0.5871	ns	onco	0.4798	ns	T-test
231	TG 44:2	control	cvd	0.6981	ns	diabetes	0.8712	ns	IBD	0.0701	ns	RA	0.3413	ns	onco	0.3506	ns	T-test
232	TG 44:3	control	cvd	0.5299	ns	diabetes	0.8716	ns	IBD	0.0449	*	RA	0.4529	ns	onco	0.5125	ns	T-test
233	TG 45:0	control	cvd	0.7014	ns	diabetes	0.9237	ns	IBD	0.2251	ns	RA	0.3357	ns	onco	0.6277	ns	T-test
234	TG 45:1	control	cvd	0.5428	ns	diabetes	0.6902	ns	IBD	0.1302	ns	RA	0.4103	ns	onco	0.6636	ns	T-test
235	TG 45:2	control	cvd	0.6908	ns	diabetes	0.7794	ns	IBD	0.0346	*	RA	0.2875	ns	onco	0.2157	ns	T-test
236	TG 46:0	control	cvd	0.9924	ns	diabetes	0.6516	ns	IBD	0.0954	ns	RA	0.3287	ns	onco	0.1654	ns	T-test
237	TG 46:1	control	cvd	0.6200	ns	diabetes	0.8609	ns	IBD	0.1051	ns	RA	0.7994	ns	onco	0.4228	ns	T-test
238	TG 46:2	control	cvd	0.9265	ns	diabetes	0.9113	ns	IBD	0.1099	ns	RA	0.5953	ns	onco	0.5782	ns	T-test
239	TG 46:3	control	cvd	0.7222	ns	diabetes	0.6084	ns	IBD	0.0603	ns	RA	0.6042	ns	onco	0.6860	ns	T-test
240	TG 46:4	control	cvd	0.0500	ns	diabetes	0.4574	ns	IBD	0.2377	ns	RA	0.4428	ns	onco	0.3005	ns	T-test
241	TG 47:0	control	cvd	0.8503	ns	diabetes	0.8852	ns	IBD	0.0998	ns	RA	0.2107	ns	onco	0.3577	ns	T-test
242	TG 47:1	control	cvd	0.6027	ns	diabetes	0.9480	ns	IBD	0.0462	*	RA	0.4976	ns	onco	0.6958	ns	T-test
243	TG 47:2	control	cvd	0.6768	ns	diabetes	0.8608	ns	IBD	0.0275	*	RA	0.3148	ns	onco	0.4967	ns	T-test
244	TG 47:3	control	cvd	0.7682	ns	diabetes	0.5658	ns	IBD	0.0079	**	RA	0.1898	ns	onco	0.3303	ns	T-test
245	TG 48:0	control	cvd	0.4922	ns	diabetes	0.4278	ns	IBD	0.1125	ns	RA	0.2415	ns	onco	0.1171	ns	T-test
246	TG 48:1	control	cvd	0.8693	ns	diabetes	0.5001	ns	IBD	0.0617	ns	RA	0.6710	ns	onco	0.2505	ns	T-test
247	TG 48:2	control	cvd	0.8958	ns	diabetes	0.4500	ns	IBD	0.0489	*	RA	0.6784	ns	onco	0.3465	ns	T-test
248	TG 48:3	control	cvd	0.7264	ns	diabetes	0.7806	ns	IBD	0.0314	*	RA	0.7490	ns	onco	0.6703	ns	T-test
249	TG 48:4	control	cvd	0.5448	ns	diabetes	0.9322	ns	IBD	0.0144	*	RA	0.5021	ns	onco	0.4357	ns	T-test

250	TG 48:5	control	cvd	0.6209	ns	diabetes	0.9381	ns	IBD	0.0201	*	RA	0.4374	ns	onco	0.4570	ns	T-test
251	TG 49:0	control	cvd	0.5989	ns	diabetes	0.9604	ns	IBD	0.0692	ns	RA	0.1518	ns	onco	0.4836	ns	T-test
252	TG 49:1	control	cvd	0.8899	ns	diabetes	0.8630	ns	IBD	0.0430	*	RA	0.4586	ns	onco	0.9277	ns	T-test
253	TG 49:2	control	cvd	0.7035	ns	diabetes	0.6696	ns	IBD	0.0373	*	RA	0.3299	ns	onco	0.7282	ns	T-test
254	TG 49:3	control	cvd	0.8497	ns	diabetes	0.8456	ns	IBD	0.0087	**	RA	0.2773	ns	onco	0.6850	ns	T-test
255	TG 49:4	control	cvd	0.7960	ns	diabetes	0.6761	ns	IBD	0.0028	**	RA	0.2576	ns	onco	0.6306	ns	T-test
256	TG 50:0	control	cvd	0.3916	ns	diabetes	0.9671	ns	IBD	0.0765	ns	RA	0.3432	ns	onco	0.2478	ns	T-test
257	TG 50:1	control	cvd	0.2789	ns	diabetes	0.0908	ns	IBD	0.1617	ns	RA	0.4168	ns	onco	0.1825	ns	T-test
258	TG 50:2	control	cvd	0.1783	ns	diabetes	0.0435	*	IBD	0.1573	ns	RA	0.4585	ns	onco	0.2111	ns	T-test
259	TG 50:3	control	cvd	0.2128	ns	diabetes	0.1432	ns	IBD	0.0643	ns	RA	0.5044	ns	onco	0.3354	ns	T-test
260	TG 50:4	control	cvd	0.1982	ns	diabetes	0.5561	ns	IBD	0.0167	*	RA	0.4088	ns	onco	0.3999	ns	T-test
261	TG 50:5	control	cvd	0.2434	ns	diabetes	0.8930	ns	IBD	0.0097	**	RA	0.3811	ns	onco	0.2843	ns	T-test
262	TG 50:6	control	cvd	0.2321	ns	diabetes	0.7260	ns	IBD	0.0132	*	RA	0.2335	ns	onco	0.0675	ns	T-test
263	TG 51:0	control	cvd	0.6564	ns	diabetes	0.7199	ns	IBD	0.0242	*	RA	0.1462	ns	onco	0.3767	ns	T-test
264	TG 51:1	control	cvd	0.3735	ns	diabetes	0.9011	ns	IBD	0.0464	*	RA	0.4007	ns	onco	0.7875	ns	T-test
265	TG 51:2	control	cvd	0.1433	ns	diabetes	0.3218	ns	IBD	0.0442	*	RA	0.5337	ns	onco	0.8129	ns	T-test
266	TG 51:3	control	cvd	0.1848	ns	diabetes	0.5239	ns	IBD	0.0270	*	RA	0.6828	ns	onco	0.8859	ns	T-test
267	TG 51:4	control	cvd	0.2474	ns	diabetes	0.9610	ns	IBD	0.0070	**	RA	0.4442	ns	onco	0.8125	ns	T-test
268	TG 51:5	control	cvd	0.3688	ns	diabetes	0.9762	ns	IBD	0.0007	***	RA	0.3948	ns	onco	0.9276	ns	T-test
269	TG 51:6	control	cvd	0.5799	ns	diabetes	0.6260	ns	IBD	0.0038	**	RA	0.3933	ns	onco	0.6588	ns	T-test
270	TG 52:0	control	cvd	0.1955	ns	diabetes	0.3285	ns	IBD	0.0313	*	RA	0.5303	ns	onco	0.2942	ns	T-test
271	TG 52:1	control	cvd	0.1732	ns	diabetes	0.5947	ns	IBD	0.0583	ns	RA	0.6197	ns	onco	0.4214	ns	T-test
272	TG 52:2	control	cvd	0.0164	*	diabetes	0.0253	*	IBD	0.1753	ns	RA	0.8614	ns	onco	0.2427	ns	T-test
273	TG 52:3	control	cvd	0.0022	**	diabetes	0.0062	**	IBD	0.1202	ns	RA	0.6560	ns	onco	0.2648	ns	T-test
274	TG 52:4	contro	cvd	0.0122	*	diabetes	0.0695	ns	IBD	0.0524	ns	RA	0.5647	ns	onco	0.4703	ns	T-test

275	TG 52:5	control	cvd	0.0750	ns	diabetes	0.4288	ns	IBD	0.0119	*	RA	0.9062	ns	onco	0.8223	ns	T-test
276	TG 52:6	control	cvd	0.0515	ns	diabetes	0.7691	ns	IBD	0.0093	**	RA	0.2834	ns	onco	0.0960	ns	T-test
277	TG 52:7	control	cvd	0.0602	ns	diabetes	0.7947	ns	IBD	0.0047	**	RA	0.2039	ns	onco	0.0595	ns	T-test
278	TG 53:1	control	cvd	0.3431	ns	diabetes	0.3717	ns	IBD	0.0132	*	RA	0.4512	ns	onco	0.7175	ns	T-test
279	TG 53:2	control	cvd	0.1224	ns	diabetes	0.2791	ns	IBD	0.0102	*	RA	0.6946	ns	onco	0.9633	ns	T-test
280	TG 53:3	control	cvd	0.0256	*	diabetes	0.4808	ns	IBD	0.0305	*	RA	0.7278	ns	onco	0.8863	ns	T-test
281	TG 53:4	control	cvd	0.0184	*	diabetes	0.4022	ns	IBD	0.0428	*	RA	0.9562	ns	onco	0.7094	ns	T-test
282	TG 53:5	control	cvd	0.0531	ns	diabetes	0.8384	ns	IBD	0.0064	**	RA	0.4337	ns	onco	0.8114	ns	T-test
283	TG 53:6	control	cvd	0.1302	ns	diabetes	0.5729	ns	IBD	0.0019	**	RA	0.2166	ns	onco	0.2836	ns	T-test
284	TG 53:7	control	cvd	0.1593	ns	diabetes	0.3652	ns	IBD	0.0095	**	RA	0.1808	ns	onco	0.3123	ns	T-test
285	TG 54:0	control	cvd	0.2611	ns	diabetes	0.1879	ns	IBD	0.0012	**	RA	0.3980	ns	onco	0.1519	ns	T-test
286	TG 54:1	control	cvd	0.2500	ns	diabetes	0.5130	ns	IBD	0.0119	*	RA	0.6782	ns	onco	0.6078	ns	T-test
287	TG 54:2	control	cvd	0.0504	ns	diabetes	0.4323	ns	IBD	0.0443	*	RA	0.8885	ns	onco	0.6500	ns	T-test
288	TG 54:3	control	cvd	0.0160	*	diabetes	0.0625	ns	IBD	0.2045	ns	RA	0.7872	ns	onco	0.6736	ns	T-test
289	TG 54:4	control	cvd	0.0075	**	diabetes	0.0960	ns	IBD	0.2023	ns	RA	0.8789	ns	onco	0.8505	ns	T-test
290	TG 54:5	control	cvd	0.0058	**	diabetes	0.0860	ns	IBD	0.0714	ns	RA	0.6373	ns	onco	0.3584	ns	T-test
291	TG 54:6	control	cvd	0.0096	**	diabetes	0.3583	ns	IBD	0.0195	*	RA	0.3672	ns	onco	0.1584	ns	T-test
292	TG 54:7	control	cvd	0.0051	**	diabetes	0.5339	ns	IBD	0.0110	*	RA	0.0877	ns	onco	0.0123	*	T-test
293	TG 54:8	control	cvd	0.0172	*	diabetes	0.8289	ns	IBD	0.0034	**	RA	0.1138	ns	onco	0.0406	*	T-test
294	TG 54:9	control	cvd	0.1039	ns	diabetes	0.3808	ns	IBD	0.0061	**	RA	0.2240	ns	onco	0.0823	ns	T-test
295	TG 55:0	control	cvd	0.2338	ns	diabetes	0.7991	ns	IBD	0.1472	ns	RA	0.2248	ns	onco	0.3510	ns	T-test
296	TG 55:1	control	cvd	0.4546	ns	diabetes	0.1665	ns	IBD	0.0017	**	RA	0.3177	ns	onco	0.4888	ns	T-test
297	TG 55:2	control	cvd	0.1852	ns	diabetes	0.4778	ns	IBD	0.0012	**	RA	0.7213	ns	onco	0.6606	ns	T-test
298	TG 55:3	control	cvd	0.0641	ns	diabetes	0.7383	ns	IBD	0.0093	**	RA	0.9185	ns	onco	0.9248	ns	T-test

299	TG 55:4	control	cvd	0.1926	ns	diabetes	0.4741	ns	IBD	0.0012	**	RA	0.5918	ns	onco	0.8391	ns	T-test
300	TG 55:5	control	cvd	0.0239	*	diabetes	0.6521	ns	IBD	0.0281	*	RA	0.3492	ns	onco	0.2551	ns	T-test
301	TG 55:6	control	cvd	0.0322	*	diabetes	0.4850	ns	IBD	0.0169	*	RA	0.5301	ns	onco	0.0358	*	T-test
302	TG 55:7	control	cvd	0.0385	*	diabetes	0.3435	ns	IBD	0.0047	**	RA	0.1797	ns	onco	0.2323	ns	T-test
303	TG 55:8	control	cvd	0.0641	ns	diabetes	0.2096	ns	IBD	0.0045	**	RA	0.2115	ns	onco	0.2410	ns	T-test
304	TG 56:0	control	cvd	0.2202	ns	diabetes	0.3450	ns	IBD	0.0076	**	RA	0.2722	ns	onco	0.2280	ns	T-test
305	TG 56:1	control	cvd	0.4724	ns	diabetes	0.3578	ns	IBD	0.0004	***	RA	0.4581	ns	onco	0.5754	ns	T-test
306	TG 56:10	control	cvd	0.0140	*	diabetes	0.9713	ns	IBD	0.1257	ns	RA	0.1766	ns	onco	0.0261	*	T-test
307	TG 56:2	control	cvd	0.1267	ns	diabetes	0.3733	ns	IBD	0.0004	***	RA	0.9544	ns	onco	0.3539	ns	T-test
308	TG 56:3	control	cvd	0.0394	*	diabetes	0.7892	ns	IBD	0.0015	**	RA	0.6578	ns	onco	0.5888	ns	T-test
309	TG 56:4	control	cvd	0.1200	ns	diabetes	0.3052	ns	IBD	0.0047	**	RA	0.8338	ns	onco	0.3266	ns	T-test
310	TG 56:5	control	cvd	0.0000	****	diabetes	0.0584	ns	IBD	0.8719	ns	RA	0.2700	ns	onco	0.0075	**	T-test
311	TG 56:6	control	cvd	0.0001	****	diabetes	0.0708	ns	IBD	0.3260	ns	RA	0.4445	ns	onco	0.0241	*	T-test
312	TG 56:7	control	cvd	0.0005	***	diabetes	0.4903	ns	IBD	0.0478	*	RA	0.1646	ns	onco	0.0193	*	T-test
313	TG 56:8	control	cvd	0.0020	**	diabetes	0.8700	ns	IBD	0.0108	*	RA	0.1354	ns	onco	0.0251	*	T-test
314	TG 56:9	control	cvd	0.0052	**	diabetes	0.9066	ns	IBD	0.0075	**	RA	0.2037	ns	onco	0.0337	*	T-test
315	TG 57:0	control	cvd	0.3639	ns	diabetes	0.8857	ns	IBD	0.5483	ns	RA	0.6918	ns	onco	0.3158	ns	T-test
316	TG 57:1	control	cvd	0.8190	ns	diabetes	0.1477	ns	IBD	0.0185	*	RA	0.4045	ns	onco	0.4471	ns	T-test
317	TG 57:2	control	cvd	0.3364	ns	diabetes	0.2737	ns	IBD	0.0007	***	RA	0.3879	ns	onco	0.3230	ns	T-test
318	TG 57:3	control	cvd	0.1620	ns	diabetes	0.9243	ns	IBD	0.0011	**	RA	0.5654	ns	onco	0.5748	ns	T-test
319	TG 57:4	control	cvd	0.1524	ns	diabetes	0.5406	ns	IBD	0.0019	**	RA	0.4698	ns	onco	0.5128	ns	T-test
320	TG 57:5	control	cvd	0.0922	ns	diabetes	0.4553	ns	IBD	0.0047	**	RA	0.3799	ns	onco	0.2785	ns	T-test
321	TG 57:6	control	cvd	0.0345	*	diabetes	0.4961	ns	IBD	0.0111	*	RA	0.3662	ns	onco	0.3323	ns	T-test
322	TG 57:7	control	cvd	0.0307	*	diabetes	0.1801	ns	IBD	0.0036	**	RA	0.2581	ns	onco	0.2139	ns	T-test
323	TG 57:8	contro	cvd	0.0166	*	diabetes	0.2426	ns	IBD	0.0059	**	RA	0.1447	ns	onco	0.1930	ns	T-test

324	TG 57:9	control	cvd	0.0148	*	diabetes	0.1896	ns	IBD	0.0094	**	RA	0.1648	ns	onco	0.1306	ns	T-test
325	TG 58:0	control	cvd	0.3198	ns	diabetes	0.8602	ns	IBD	0.0408	*	RA	0.1802	ns	onco	0.2522	ns	T-test
326	TG 58:1	control	cvd	0.5205	ns	diabetes	0.1341	ns	IBD	0.0006	***	RA	0.7113	ns	onco	0.4405	ns	T-test
327	TG 58:10	control	cvd	0.0010	**	diabetes	0.8260	ns	IBD	0.0258	*	RA	0.1203	ns	onco	0.0041	**	T-test
328	TG 58:11	control	cvd	0.0027	**	diabetes	0.7338	ns	IBD	0.0322	*	RA	0.1647	ns	onco	0.0173	*	T-test
329	TG 58:2	control	cvd	0.3317	ns	diabetes	0.1610	ns	IBD	0.0001	***	RA	0.9408	ns	onco	0.5644	ns	T-test
330	TG 58:3	control	cvd	0.1411	ns	diabetes	0.4216	ns	IBD	0.0001	***	RA	0.8889	ns	onco	0.3998	ns	T-test
331	TG 58:4	control	cvd	0.1140	ns	diabetes	0.4950	ns	IBD	0.0001	****	RA	0.9849	ns	onco	0.3200	ns	T-test
332	TG 58:5	control	cvd	0.0069	**	diabetes	0.0576	ns	IBD	0.8998	ns	RA	0.5442	ns	onco	0.1739	ns	T-test
333	TG 58:6	control	cvd	0.0168	*	diabetes	0.7736	ns	IBD	0.0162	*	RA	0.7043	ns	onco	0.1475	ns	T-test
334	TG 58:7	control	cvd	0.0056	**	diabetes	0.8508	ns	IBD	0.0084	**	RA	0.4261	ns	onco	0.0351	*	T-test
335	TG 58:8	control	cvd	0.0017	**	diabetes	0.8717	ns	IBD	0.0326	*	RA	0.1582	ns	onco	0.0172	*	T-test
336	TG 58:9	control	cvd	0.0112	*	diabetes	0.7852	ns	IBD	0.0158	*	RA	0.3135	ns	onco	0.0698	ns	T-test
337	TG 59:0	control	cvd	0.4094	ns	diabetes	0.6037	ns	IBD	0.6478	ns	RA	0.4306	ns	onco	0.0873	ns	T-test
338	TG 59:1	control	cvd	0.9408	ns	diabetes	0.0674	ns	IBD	0.0144	*	RA	0.3082	ns	onco	0.2431	ns	T-test
339	TG 59:2	control	cvd	0.8914	ns	diabetes	0.0304	*	IBD	0.0016	**	RA	0.6994	ns	onco	0.6626	ns	T-test
340	TG 59:3	control	cvd	0.1880	ns	diabetes	0.3330	ns	IBD	0.0090	**	RA	0.6432	ns	onco	0.5653	ns	T-test
341	TG 60:0	control	cvd	0.3307	ns	diabetes	0.5684	ns	IBD	0.3036	ns	RA	0.2008	ns	onco	0.0878	ns	T-test
342	TG 60:1	control	cvd	0.7357	ns	diabetes	0.0575	ns	IBD	0.0009	***	RA	0.5835	ns	onco	0.3023	ns	T-test
343	TG 60:10	control	cvd	0.0003	***	diabetes	0.5271	ns	IBD	0.0974	ns	RA	0.0642	ns	onco	0.0023	**	T-test
344	TG 60:11	control	cvd	0.0005	***	diabetes	0.9801	ns	IBD	0.0711	ns	RA	0.0720	ns	onco	0.0041	**	T-test
345	TG 60:12	control	cvd	0.0038	**	diabetes	0.6018	ns	IBD	0.0424	*	RA	0.0683	ns	onco	0.0088	**	T-test
346	TG 60:2	control	cvd	0.3827	ns	diabetes	0.1132	ns	IBD	0.0003	***	RA	0.9859	ns	onco	0.5879	ns	T-test
347	TG 60:3	control	cvd	0.2416	ns	diabetes	0.1700	ns	IBD	0.0001	****	RA	0.8853	ns	onco	0.5575	ns	T-test

348	TG 60:4	control	cvd	0.1248	ns	diabetes	0.9390	ns	IBD	0.0000	****	RA	0.6824	ns	onco	0.4203	ns	T-test
349	TG 60:5	control	cvd	0.2113	ns	diabetes	0.1808	ns	IBD	0.0001	****	RA	0.7192	ns	onco	0.2281	ns	T-test
350	TG 60:6	control	cvd	0.3997	ns	diabetes	0.2410	ns	IBD	0.0002	***	RA	0.6911	ns	onco	0.0697	ns	T-test
351	TG 60:7	control	cvd	0.0084	**	diabetes	0.9274	ns	IBD	0.3974	ns	RA	0.5947	ns	onco	0.0172	*	T-test
352	TG 60:8	control	cvd	0.1948	ns	diabetes	0.7854	ns	IBD	0.0017	**	RA	0.4821	ns	onco	0.0367	*	T-test
353	TG 60:9	control	cvd	0.0009	***	diabetes	0.2649	ns	IBD	0.0211	*	RA	0.1917	ns	onco	0.0029	**	T-test
354	TG 61:2	control	cvd	0.8824	ns	diabetes	0.0242	*	IBD	0.0200	*	RA	0.4391	ns	onco	0.3639	ns	T-test
355	TG 62:0	control	cvd	0.6124	ns	diabetes	0.2043	ns	IBD	0.6848	ns	RA	0.3678	ns	onco	0.1183	ns	T-test
356	TG 62:1	control	cvd	0.8995	ns	diabetes	0.0332	*	IBD	0.0013	**	RA	0.4261	ns	onco	0.2547	ns	T-test
357	TG 62:10	control	cvd	0.1239	ns	diabetes	0.3618	ns	IBD	0.0075	**	RA	0.6164	ns	onco	0.0090	**	T-test
358	TG 62:11	control	cvd	0.0400	*	diabetes	0.4028	ns	IBD	0.0233	*	RA	0.2034	ns	onco	0.0120	*	T-test
359	TG 62:12	control	cvd	0.0144	*	diabetes	0.5046	ns	IBD	0.0485	*	RA	0.1175	ns	onco	0.0083	**	T-test
360	TG 62:13	control	cvd	0.0225	*	diabetes	0.3817	ns	IBD	0.0717	ns	RA	0.1323	ns	onco	0.0162	*	T-test
361	TG 62:2	control	cvd	0.7197	ns	diabetes	0.0246	*	IBD	0.0005	***	RA	0.8152	ns	onco	0.4904	ns	T-test
362	TG 62:3	control	cvd	0.2936	ns	diabetes	0.1245	ns	IBD	0.0008	***	RA	0.8993	ns	onco	0.4918	ns	T-test
363	TG 62:4	control	cvd	0.1828	ns	diabetes	0.0969	ns	IBD	0.0002	***	RA	0.9820	ns	onco	0.3198	ns	T-test
364	TG 62:5	control	cvd	0.2017	ns	diabetes	0.0794	ns	IBD	0.0004	***	RA	0.9303	ns	onco	0.1632	ns	T-test
365	TG 62:6	control	cvd	0.8624	ns	diabetes	0.0311	*	IBD	0.0002	***	RA	0.6867	ns	onco	0.3072	ns	T-test
366	TG 62:7	control	cvd	0.5713	ns	diabetes	0.1030	ns	IBD	0.0105	*	RA	0.9867	ns	onco	0.0671	ns	T-test
367	TG 62:8	control	cvd	0.0425	*	diabetes	0.8682	ns	IBD	0.1464	ns	RA	0.8148	ns	onco	0.0392	*	T-test
368	TG 62:9	control	cvd	0.1981	ns	diabetes	0.1342	ns	IBD	0.0098	**	RA	0.2949	ns	onco	0.0558	ns	T-test
369	TG 64:0	control	cvd	0.0238	*	diabetes	0.4852	ns	IBD	0.4260	ns	RA	0.0113	*	onco	0.0056	**	T-test
370	TG 64:1	control	cvd	0.5471	ns	diabetes	0.0181	*	IBD	0.0113	*	RA	0.7371	ns	onco	0.0492	*	T-test
371	TG 64:2	control	cvd	0.9954	ns	diabetes	0.4109	ns	IBD	0.0001	****	RA	0.6911	ns	onco	0.7146	ns	T-test

Supplement Table 7 Overview of the T-test between lipid species and lipid subclasses of healthy condition (group 1) and cardiovascular diseases (cvd), diabetes, rheumatoid arthritis (RA) and inflammation bowel diseases (IBD) (group 2) of the FoCus cohort.

ID	Lipid class	group 1	group2	p-value	p.signif	group2	p-value	p.signif	group2	p-value	p.signif	group2	p-value	p.signif	group2	p-value	p.signif	method
1	aPE	control	cvd	0.0838	ns	diabetes	0.2161	ns	IBD	0.0541	ns	RA	0.8688	ns	onco	0.5374	ns	T-test
2	CE	control	cvd	0.5211	ns	diabetes	0.6072	ns	IBD	0.5559	ns	RA	0.8846	ns	onco	0.6512	ns	T-test
3	CER	control	cvd	0.0234	*	diabetes	0.8130	ns	IBD	0.1777	ns	RA	0.8492	ns	onco	0.1324	ns	T-test
4	CHOL	control	cvd	0.1797	ns	diabetes	0.2584	ns	IBD	0.0269	*	RA	0.9824	ns	onco	0.1066	ns	T-test
5	CoQ	control	cvd	0.5904	ns	diabetes	0.2737	ns	IBD	0.6591	ns	RA	0.8740	ns	onco	0.9685	ns	T-test
6	DG	control	cvd	0.1982	ns	diabetes	0.1880	ns	IBD	0.4462	ns	RA	0.8307	ns	onco	0.7034	ns	T-test
7	HEXCer	control	cvd	0.8670	ns	diabetes	0.6845	ns	IBD	0.3780	ns	RA	0.6558	ns	onco	0.8259	ns	T-test
8	LPC	control	cvd	0.7036	ns	diabetes	0.3259	ns	IBD	0.5112	ns	RA	0.6718	ns	onco	0.9472	ns	T-test
9	LPE	control	cvd	0.8946	ns	diabetes	0.1269	ns	IBD	0.7904	ns	RA	0.8376	ns	onco	0.7255	ns	T-test
10	PC	control	cvd	0.8584	ns	diabetes	0.2178	ns	IBD	0.1322	ns	RA	0.9174	ns	onco	0.2283	ns	T-test
11	PE	control	cvd	0.9965	ns	diabetes	0.1684	ns	IBD	0.1385	ns	RA	0.8240	ns	onco	0.4384	ns	T-test
12	PI	control	cvd	0.2824	ns	diabetes	0.1856	ns	IBD	0.1751	ns	RA	0.5095	ns	onco	0.5410	ns	T-test
13	SM	control	cvd	0.2074	ns	diabetes	0.5191	ns	IBD	0.3820	ns	RA	0.9819	ns	onco	0.1132	ns	T-test
14	TG	control	cvd	0.0001	***	diabetes	0.5482	ns	IBD	0.0000	****	RA	0.0047	**	onco	0.0001	***	T-test

ID	Lipid species	group 1	group2	p-value	p.signif	group2	p-value	p.signif	group2	p-value	p.signif	group2	p-value	p.signif	group2	p-value	p.signif	method
1	aPE 34:1	control	cvd	0.2559	ns	diabetes	0.6779	ns	IBD	0.0218	*	RA	0.9514	ns	onco	0.9318	ns	T-test
2	aPE 34:2	control	cvd	0.4986	ns	diabetes	0.1476	ns	IBD	0.0392	*	RA	0.5431	ns	onco	0.2251	ns	T-test
3	aPE 36:1	control	cvd	0.1089	ns	diabetes	0.5822	ns	IBD	0.0848	ns	RA	0.3792	ns	onco	0.6393	ns	T-test
4	aPE 36:2	control	cvd	0.8964	ns	diabetes	0.0846	ns	IBD	0.0830	ns	RA	0.8287	ns	onco	0.5631	ns	T-test

5	aPE 36:3	control	cvd	0.9169	ns	diabetes	0.2896	ns	IBD	0.0947	ns	RA	0.2427	ns	onco	0.5831	ns	T-test
6	aPE 36:4	control	cvd	0.0064	**	diabetes	0.3241	ns	IBD	0.0409	*	RA	0.8359	ns	onco	0.4733	ns	T-test
7	aPE 36:5	control	cvd	0.0060	**	diabetes	0.5150	ns	IBD	0.0706	ns	RA	0.4383	ns	onco	0.8072	ns	T-test
8	aPE 38:1	control	cvd	0.2440	ns	diabetes	0.0688	ns	IBD	0.0455	*	RA	0.6001	ns	onco	0.5246	ns	T-test
9	aPE 38:2	control	cvd	0.8366	ns	diabetes	0.0044	**	IBD	0.0735	ns	RA	0.9760	ns	onco	0.9982	ns	T-test
10	aPE 38:3	control	cvd	0.7040	ns	diabetes	0.2859	ns	IBD	0.3113	ns	RA	0.9283	ns	onco	0.4777	ns	T-test
11	aPE 38:4	control	cvd	0.0012	**	diabetes	0.5720	ns	IBD	0.2794	ns	RA	0.5072	ns	onco	0.1472	ns	T-test
12	aPE 38:5	control	cvd	0.0065	**	diabetes	0.4885	ns	IBD	0.0409	*	RA	0.9320	ns	onco	0.1462	ns	T-test
13	aPE 38:6	control	cvd	0.0271	*	diabetes	0.6415	ns	IBD	0.0071	**	RA	0.1843	ns	onco	0.0480	*	T-test
14	aPE 40:2	control	cvd	0.6159	ns	diabetes	0.0097	**	IBD	0.0339	*	RA	0.5618	ns	onco	0.8858	ns	T-test
15	aPE 40:3	control	cvd	0.8803	ns	diabetes	0.0645	ns	IBD	0.0825	ns	RA	0.1546	ns	onco	0.8552	ns	T-test
16	aPE 40:4	control	cvd	0.5815	ns	diabetes	0.1516	ns	IBD	0.3627	ns	RA	0.6271	ns	onco	0.9734	ns	T-test
17	aPE 40:5	control	cvd	0.0580	ns	diabetes	0.2205	ns	IBD	0.0429	*	RA	0.5802	ns	onco	0.7812	ns	T-test
18	aPE 42:4	control	cvd	0.0027	**	diabetes	0.3756	ns	IBD	0.2822	ns	RA	0.7232	ns	onco	0.0667	ns	T-test
19	aPE 42:5	control	cvd	0.0143	*	diabetes	0.5072	ns	IBD	0.5404	ns	RA	0.3483	ns	onco	0.2372	ns	T-test
20	aPE 42:6	control	cvd	0.1493	ns	diabetes	0.0090	**	IBD	0.2026	ns	RA	0.3874	ns	onco	0.1936	ns	T-test
21	aPE 42:7	control	cvd	0.0200	*	diabetes	0.5548	ns	IBD	0.3462	ns	RA	0.3174	ns	onco	0.0496	*	T-test
22	CE 16:0	control	cvd	0.7900	ns	diabetes	0.5155	ns	IBD	0.0349	*	RA	0.6207	ns	onco	0.3187	ns	T-test
23	CE 16:1	control	cvd	0.6630	ns	diabetes	0.3273	ns	IBD	0.9644	ns	RA	0.5819	ns	onco	0.0748	ns	T-test
24	CE 18:1	control	cvd	0.6662	ns	diabetes	0.9926	ns	IBD	0.0532	ns	RA	0.0969	ns	onco	0.8864	ns	T-test
25	CE 18:2	control	cvd	0.4647	ns	diabetes	0.6724	ns	IBD	0.0412	*	RA	0.0531	ns	onco	0.5783	ns	T-test
26	CE 18:3	control	cvd	0.5449	ns	diabetes	0.4037	ns	IBD	0.0592	ns	RA	0.4792	ns	onco	0.5976	ns	T-test
27	CE 20:2	control	cvd	0.0975	ns	diabetes	0.9471	ns	IBD	0.7928	ns	RA	0.0066	**	onco	0.2914	ns	T-test
28	CE 20:3	control	cvd	0.8624	ns	diabetes	0.3072	ns	IBD	0.5972	ns	RA	0.7612	ns	onco	0.4140	ns	T-test
29	CE 20:4	control	cvd	0.0087	**	diabetes	0.0841	ns	IBD	0.7715	ns	RA	0.4628	ns	onco	0.0794	ns	T-test

30	CE 20:5	control	cvd	0.0055	**	diabetes	0.8398	ns	IBD	0.0543	ns	RA	0.7516	ns	onco	0.1255	ns	T-test
31	CE 22:5	control	cvd	0.1408	ns	diabetes	0.7603	ns	IBD	0.2722	ns	RA	0.4645	ns	onco	0.2241	ns	T-test
32	CE 22:6	control	cvd	0.0513	ns	diabetes	0.6721	ns	IBD	0.2973	ns	RA	0.3035	ns	onco	0.1594	ns	T-test
33	CER 32:1	control	cvd	0.0099	**	diabetes	0.7908	ns	IBD	0.3436	ns	RA	0.0977	ns	onco	0.0139	*	T-test
34	CER 34:1	control	cvd	0.0124	*	diabetes	0.4818	ns	IBD	0.1197	ns	RA	0.1148	ns	onco	0.1140	ns	T-test
35	CER 34:2	control	cvd	0.0048	**	diabetes	0.0031	**	IBD	0.5255	ns	RA	0.3872	ns	onco	0.7905	ns	T-test
36	CER 36:1	control	cvd	0.0018	**	diabetes	0.0547	ns	IBD	0.0088	**	RA	0.0253	*	onco	0.0537	ns	T-test
37	CER 38:1	control	cvd	0.0157	*	diabetes	0.4912	ns	IBD	0.1623	ns	RA	0.7718	ns	onco	0.0998	ns	T-test
38	CER 39:1	control	cvd	0.7889	ns	diabetes	0.0609	ns	IBD	0.0007	***	RA	0.7947	ns	onco	0.4467	ns	T-test
39	CER 40:1	control	cvd	0.1028	ns	diabetes	0.8877	ns	IBD	0.0750	ns	RA	0.9759	ns	onco	0.6833	ns	T-test
40	CER 40:2	control	cvd	0.0063	**	diabetes	0.8939	ns	IBD	0.4590	ns	RA	0.9985	ns	onco	0.1855	ns	T-test
41	CER 41:1	control	cvd	0.4081	ns	diabetes	0.1410	ns	IBD	0.0051	**	RA	0.9312	ns	onco	0.6944	ns	T-test
42	CER 41:2	control	cvd	0.2991	ns	diabetes	0.2171	ns	IBD	0.0440	*	RA	0.9631	ns	onco	0.5501	ns	T-test
43	CER 42:1	control	cvd	0.2169	ns	diabetes	0.5859	ns	IBD	0.0456	*	RA	0.7297	ns	onco	0.5865	ns	T-test
44	CER 42:2	control	cvd	0.0010	***	diabetes	0.1729	ns	IBD	0.1642	ns	RA	0.8142	ns	onco	0.0598	ns	T-test
45	CER 42:3	control	cvd	0.0025	**	diabetes	0.1903	ns	IBD	0.4612	ns	RA	0.5437	ns	onco	0.0562	ns	T-test
46	CER 43:1	control	cvd	0.4366	ns	diabetes	0.1517	ns	IBD	0.0338	*	RA	0.5649	ns	onco	0.7405	ns	T-test
47	CER 43:2	control	cvd	0.0027	**	diabetes	0.3604	ns	IBD	0.7057	ns	RA	0.5263	ns	onco	0.9201	ns	T-test
48	CER 43:3	control	cvd	0.6522	ns	diabetes	0.4597	ns	IBD	0.0677	ns	RA	0.7202	ns	onco	0.2736	ns	T-test
49	CER 43:4	control	cvd	0.6415	ns	diabetes	0.3017	ns	IBD	0.9796	ns	RA	0.5452	ns	onco	0.0721	ns	T-test
50	CER 44:1	control	cvd	0.4170	ns	diabetes	0.6567	ns	IBD	0.0190	*	RA	0.7030	ns	onco	0.7696	ns	T-test
51	CER 44:2	control	cvd	0.0508	ns	diabetes	0.7691	ns	IBD	0.1331	ns	RA	0.3705	ns	onco	0.0982	ns	T-test
52	CHOL 0:0	control	cvd	0.1797	ns	diabetes	0.2584	ns	IBD	0.0269	*	RA	0.9824	ns	onco	0.1066	ns	T-test
53	CoQ 50:10	control	cvd	0.0330	*	diabetes	0.4757	ns	IBD	0.1823	ns	RA	0.9165	ns	onco	0.2488	ns	T-test

54	CoQ 35:7	control	cvd	0.5701	ns	diabetes	0.0041	**	IBD	0.4937	ns	RA	0.6270	ns	onco	0.8221	ns	T-test
55	DG 36:2	control	cvd	0.0977	ns	diabetes	0.0201	*	IBD	0.2020	ns	RA	0.4965	ns	onco	0.6925	ns	T-test
56	DG 36:3	control	cvd	0.0985	ns	diabetes	0.0810	ns	IBD	0.0782	ns	RA	0.9876	ns	onco	0.8719	ns	T-test
57	DG 36:4	control	cvd	0.0733	ns	diabetes	0.0930	ns	IBD	0.6633	ns	RA	0.4419	ns	onco	0.4033	ns	T-test
58	HEXCer 34:1	control	cvd	0.7036	ns	diabetes	0.8657	ns	IBD	0.7335	ns	RA	0.6880	ns	onco	0.7253	ns	T-test
59	HEXCer 36:1	control	cvd	0.5988	ns	diabetes	0.6736	ns	IBD	0.0655	ns	RA	0.7491	ns	onco	0.6250	ns	T-test
60	HEXCer 38:1	control	cvd	0.4649	ns	diabetes	0.8039	ns	IBD	0.8166	ns	RA	0.6525	ns	onco	0.2687	ns	T-test
61	HEXCer 38:2	control	cvd	0.0504	ns	diabetes	0.1365	ns	IBD	0.6315	ns	RA	0.8352	ns	onco	0.6261	ns	T-test
62	HEXCer 40:1	control	cvd	0.8288	ns	diabetes	0.0956	ns	IBD	0.1878	ns	RA	0.2862	ns	onco	0.7475	ns	T-test
63	HEXCer 40:2	control	cvd	0.7488	ns	diabetes	0.9135	ns	IBD	0.2138	ns	RA	0.5771	ns	onco	0.1178	ns	T-test
64	HEXCer 41:1	control	cvd	0.9149	ns	diabetes	0.0165	*	IBD	0.0900	ns	RA	0.2720	ns	onco	0.4302	ns	T-test
65	HEXCer 42:1	control	cvd	0.0348	*	diabetes	0.2424	ns	IBD	0.6192	ns	RA	0.5673	ns	onco	0.9932	ns	T-test
66	HEXCer 42:2	control	cvd	0.3181	ns	diabetes	0.6813	ns	IBD	0.3340	ns	RA	0.3644	ns	onco	0.1310	ns	T-test
67	LPC 15:0	control	cvd	0.1255	ns	diabetes	0.3169	ns	IBD	0.0205	*	RA	0.4511	ns	onco	0.4358	ns	T-test
68	LPC 16:0	control	cvd	0.4869	ns	diabetes	0.8805	ns	IBD	0.8814	ns	RA	0.8864	ns	onco	0.6988	ns	T-test
69	LPC 18:0	control	cvd	0.2586	ns	diabetes	0.5980	ns	IBD	0.3415	ns	RA	0.6207	ns	onco	0.1476	ns	T-test
70	LPC 18:3	control	cvd	0.4880	ns	diabetes	0.0622	ns	IBD	0.1617	ns	RA	0.1815	ns	onco	0.7491	ns	T-test
71	LPC 19:0	control	cvd	0.3294	ns	diabetes	0.0380	*	IBD	0.0269	*	RA	0.1864	ns	onco	0.0806	ns	T-test
72	LPC 19:1	control	cvd	0.4142	ns	diabetes	0.1465	ns	IBD	0.6059	ns	RA	0.4346	ns	onco	0.0934	ns	T-test
73	LPC 20:0	control	cvd	0.4995	ns	diabetes	0.0617	ns	IBD	0.0200	*	RA	0.0456	*	onco	0.4165	ns	T-test
74	LPC 20:1	control	cvd	0.2835	ns	diabetes	0.3390	ns	IBD	0.2162	ns	RA	0.1502	ns	onco	0.6655	ns	T-test
75	LPC 20:2	control	cvd	0.6823	ns	diabetes	0.1331	ns	IBD	0.1491	ns	RA	0.3730	ns	onco	0.6855	ns	T-test
76	LPC 20:3	control	cvd	0.9470	ns	diabetes	0.5315	ns	IBD	0.5132	ns	RA	0.5057	ns	onco	0.3063	ns	T-test
77	LPC 20:4	control	cvd	0.0076	**	diabetes	0.9756	ns	IBD	0.6490	ns	RA	0.6708	ns	onco	0.2127	ns	T-test
78	LPC 20:5	contro	cvd	0.0175	*	diabetes	0.1779	ns	IBD	0.0898	ns	RA	0.6888	ns	onco	0.2500	ns	T-test

		control	cvd			diabetes			IBD			RA			onco			T-test
79	LPC 21:0	control	cvd	0.2227	ns	diabetes	0.0060	**	IBD	0.1163	ns	RA	0.0557	ns	onco	0.1830	ns	T-test
80	LPC 22:0	control	cvd	0.7429	ns	diabetes	0.0404	*	IBD	0.0645	ns	RA	0.0862	ns	onco	0.2751	ns	T-test
81	LPC 22:1	control	cvd	0.2112	ns	diabetes	0.6221	ns	IBD	0.0708	ns	RA	0.1556	ns	onco	0.4353	ns	T-test
82	LPC 22:4	control	cvd	0.5941	ns	diabetes	0.7458	ns	IBD	0.0753	ns	RA	0.6744	ns	onco	0.8034	ns	T-test
83	LPC 22:5	control	cvd	0.0090	**	diabetes	0.2018	ns	IBD	0.2183	ns	RA	0.7450	ns	onco	0.8617	ns	T-test
84	LPC 22:6	control	cvd	0.0143	*	diabetes	0.1799	ns	IBD	0.8060	ns	RA	0.0835	ns	onco	0.0896	ns	T-test
85	LPC 24:1	control	cvd	0.1530	ns	diabetes	0.3695	ns	IBD	0.4276	ns	RA	0.5354	ns	onco	0.5383	ns	T-test
86	LPE 16:1	control	cvd	0.6277	ns	diabetes	0.4426	ns	IBD	0.6719	ns	RA	0.4482	ns	onco	0.5468	ns	T-test
87	LPE 18:0	control	cvd	0.8244	ns	diabetes	0.0037	**	IBD	0.4015	ns	RA	0.7208	ns	onco	0.8510	ns	T-test
88	LPE 18:3	control	cvd	0.4236	ns	diabetes	0.0237	*	IBD	0.3273	ns	RA	0.1165	ns	onco	0.6409	ns	T-test
89	LPE 20:3	control	cvd	0.7414	ns	diabetes	0.0744	ns	IBD	0.5918	ns	RA	0.6510	ns	onco	0.8297	ns	T-test
90	LPE 20:4	control	cvd	0.1231	ns	diabetes	0.0435	*	IBD	0.7273	ns	RA	0.6399	ns	onco	0.4307	ns	T-test
91	LPE 22:5	control	cvd	0.1415	ns	diabetes	0.1801	ns	IBD	0.2584	ns	RA	0.5984	ns	onco	0.3890	ns	T-test
92	LPE 22:6	control	cvd	0.0238	*	diabetes	0.0279	*	IBD	0.8429	ns	RA	0.0901	ns	onco	0.0357	*	T-test
93	PC 24:0.IS	control	cvd	0.1576	ns	diabetes	0.3848	ns	IBD	0.3197	ns	RA	0.4795	ns	onco	0.2884	ns	T-test
94	PC 26:0	control	cvd	0.6742	ns	diabetes	0.9470	ns	IBD	0.3142	ns	RA	0.2005	ns	onco	0.6925	ns	T-test
95	PC 29:0	control	cvd	0.0146	*	diabetes	0.0162	*	IBD	0.0346	*	RA	0.7888	ns	onco	0.6987	ns	T-test
96	PC 30:0	control	cvd	0.0919	ns	diabetes	0.1068	ns	IBD	0.3079	ns	RA	0.6492	ns	onco	0.0863	ns	T-test
97	PC 30:1	control	cvd	0.0960	ns	diabetes	0.6519	ns	IBD	0.5019	ns	RA	0.7052	ns	onco	0.0680	ns	T-test
98	PC 31:0	control	cvd	0.0654	ns	diabetes	0.0237	*	IBD	0.1526	ns	RA	0.8105	ns	onco	0.9491	ns	T-test
99	PC 31:1	control	cvd	0.0921	ns	diabetes	0.3027	ns	IBD	0.3924	ns	RA	0.6958	ns	onco	0.5403	ns	T-test
100	PC 32:0	control	cvd	0.8102	ns	diabetes	0.2316	ns	IBD	0.6002	ns	RA	0.7420	ns	onco	0.1276	ns	T-test
101	PC 32:1	control	cvd	0.4049	ns	diabetes	0.7975	ns	IBD	0.7976	ns	RA	0.8210	ns	onco	0.0722	ns	T-test
102	PC 32:2	control	cvd	0.1177	ns	diabetes	0.2377	ns	IBD	0.0063	**	RA	0.3377	ns	onco	0.2169	ns	T-test

L

103	PC 32:3	control	cvd	0.1228	ns	diabetes	0.1441	ns	IBD	0.0210	*	RA	0.1877	ns	onco	0.4259	ns	T-test
104	PC 33:1	control	cvd	0.0387	*	diabetes	0.1687	ns	IBD	0.4056	ns	RA	0.6245	ns	onco	0.8195	ns	T-test
105	PC 33:2	control	cvd	0.0321	*	diabetes	0.0158	*	IBD	0.0043	**	RA	0.3689	ns	onco	0.2776	ns	T-test
106	PC 34:0	control	cvd	0.2841	ns	diabetes	0.3198	ns	IBD	0.1251	ns	RA	0.8251	ns	onco	0.2818	ns	T-test
107	PC 34:2	control	cvd	0.5266	ns	diabetes	0.5158	ns	IBD	0.1439	ns	RA	0.3801	ns	onco	0.7506	ns	T-test
108	PC 34:4	control	cvd	0.9056	ns	diabetes	0.7938	ns	IBD	0.0909	ns	RA	0.7397	ns	onco	0.0096	**	T-test
109	PC 34:5	control	cvd	0.4905	ns	diabetes	0.3509	ns	IBD	0.0113	*	RA	0.7569	ns	onco	0.0508	ns	T-test
110	PC 35:4	control	cvd	0.8974	ns	diabetes	0.3578	ns	IBD	0.0648	ns	RA	0.2728	ns	onco	0.2205	ns	T-test
111	PC 35:5	control	cvd	0.5664	ns	diabetes	0.0973	ns	IBD	0.0032	**	RA	0.5500	ns	onco	0.4627	ns	T-test
112	PC 36:0	control	cvd	0.3063	ns	diabetes	0.0108	*	IBD	0.2751	ns	RA	0.2575	ns	onco	0.3179	ns	T-test
113	PC 36:1	control	cvd	0.3559	ns	diabetes	0.3173	ns	IBD	0.3522	ns	RA	0.2650	ns	onco	0.4953	ns	T-test
114	PC 36:2	control	cvd	0.9143	ns	diabetes	0.3586	ns	IBD	0.1368	ns	RA	0.3547	ns	onco	0.9520	ns	T-test
115	PC 36:4	control	cvd	0.1541	ns	diabetes	0.4822	ns	IBD	0.6079	ns	RA	0.2205	ns	onco	0.0024	**	T-test
116	PC 36:5	control	cvd	0.1364	ns	diabetes	0.2283	ns	IBD	0.0345	*	RA	0.6113	ns	onco	0.0753	ns	T-test
117	PC 36:6	control	cvd	0.7754	ns	diabetes	0.1778	ns	IBD	0.0056	**	RA	0.3039	ns	onco	0.0184	*	T-test
118	PC 37:6	control	cvd	0.6469	ns	diabetes	0.0281	*	IBD	0.0087	**	RA	0.1644	ns	onco	0.6677	ns	T-test
119	PC 38:3	control	cvd	0.7227	ns	diabetes	0.3450	ns	IBD	0.5907	ns	RA	0.4264	ns	onco	0.0845	ns	T-test
120	PC 38:4	control	cvd	0.0010	**	diabetes	0.2813	ns	IBD	0.4154	ns	RA	0.1397	ns	onco	0.0020	**	T-test
121	PC 38:5	control	cvd	0.3083	ns	diabetes	0.1750	ns	IBD	0.6340	ns	RA	0.2358	ns	onco	0.7727	ns	T-test
122	PC 38:6	control	cvd	0.2072	ns	diabetes	0.1572	ns	IBD	0.2228	ns	RA	0.0757	ns	onco	0.0337	*	T-test
123	PC 38:7	control	cvd	0.6535	ns	diabetes	0.0545	ns	IBD	0.0022	**	RA	0.8842	ns	onco	0.4615	ns	T-test
124	PC 38:8	control	cvd	0.4282	ns	diabetes	0.3267	ns	IBD	0.1863	ns	RA	0.8582	ns	onco	0.3193	ns	T-test
125	PC 39:3	control	cvd	0.3059	ns	diabetes	0.4444	ns	IBD	0.0120	*	RA	0.7569	ns	onco	0.2833	ns	T-test
126	PC 39:4	control	cvd	0.3628	ns	diabetes	0.1899	ns	IBD	0.0710	ns	RA	0.8653	ns	onco	0.1385	ns	T-test
127	PC 39:5	contro	cvd	0.4743	ns	diabetes	0.0086	**	IBD	0.4416	ns	RA	0.2126	ns	onco	0.7264	ns	T-test

LI

128	PC 40:4	control	cvd	0.4655	ns	diabetes	0.2142	ns	IBD	0.3305	ns	RA	0.8961	ns	onco	0.1337	ns	T-test
129	PC 40:5	control	cvd	0.0150	*	diabetes	0.6903	ns	IBD	0.6473	ns	RA	0.5077	ns	onco	0.4924	ns	T-test
130	PC 40:6	control	cvd	0.0414	*	diabetes	0.7622	ns	IBD	0.3368	ns	RA	0.0947	ns	onco	0.0214	*	T-test
131	PC 41:6	control	cvd	0.7517	ns	diabetes	0.0703	ns	IBD	0.0270	*	RA	0.5772	ns	onco	0.2705	ns	T-test
132	PC 42:10	control	cvd	0.3130	ns	diabetes	0.0246	*	IBD	0.0647	ns	RA	0.4383	ns	onco	0.2016	ns	T-test
133	PC 42:2	control	cvd	0.2745	ns	diabetes	0.0986	ns	IBD	0.0062	**	RA	0.0183	*	onco	0.9948	ns	T-test
134	PC 42:3	control	cvd	0.9243	ns	diabetes	0.2211	ns	IBD	0.0240	*	RA	0.5229	ns	onco	0.4410	ns	T-test
135	PC 42:4	control	cvd	0.8671	ns	diabetes	0.4271	ns	IBD	0.1431	ns	RA	0.9577	ns	onco	0.0531	ns	T-test
136	PC 42:5	control	cvd	0.0337	*	diabetes	0.0102	*	IBD	0.1081	ns	RA	0.1609	ns	onco	0.9317	ns	T-test
137	PC 42:7	control	cvd	0.2734	ns	diabetes	0.7381	ns	IBD	0.0314	*	RA	0.9006	ns	onco	0.1137	ns	T-test
138	PC 42:8	control	cvd	0.9254	ns	diabetes	0.7752	ns	IBD	0.4144	ns	RA	0.8559	ns	onco	0.1572	ns	T-test
139	PC 42:9	control	cvd	0.1416	ns	diabetes	0.2419	ns	IBD	0.9848	ns	RA	0.5217	ns	onco	0.5872	ns	T-test
140	PC 44:5	control	cvd	0.0564	ns	diabetes	0.8221	ns	IBD	0.3509	ns	RA	0.8943	ns	onco	0.0569	ns	T-test
141	PE 22:0	control	cvd	0.9336	ns	diabetes	0.0942	ns	IBD	0.0413	*	RA	0.7853	ns	onco	0.8423	ns	T-test
142	PE 23:0	control	cvd	0.8717	ns	diabetes	0.3052	ns	IBD	0.0585	ns	RA	0.5087	ns	onco	0.8412	ns	T-test
143	PE 24:0.IS	control	cvd	0.5694	ns	diabetes	0.7749	ns	IBD	0.2485	ns	RA	0.8189	ns	onco	0.6557	ns	T-test
144	PE 25:0	control	cvd	0.6254	ns	diabetes	0.3394	ns	IBD	0.4813	ns	RA	0.3898	ns	onco	0.3231	ns	T-test
145	PE 26:0	control	cvd	0.6337	ns	diabetes	0.1098	ns	IBD	0.1949	ns	RA	0.9921	ns	onco	0.4716	ns	T-test
146	PE 32:1	control	cvd	0.6363	ns	diabetes	0.9375	ns	IBD	0.5962	ns	RA	0.8315	ns	onco	0.2059	ns	T-test
147	PE 34:1	control	cvd	0.9858	ns	diabetes	0.6825	ns	IBD	0.3417	ns	RA	0.9166	ns	onco	0.1853	ns	T-test
148	PE 34:2	control	cvd	0.3558	ns	diabetes	0.0381	*	IBD	0.2245	ns	RA	0.8585	ns	onco	0.8547	ns	T-test
149	PE 34:3	control	cvd	0.2941	ns	diabetes	0.1329	ns	IBD	0.0798	ns	RA	0.3635	ns	onco	0.7504	ns	T-test
150	PE 35:1	control	cvd	0.4774	ns	diabetes	0.1422	ns	IBD	0.1296	ns	RA	0.6113	ns	onco	0.9354	ns	T-test
151	PE 35:2	control	cvd	0.0728	ns	diabetes	0.0206	*	IBD	0.1097	ns	RA	0.5103	ns	onco	0.9225	ns	T-test

152	PE 36:1	control	cvd	0.7095	ns	diabetes	0.2904	ns	IBD	0.0341	*	RA	0.7262	ns	onco	0.4317	ns	T-test
153	PE 36:2	control	cvd	0.7156	ns	diabetes	0.0441	*	IBD	0.0947	ns	RA	0.9371	ns	onco	0.8089	ns	T-test
154	PE 36:3	control	cvd	0.2055	ns	diabetes	0.0099	**	IBD	0.1850	ns	RA	0.6623	ns	onco	0.7210	ns	T-test
155	PE 36:4	control	cvd	0.9932	ns	diabetes	0.1248	ns	IBD	0.8681	ns	RA	0.8944	ns	onco	0.1225	ns	T-test
156	PE 36:5	control	cvd	0.7424	ns	diabetes	0.0496	*	IBD	0.1519	ns	RA	0.9030	ns	onco	0.2369	ns	T-test
157	PE 38:3	control	cvd	0.9653	ns	diabetes	0.9310	ns	IBD	0.2242	ns	RA	0.6352	ns	onco	0.4146	ns	T-test
158	PE 38:4	control	cvd	0.1471	ns	diabetes	0.1587	ns	IBD	0.6802	ns	RA	0.7942	ns	onco	0.1037	ns	T-test
159	PE 38:5	control	cvd	0.9820	ns	diabetes	0.0111	*	IBD	0.5315	ns	RA	0.9436	ns	onco	0.1695	ns	T-test
160	PE 38:6	control	cvd	0.3177	ns	diabetes	0.1608	ns	IBD	0.6827	ns	RA	0.4681	ns	onco	0.1211	ns	T-test
161	PE 40:3	control	cvd	0.3293	ns	diabetes	0.4129	ns	IBD	0.0539	ns	RA	0.2732	ns	onco	0.2089	ns	T-test
162	PE 40:4	control	cvd	0.7849	ns	diabetes	0.9402	ns	IBD	0.7269	ns	RA	0.8815	ns	onco	0.4506	ns	T-test
163	PE 40:5	control	cvd	0.1117	ns	diabetes	0.4335	ns	IBD	0.7522	ns	RA	0.6678	ns	onco	0.5706	ns	T-test
164	PE 40:6	control	cvd	0.0472	*	diabetes	0.5435	ns	IBD	0.4667	ns	RA	0.2182	ns	onco	0.0395	*	T-test
165	PE 40:7	control	cvd	0.5722	ns	diabetes	0.0320	*	IBD	0.5357	ns	RA	0.9392	ns	onco	0.4183	ns	T-test
166	PE 40:8	control	cvd	0.6250	ns	diabetes	0.0506	ns	IBD	0.6182	ns	RA	0.1841	ns	onco	0.5189	ns	T-test
167	PI 32:0	control	cvd	0.0049	**	diabetes	0.2324	ns	IBD	0.1099	ns	RA	0.5173	ns	onco	0.9125	ns	T-test
168	PI 32:1	control	cvd	0.1258	ns	diabetes	0.3006	ns	IBD	0.6670	ns	RA	0.5571	ns	onco	0.2258	ns	T-test
169	PI 34:1	control	cvd	0.0694	ns	diabetes	0.2300	ns	IBD	0.1157	ns	RA	0.8506	ns	onco	0.6720	ns	T-test
170	PI 34:2	control	cvd	0.0902	ns	diabetes	0.6533	ns	IBD	0.1064	ns	RA	0.9353	ns	onco	0.2935	ns	T-test
171	PI 36:1	control	cvd	0.2638	ns	diabetes	0.0339	*	IBD	0.0020	**	RA	0.4113	ns	onco	0.8039	ns	T-test
172	PI 36:2	control	cvd	0.2136	ns	diabetes	0.3997	ns	IBD	0.0168	*	RA	0.4358	ns	onco	0.5478	ns	T-test
173	PI 36:3	control	cvd	0.0190	*	diabetes	0.1543	ns	IBD	0.3017	ns	RA	0.4509	ns	onco	0.5125	ns	T-test
174	PI 36:4	control	cvd	0.8121	ns	diabetes	0.9046	ns	IBD	0.9138	ns	RA	0.8065	ns	onco	0.3559	ns	T-test
175	PI 38:2	control	cvd	0.3979	ns	diabetes	0.0177	*	IBD	0.0006	***	RA	0.3470	ns	onco	0.2012	ns	T-test
176	PI 38:3	control	cvd	0.5925	ns	diabetes	0.2186	ns	IBD	0.0694	ns	RA	0.6204	ns	onco	0.4954	ns	T-test

177	PI 38:4	control	cvd	0.0019	**	diabetes	0.5216	ns	IBD	0.8271	ns	RA	0.8250	ns	onco	0.1412	ns	T-test
178	PI 38:5	control	cvd	0.5018	ns	diabetes	0.2670	ns	IBD	0.7335	ns	RA	0.8689	ns	onco	0.4914	ns	T-test
179	PI 38:6	control	cvd	0.1438	ns	diabetes	0.0202	*	IBD	0.2165	ns	RA	0.4169	ns	onco	0.1297	ns	T-test
180	PI 40:4	control	cvd	0.8066	ns	diabetes	0.2562	ns	IBD	0.9850	ns	RA	0.3676	ns	onco	0.9715	ns	T-test
181	PI 40:5	control	cvd	0.0807	ns	diabetes	0.1718	ns	IBD	0.7901	ns	RA	0.8971	ns	onco	0.2630	ns	T-test
182	PI 40:6	control	cvd	0.7877	ns	diabetes	0.0080	**	IBD	0.2113	ns	RA	0.3935	ns	onco	0.0783	ns	T-test
183	SM 30:1	control	cvd	0.4859	ns	diabetes	0.5893	ns	IBD	0.1052	ns	RA	0.7917	ns	onco	0.1525	ns	T-test
184	SM 31:1	control	cvd	0.2908	ns	diabetes	0.0906	ns	IBD	0.0329	*	RA	0.5515	ns	onco	0.7806	ns	T-test
185	SM 32:1	control	cvd	0.2145	ns	diabetes	0.5048	ns	IBD	0.0017	**	RA	0.9394	ns	onco	0.1262	ns	T-test
186	SM 32:2	control	cvd	0.1075	ns	diabetes	0.0393	*	IBD	0.5313	ns	RA	0.2723	ns	onco	0.0340	*	T-test
187	SM 33:1	control	cvd	0.6464	ns	diabetes	0.4029	ns	IBD	0.0128	*	RA	0.6082	ns	onco	0.7948	ns	T-test
188	SM 34:1	control	cvd	0.6852	ns	diabetes	0.4517	ns	IBD	0.6951	ns	RA	0.6277	ns	onco	0.6336	ns	T-test
189	SM 34:2	control	cvd	0.0117	*	diabetes	0.0136	*	IBD	0.6007	ns	RA	0.2788	ns	onco	0.0466	*	T-test
190	SM 34:3	control	cvd	0.0667	ns	diabetes	0.0130	*	IBD	0.7235	ns	RA	0.1032	ns	onco	0.2099	ns	T-test
191	SM 35:1	control	cvd	0.2082	ns	diabetes	0.9526	ns	IBD	0.1870	ns	RA	0.6280	ns	onco	0.5033	ns	T-test
192	SM 35:2	control	cvd	0.0557	ns	diabetes	0.5217	ns	IBD	0.2024	ns	RA	0.1633	ns	onco	0.1367	ns	T-test
193	SM 36:1	control	cvd	0.0194	*	diabetes	0.4408	ns	IBD	0.1223	ns	RA	0.4303	ns	onco	0.1268	ns	T-test
194	SM 36:2	control	cvd	0.0102	*	diabetes	0.1131	ns	IBD	0.4903	ns	RA	0.1506	ns	onco	0.0191	*	T-test
195	SM 36:3	control	cvd	0.0104	*	diabetes	0.0650	ns	IBD	0.8600	ns	RA	0.3195	ns	onco	0.2237	ns	T-test
196	SM 36:4	control	cvd	0.9005	ns	diabetes	0.0158	*	IBD	0.0036	**	RA	0.0746	ns	onco	0.7649	ns	T-test
197	SM 37:1	control	cvd	0.1776	ns	diabetes	0.8578	ns	IBD	0.0442	*	RA	0.5885	ns	onco	0.2056	ns	T-test
198	SM 37:2	control	cvd	0.3588	ns	diabetes	0.3995	ns	IBD	0.5611	ns	RA	0.5787	ns	onco	0.4606	ns	T-test
199	SM 38:1	control	cvd	0.2237	ns	diabetes	0.2998	ns	IBD	0.0058	**	RA	0.9499	ns	onco	0.0246	*	T-test
200	SM 38:2	control	cvd	0.1843	ns	diabetes	0.6890	ns	IBD	0.6388	ns	RA	0.3645	ns	onco	0.0189	*	T-test

201	SM 38:3	control	cvd	0.0211	*	diabetes	0.0080	**	IBD	0.5733	ns	RA	0.1672	ns	onco	0.0120	*	T-test
202	SM 39:1	control	cvd	0.8809	ns	diabetes	0.0726	ns	IBD	0.0001	****	RA	0.6991	ns	onco	0.1597	ns	T-test
203	SM 39:2	control	cvd	0.3070	ns	diabetes	0.2204	ns	IBD	0.6645	ns	RA	0.5167	ns	onco	0.2224	ns	T-test
204	SM 40:1	control	cvd	0.1961	ns	diabetes	0.7359	ns	IBD	0.1142	ns	RA	0.8806	ns	onco	0.2652	ns	T-test
205	SM 40:2	control	cvd	0.4318	ns	diabetes	0.7391	ns	IBD	0.0716	ns	RA	0.9822	ns	onco	0.0953	ns	T-test
206	SM 40:3	control	cvd	0.0076	**	diabetes	0.0146	*	IBD	0.7398	ns	RA	0.2223	ns	onco	0.0034	**	T-test
207	SM 40:4	control	cvd	0.0487	*	diabetes	0.0053	**	IBD	0.4050	ns	RA	0.0705	ns	onco	0.0206	*	T-test
208	SM 40:5	control	cvd	0.6327	ns	diabetes	0.0675	ns	IBD	0.0380	*	RA	0.8376	ns	onco	0.7551	ns	T-test
209	SM 41:1	control	cvd	0.8035	ns	diabetes	0.1118	ns	IBD	0.0049	**	RA	0.4989	ns	onco	0.1479	ns	T-test
210	SM 42:1	control	cvd	0.3716	ns	diabetes	0.2528	ns	IBD	0.0322	*	RA	0.3893	ns	onco	0.1851	ns	T-test
211	SM 42:2	control	cvd	0.0066	**	diabetes	0.0983	ns	IBD	0.3910	ns	RA	0.9550	ns	onco	0.0204	*	T-test
212	SM 42:3	control	cvd	0.0077	**	diabetes	0.0743	ns	IBD	0.3133	ns	RA	0.5437	ns	onco	0.0070	**	T-test
213	SM 42:4	control	cvd	0.1989	ns	diabetes	0.0488	*	IBD	0.3413	ns	RA	0.1214	ns	onco	0.0172	*	T-test
214	SM 43:1	control	cvd	0.2283	ns	diabetes	0.3851	ns	IBD	0.0368	*	RA	0.9332	ns	onco	0.5847	ns	T-test
215	SM 43:2	control	cvd	0.0046	**	diabetes	0.4152	ns	IBD	0.4555	ns	RA	0.6255	ns	onco	0.4037	ns	T-test
216	SM 43:3	control	cvd	0.9901	ns	diabetes	0.8406	ns	IBD	0.0417	*	RA	0.0664	ns	onco	0.3163	ns	T-test
217	SM 44:1	control	cvd	0.2946	ns	diabetes	0.3517	ns	IBD	0.0161	*	RA	0.3150	ns	onco	0.6953	ns	T-test
218	SM 44:2	control	cvd	0.0876	ns	diabetes	0.1337	ns	IBD	0.1047	ns	RA	0.1937	ns	onco	0.1024	ns	T-test
219	SM 44:3	control	cvd	0.0771	ns	diabetes	0.4944	ns	IBD	0.1069	ns	RA	0.7765	ns	onco	0.0678	ns	T-test
220	SM 44:4	control	cvd	0.4496	ns	diabetes	0.2554	ns	IBD	0.4184	ns	RA	0.6249	ns	onco	0.1238	ns	T-test
221	TG 40:0	control	cvd	0.9859	ns	diabetes	0.5898	ns	IBD	0.1703	ns	RA	0.3570	ns	onco	0.4641	ns	T-test
222	TG 41:0	control	cvd	0.9505	ns	diabetes	0.7704	ns	IBD	0.2451	ns	RA	0.4384	ns	onco	0.6129	ns	T-test
223	TG 42:0	control	cvd	0.7418	ns	diabetes	0.9252	ns	IBD	0.3049	ns	RA	0.3767	ns	onco	0.3783	ns	T-test
224	TG 42:1	control	cvd	0.9933	ns	diabetes	0.9625	ns	IBD	0.1859	ns	RA	0.4711	ns	onco	0.5087	ns	T-test
225	TG 42:2	control	cvd	0.9528	ns	diabetes	0.9236	ns	IBD	0.1812	ns	RA	0.4249	ns	onco	0.6257	ns	T-test

226	TG 43:0	control	cvd	0.8951	ns	diabetes	0.7286	ns	IBD	0.3525	ns	RA	0.3652	ns	onco	0.4726	ns	T-test
227	TG 43:1	control	cvd	0.9797	ns	diabetes	0.9771	ns	IBD	0.1139	ns	RA	0.2790	ns	onco	0.3535	ns	T-test
228	TG 43:2	control	cvd	0.8655	ns	diabetes	0.8520	ns	IBD	0.0279	*	RA	0.3202	ns	onco	0.1964	ns	T-test
229	TG 44:0	control	cvd	0.7852	ns	diabetes	0.6992	ns	IBD	0.1948	ns	RA	0.4052	ns	onco	0.2858	ns	T-test
230	TG 44:1	control	cvd	0.8502	ns	diabetes	0.9198	ns	IBD	0.1947	ns	RA	0.5871	ns	onco	0.4798	ns	T-test
231	TG 44:2	control	cvd	0.6981	ns	diabetes	0.8712	ns	IBD	0.0701	ns	RA	0.3413	ns	onco	0.3506	ns	T-test
232	TG 44:3	control	cvd	0.5299	ns	diabetes	0.8716	ns	IBD	0.0449	*	RA	0.4529	ns	onco	0.5125	ns	T-test
233	TG 45:0	control	cvd	0.7014	ns	diabetes	0.9237	ns	IBD	0.2251	ns	RA	0.3357	ns	onco	0.6277	ns	T-test
234	TG 45:1	control	cvd	0.5428	ns	diabetes	0.6902	ns	IBD	0.1302	ns	RA	0.4103	ns	onco	0.6636	ns	T-test
235	TG 45:2	control	cvd	0.6908	ns	diabetes	0.7794	ns	IBD	0.0346	*	RA	0.2875	ns	onco	0.2157	ns	T-test
236	TG 46:0	control	cvd	0.9924	ns	diabetes	0.6516	ns	IBD	0.0954	ns	RA	0.3287	ns	onco	0.1654	ns	T-test
237	TG 46:1	control	cvd	0.6200	ns	diabetes	0.8609	ns	IBD	0.1051	ns	RA	0.7994	ns	onco	0.4228	ns	T-test
238	TG 46:2	control	cvd	0.9265	ns	diabetes	0.9113	ns	IBD	0.1099	ns	RA	0.5953	ns	onco	0.5782	ns	T-test
239	TG 46:3	control	cvd	0.7222	ns	diabetes	0.6084	ns	IBD	0.0603	ns	RA	0.6042	ns	onco	0.6860	ns	T-test
240	TG 46:4	control	cvd	0.0500	ns	diabetes	0.4574	ns	IBD	0.2377	ns	RA	0.4428	ns	onco	0.3005	ns	T-test
241	TG 47:0	control	cvd	0.8503	ns	diabetes	0.8852	ns	IBD	0.0998	ns	RA	0.2107	ns	onco	0.3577	ns	T-test
242	TG 47:1	control	cvd	0.6027	ns	diabetes	0.9480	ns	IBD	0.0462	*	RA	0.4976	ns	onco	0.6958	ns	T-test
243	TG 47:2	control	cvd	0.6768	ns	diabetes	0.8608	ns	IBD	0.0275	*	RA	0.3148	ns	onco	0.4967	ns	T-test
244	TG 47:3	control	cvd	0.7682	ns	diabetes	0.5658	ns	IBD	0.0079	**	RA	0.1898	ns	onco	0.3303	ns	T-test
245	TG 48:0	control	cvd	0.4922	ns	diabetes	0.4278	ns	IBD	0.1125	ns	RA	0.2415	ns	onco	0.1171	ns	T-test
246	TG 48:1	control	cvd	0.8693	ns	diabetes	0.5001	ns	IBD	0.0617	ns	RA	0.6710	ns	onco	0.2505	ns	T-test
247	TG 48:2	control	cvd	0.8958	ns	diabetes	0.4500	ns	IBD	0.0489	*	RA	0.6784	ns	onco	0.3465	ns	T-test
248	TG 48:3	control	cvd	0.7264	ns	diabetes	0.7806	ns	IBD	0.0314	*	RA	0.7490	ns	onco	0.6703	ns	T-test
249	TG 48:4	control	cvd	0.5448	ns	diabetes	0.9322	ns	IBD	0.0144	*	RA	0.5021	ns	onco	0.4357	ns	T-test

250	TG 48:5	control	cvd	0.6209	ns	diabetes	0.9381	ns	IBD	0.0201	*	RA	0.4374	ns	onco	0.4570	ns	T-test
251	TG 49:0	control	cvd	0.5989	ns	diabetes	0.9604	ns	IBD	0.0692	ns	RA	0.1518	ns	onco	0.4836	ns	T-test
252	TG 49:1	control	cvd	0.8899	ns	diabetes	0.8630	ns	IBD	0.0430	*	RA	0.4586	ns	onco	0.9277	ns	T-test
253	TG 49:2	control	cvd	0.7035	ns	diabetes	0.6696	ns	IBD	0.0373	*	RA	0.3299	ns	onco	0.7282	ns	T-test
254	TG 49:3	control	cvd	0.8497	ns	diabetes	0.8456	ns	IBD	0.0087	**	RA	0.2773	ns	onco	0.6850	ns	T-test
255	TG 49:4	control	cvd	0.7960	ns	diabetes	0.6761	ns	IBD	0.0028	**	RA	0.2576	ns	onco	0.6306	ns	T-test
256	TG 50:0	control	cvd	0.3916	ns	diabetes	0.9671	ns	IBD	0.0765	ns	RA	0.3432	ns	onco	0.2478	ns	T-test
257	TG 50:1	control	cvd	0.2789	ns	diabetes	0.0908	ns	IBD	0.1617	ns	RA	0.4168	ns	onco	0.1825	ns	T-test
258	TG 50:2	control	cvd	0.1783	ns	diabetes	0.0435	*	IBD	0.1573	ns	RA	0.4585	ns	onco	0.2111	ns	T-test
259	TG 50:3	control	cvd	0.2128	ns	diabetes	0.1432	ns	IBD	0.0643	ns	RA	0.5044	ns	onco	0.3354	ns	T-test
260	TG 50:4	control	cvd	0.1982	ns	diabetes	0.5561	ns	IBD	0.0167	*	RA	0.4088	ns	onco	0.3999	ns	T-test
261	TG 50:5	control	cvd	0.2434	ns	diabetes	0.8930	ns	IBD	0.0097	**	RA	0.3811	ns	onco	0.2843	ns	T-test
262	TG 50:6	control	cvd	0.2321	ns	diabetes	0.7260	ns	IBD	0.0132	*	RA	0.2335	ns	onco	0.0675	ns	T-test
263	TG 51:0	control	cvd	0.6564	ns	diabetes	0.7199	ns	IBD	0.0242	*	RA	0.1462	ns	onco	0.3767	ns	T-test
264	TG 51:1	control	cvd	0.3735	ns	diabetes	0.9011	ns	IBD	0.0464	*	RA	0.4007	ns	onco	0.7875	ns	T-test
265	TG 51:2	control	cvd	0.1433	ns	diabetes	0.3218	ns	IBD	0.0442	*	RA	0.5337	ns	onco	0.8129	ns	T-test
266	TG 51:3	control	cvd	0.1848	ns	diabetes	0.5239	ns	IBD	0.0270	*	RA	0.6828	ns	onco	0.8859	ns	T-test
267	TG 51:4	control	cvd	0.2474	ns	diabetes	0.9610	ns	IBD	0.0070	**	RA	0.4442	ns	onco	0.8125	ns	T-test
268	TG 51:5	control	cvd	0.3688	ns	diabetes	0.9762	ns	IBD	0.0007	***	RA	0.3948	ns	onco	0.9276	ns	T-test
269	TG 51:6	control	cvd	0.5799	ns	diabetes	0.6260	ns	IBD	0.0038	**	RA	0.3933	ns	onco	0.6588	ns	T-test
270	TG 52:0	control	cvd	0.1955	ns	diabetes	0.3285	ns	IBD	0.0313	*	RA	0.5303	ns	onco	0.2942	ns	T-test
271	TG 52:1	control	cvd	0.1732	ns	diabetes	0.5947	ns	IBD	0.0583	ns	RA	0.6197	ns	onco	0.4214	ns	T-test
272	TG 52:2	control	cvd	0.0164	*	diabetes	0.0253	*	IBD	0.1753	ns	RA	0.8614	ns	onco	0.2427	ns	T-test
273	TG 52:3	control	cvd	0.0022	**	diabetes	0.0062	**	IBD	0.1202	ns	RA	0.6560	ns	onco	0.2648	ns	T-test
274	TG 52:4	control	cvd	0.0122	*	diabetes	0.0695	ns	IBD	0.0524	ns	RA	0.5647	ns	onco	0.4703	ns	T-test

275	TG 52:5	control	cvd	0.0750	ns	diabetes	0.4288	ns	IBD	0.0119	*	RA	0.9062	ns	onco	0.8223	ns	T-test
276	TG 52:6	control	cvd	0.0515	ns	diabetes	0.7691	ns	IBD	0.0093	**	RA	0.2834	ns	onco	0.0960	ns	T-test
277	TG 52:7	control	cvd	0.0602	ns	diabetes	0.7947	ns	IBD	0.0047	**	RA	0.2039	ns	onco	0.0595	ns	T-test
278	TG 53:1	control	cvd	0.3431	ns	diabetes	0.3717	ns	IBD	0.0132	*	RA	0.4512	ns	onco	0.7175	ns	T-test
279	TG 53:2	control	cvd	0.1224	ns	diabetes	0.2791	ns	IBD	0.0102	*	RA	0.6946	ns	onco	0.9633	ns	T-test
280	TG 53:3	control	cvd	0.0256	*	diabetes	0.4808	ns	IBD	0.0305	*	RA	0.7278	ns	onco	0.8863	ns	T-test
281	TG 53:4	control	cvd	0.0184	*	diabetes	0.4022	ns	IBD	0.0428	*	RA	0.9562	ns	onco	0.7094	ns	T-test
282	TG 53:5	control	cvd	0.0531	ns	diabetes	0.8384	ns	IBD	0.0064	**	RA	0.4337	ns	onco	0.8114	ns	T-test
283	TG 53:6	control	cvd	0.1302	ns	diabetes	0.5729	ns	IBD	0.0019	**	RA	0.2166	ns	onco	0.2836	ns	T-test
284	TG 53:7	control	cvd	0.1593	ns	diabetes	0.3652	ns	IBD	0.0095	**	RA	0.1808	ns	onco	0.3123	ns	T-test
285	TG 54:0	control	cvd	0.2611	ns	diabetes	0.1879	ns	IBD	0.0012	**	RA	0.3980	ns	onco	0.1519	ns	T-test
286	TG 54:1	control	cvd	0.2500	ns	diabetes	0.5130	ns	IBD	0.0119	*	RA	0.6782	ns	onco	0.6078	ns	T-test
287	TG 54:2	control	cvd	0.0504	ns	diabetes	0.4323	ns	IBD	0.0443	*	RA	0.8885	ns	onco	0.6500	ns	T-test
288	TG 54:3	control	cvd	0.0160	*	diabetes	0.0625	ns	IBD	0.2045	ns	RA	0.7872	ns	onco	0.6736	ns	T-test
289	TG 54:4	control	cvd	0.0075	**	diabetes	0.0960	ns	IBD	0.2023	ns	RA	0.8789	ns	onco	0.8505	ns	T-test
290	TG 54:5	control	cvd	0.0058	**	diabetes	0.0860	ns	IBD	0.0714	ns	RA	0.6373	ns	onco	0.3584	ns	T-test
291	TG 54:6	control	cvd	0.0096	**	diabetes	0.3583	ns	IBD	0.0195	*	RA	0.3672	ns	onco	0.1584	ns	T-test
292	TG 54:7	control	cvd	0.0051	**	diabetes	0.5339	ns	IBD	0.0110	*	RA	0.0877	ns	onco	0.0123	*	T-test
293	TG 54:8	control	cvd	0.0172	*	diabetes	0.8289	ns	IBD	0.0034	**	RA	0.1138	ns	onco	0.0406	*	T-test
294	TG 54:9	control	cvd	0.1039	ns	diabetes	0.3808	ns	IBD	0.0061	**	RA	0.2240	ns	onco	0.0823	ns	T-test
295	TG 55:0	control	cvd	0.2338	ns	diabetes	0.7991	ns	IBD	0.1472	ns	RA	0.2248	ns	onco	0.3510	ns	T-test
296	TG 55:1	control	cvd	0.4546	ns	diabetes	0.1665	ns	IBD	0.0017	**	RA	0.3177	ns	onco	0.4888	ns	T-test
297	TG 55:2	control	cvd	0.1852	ns	diabetes	0.4778	ns	IBD	0.0012	**	RA	0.7213	ns	onco	0.6606	ns	T-test
298	TG 55:3	control	cvd	0.0641	ns	diabetes	0.7383	ns	IBD	0.0093	**	RA	0.9185	ns	onco	0.9248	ns	T-test

299	TG 55:4	control	cvd	0.1926	ns	diabetes	0.4741	ns	IBD	0.0012	**	RA	0.5918	ns	onco	0.8391	ns	T-test
300	TG 55:5	control	cvd	0.0239	*	diabetes	0.6521	ns	IBD	0.0281	*	RA	0.3492	ns	onco	0.2551	ns	T-test
301	TG 55:6	control	cvd	0.0322	*	diabetes	0.4850	ns	IBD	0.0169	*	RA	0.5301	ns	onco	0.0358	*	T-test
302	TG 55:7	control	cvd	0.0385	*	diabetes	0.3435	ns	IBD	0.0047	**	RA	0.1797	ns	onco	0.2323	ns	T-test
303	TG 55:8	control	cvd	0.0641	ns	diabetes	0.2096	ns	IBD	0.0045	**	RA	0.2115	ns	onco	0.2410	ns	T-test
304	TG 56:0	control	cvd	0.2202	ns	diabetes	0.3450	ns	IBD	0.0076	**	RA	0.2722	ns	onco	0.2280	ns	T-test
305	TG 56:1	control	cvd	0.4724	ns	diabetes	0.3578	ns	IBD	0.0004	***	RA	0.4581	ns	onco	0.5754	ns	T-test
306	TG 56:10	control	cvd	0.0140	*	diabetes	0.9713	ns	IBD	0.1257	ns	RA	0.1766	ns	onco	0.0261	*	T-test
307	TG 56:2	control	cvd	0.1267	ns	diabetes	0.3733	ns	IBD	0.0004	***	RA	0.9544	ns	onco	0.3539	ns	T-test
308	TG 56:3	control	cvd	0.0394	*	diabetes	0.7892	ns	IBD	0.0015	**	RA	0.6578	ns	onco	0.5888	ns	T-test
309	TG 56:4	control	cvd	0.1200	ns	diabetes	0.3052	ns	IBD	0.0047	**	RA	0.8338	ns	onco	0.3266	ns	T-test
310	TG 56:5	control	cvd	0.0000	****	diabetes	0.0584	ns	IBD	0.8719	ns	RA	0.2700	ns	onco	0.0075	**	T-test
311	TG 56:6	control	cvd	0.0001	****	diabetes	0.0708	ns	IBD	0.3260	ns	RA	0.4445	ns	onco	0.0241	*	T-test
312	TG 56:7	control	cvd	0.0005	***	diabetes	0.4903	ns	IBD	0.0478	*	RA	0.1646	ns	onco	0.0193	*	T-test
313	TG 56:8	control	cvd	0.0020	**	diabetes	0.8700	ns	IBD	0.0108	*	RA	0.1354	ns	onco	0.0251	*	T-test
314	TG 56:9	control	cvd	0.0052	**	diabetes	0.9066	ns	IBD	0.0075	**	RA	0.2037	ns	onco	0.0337	*	T-test
315	TG 57:0	control	cvd	0.3639	ns	diabetes	0.8857	ns	IBD	0.5483	ns	RA	0.6918	ns	onco	0.3158	ns	T-test
316	TG 57:1	control	cvd	0.8190	ns	diabetes	0.1477	ns	IBD	0.0185	*	RA	0.4045	ns	onco	0.4471	ns	T-test
317	TG 57:2	control	cvd	0.3364	ns	diabetes	0.2737	ns	IBD	0.0007	***	RA	0.3879	ns	onco	0.3230	ns	T-test
318	TG 57:3	control	cvd	0.1620	ns	diabetes	0.9243	ns	IBD	0.0011	**	RA	0.5654	ns	onco	0.5748	ns	T-test
319	TG 57:4	control	cvd	0.1524	ns	diabetes	0.5406	ns	IBD	0.0019	**	RA	0.4698	ns	onco	0.5128	ns	T-test
320	TG 57:5	control	cvd	0.0922	ns	diabetes	0.4553	ns	IBD	0.0047	**	RA	0.3799	ns	onco	0.2785	ns	T-test
321	TG 57:6	control	cvd	0.0345	*	diabetes	0.4961	ns	IBD	0.0111	*	RA	0.3662	ns	onco	0.3323	ns	T-test
322	TG 57:7	control	cvd	0.0307	*	diabetes	0.1801	ns	IBD	0.0036	**	RA	0.2581	ns	onco	0.2139	ns	T-test
323	TG 57:8	control	cvd	0.0166	*	diabetes	0.2426	ns	IBD	0.0059	**	RA	0.1447	ns	onco	0.1930	ns	T-test

324	TG 57:9	control	cvd	0.0148	*	diabetes	0.1896	ns	IBD	0.0094	**	RA	0.1648	ns	onco	0.1306	ns	T-test
325	TG 58:0	control	cvd	0.3198	ns	diabetes	0.8602	ns	IBD	0.0408	*	RA	0.1802	ns	onco	0.2522	ns	T-test
326	TG 58:1	control	cvd	0.5205	ns	diabetes	0.1341	ns	IBD	0.0006	***	RA	0.7113	ns	onco	0.4405	ns	T-test
327	TG 58:10	control	cvd	0.0010	**	diabetes	0.8260	ns	IBD	0.0258	*	RA	0.1203	ns	onco	0.0041	**	T-test
328	TG 58:11	control	cvd	0.0027	**	diabetes	0.7338	ns	IBD	0.0322	*	RA	0.1647	ns	onco	0.0173	*	T-test
329	TG 58:2	control	cvd	0.3317	ns	diabetes	0.1610	ns	IBD	0.0001	***	RA	0.9408	ns	onco	0.5644	ns	T-test
330	TG 58:3	control	cvd	0.1411	ns	diabetes	0.4216	ns	IBD	0.0001	***	RA	0.8889	ns	onco	0.3998	ns	T-test
331	TG 58:4	control	cvd	0.1140	ns	diabetes	0.4950	ns	IBD	0.0001	****	RA	0.9849	ns	onco	0.3200	ns	T-test
332	TG 58:5	control	cvd	0.0069	**	diabetes	0.0576	ns	IBD	0.8998	ns	RA	0.5442	ns	onco	0.1739	ns	T-test
333	TG 58:6	control	cvd	0.0168	*	diabetes	0.7736	ns	IBD	0.0162	*	RA	0.7043	ns	onco	0.1475	ns	T-test
334	TG 58:7	control	cvd	0.0056	**	diabetes	0.8508	ns	IBD	0.0084	**	RA	0.4261	ns	onco	0.0351	*	T-test
335	TG 58:8	control	cvd	0.0017	**	diabetes	0.8717	ns	IBD	0.0326	*	RA	0.1582	ns	onco	0.0172	*	T-test
336	TG 58:9	control	cvd	0.0112	*	diabetes	0.7852	ns	IBD	0.0158	*	RA	0.3135	ns	onco	0.0698	ns	T-test
337	TG 59:0	control	cvd	0.4094	ns	diabetes	0.6037	ns	IBD	0.6478	ns	RA	0.4306	ns	onco	0.0873	ns	T-test
338	TG 59:1	control	cvd	0.9408	ns	diabetes	0.0674	ns	IBD	0.0144	*	RA	0.3082	ns	onco	0.2431	ns	T-test
339	TG 59:2	control	cvd	0.8914	ns	diabetes	0.0304	*	IBD	0.0016	**	RA	0.6994	ns	onco	0.6626	ns	T-test
340	TG 59:3	control	cvd	0.1880	ns	diabetes	0.3330	ns	IBD	0.0090	**	RA	0.6432	ns	onco	0.5653	ns	T-test
341	TG 60:0	control	cvd	0.3307	ns	diabetes	0.5684	ns	IBD	0.3036	ns	RA	0.2008	ns	onco	0.0878	ns	T-test
342	TG 60:1	control	cvd	0.7357	ns	diabetes	0.0575	ns	IBD	0.0009	***	RA	0.5835	ns	onco	0.3023	ns	T-test
343	TG 60:10	control	cvd	0.0003	***	diabetes	0.5271	ns	IBD	0.0974	ns	RA	0.0642	ns	onco	0.0023	**	T-test
344	TG 60:11	control	cvd	0.0005	***	diabetes	0.9801	ns	IBD	0.0711	ns	RA	0.0720	ns	onco	0.0041	**	T-test
345	TG 60:12	control	cvd	0.0038	**	diabetes	0.6018	ns	IBD	0.0424	*	RA	0.0683	ns	onco	0.0088	**	T-test
346	TG 60:2	control	cvd	0.3827	ns	diabetes	0.1132	ns	IBD	0.0003	***	RA	0.9859	ns	onco	0.5879	ns	T-test
347	TG 60:3	control	cvd	0.2416	ns	diabetes	0.1700	ns	IBD	0.0001	****	RA	0.8853	ns	onco	0.5575	ns	T-test

348	TG 60:4	control	cvd	0.1248	ns	diabetes	0.9390	ns	IBD	0.0000	****	RA	0.6824	ns	onco	0.4203	ns	T-test
349	TG 60:5	control	cvd	0.2113	ns	diabetes	0.1808	ns	IBD	0.0001	****	RA	0.7192	ns	onco	0.2281	ns	T-test
350	TG 60:6	control	cvd	0.3997	ns	diabetes	0.2410	ns	IBD	0.0002	***	RA	0.6911	ns	onco	0.0697	ns	T-test
351	TG 60:7	control	cvd	0.0084	**	diabetes	0.9274	ns	IBD	0.3974	ns	RA	0.5947	ns	onco	0.0172	*	T-test
352	TG 60:8	control	cvd	0.1948	ns	diabetes	0.7854	ns	IBD	0.0017	**	RA	0.4821	ns	onco	0.0367	*	T-test
353	TG 60:9	control	cvd	0.0009	***	diabetes	0.2649	ns	IBD	0.0211	*	RA	0.1917	ns	onco	0.0029	**	T-test
354	TG 61:2	control	cvd	0.8824	ns	diabetes	0.0242	*	IBD	0.0200	*	RA	0.4391	ns	onco	0.3639	ns	T-test
355	TG 62:0	control	cvd	0.6124	ns	diabetes	0.2043	ns	IBD	0.6848	ns	RA	0.3678	ns	onco	0.1183	ns	T-test
356	TG 62:1	control	cvd	0.8995	ns	diabetes	0.0332	*	IBD	0.0013	**	RA	0.4261	ns	onco	0.2547	ns	T-test
357	TG 62:10	control	cvd	0.1239	ns	diabetes	0.3618	ns	IBD	0.0075	**	RA	0.6164	ns	onco	0.0090	**	T-test
358	TG 62:11	control	cvd	0.0400	*	diabetes	0.4028	ns	IBD	0.0233	*	RA	0.2034	ns	onco	0.0120	*	T-test
359	TG 62:12	control	cvd	0.0144	*	diabetes	0.5046	ns	IBD	0.0485	*	RA	0.1175	ns	onco	0.0083	**	T-test
360	TG 62:13	control	cvd	0.0225	*	diabetes	0.3817	ns	IBD	0.0717	ns	RA	0.1323	ns	onco	0.0162	*	T-test
361	TG 62:2	control	cvd	0.7197	ns	diabetes	0.0246	*	IBD	0.0005	***	RA	0.8152	ns	onco	0.4904	ns	T-test
362	TG 62:3	control	cvd	0.2936	ns	diabetes	0.1245	ns	IBD	0.0008	***	RA	0.8993	ns	onco	0.4918	ns	T-test
363	TG 62:4	control	cvd	0.1828	ns	diabetes	0.0969	ns	IBD	0.0002	***	RA	0.9820	ns	onco	0.3198	ns	T-test
364	TG 62:5	control	cvd	0.2017	ns	diabetes	0.0794	ns	IBD	0.0004	***	RA	0.9303	ns	onco	0.1632	ns	T-test
365	TG 62:6	control	cvd	0.8624	ns	diabetes	0.0311	*	IBD	0.0002	***	RA	0.6867	ns	onco	0.3072	ns	T-test
366	TG 62:7	control	cvd	0.5713	ns	diabetes	0.1030	ns	IBD	0.0105	*	RA	0.9867	ns	onco	0.0671	ns	T-test
367	TG 62:8	control	cvd	0.0425	*	diabetes	0.8682	ns	IBD	0.1464	ns	RA	0.8148	ns	onco	0.0392	*	T-test
368	TG 62:9	control	cvd	0.1981	ns	diabetes	0.1342	ns	IBD	0.0098	**	RA	0.2949	ns	onco	0.0558	ns	T-test
369	TG 64:0	control	cvd	0.0238	*	diabetes	0.4852	ns	IBD	0.4260	ns	RA	0.0113	*	onco	0.0056	**	T-test
370	TG 64:1	control	cvd	0.5471	ns	diabetes	0.0181	*	IBD	0.0113	*	RA	0.7371	ns	onco	0.0492	*	T-test
371	TG 64:2	control	cvd	0.9954	ns	diabetes	0.4109	ns	IBD	0.0001	****	RA	0.6911	ns	onco	0.7146	ns	T-test

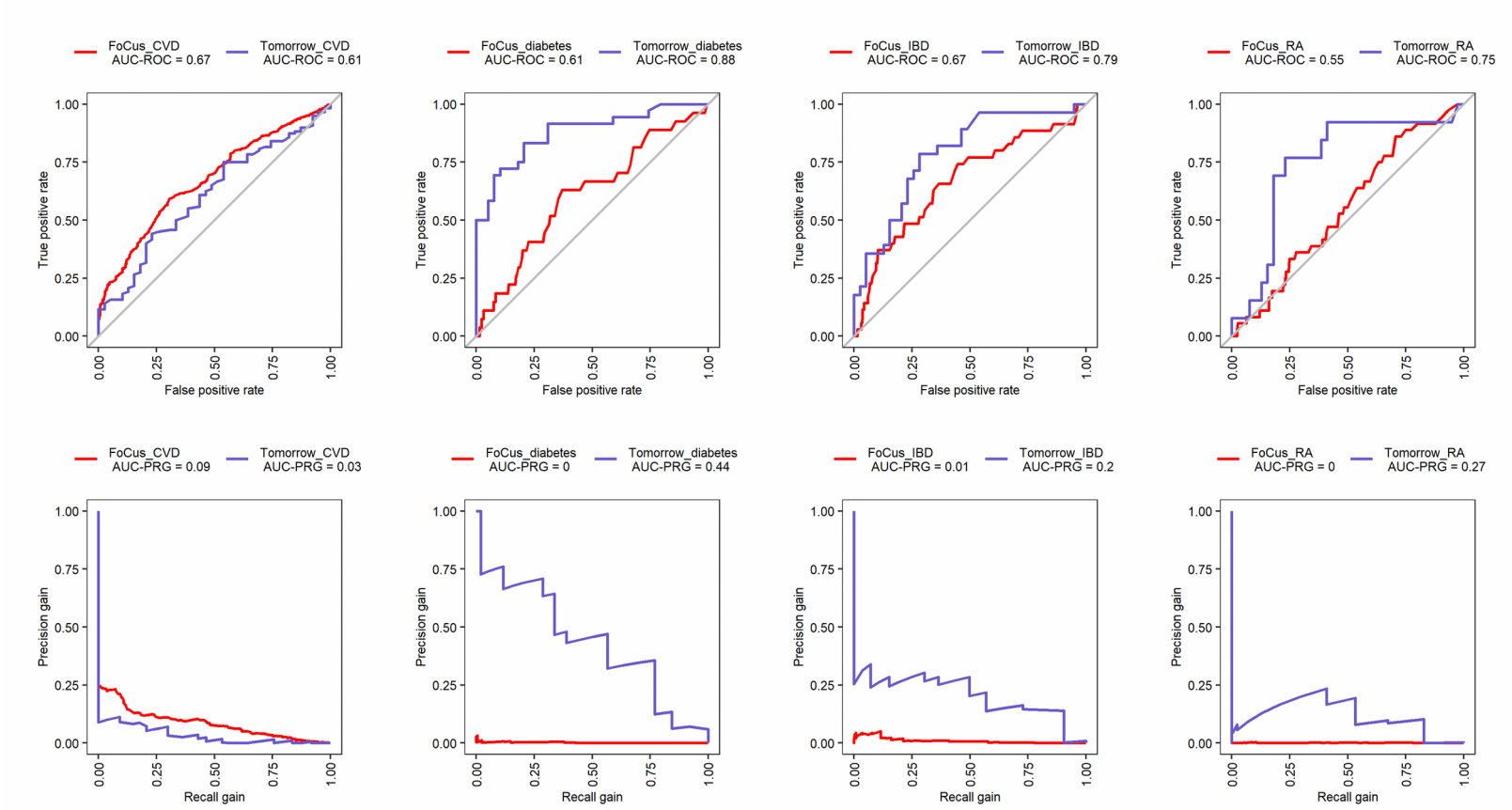

Supplement Figure 14 ROC (top) and Precision-Recall-Gain (bottom) curves of the health status groups of the top20 discrimination lipid species found in the OPLS-DA model in the Tomorrow cohort and which was validated with the FoCus cohort.